

# **Synthesis of a High Performance Surfactant for Application in Alkaline-Surfactant-Polymer Flooding in Extreme Reservoirs**

By

**Samya Daniela de Sousa Elias**

In fulfillment of the Requirement for the Degree of Masters of Engineering:  
Chemical Engineering, Faculty of Engineering, Cape Peninsula  
University of Technology.

Cape Town  
September 2016

**Synthesis of a High Performance Surfactant for Application in Alkaline-Surfactant-Polymer Flooding in Extreme Reservoirs**

---



By

**Samya Daniela de Sousa Elias**

**Supervisors:**

**Ademola Rabi  
Oluwaseun Oyekola**

## DECLARATION

I, **Samya Daniela De Sousa Elias**, declare that the contents of this thesis/dissertation represent my own unaided work, and that it has not previously been submitted for academic examination towards any qualification. In addition, all the sources I have utilized or quoted have been indicated or acknowledge as full references.

Samya Elias

November 2016

Signed

## ABSTRACT

Due to the rising cost involve with bringing new fields on stream, of producing residual crude from matured fields, and the significant enhancement in oil recovery provided when compared to conventional water-flooding, increasing attention is being given to chemical flooding technologies. This is particular of interest in mature fields that had previously undergone water flooding. These methods entail injecting chemicals such as surfactant, alkali, and polymer often in mixture into reservoirs to improve oil recovery. In this study a sulfonated surfactant was produced from cheap waste vegetable oils and its performance was assessed in terms of thermal stability at reservoir conditions, adsorption on different reservoir materials, gas chromatography characterization and a limited interfacial tension measurement to evaluate its ability to improve the recovery of crude oil. Waste vegetable oils have great potential as a sustainable and low cost feedstock as well as its low toxicity.

This study consists of two sections. The first section focussed on formulation of a bifunctional catalyst that facilitated a simultaneous esterification/transesterification reactions and optimum reaction conditions for the production of Fatty Acid Methyl Esters (FAME) from waste oils. The methyl esters were then sulfonated to produce the surfactant via the epoxidation step. The performance evaluation of the sulfonated surfactant produced is the subject matter of the second part. The transesterification step with methanol was investigated over the catalyst in a well stirred batch reactor at the optimum reaction conditions. The catalyst was produced via co-precipitation method and characterized using thermal gravimetric analysis (TGA), x-ray diffraction (XRD), Brunner-Emmett-Teller surface area measurement (BET), scanning electron microscopy with energy dispersive X-ray (SEM-EDX) and transmission electron microscopy (TEM). The characterization of the raw materials used and the methyl ester products were carried out with Gas Chromatography-Flame Ionization Detector (GC-FID) and Gas Chromatography-Mass Spectrometry (GC-MS).

The fatty acid methyl esters were subjected to epoxidation reaction in the presence and absence of a solvent at 25 °C, 30 °C and 50 °C so as to reduce the saturated fatty acid and convert the unsaturated fatty acid methyl esters to epoxy or oxirane groups. The epoxy originating from the esters were consequently sulfonated to produce the Sodium Epoxidized Methyl Ester Sulfonate (SEMES). The SEMES was produced by reacting the epoxy FAME with chlorosulfonic acid. The sulfonated functional group (S=O) was detected in the SEMES by FTIR analysis.

The effectiveness of the formulated surfactant was evaluated via the interfacial tension (IFT) between the crude oil and brine/surfactant solution test, its thermal behaviour at

reservoir conditions as well as the adsorption pattern of the SEMES against commercial cationic and anionic surfactants onto the common reservoir rock material and drilling mud weighing agent. The adsorption test was investigated at various surfactants, salinity and pH. The indirect method of residual equilibrium surfactant concentration measurement was employed to obtain and compare the adsorption isotherms of cetyltrimethylammonium bromide (CTAB), sodium dodecyl sulphate (SDS) and the synthesized sodium epoxidized methyl ester sulfonate (SEMES) on kaolin, silica, alumina and ilmenite materials. Surfactant concentration was varied from 50-600 ppm and the conductivity of the equilibrated media at room temperature is measured at various brine concentration and pH. The optimum catalyst ratios for production of fatty acid methyl esters via simultaneous esterification and transesterification reaction with the waste vegetable oil were found to be a reaction time of 4h, temperature of 65 °C and a methanol:oil ratio of 9:1. The CaO/Al<sub>2</sub>O<sub>3</sub> ratio of 60/40 % by wt and 4wt % catalyst loading for waste palm oil but a CaO/Al<sub>2</sub>O<sub>3</sub> ratio of 80/20 % by wt for the waste sunflower oil at the same reaction conditions. The maximum yield of FAME is found to be 89 % for waste palm oil and 98% for waste sunflower oil.

Both surfactants were found to adsorb strongly onto the rock materials while stabilization in the level of adsorption in the region above the CMC was observed as the monomer concentration falls due to micelles formation. At same level of salinity, it was found that cationic surfactant adsorbed more strongly on the rock materials than the anionic surfactant. The volume adsorbed was found to increase up to a maximum of 1.170 mg/g, 1.8249 mg/g and 0.7935 for SDS, CTAB and the synthesized SEMES respectively on kaolin and ilmenite for instance, as the concentration was increased at constant salinity. The same trend was noted as the brine concentration was varied with adsorption increasing with salinity for anionic surfactant. As pH increases the volume adsorption for SDS as well as for the synthesized surfactant decreases while the opposite was the case with the cationic surfactant, CTAB which increase with the alkalinity of the solution.

Thermal degradation analysis revealed that the sodium epoxidized methyl ester sulfonate demonstrated good surface thermal stability at reservoir temperature of up to 500 °C, where approximately 10% mass loss was observed.

## ACKNOWLEDGEMENTS

I would like to humbly acknowledge the following for the untiring support rendered to me during the course of my research study:

My Creator, for the knowledge and wisdom He has given me.

My supervisor, Ademola Rabi, for his relentless support, sincere encouragement and patience with my research thesis. His enlightening guidance, knowledgeable ideas and counsel played a critical role in the success of this study. Thanks for allowing me to be part of the Petroleum Research Group.

Genuine thanks to my co-supervisor, Oluwaseun Oyekola, for his considerable and invaluable help and technical assistance during the course of my research work.

My family, whose moral support always rekindled my beacon of hope during the tough moments during the course of this study. Special thanks goes to Bruno Marcos Elias who never stopped believing in me when I did not believe in myself. I would like to say I love him very much. And thanks to my friends for all the encouragement.

All my fellow postgraduate colleagues whose contributions and continuous support could not go without being mentioned. The Chemical Engineering staff for being a helping hand.

A great thanks goes to Cedrick from Suppa Oil Company, for donating resources (waste vegetable oils) to this research.

The Cape Peninsula University of technology and the Total Angola Group, for the financial support towards this research study which contributed beyond measure for its realization.

## TABLE OF CONTENT

DECLARATION.....	iii
ACKNOWLEDGEMENTS .....	vi
TABLE OF CONTENT .....	vii
LIST OF FIGURES.....	xi
LIST OF TABLES.....	xiv
NOMENCLATURE.....	xvii
ABBREVIATIONS.....	xix
<b>CHAPTER 1: INTRODUCTION .....</b>	<b>1</b>
1.1 GENERAL BACKGROUND .....	1
1.2 ENHANCED OIL RECOVERY .....	2
1.3 CHEMICAL ENHANCED OIL RECOVERY.....	5
1.4 SURFACTANT PRODUCTION FROM SUSTAINABLE FEEDSTOCK.....	6
1.5 PROBLEM STATEMENT.....	8
1.6 AIM AND OBJECTIVES OF THE STUDY .....	8
1.7 RESEARCH QUESTIONS.....	8
1.8 SCOPE OF THE STUDY .....	9
1.9 EXPECTED CONTRIBUTION TO KNOWLEDGE.....	9
1.10 THESIS OUTLINE.....	10
<b>CHAPTER 2: CURRENT TRENDS IN CHEMICAL ENHANCED OIL RECOVERY TECHNIQUES.....</b>	<b>12</b>
2. OVERVIEW.....	12
2.1 GENERAL CONCEPTS OF ENHANCED OIL RECOVERY .....	13
2.1.1 Improvement of the mobility ratio .....	13
2.1.2 Increasing the Capillary Number .....	14
2.1.3 Interfacial Tension .....	15
2.1.4 Wettability .....	15
2.2 SURFACTANT FLOODING .....	17
2.2.3 Structure and Classification of Surfactants .....	20
2.2.4 Selection of Surfactants for Surfactant Flooding .....	23
2.2.5 Effect of Surfactant on Wettability Alteration .....	25
2.2.6 Temperature and Pressure .....	26
2.2.7 Surfactant Retention.....	27
2.3 ALKALINE FLOODING .....	27
2.4 POLYMER FLOODING .....	31
2.5 ALKALINE-SURFACTANT-POLYMER FLOODING.....	34
<b>CHAPTER 3: PRODUCTION OF FAME FROM WASTE VEGETABLE OILS.....</b>	<b>39</b>

3.1	OVERVIEW.....	39
3.2	CHARACTERISTICS OF FATTY ACID METHYL ESTERS.....	40
3.3	ESTERIFICATION REACTION .....	42
3.4	TRANSESTERIFICATION REACTION.....	42
3.4.1	Reagents.....	43
3.4.2	Factors Affecting the Yield of Fatty Acid Methyl Esters.....	44
3.4.2.1	The Effect of Free Fatty Acids.....	45
3.4.2.2	Molar Ratio of Alcohol to Oil.....	45
3.4.2.3	Reaction Time.....	46
3.4.2.4	Reaction Temperature .....	46
3.4.2.5	Catalyst Weight .....	47
3.4.2.6	The Effect of Mixing.....	47
3.4.3	Transesterification using Homogeneous Catalysts.....	47
3.4.3.1	Homogeneous Alkali-Catalysis.....	48
3.4.3.2	Homogeneous Acid-Catalysis .....	49
3.4.4	Transesterification using Heterogeneous Catalysts .....	50
3.4.5	Catalysts for Simultaneous Esterification and Transesterification .....	53
3.4.6	Enzymatic Transesterification .....	55
3.4.7	Non-catalytic transesterification .....	56
3.5	SOLID CATALYSTS PREPARATION .....	57
3.5.1	Impregnation .....	57
3.5.2	Precipitation and Co-Precipitation.....	58
3.6	CATALYST CHARACTERIZATION TECHNIQUES .....	61
3.6.1	Thermo-Gravimetric Analysis (TGA) .....	61
3.6.2	X-Ray Diffraction (XRD) .....	61
3.6.3	Brunauer-Emmett-Teller (BET) Characterization .....	62
3.6.4	Scanning Electron Microscopy and Energy Dispersive X-ray Spectroscopy.....	62
3.6.5	Transmission Electron Microscopy (TEM).....	63
3.7	EXPERIMENTALS .....	64
3.7.1	Preparation of Catalyst.....	65
3.7.2	Catalyst Characterization.....	66
3.7.3	Fatty Acids Methyl Esters Production .....	67
3.7.4	Products Analyses.....	69
3.7.5	Catalyst Reusability .....	71
3.8	RESULTS .....	71
3.8.1	Catalyst Characterization.....	71



3.8.2	Fatty Acid Profiles of Oil Samples .....	77
3.8.3	Yield of Fatty Acid Methyl Esters.....	80
3.8.4	Catalyst Reusability .....	82
3.9	SUMMARY.....	83
<b>CHAPTER 4: METHLY ESTERS EPOXIDATION AND SULFONATION .....</b>		<b>85</b>
4.1	EPOXIDATION OF FATTY ACID METHYL ESTERS .....	85
4.1.1	Enzymatic Epoxidation .....	90
4.1.2	Epoxidation using Heterogeneous Catalysts .....	91
4.2	SULFONATION OF FATTY ACID METHYL ESTERS .....	93
4.3	EXPERIMENTALS .....	95
4.3.1	Production of Epoxidized Fatty Acid Methyl Esters .....	96
4.3.2	Epoxidation with no solvent .....	97
4.3.3	Epoxidation with solvent.....	98
4.3.4	Analyses of Epoxy Fatty Acid Methyl Esters .....	98
4.3.5	Sulfonation of the Epoxidized Methyl Esters for Surfactant Production .....	99
4.3.6	Surfactants Analysis .....	101
4.4	RESULTS AND DISCUSSIONS .....	101
4.4.1	Epoxidation of FAME .....	101
4.4.2	Thermo-gravimetric Analysis of FAME and EFAME .....	111
4.4.3	Surfactant Analyses .....	112
4.5	SUMMARY.....	115
<b>CHAPTER 5: CHARACTERIZATION OF THE SURFACTANTS.....</b>		<b>116</b>
5.1	INTRODUCTION .....	116
5.2	SURFACTANT ADSORPTION ON RESERVOIR ROCKS .....	118
5.2.1	Selection of Surfactants for Micellar Flooding .....	119
5.2.2	Effect of pH and Salinity on Surfactants Adsorption .....	121
5.2.3	Thermal Stability of Surfactants .....	122
5.3	TECHNIQUES TO DETERMINE ADSORPTION.....	122
5.3.1	Langmuir Adsorption Isotherm.....	125
5.3.2	Freundlich Adsorption Isotherm .....	125
5.3.3	Critical Micelle Concentration .....	126
5.4	EXPERIMENTALS .....	127
5.4.1	Static Adsorption Experiments .....	128
5.4.2	Thermal Stability test .....	129
5.5	RESULTS.....	129
5.5.1	Analyses of Reservoir Rock Materials.....	129

5.5.2	Adsorption of Surfactants at Constant Salinity .....	132
5.5.3	Effect of pH on the Surfactant Adsorption Isotherm .....	137
5.5.4	Effect of Salinity on the Adsorption Isotherm of Surfactants .....	139
5.5.5	Adsorption of Mixed Anionic-Cationic Surfactants System .....	140
5.5.6	Sub-CMC Adsorption Isotherms .....	141
5.6	THERMAL STABILITY ANALYSIS .....	144
5.7	SUMMARY.....	146
<b>CHAPTER 6: CONCLUSIONS AND RECOMMENDATIONS .....</b>		<b>147</b>
6.1	GENERAL CONCLUSIONS.....	147
6.2	RECOMMENDATIONS.....	150
<b>REFERENCES.....</b>		<b>151</b>
Appendix A - Sample Calculations on FAME Production .....		178
A.1	Free fatty acids determination.....	178
A.2.	FAME Production Calculations .....	179
A.3.	FAME Production Calculations .....	180
Appendix B - Spectrum and Chromatograms of Epoxidized Fatty Acid Methyl esters .....		190
Appendix C - Sample Calculations for Adsorption Density Determination.....		195
C.1.	Adsorption of CTAB on kaolin clay powder.....	195

## LIST OF FIGURES

Figure 1: Normalized residual saturation of the oil vs capillary number ( $N_c$ ) .....	14
Figure 2: Force balance at three phase contact line (Rao <i>et al.</i> , 2006).....	16
Figure 3: Schematics diagram of flooding showing trapped residual oil trapped in the reservoir	18
Figure 4: Surfactant flooding process (Berger & Lee, 2006) .....	18
Figure 5: Surfactant molecule and its orientation in water (Pashley & Karaman, 2004) .....	21
Figure 6: Schematic Alkaline process (Zhang <i>et al.</i> , 2005) .....	31
Figure 7: Schematic diagram of polymer flooding (Sadikhzadeh, 2006).....	31
Figure 8: HPAM structure (Sadikhzadeh, 2006) .....	33
Figure 9: ASP flooding process (Gan-Zuo <i>et al.</i> , 2000) .....	35
Figure 10: Fatty acid profile of diverse feedstock (Babajide <i>et al.</i> , 2011).....	40
Figure 11: Typical composition of a triglyceride (Babajide <i>et al.</i> , 2011) .....	41
Figure 12: SEM layout and function (Goodhew <i>et al.</i> , 2001) .....	63
Figure 13: An electron beam hitting the catalyst surface begins various processes; the electrons that are transmitted by the sample test are used for generating the TEM image (demonstrating gold and silver nano-particles supported on g-alumina (Wang <i>et al.</i> , 2004).....	64
Figure 14: Reactor used for the calcination of the catalysts .....	66
Figure 15: Simultaneous esterification and transesterification set-up.....	69
Figure 16: Thermal-gravimetric analysis of 80% Ca/ 20% Al filtrate .....	72
Figure 17: Weight loss vs Temperature curve for 80% Ca/ 20% Al filtrate .....	72
Figure 18: SEM-EDX micrograph of (a) the 80 CaO/20 Al <sub>2</sub> O <sub>3</sub> and (b) showing the areas chosen for EDX analysis at different magnifications. ....	73
Figure 19: 80%CaO/Al <sub>2</sub> O <sub>3</sub> EDX Spectrum.....	75
Figure 20: TEM images and structural information of 80%CaO/Al <sub>2</sub> O <sub>3</sub> catalyst .....	75
Figure 21: XRD pattern of 60%, 70% and 80% CaO on Al <sub>2</sub> O <sub>3</sub> catalysts .....	77
Figure 22: Fatty acid methyl ester yield versus catalyst ratio (60%, 70% and 80% CaO/Al <sub>2</sub> O <sub>3</sub> catalysts for 4 h of reaction time and methanol to oil molar ratio of 9:1 .....	81
Figure 23: Reusability of CaO/Al <sub>2</sub> O <sub>3</sub> catalysts at optimum reaction conditions (60% and 80% CaO/Al <sub>2</sub> O <sub>3</sub> , 9:1 methanol to oil molar ratio, 4 wt. % catalyst loading at 65 °C for 4 h).....	83
Figure 24: Epoxidation reaction of double bonds in the organic phase, using PFA generated in the aqueous (polar) phase from hydrogen peroxide (Campanella <i>et al.</i> , 2008) .....	88

Figure 25: Schematic illustration of proposed chemical reaction for Sodium Methyl Ester Sulfonate surfactant (Babu <i>et al.</i> , 2015).....	100
Figure 26: Mass spectrum of fatty acid methyl esters .....	102
Figure 27: Chromatogram from the GC-MS of the Fatty acid methyl esters .....	103
Figure 28: Mass spectrum of FAME derivatives: <i>Methyl (11R, 12R, 13S)-(Z)-12, 13-epoxy-11-methoxy-9-octadecenoate</i> .....	111
Figure 29: TGA curve of FAME and epoxidized FAME in O <sub>2</sub> .....	112
Figure 30: FTIR spectrum of SEMES.....	113
Figure 31: Infrared Spectrum of SDS.....	114
Figure 32: Infrared Spectrum of CTAB.....	114
Figure 33: Diagram of a typical four region isotherm (Behrens, 2013).....	124
Figure 34: A typical illustration of a spherical micelle (Holmberg <i>et al.</i> , 2003).....	126
Figure 35: IFT variation with surfactant concentration .....	127
Figure 36: XRD spectrum of silica .....	130
Figure 37: XRD spectrum of kaolin clay.....	131
Figure 38: XRD spectrum of synthetic ilmenite.....	131
Figure 39: XRD spectrum of alumina.....	132
Figure 40: Static adsorption of SDS, CTAB and SEMES onto synthetic kaolin clay.....	133
Figure 41: Static adsorption of SDS, CTAB and SEMES onto ilmenite .....	134
Figure 42: Static adsorption of SDS, CTAB and SEMES on silica.....	134
Figure 43: Comparison of static adsorption of SDS, CTAB and SEMES on alumina.....	135
Figure 44: The effect of different alkali concentrations on the adsorption isotherms of SDS, CTAB and SEMES on kaolin at ambient temperature .....	138
Figure 45: Adsorption Isotherm of SDS and CTAB at different NaCl salt concentrations at ambient temperature.....	139
Figure 46: Adsorption isotherm of SDS+CTAB and SEMES+CTAB systems with fixed salinity at ambient temperature.....	141
Figure 47: Thermal stability analysis for SDS and CTAB and SEMES as a function of temperature.....	144
Figure 48: Weight loss of SDS, CTAB and SEMES as a function of temperature .....	145
Figure 49: Mass spectrum of solvent-free EFAME at 25 °C.....	190
Figure 50: GC-MS Chromatogram of solvent-free EFAME at 25 °C .....	190
Figure 51: Mass spectrum of EFAME with toluene at 25 °C .....	191

Figure 52: GC-MS Chromatogram of EFAME with toluene at 25 °C .....	191
Figure 53: Mass spectrum of EFAME with propan-2-ol at 30 °C.....	191
Figure 54: GC-MS Chromatogram of EFAME with propan-2-ol at 30 °C .....	192
Figure 55: Mass spectrum of EFAME with n-hexane at 30 °C .....	192
Figure 56: GC-MS chromatogram of EFAME with n-hexane at 30 °C.....	192
Figure 57: Mass spectrum of EFAME with n-hexane at 50 °C .....	193
Figure 58: GC-MS chromatogram of EFAME with n-hexane at 50 °C.....	193
Figure 59: Mass spectrum of EFAME with propan-2-ol at 50 °C.....	193
Figure 60: GC-MS chromatogram of EFAME with propan-2-ol at 50 °C .....	194
Figure 61: Mass spectrum of EFAME with toluene at 50 °C .....	194
Figure 62: GC-MS chromatogram of EFAME with toluene at 50 °C.....	194

## LIST OF TABLES

Table 1: Types of Surfactant Flooding.....	19
Table 2: EDX analysis of the selected areas (weight %) of 80 CaO/20 Al <sub>2</sub> O <sub>3</sub> .....	74
Table 3: Catalysts Morphological Properties .....	76
Table 4: Analysis of fatty acid content of the waste oils.....	78
Table 5: Analysis of fatty acid content of waste sunflower oil .....	78
Table 6: Analysis of fatty acid content of waste palm oil .....	79
Table 7: Chemicals properties and their structures .....	96
Table 8: GC-MS Specifications.....	99
Table 9: Oven Temperature Program.....	99
Table 10: Percentage composition of Fatty acid methyl esters .....	101
Table 11: Composition of solvent-free epoxidized fatty acid methyl esters at 25 °C.....	104
Table 12: Composition of epoxidized fatty acid methyl esters produced with toluene at 25 °C ...	105
Table 13: Composition of epoxidized fatty acid methyl esters produced with propan-2-ol at 30 °C .....	106
Table 14: Composition of epoxidized fatty acid methyl esters produced with n-hexane at 30 °C	106
Table 15: Composition of epoxidized fatty acid methyl esters produced with toluene at 30 °C ...	107
Table 16: Composition of epoxidized fatty acid methyl esters produced with n-hexane at 50 °C	107
Table 17: Composition of epoxidized fatty acid methyl esters produced with propan-2-ol at 50 °C .....	107
Table 18: Composition of epoxidized fatty acid methyl esters with toluene at 50 °C .....	108
Table 19: BET characterization .....	129
Table 20: Atomic surface composition for the reservoir materials using ICP-OES analysis.....	129
Table 21: Parameters for Langmuir model fitted to synthetic kaolin clay data.....	142
Table 22: Parameters for Langmuir model fitted to silica data.....	142
Table 23: Parameters for Langmuir model fitted to alumina data .....	142
Table 24: Parameters for Langmuir model fitted to ilmenite data .....	142
Table 25: Parameters for Freundlich model fitted to synthetic kaolin clay data .....	143
Table 26: Parameters for Freundlich model fitted to silica data .....	143
Table 27: Parameters for Freundlich model fitted to alumina data.....	143
Table 28: Parameters for Freundlich model fitted to ilmenite data .....	143

Table 29: Titration readings for WPO .....	178
Table 30: Titration readings for WSO .....	179
Table 31: Effect of catalyst ratio on the FAME yield of WSO using 60% CaO/Al <sub>2</sub> O <sub>3</sub> at reaction temperature of 65 °C, methanol/oil molar ratio of 9:1 and reaction time of 4 hours and agitation speed of 800 rpm .....	182
Table 32: Effect of catalyst ratio on the FAME yield of WSO using 70% CaO/Al <sub>2</sub> O <sub>3</sub> at reaction temperature of 65 °C, methanol/oil molar ratio of 9:1 and reaction time of 4 hours and agitation speed of 800 rpm .....	183
Table 33: Effect of catalyst ratio on the FAME yield of WSO using 80% CaO/Al <sub>2</sub> O <sub>3</sub> at reaction temperature of 65 °C, methanol/oil molar ratio of 9:1 and reaction time of 4 hours and agitation speed of 800 rpm .....	184
Table 34: Effect of catalyst ratio on the FAME yield of WPO using 60% CaO/Al <sub>2</sub> O <sub>3</sub> at reaction temperature of 65 °C, methanol/oil molar ratio of 9:1 and reaction time of 4 hours and agitation speed of 800 rpm .....	185
Table 35: Effect of catalyst ratio on the FAME yield of WPO using 70% CaO/Al <sub>2</sub> O <sub>3</sub> at reaction temperature of 65 °C, methanol/oil molar ratio of 9:1 and reaction time of 4 hours and agitation speed of 800 rpm .....	186
Table 36: Effect of catalyst ratio on the FAME yield of WPO using 80% CaO/Al <sub>2</sub> O <sub>3</sub> at reaction temperature of 65 °C, methanol/oil molar ratio of 9:1 and reaction time of 4 hours and agitation speed of 800 rpm .....	187
Table 37: Effect of catalyst ratio on the FAME yield of WPO using 60% CaO/Al <sub>2</sub> O <sub>3</sub> at reaction temperature of 65 °C, methanol/oil molar ratio of 9:1 and reaction time of 4 hours and agitation speed of 800 rpm .....	188
Table 38: Effect of catalyst ratio on the FAME yield of WSO using 80% CaO/Al <sub>2</sub> O <sub>3</sub> at reaction temperature of 65 °C, methanol/oil molar ratio of 9:1 and reaction time of 4 hours and agitation speed of 800 rpm .....	188
Table 39: Total volumes of CTAB solutions prepared and initial CTAB concentrations measured in part per million before adsorption on kaolin powder .....	195
Table 40: CTAB equilibrium surfactant concentration after filtration .....	195
Table 41: Static adsorption density of CTAB at different concentrations on kaolin clay at in 2 vol% NaCl solution at ambient temperature .....	196
Table 42: Total volumes of SDS solutions prepared and initial SDS concentrations measured in part per million before adsorption on kaolin clay powder .....	197
Table 43: Residual concentrations and static adsorption density of SDS at different concentrations on kaolin clay in 2 vol % NaCl solution at ambient temperature .....	197

Table 44: Total volumes of CTAB solutions prepared and initial CTAB concentrations measured in part per million before adsorption on alumina .....	198
Table 49: Residual concentration and static adsorption density of CTAB at different concentrations on alumina in 2 vol. % NaCl solution at ambient temperature .....	199
Table 46: Total volumes of SDS solutions prepared and initial SDS concentrations measured in part per million before adsorption on alumina .....	199
Table 47: Residual concentrations and static adsorption density of SDS at different concentrations on alumina in 2 vol. % NaCl solution at ambient temperature .....	200
Table 48: Total volumes of CTAB solutions prepared and initial CTAB concentrations measured in part per million before adsorption on silica .....	200
Table 49: Residual CTAB concentrations and static adsorption density of CTAB at different concentrations on silica in 2 vol. % NaCl solution at ambient temperature.....	201
Table 50: Total volumes of SDS solutions prepared and initial SDS concentrations measured in part per million before adsorption on silica .....	201
Table 51: Residual SDS concentrations and static adsorption density of SDS at different concentrations on silica in 2 vol. % NaCl solution at ambient temperature.....	202
Table 52: Total volumes of CTAB solutions prepared and initial CTAB concentrations measured in part per million before adsorption on ilmenite.....	203
Table 53: Residual CTAB concentrations and static adsorption density of CTAB at different concentrations on ilmenite in 2 vol. % NaCl solution at ambient temperature .....	203
Table 54: Total volumes of SDS solutions prepared and initial SDS concentrations measured in part per million before adsorption on ilmenite .....	204
Table 55: Residual SDS concentrations and static adsorption density of SDS at different concentrations on ilmenite in 2 wt. % NaCl solution at ambient temperature .....	204
Table 56: The effect of different alkali concentrations on the adsorption isotherms of SDS.....	204
Table 57: The effect of different alkali concentrations on the adsorption isotherms of CTAB.....	205
Table 58: The effect of different alkali concentrations on the adsorption isotherms of SEMES..	205
Table 59: The effect of different salt concentrations on the adsorption isotherms of SDS .....	205
Table 60: The effect of different salt concentrations on the adsorption isotherms of CTAB .....	206
Table 61: Adsorption data for the adsorption isotherm of SDS+CTAB system with fixed salinity .....	206
Table 62: Adsorption data for the adsorption isotherm of SEMES+CTAB system with fixed salinity .....	206



## NOMENCLATURE

<u>Symbol</u>	<u>Description</u>	<u>Unit</u>
$v$	Darcy velocity	m/s or cm/s
$\lambda$	Mobility of a fluid	-
$k$	Effective permeability of the displaced fluid	m <sup>2</sup> or mD
$\theta$	Contact angle	Degree
$\mu$	Fluid viscosity	cp
$i$	Oil, water or gas	-
$\sigma$	Interfacial tension	N/m or mN/m
$\omega$	Rotational velocity	rpm
$\sigma_{ow}$	Interfacial tension between the oil and water phases	mN/m
$\sigma_{os}$	surface energy between the oil phase and substrate	
$\sigma_{ws}$	surface energy between the water and substrate	
$\rho$	Density	g/cm <sup>3</sup>
$r$	Radius of the cylindrical drop	Cm
$A_1$	Area under the secondary water-drainage curve	
$A_2$	Area under the imbibition curve falling below the zero- $P_c$ axis	
$d_{BET}$	Average crystallite diameter equivalent to the volume-weighted	m or cm
$HA_w$	Acid in aqueous phase	-
$HA_o$	Acid in oil phase	-
$2H$	Curvature of interface	-
$M$	Mobility ratio	m <sup>3</sup> .s/kg / m <sup>3</sup> .s/kg
$N_c$	Capillary number	-
$N_w$	Wettability number	
$P_c$	Capillary pressure	dynes/cm <sup>3</sup>
$P_w$	Pressure of the wetting phase at the interface (water)	Dynes
$P_{NW}$	Pressure of the non-wetting phase at the interface (oil)	Dynes
$\Delta\rho$	Change in density between the rotational velocity of the drop and the drop	g/cm <sup>3</sup>
$\Delta P/L$	Pressure gradient across a distance	Pa/m
$p_A$ and $p_B$	Bulk phase pressures	

$S_g$	BET surface area	$\text{cm}^2/\text{g}$
$S_{or}$	Residual Oil Saturation	%
$\Delta S_{ws}$	Increase in water saturation during water spontaneous imbibition	%
$\Delta S_{os}$	Increase in oil saturation during oil spontaneous imbibition	%
$\Delta S_{wt}$	Total increase in water saturation during spontaneous and forced displacement of oil	%
$S_{wi}$	Initial water saturation	%
$\Delta S_{ot}$	Total increase in oil saturation during spontaneous and forced imbibition of water	%

## ABBREVIATIONS

<b>AS</b>	Alkaline-Surfactant
<b>ASP</b>	Alkaline-Surfactant-Polymer
<b>AAS</b>	Atomic Adsorption Spectrophotometry
<b>BET</b>	Brunauer-Emmett-Teller
<b>bb1</b>	Barrel
<b>EOR</b>	Enhanced Oil Recovery
<b>IOR</b>	Improved Oil Recovery
<b>CEOR</b>	Chemical Enhanced Oil Recovery
<b>CTAB</b>	Cetyltrimethylammonia bromide
<b>CMC</b>	Critical Micelle Concentration
<b>FAME</b>	Fatty Methyl Ester
<b>FFA</b>	Free Fatty Acid
<b>FCM</b>	First Contact Miscible
<b>GC-MS</b>	Gas Chromatography-Mass Spectrometry
<b>GC-FID</b>	Gas-Chromatography-Flame Ionization Detector
<b>HAPAM</b>	Hydrophobically Modified Associating Polyacrylamide
<b>IFT</b>	Interfacial Tension
<b>kV</b>	Kilovolts
<b>LPG</b>	Liquefied Petroleum gas
<b>MEOR</b>	Microbial Enhanced Oil Recovery
<b>OOIP</b>	Original Oil-in-Place
<b>OHIP</b>	Original Hydrocarbon in Place
<b>PFA</b>	Performic Acid
<b>PAM</b>	Polyacrylamides
<b>ROIP</b>	Residual Oil-in-Place
<b>XRD</b>	X-Ray Diffraction
<b>SF</b>	Surfactant
<b>SEM-EDX</b>	Scanning Electron Microscopy–Energy Dispersive X-ray Spectroscopy
<b>SDS</b>	Sodium Dodecyl Sulfate
<b>SEMES</b>	Sodium Epoxidized Methyl Ester Sulfonate
<b>TCD</b>	Thermal Conductivity Detector
<b>TGA</b>	Thermo-gravimetric Analysis

<b>TEM</b>	Transmission Electron Microscopy
<b>TPR</b>	Temperature Programmed Reduction
<b>USBM</b>	United States Bureau of Mines
<b>W/O, O/W</b>	Water-Oil, Oil-Water contact
<b>WPO</b>	Waste Palm Oil
<b>WSO</b>	Waste Sunflower Oil
<b>WVO</b>	Waste Vegetable Oil

## INTRODUCTION

---

*This chapter deals with the introduction to the study in which the general background of the study, the problem statement, aims and objectives, research questions, research approach and scope of the study are outlined. The basic concepts of Enhanced Oil Recovery (EOR), its mechanisms, and the common chemical EOR techniques including surfactant, polymer, alkaline-surfactant and alkaline-surfactant-polymer floodings are also briefly presented.*

### 1.1 GENERAL BACKGROUND

Petroleum undoubtedly currently plays a major role in the world economy. Humans depend on it for energy and transportation. There has not been found a single energy supply yet to substitute crude oil that is extensively integrated. To meet the high demand of energy there is a major need to produce more oil. About 30-60% of the Original Oil in Place (OOIP) can be recovered through primary and secondary recovery methods (Elraies *et al.*, 2011a). The remaining oil droplets are trapped in reservoir pores owing to the surface and high interfacial forces (capillary forces), viscosity forces and reservoir heterogeneities that results in poor dislocation efficiency (Mohan, 2009; Wang and Mohanty, 2013). To overcome this problem and to meet the high demand for oil, Chemical Enhanced Oil Recovery (CEOR) techniques have vastly been developed as a significant way of recovering the remaining oil in addition to reducing the chemical cost relative to crude oil prices (Liu, 2008).

Alkaline-Surfactant-Polymer (ASP) flooding has demonstrated significant potential as an EOR method. It generally involves the injection of fluids containing surfactants, alkalis and polymers into the reservoir. As a result, surfactants structures have been extensively researched and improved to suit a much wider range of reservoir conditions and oil properties. With increasingly harsh conditions (salinity, oil properties, water hardness, reservoir temperature and pressure), there is an ever-increasing need for new surfactants for efficient oil recovery. When in contact with the trapped crude oil, surfactants are able to reduce the Interfacial Tension (IFT) between the oil and the injected water to ultra-low levels which leads to the mobilization of more crude oil, and, therefore improve oil recovery (Gan-Zuo *et al.*, 2000). Polymers are added to the process to improve and control the mobility ratio of Water-Oil (W/O) as well as increase the

injected water viscosity (Sydansk, 2006). Alkaline chemicals are also injected to reduce surfactant retention, increase pH and alter the wettability of reservoir rock in order to create favourable conditions for oil production increase. In this process, these chemicals are combined for effective and efficient mobilisation of trapped crude droplets. ASP flooding can be applied as an improved water flooding method which uses a large slug with low surfactant concentration making it a significant technique for enhancement of oil recovery (Pingping *et al.*, 2009). The production rates of the largest oilfields in the world are all declining past plateau production, the challenge is to come up with EOR processes which ensure a cost-effective tail end production from these fields. Many field applications of ASP have resulted in significant recovery of residual oils. For instance in Daqing oil field in China, an additional oil recovery of more than 20% was achieved (Yang *et al.*, 2003). Pitts *et al.* (2006) and Qiao *et al.* (2000) also reported an increase of 24% of the OOIP in Karamay oil field in China and of 10% in the Tanner oil field.

One of the biggest problems associated with the ASP process is that surfactants are toxic to marine organisms and the costal environment on top of being expensive, and so the search for environmentally friendly and cost effective formulations is attracting growing interest (Pitts *et al.*, 2006). Therefore, this thesis focuses on the formulation of a sulfonated surfactant for the ASP process from waste vegetable oils. The goal is to synthesize a cheaper and less hazardous surfactant that will be both economical and effective for IFT reduction as well as reservoir rock wettability alteration for a significant improvement in oil recovery.

## 1.2 ENHANCED OIL RECOVERY

The life of crude oil undergoes three different stages where various methods are used to maintain oil production at desirable levels. Primary recovery is when oil is produced by the natural pressure in the reservoir. In the second stage or secondary recovery, normally gas or water is injected into the production zone to maintain reservoir pressure and hence sweep oil from the reservoir to the well bore. The main purpose of these methods is to force oil into the wellhead where it can easily flow to the surface. Methods used during the third stage are usually known as Enhanced Oil Recovery (EOR). EOR is the recovery of oil that is trapped in the reservoir rock after primary and secondary recovery methods are either ineffective or no longer economical (Sheng, 2011). Currently, many EOR techniques are used to improve oil extraction effectiveness significantly. Depending on the producing life of a reservoir, oil recovery can be classified into three important stages (Emegwalu, 2010):

- Primary recovery
- Secondary recovery
- Tertiary recovery

**Primary recovery** refers to the first oil out (the "easy oil") by natural forces prevailing in the reservoir; no additional energy is required to produce the oil or gas (Gan-Zuo *et al.*, 2000). Here, the oil inside the reservoir will be driven to the surface through the well only by pressure. The pressure differences within the reservoir cause the oil to flow from the zones of high pressure to the zones of lower pressure (Emegwalu, 2010). Meaning that, the trapped oil flows naturally to the surface through the drilled well, only by the force of pressure differences and sometimes by artificial lift through a wellbore. About 10-19% of the Original Oil in Place (OOIP) is recovered (Liu, 2008).

**Secondary recovery** is a physical technique, used after primary recovery when the underground pressure is insufficient to move the remaining oil. This method involves the use of artificial energy into the reservoir through one wellbore and production of crude oil and/or gas from another wellbore (Emegwalu, 2010). External fluids such as water and/ gas or gas-water combined (process known as water-alternating gas injection) are injected into the reservoir to increase (or maintain) the pressure and force the trapped oil to flow to the production well (Holmberg *et al.*, 2003). The recovery is between 25-45% of OOIP (Mohan, 2009)

After both primary and secondary recovery techniques, there is still a percentage of the Original Oil in Place (OOIP). The **tertiary recovery** makes use of miscible gases, chemical fluids and/or heat to reduce viscosity and displace the remaining oil after the secondary recovery process becomes uneconomical (Schramm, 2012). If the crude oil is too viscous, it will not flow at economic rates under natural forces, so primary and secondary productions are of no use. For this reason; thermal processes might have to be used as the only way to recover a considerable quantity of oil. As a result, the tertiary process becomes the 1<sup>st</sup> stage and the term EOR or IOR (Improved Oil Recovery) is used to replace it. IOR usually includes taking measures during, not after the primary or secondary steps, to enhance oil recovery. Tertiary recovery is not a synonym for EOR and should not be used as such. This is because, some EOR techniques functions reasonably well as either secondary or tertiary processes, like CO<sub>2</sub> flooding whereas others, such as steam, or polymer flooding are more successful as enhanced secondary processes.

There is over 50% of residual oil still trapped in reservoirs, where facilities and wells are already in use. The Department of Energy, in Saskatchewan (Canada) estimated that improvement of EOR processes applicable to thin, unconsolidated sand reservoirs could signify the recovery of about 4 Billion bbls of heavy oil (Mohan, 2009). Production of oil from EOR developments keep on supplying an increase percentage of the world's oil. About 3% of the global production originates from EOR (Pope, 2011). Hence, the need for the development of EOR is clear and undeniable.

EOR techniques involve the injection of gas, chemical fluid/fluids and energy of some sort into a reservoir (Arihara *et al.*, 2006). The injected fluids and processes act as enhancement to the natural energy present in the reservoir which creates favourable conditions for high oil recovery. The conditions include lowering the IFT, reducing the viscosity, alter wettability, adjust the driving fluid mobility, alter the permeability of selected zones, change fluid properties or stabilize pressure gradients necessary to overcome retaining forces (Elraies *et al.*, 2011). These changes are caused by physical and chemical mechanisms and by the production or injection of thermal energy. Enhanced Oil Recovery is divided into five main categories (Maheshwari, 2011):

- Chemical Processes
- Miscible Processes
- Microbial EOR Processes
- Thermal Processes

**Chemical Processes** aims to reduce the IFT between the displacing fluid (usually water) and oil as well as cause an alteration in the wettability of the reservoir rock (Flaaten *et al.*, 2008). It involves the injection of a solution containing surfactant and a polymer or alkali into the reservoir, leading to the displacement of more crude oil. Surfactants and polymer flooding have demonstrated potential for a higher EOR than any other technique (Wang *et al.*, 2001). The surfactant injection can only be justified when oil prices are relatively high and if the residual oil saturation after water-flooding process is high. This is because surfactants are expensive.

The main purpose of the **miscible process** is to displace oil with a fluid that is miscible with the oil in all proportions (Zhang *et al.*, 2005). This will reduce the IFT between oil and water consequently leading to better oil sweep. Two major variations are distinguished in this process. One is the first-contact-miscible (FCM) process where the injected fluid becomes directly miscible with the residual oil immediately on contact (Liu, 2008). In this process fluids such as liquefied petroleum gases (LPG) and alcohols are injected. The other is the Multiple-Contact, or dynamic, miscible process where miscibility comes from modifying the composition of the injected fluid as it goes through the reservoir (Liu, 2008). An example of this process is the injection of CO<sub>2</sub>, methane, inert fluids into the reservoir. This method is especially used in low permeability, high pressure and lighter oil.

**Thermal Recovery** is the most attractive method for maximization of the value and reserves from heavy oil assets (Greaser, 2001). It involves making use of thermal energy to recover crude oil. A hot phase like steam, hot water or a combustible gas is injected into the reservoir to increase the temperature of the trapped oil and gas thus reducing the viscosity of the crude oil (Liu, 2008). This causes the oil to flow much easier to the



production well by reducing the pressure and its resistance to flow. Thermal methods are not as advantageous for light crudes as for heavy crudes where the viscosity reduction is less.

**Microbial Enhanced Oil Recovery (MEOR)** refers to the injection of microorganisms or selected natural bacteria down injection wells. The microorganisms metabolically produce products such as acids, surfactants and certain gases (carbon dioxide and hydrogen) (Wang *et al.*, 2001). The products act upon the oil by facilitating its movement through the reservoir to the production wells. There are two methods which make use of microbial techniques to enhance oil production: Cyclic microbial recovery and microbial flooding.

### 1.3 CHEMICAL ENHANCED OIL RECOVERY

Deployment of Chemical Enhanced Oil Recovery (CEOR) processes peaked during the 1980's and most active, particularly in the United States, around 1986, which coincided with the period of high oil prices. Attention on CEOR methods have increased over the last few years due to the high enhancement in oil recovery provided when compared to conventional water-flooding. These methods entail using chemicals such as surfactant, alkali, and polymer for improvement in the recovery of oil. Surfactants lower the IFT between oil and brine by reducing the capillary forces which makes easier for the oil to flow throughout the reservoir, and more oil can therefore be mobilized (Emegwalu, 2010). Alkali reacts with acidic compounds in the oil to generate *in-situ* surfactants which together with the injected surfactant are able to reduce the IFT between water and oil even more.

A polymer, preferably water soluble, is usually injected either on its own or mixed with the alkali surfactant solution to achieve a more viscous phase of the injected solution (Guo, 2000). This serves to improve the mobility ratio of the process and to achieve higher oil rates of recovery. There are other CEOR processes including alkaline flooding, alkali-surfactant flooding, micelles flooding, alkali-surfactant-polymer (ASP) and others where alcohols are introduced. In alkaline flooding, alkaline chemicals are pumped into the reservoir, where they react with certain components in the oil to generate surfactants *in-situ* (Flaaten *et al.*, 2008). The effectiveness of the CEOR depends on the viscosities of the liquid, interfacial tensions, relative permeability, wettability, and capillary pressures (Zhang *et al.*, 2005). Even if the injected chemicals come in contact with all the oil, some oil droplets would still be trapped in the reservoir pores. This is due to capillary forces, high interfacial tension (IFT) between water and oil.

- **Surfactant Flooding** - is a very promising EOR method. After continuing water-flooding process, a percentage of crude oil is left trapped in the reservoir owing to high

capillary forces. To mobilize the remaining oil, surfactant agents are pumped into the reservoir to improve oil recovery by reducing the IFT between water and oil (Emegwalu, 2010). An oil bank will start to flow, gathering together any remaining oil in front. The coalescence of these oil droplets causes a local increase in oil saturation.

- **Alkaline-Surfactant Flooding** - is a process where a slug mixture of alkali and synthetic surfactant are injected into the reservoir pores, followed by chase water (Chang *et al.*, 2006). Combining the two chemicals is more effective than injecting them individually. Surfactant is added to the mixture to reduce the IFT between oil and water, resulting in more trapped crude oil being mobilized. The alkali is a crucial component when it comes to decreasing the adsorption of the surfactant displacement through the reservoir rock (Maheshwari, 2011). Furthermore, the injected alkali reacts with the naphthenic acid in the crude oil to generate soap *in-situ*. As alkali is reasonably priced, this facilitates the reduction of the overall cost of the process.

- **Polymer Flooding** - is another EOR method where polymer solutions are often used to increase oil recovery by raising the viscosity of the injected water and decreasing the water/oil (W/O) mobility ratio (Sadikhzadeh, 2006). During this process, a polymer (which is soluble in water) is added to the injected water containing surfactant to increase the viscosity of water and maintain mobility control and reduce the effective permeability to water depending on the type of polymer used (Sydansk, 2006). The success of polymer flooding depends on reservoir temperature and reservoir water chemical properties (Pope, 2011). The mostly used types of polymers include polyacrylamides (PAM) and biopolymers.

- **Alkaline-Surfactant-Polymer Flooding** - This technique combines three processes that is, alkaline, surfactant and polymer flooding where the three slugs are used sequentially. The three fluids can be mixed simultaneously and injected as a single slug. ASP flood uses chemicals such as a surfactant alkali ( $\text{Na}_2\text{CO}_3$  or  $\text{NaOH}$ ), and a polymer. The main objective of this process is to reduce the large consumption of chemicals per unit volume of oil needed and consequently a decrease in cost (Gan-Zuo *et al.*, 2000).

#### 1.4 SURFACTANT PRODUCTION FROM SUSTAINABLE FEEDSTOCK

In the 2000s, the majority of field tests on surfactant-polymer and alkaline-surfactant-polymer flooding revealed that a higher oil recovery factor was achieved compared with those in the late 1970s and 1980s (Elraies & Tan, 2003). Upgrading in the chemicals functionality and an improved comprehension of the process schemes are the principal reasons for this accomplishment. This field pilot test is an indication that the use of surfactant for SP and ASP flooding and its disparities can be in principle efficacious.

Since then surfactants have been considered as good enhanced oil recovery agents due to the fact that they can considerably reduce the interfacial tension (IFT) and modify wetting properties. Nevertheless, the principal issue related to the application of chemical EOR methods still is the high cost of raw materials as well as the costs involved during the production of surfactants. In some instances the oil recovered by these processes is reasonably priced in addition to the technical risks which are quite high compared to the price of oil (Austad & Milter, 2000).

Currently, several works have been conducted to develop cost-effective surfactants because the existing commercial surfactants are mostly produced from slowly degradable compounds (from petrochemicals). In some instances the products from their degradation can be, detrimental to the environment or to humans (Gregorio, 2005; Li *et al.*, 2000; Wuest *et al.*, 1994). Additionally, the price of commercial surfactants is a bottleneck for their use in CEOR. Therefore, to cut down on the surfactant production cost and to satisfy EOR requirements, much attention is being giving to agriculturally originated oleochemicals (or natural oils) as substitute source of raw materials for surfactants manufacturing. The most popular oils used as oleochemical feedstock to obtain fatty alcohol and esters are coconut and soybean oils (Elraies *et al.*, 2009). In contrast, these surfactants are produced using edible vegetable oils and in a long-term it will compete with the food supply. Furthermore, as the cost and demand of edible oils tend to rise, the cost of their derivative surfactant increases as well (Gregorio, 2005).

Consequently, it is essential to use non-edible or waste vegetable oils as alternative feedstock for the production of environmentally friendly and renewable surfactants which in turn will minimize surfactant production cost. Non-edible oil sources such as *Jatropha curcas* is quite difficult to be cultivated in South Africa, however, large amounts of waste vegetable oil (WVO) are generated by homes and restaurants at an increasing rate as a result of massive growth in population as well as food consumption. It is estimated that South Africa on its own, produces approximately 28 million tons of WVO annually, which requires an economical and eco-friendly disposal method, such as its use as feedstock for bio-based materials production (Yaakob *et al.*, 2013).

Processes involved in the production of surfactants entails production of alkyl esters (majorly methyl or ethyl esters) using either homogeneous or heterogeneous catalysis. This is further subjected to epoxidation reaction to reduce FAME double-bonds and obtain more stable structures, epoxides. Finally, the sulfonated surfactant is produced using sulfonating agents such as sulfuric acid, oleum or chlorosulphonic acid. In this work the intention is to produce FAME from waste vegetable oils to promote the production of bio-based surfactants.

## **1.5 PROBLEM STATEMENT**

With the discoveries of new fields declining and the cost of exploration and development skyrocketing while the cumulative demand for crude oil is growing, there is need to recover more of the residual trapped crude oil in matured and abandoned wells. More effective EOR methods that ensure an economical tail end (trapped oil) production from these oil fields are being continuously researched. Alkaline-Surfactant-Polymer flooding (ASP) has been employed in the oil industry for enhancement of oil recovery through the reduction of interfacial tension (IFT) between oil and water, reservoir rock wettability alteration and an increase in mobility ratio. However, commercial surfactants used in this process are usually expensive, toxic and required in high quantities which renders this technique uneconomical. Thus, the need for a less hazardous and cost effective but high performance surfactant formulation for an efficient oil recovery is required. This study will investigate the production of an anionic surfactant from cheap waste vegetable oils using heterogeneous catalysis processes and assess its performance for application under extreme reservoir conditions.

## **1.6 AIM AND OBJECTIVES OF THE STUDY**

The project seeks to develop a cost effective process to produce surfactant from sustainable sources. This will be used in petroleum industry to enhance oil recovery from matured oil fields at declining production phase. The research focused specifically on formulating a natural sulfonate surfactant and investigating its effectiveness for application in extreme petroleum reservoirs. Therefore, the main aim of this study is to synthesize a relatively inexpensive and non-hazardous but high performance surfactant for the ASP flooding. To realize this aim, the study will investigate the following specific objectives:

- a) Optimizing the process conditions for FAME production from high free fatty acid waste vegetable oils, focusing mainly on bi-functional catalysts formulation and loading.
- b) Optimizing the epoxidation stage process conditions to minimize the amount of poly-unsaturated fatty acids using different solvents and reaction temperatures.
- c) Investigate the thermal behavior of the surfactant at typical reservoir temperature.
- d) Investigate the adsorption characteristics of the surfactant on various reservoir rock materials to quantify loss during flooding.

## **1.7 RESEARCH QUESTIONS**

- a) What are the process conditions that will produce a very high yield of Fatty Acid Methyl Ester (FAME) from oils with high FFA content?

- b) Will the use of solvent(s) during epoxidation of FAME influence the poly-unsaturated fatty acids content?
- c) Will the surfactant produced be suitable for high reservoir temperature operations?
- d) For which types of reservoirs materials will the synthesized surfactant be suitable and economical?

## 1.8 SCOPE OF THE STUDY

This thesis will focus on the optimization of the parameters that affect the yield of FAME from the waste vegetable oils. The effects of the morphological properties of the acid/basic solid catalysts used will not be investigated. The epoxidation and sulfonation steps for the surfactant production will be carried out using the approach of Campanella *et al.* (2008) and Elraies *et al.* (2009) respectively. As regards the performance of the surfactant in real EOR field operations, the thermal behaviour and adsorption unto reservoir rocks will be used for comparison with commercial surfactants.

## 1.9 EXPECTED CONTRIBUTIONS TO KNOWLEDGE

A steady and sustainable supply of energy sources, particularly, crude oil and natural gas is of enormous importance to economy and national security. More than half of the Original Oil in Place (OOIP) remains trapped in the reservoirs, after conventional production operations. This is attributed to poor sweep and to oil droplets being trapped by capillary forces due to high IFT between oil and water. Enhanced oil recovery techniques generally employ thermal, chemical, miscible and immiscible gas displacement and even microbial to produce this *hard-to-recover* oils in older fields. The chemical EOR method of alkaline-surfactant-polymer flooding has recorded as much as 68% improved recovery from abandoned and depleted oilfield, particularly field past its peak production stage. CEOR techniques have vastly been developed as a significant way of recovering the remaining oil in addition to reducing the chemical cost relative to crude oil prices (Liu, 2008).

Surfactant flooding is widely used as an EOR method, which is performed by injecting the surfactant and typically co-surfactants together with alkali and/or polymer into the reservoir. With increasingly harsh conditions encountered in reservoirs, there is an ever-increasing need for better performing surfactants for efficient oil recovery. This project is aimed at formulating a less hazardous surfactant from waste vegetable oils that will be economical and effective for interfacial tension reduction, viscosity control, minimal reservoir adsorption, and wettability alteration as well as able to withstand high pressures and temperatures.

South Africa though a fringe player in crude oil production has substantial natural gas deposits and a huge deposit of shale gas in the Karoo. There is therefore the need to develop local and home grown expertise in petroleum production and processing technologies. The surfactant produced has potential use in formulation of drilling fluids and possibly hydraulic fracturing fluids for shale gas production.

## 1.10 THESIS OUTLINE

This study is divided into 6 chapters and an appendix. **Chapter 1** gives the general background and motivation of the research project. The objectives of the thesis are concisely outlined. It also describes and introduces Enhanced Oil Recovery (EOR) processes and some chemical recovery mechanisms are reviewed, especially for the surfactant, alkaline-surfactant, alkaline-surfactant-polymer and polymer flooding systems.

**Chapter 2** gives emphasis to the use of surfactant, alkali, and polymer for the improvement in oil recovery over conventional water-flooding. Surfactant, alkaline and polymer flooding and their general classification and chemistry will be discussed. A detailed review of surfactant flooding as well as ASP techniques will be given in order to understand the status quo with respect to this subject.

**Chapter 3** succinctly reviews and discusses the production of Fatty Acid Methyl Esters (FAME) produced via esterification and transesterification of non-edible, edible and waste vegetable oils via homogeneous, heterogeneous, enzymatic, ultrasonic, supercritical catalytic processes. The theoretical background and usage of solid acidic and base catalysts is explained and reported in brief individually. The aspects of simultaneous esterification-transesterification using bifunctional heterogeneous catalysts are also reviewed. Parameters affecting transesterification reaction are explained based on the most recent developments. Methods for catalysts preparation and its characterization are presented here. It presents the methods of preparation and the characterization techniques used for the solid catalysts. It also discusses the synthesis, characterization and testing of  $\text{CaO}/\text{Al}_2\text{O}_3$  bifunctional heterogeneous catalysts for the simultaneous esterification and transesterification of high free fatty acid oils (waste palm oil and waste sunflower oil) into FAME. The impact of the different catalysts ratios for transesterification reaction of waste vegetable oils containing high free fatty acids was also studied and results presented in this chapter. Sample analyses were done using Gas Chromatograph-Flame Ionisation Detector (GC-FID) and a Gas Chromatograph-Mass Spectrometer (GC-MS) techniques.

In **Chapter 4** the process for the epoxidation of FAME for surfactant production is presented. Peroxyformic acid prepared *in-situ* was employed for epoxidation of the unsaturated double bonds on the chains of the methyl esters in the absence and presence of different solvents and temperatures. A summary of the sulfonation reaction and its various sulfonating agents is given. The methods and consequential results on epoxidation of FAME and sulfonation of Epoxy Methyl Esters are also presented herein.

**Chapter 5** focuses on the chemical composition of the surfactant and its physical and chemical properties which includes its capacity to lower the interfacial tension (IFT) between the oil and water, critical micelle concentration (CMC) and thermal stability at reservoir temperatures. It lays out the adsorption of surfactants onto different solid mineral surfaces. It also incorporates a description of the experimental procedure and materials used. Experimental results on the characterization of the surfactants are discussed.

**Chapter 6** is devoted to conclusions of this thesis where the results are summarized and also recommendations for future research work. This chapter is followed by all the references that have been combined into a list.

## CURRENT TRENDS IN CHEMICAL ENHANCED OIL RECOVERY TECHNIQUES

---

*The present chapter re-examines the improvement of CEOR techniques over the last few decades and identifies the gaps existing in the literature which justify the need for this study. The first section defines some basic concepts: mobility ratio, capillary number, capillary pressure, IFT as well as wettability. The second describes the role of surfactants in improving oil recovery. The second section explains how alkalis generate emulsifying agents in-situ and support EOR. The third section reviews the use of polymers in the petroleum industry for providing a better mobility control to the displacement process. In the fourth section, the benefit of combining all the chemicals for better EOR is also discussed. This process is usually referred to as the ASP (Alkali Surfactant Polymer) process where microemulsions, with ultra-low interfacial tensions are generated.*

### 2. OVERVIEW

The largest amount of the oil produced currently comes from older fields. Enhancing oil production from the matured and aging resources is therefore a major concern for oil companies and the government (Zhang *et al.*, 2006). This is because sometimes production does not meet the growing energy demand. Additionally, the production from matured fields are declining at a rate faster than the discoveries and production of new fields needed to maintain or increase the production rate to meet the energy demand recently (Zhang *et al.*, 2005). Therefore, money, effort and time are being put towards maximizing oil extraction from maturing reservoir systems and other tight rock resources. There still remains, however, a very large amount of known residual oil resources in countless "usual reservoirs". Secondary recovery techniques, such as water-flooding, have been demonstrating their significance in recovering incremental oil for decades in reservoirs all over the world (Zhang *et al.*, 2005; Liu *et al.*, 2008).

Currently, with the growing demand for more effective EOR methods, surfactant, ASP and polymer flooding techniques are progressively making their mark in extracting more crude oil from maturing fields; with the ASP flooding being the most cost effective technique. ASP chemical flooding, which includes the injection of alkalis, surfactant and



polymer simultaneously into the reservoir, is considered a promising EOR technique due to the fact that it employs the synergy of the three techniques and it has been applied in a limited number of fields around the world (for example China, India, Alberta and Wyoming, etc.) for over 20 years.

## 2.1 GENERAL CONCEPTS OF ENHANCED OIL RECOVERY

The principal purpose of all EOR methods is to increase the volumetric sweep efficiency and to improve the displacement efficiency, when compared to conventional water-flooding. This is achieved by causing a reduction in the mobility ratio or the capillary forces (Liu, 2008).

### 2.1.1 Improvement of the mobility ratio

Mobility ratio is described as the ratio between mobility of displaced fluid and displacing fluid where  $\lambda$  is the mobility (Liu, 2008). It is represented in Equation 1:

$$\mathbf{M} = \frac{\lambda_{\text{displacing}}}{\lambda_{\text{displaced}}} \quad (1)$$

Mobility of a fluid refers to how easy the fluid flows in a porous media (Arihara *et al.*, 2006; Liu, 2008). The mobility of a fluid is described as the ratio of the effective permeability to the viscosity of the fluid. The mobility ( $\lambda$ ) of a fluid is shown in Equation 2 (Emegwalu, 2010):

$$\lambda = k_i / \mu_i \quad (2)$$

where  $k$  represents effective permeability ( $\text{m}^2$ ),  $\mu$  is the fluid viscosity ( $\text{kg/m. s}$  or  $\text{cp}$ ) and  $i$  represents oil, water or gas.

For a more effective displacement,  $M$  has to be less than 1. The mobility ratio can be improved by increasing the effective permeability to oil, decreasing the effective permeability to the displacing fluid, reducing the viscosity of the displaced fluid or by increasing the viscosity of the displaced fluid (Sheng, 2011). Polymers are added to the injected fluid to increase the viscosity of oil while decreasing the relative permeability of water. This will lead to an improved sweep efficiency compare to water flooding (Sadikhzadeh, 2006).

### 2.1.2 Increasing the Capillary Number

Capillary forces have a huge effect on oil recovery technique effectiveness, varying from non-fractured to fractured reservoirs. During water-flooding in a non-fractured reservoir, strong capillary forces will trap oil and cause quite high residual oil saturation (Liu, 2008; Sheng, 2011). A decrease in the oil-water IFT remobilizes more residual oil, which is the preferred condition. Capillary pressure is described as the pressure of the non-wetting fluid minus the pressure of the wetting fluid (Berger and Lee, 2006). Water is considered as a wetting phase in oil/water systems and represented by Equation 3 where  $P_c$  is the capillary pressure,  $P_w$  is the pressure of the wetting phase at the interface (water) and  $P_{NW}$  is the pressure of the non-wetting phase at the interface (oil) (Liu, 2008)

$$P_c = P_o - P_w = P_{NW} - P_w \quad (3)$$

The forces acting on an entrapped droplet of oil within a porous media is expressed by the capillary number ( $N_c$ ). It is the dimensionless ratio between the capillary and viscous forces (Berger & Lee, 2006; Liu, 2008). The capillary number is a function of the Darcy velocity ( $v$ ; m/s), the viscosity ( $\mu$ ; cp) of the displaced fluid and the interfacial tension ( $\sigma$ ; N/m) between the displacing and the displaced fluids (Berger & Lee, 2006).

$$N_c = \frac{\mu v}{\sigma} \quad \text{or} \quad \frac{k\Delta P}{\sigma L} \quad (4)$$

where  $\Delta P/L$  is the pressure gradient (Pa/m) across a distance  $L$  and  $k$  is the effective permeability (mD) to the displaced fluid (Berger & Lee, 2006).

Figure 1 shows that the residual oil saturation reduces with an increase in capillary number.

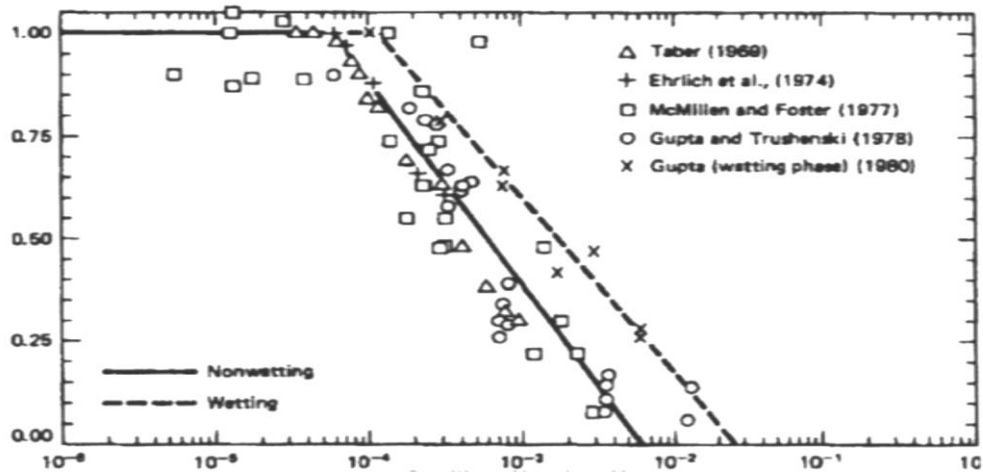


**Figure 1:** Normalized residual saturation of the oil vs capillary number ( $N_c$ ) (Sheng, 2011)

This trend is beneficial to high recovery efficiency due to the fact that large capillary number gives smaller residual oil fractions. The most reasonable manner to increase the  $N_c$  is to reduce the IFT. On the other hand, for a significant residual oil to be generated, the critical value of  $\Delta P/L\sigma$  has to be exceeded by an increase in the rate of water flooding (Berger & Lee, 2006; Zhou & Liu, 2005). Therefore, the aim of the chemical process is to decrease the interfacial tension so that the recovery performance will be improved (Sheng, 2011).

### 2.1.3 Interfacial Tension

Interfacial tension (IFT) is defined as the force per unit length parallel to the interface which is perpendicular to the local density and concentration gradient (Rosen *et al.*, 2005). It is also described as the extra free energy per unit area in the thermodynamic approach. Both descriptions, force per unit length and energy per unit area, are dimensionally alike. The IFT can be altered by salinity and temperature. The use of surfactants can produce a considerable decrease in IFT (Curbelo *et al.*, 2007). The Young-Laplace Equation (5) is used to determine the IFT by different methods such as the sessile bubble, spinning drop or pendant bubble (Rosen *et al.*, 2005).

$$p_A - p_B = -2H\sigma \quad (5)$$

where  $p_A$  and  $p_B$  are the two bulk phase pressures,  $\sigma$  is the interfacial tension between two liquid phases and  $2H$  the mean curvature of interface.

### 2.1.4 Wettability

Wettability in the petroleum industry is defined as the ability of one fluid to spread or adhere to the reservoir rock surface in the presence of another immiscible fluid (Spinler *et al.*, 2002). In general, most reservoirs are oil-wet, due to the long term presence of oil and at the prevailing elevated pressures and temperatures (Liu *et al.*, 2008). The homogenous wettability can be classified as water-wet ( $\theta < 70^\circ$ ), intermediate-wet ( $70^\circ < \theta < 115^\circ$ ), oil-wet ( $\theta > 115^\circ$ ) as well as mixed-wet state (Agbalaka *et al.*, 2008). The techniques being employed to measure the wettability of a reservoir system includes the contact angle test, Amott imbibition and the United States Bureau of Mines (USBM) tests. The most used however is the contact angle ( $\theta$ ) tests through the denser fluid. Figure 2 illustrates the force balance for the contact angle tests.

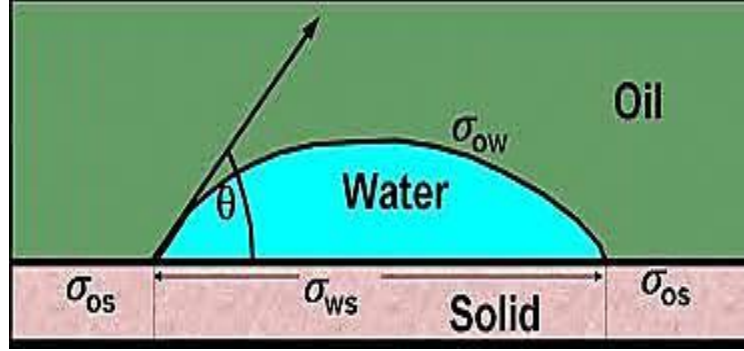


Figure 2: Force balance at three phase contact line (Rao *et al.*, 2006)

The equilibrium contact angle is described by Equation (6) (Rao *et al.*, 2006):

$$\sigma_{ow} \cos \theta = \sigma_{os} - \sigma_{ws} \quad (6)$$

where  $\theta$  is the contact angle,  $\sigma_{ow}$  is the interfacial tension between the oil and water phases,  $\sigma_{os}$  is the surface energy between the oil phase and surface; and  $\sigma_{ws}$  is the surface energy between the water and the surface being wetted.

Even though contact angle method is universally recognized, there are some limitations, which can lead to a wrong categorization of wettability and reproducibility problems. As a matter of fact, it is not possible to observe the contact angle in the rock pores (Zhu *et al.*, 2013). In addition, this angle can differ from point to point in the rock, and also if there is adsorption involved the contact time or rate also of great importance. For this reason, the most used technique for wettability measurement is the relative permeability measurements utilizing the fluids in the reservoir at reservoir states of pressure and temperature. The contact angles can be very susceptible to contamination by trace quantities of copper, nickel ions as well as products generated by crude oil oxidation (Donaldson, 2008).

#### 2.1.4.1 Wettability Alteration

A change in wettability across the entire reservoir happens during production of oil (Milter, 1996). Redistribution of capillary forces may occur as the oil flows out of the reservoir, and typically water-wet sandstone can change its wettability and become oil-wet or mixed (Karimov, 2011). In nature, fractured chalk oil reservoirs containing low initial water saturation typically have mixed-wet behavior (Austad & Milter, 2000; Milter, 1996). The saturation record of the substance may have an impact on the surface wettability with the zones that make contact with oil become oil-wet whereas the zones without it continue to be water-wet. Milter (1996) also proved that the wettability of low permeability, chalk substance can be altered by incubating the core material into the oil. This characteristic is utilized to prepare cores that are more oil-wet.

The composition of oil is the main factor responsible for wettability alteration of a naturally water-wet surface (Abdallah *et al.*, 2007). In asphaltenes and resins with hydrophilic and hydrophobic characteristics, the polar components determine the solubility. Oil that is a poor solvent for surfactants will have a greater tendency to alter wettability in comparison with the one that is an excellent solvent. In this situation, the wettability change does not have a relation with the asphaltenes precipitation, but rather with the adsorption of surfactant onto the solid surface. If precipitation was the cause for the wettability alteration, subsequently oil with the largest fraction of n-heptane should present the maximum change in wettability (owing to the fact that the heptanes make the asphaltenes to precipitate, and alter the wettability). Seethepalli *et al.* (2004) assessed numerous sulfates with low amount of alkali. It was observed that IFT is reduced to ultra-low levels, approximately  $10^{-3}$  mN/m, wettability is altered and imbibition improved by more than 35% OOIP, utilizing very dilute anionic surfactant/alkali solutions.

## 2.2 SURFACTANT FLOODING

Surfactant are employed in all stages of crude oil recovery and processing industries, from oil reservoir injection, well drilling, oil well production and surface plant process to pipeline and seagoing transportation of petroleum emulsion. Usual applications include the application of nonionics as demulsifiers agents, anionics as defoamers and amphoteric and cationics as corrosion inhibitors and biocides. Surfactants are also essential additives in drilling process operations (Dwight, 2008). They are normally utilized in drilling muds and drilling fluids to give lubricity (for better flow) and pumpability (for foam control), emulsification for corrosion and biocidal control as well as to diminish water losses during the drilling process. During natural gas and coal bed methane down hole drilling, surfactants are utilized for gas well stimulation in foaming systems which are accountable for formation blocking and fracturing with cationic quaternary ammonium compounds thus reducing corrosion and water loading, and increase the production of gas (Dwight, 2008).

Surfactant flooding process refers to the injection of one or more liquid chemicals and surfactants into the reservoir to increase oil recovery by effectively decreasing the interfacial tension (IFT) between the crude oil and the water (Touhami *et al.*, 2001). Very low oil-water, O/W interfacial tension is required for the movement of oil through the thin capillary pores. An ultra-low IFT of 0.001 mNm is preferable. A diagram illustrating the process is shown in Figure 3.

The injected surfactant will mobilize the trapped oil droplets or ganglions and bank it up until all the surfactant is diluted or if not lost owing to adsorption by the reservoir rock and can no longer be available to lower the IFT between the oil and the water and mobilize residual oil anymore (Berger & Lee, 2006).

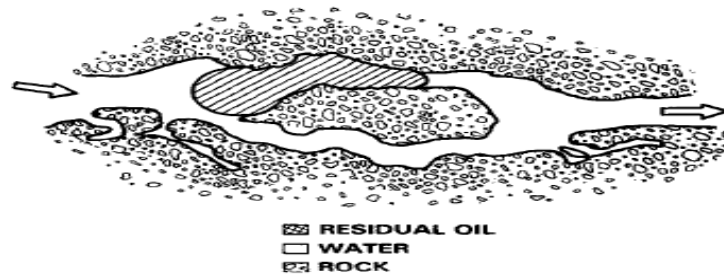


**Figure 3:** Diagram of flooding showing trapped residual oil trapped in the reservoir (Touhami *et al.*, 2001)

Behind the oil bank, the surfactant prevents the mobilized oil from being re-trapped as shown in Figure 4.

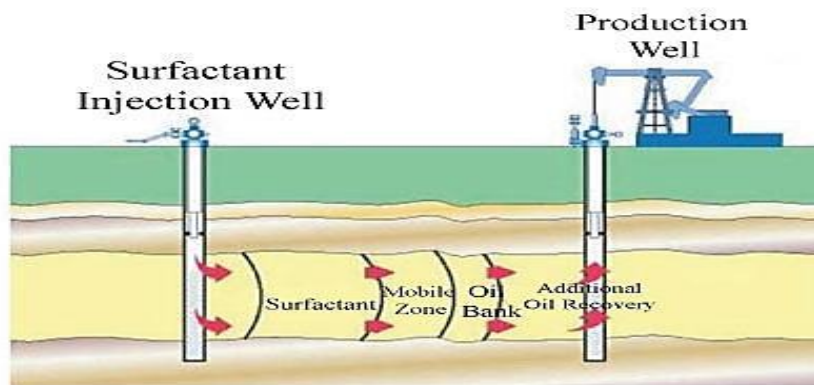


**Figure 4:** Surfactant flooding process (Berger & Lee, 2006)

In most cases, surfactants are injected only in a small portion of the pore volume due to its high cost. Thus, the surfactant slug has to be propelled with water, in several cases containing polymer to prevent fingering and break down of the slug (Emegwalu, 2010). De Groot first introduced the concept of recovering crude oil by surfactant flooding back in 1929 when he was granted a patent for water-soluble surfactants that are capable of improving oil recovery yield. The surfactant was able to lower the IFT between the brine and remaining crude oil. The utilization of appropriate surfactant can efficiently reduce the IFT which results in an equivalent increase in the capillary number (Berger & Lee, 2006).

It is also very important that when a surfactant is injected into the reservoir, it has to be able to facilitate an ultra-low IFT while preserving its integrity. However, this does not always happen; surfactants are typically compromised by some undesirable effect in the reservoir. Pope *et al.* (2010) performed studies on the role of co-surfactants and co-solvents in making CEOR processes more efficient. Co-surfactants/co-solvents are mixed into the liquid surfactant solution so as to improve the properties of the surfactant solution. It acts as a promoter or as an active agent in the surfactant solution, causes a change in the surface energy or in the viscosity of the liquids and also provides favourable conditions with regard to salinity, pressure and temperature (Pope *et al.*, 2010). Their studies showed that adding a co-surfactant or co-solvent facilitates the achievement of aqueous phase stability which ensures the transport of injected mixture in the reservoir over long distances with low retention. During two core flood experiments, they observed that the addition of a low concentration of co-surfactant improved drastically the performance of the chemical formulation and a clear ASP slug was also achieved. They also noticed that alcohol ethoxylates demonstrate outstanding solvent-surfactant properties comparing to glycol ethers and simple alcohols (Pope *et al.*, 2010).

Surfactants are used in various formulations such as surfactant-polymer flooding, surfactant-alkali flooding and alkali-surfactant-polymer. Generally there are three types of surfactant flooding for EOR (Rosen *et al.*, 2005) as shown in Table 1.

**Table 1:** Types of Surfactant Flooding

Type of Surfactant Flooding	Technique	Note
<b>Microemulsion flooding</b>	Surfactants, co-surfactants, alcohol and brine are injected into the reservoir to form microemulsions to obtain ultra-low IFT.	Can be designed to perform well in for example, high temperature or salinity or low permeable areas where polymer and/or alkali cannot work.
<b>Miceller/Polymer flooding</b>	A micelle slug normally of surfactant, co-surfactant, alcohol, brine and oil is injected into the reservoir.	Displacement efficiency close to 100 % (measured in laboratory).
<b>Alkaline/surfactant/polymer</b>	The addition of alkaline chemicals reduce the IFT at significantly lower surfactant concentrations.	Lower concentration of surfactants are involved in this process, which reduces the cost of chemicals.

In 1959, Reisberg and Doscher (1960) proposed the idea of combining alkalis and surfactants. It involved mixing non-ionic surfactants and alkali in order to enhance oil

recovery at laboratory level. Studies have shown that when an alkali is added to the surfactant solution, it not only decreases the IFT, but it also causes a reduction in the surfactant adsorption onto the negatively charged sand surface (Touhami *et al.*, 2001). Combining an inexpensive alkali with expensive surfactants can be used in order to achieve both a successful and cost-effective flooding. To design an efficient surfactant-alkali flooding formulation, it is crucial to utilize the synergistic effect between the alkali and surfactant. Surfactants have a tendency to accumulate at the water and oil interface where the hydrophobic and hydrophilic ends of the molecules are in a minimal energy state (Elraies *et al.*, 2011). This causes an increase in the surface pressure and a decrease in both IFT and the interfacial energy. Wesson & Harwell (2010) came to the conclusion that the mechanism of the synergistic effect involves the formation of mixed micelles of the surfactants and the generated *in-situ* surfactant. The mixed micelles cause the IFT to reduce considerably.

Simultaneously, surfactant adsorption on sand is significantly reduced by the presence of alkali. The sand surface will become gradually more negatively charged with an increase in pH level and will thus delay the adsorption of the anionic surfactant (Spinler *et al.*, 2002). (Zhang *et al.*, 2006) also observed that  $\text{Na}_2\text{CO}_3$  decreases the adsorption of anionic surfactant on carbonate minerals, thus when it is used it makes chemical flooding of carbonate reservoirs more economical and very profitable. The success of these processes in a real reservoir not only depends on how well but also on how long the surfactant generated internally and the added surfactant work together as planned. Based on field tests, Mayer *et al.* (1983) summarized the quantity of alkali that is injected and the performance results for premature alkaline flooding methods. Most of the performed projects were found to be not as profitable as expected. Falls *et al.* (1992) obtained successful field results when performing alkaline-surfactant flooding to recover water-flood residual oil from sandstone reservoir in USA. This process recovered no less than 38% of OOIP.

### 2.2.3 Structure and Classification of Surfactants

Surfactants are polymeric molecules and consists of an amphiphilic molecule, with a hydrophilic part (that is, water soluble, water loving or polar), a hydrophobic or lipophilic part (that is, dislikes water, oil soluble, and oil loving or non-polar) (Pashley & Karaman, 2004). In surfactant flooding, the hydrophilic head interacts with water molecules and the hydrophobic tail interacts with the trapped oil as seen is Figure 5. Hence, they can dissolve in both aqueous phase (water) and oleic phase (or organic solvents) by lowering the interfacial tensions between the phases as well as alter the wettability of the reservoir rock surface by adsorbing to the liquid-rock interface, thus making the rock surface have a strong attraction towards one of the immiscible fluids, preferably water (Elraies *et al.*, 2011).



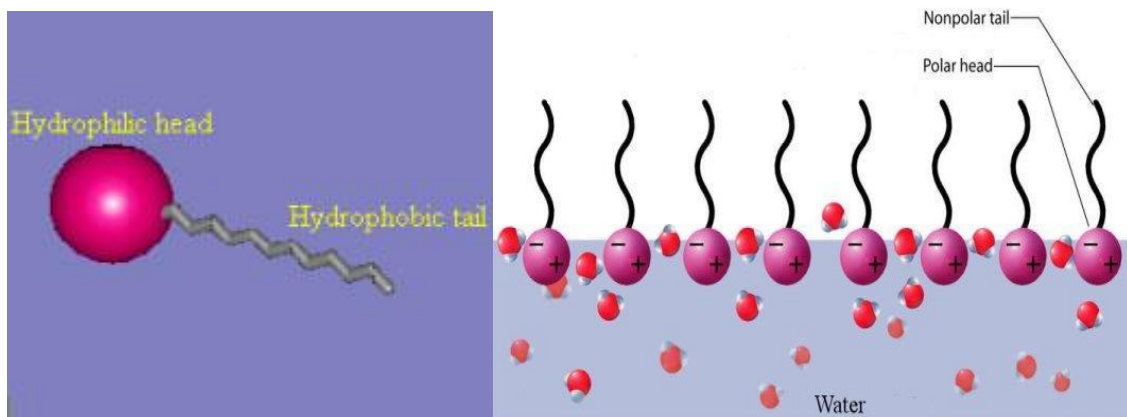


**Figure 5:** Surfactant molecule and its orientation in water (Pashley & Karaman, 2004)

The extent of reduction in surface tension strongly depends on the amount of the surfactant in the solution (Pashley & Karaman, 2004) as well as the surfactant structure. A number of surfactants have the ability to reduce the IFTs to ultra-low values even if present in very small amounts. When added, the molecules of the dissolved surfactant in water gets separated into single molecules named monomers. The maximum concentration of monomers in the solution is a function of molecular structure of the surfactant, as well as the environment (such as impurities, temperature and pH) (Hanna & Somasundaran, n.d.). The maximum concentration of the monomers in any solution is referred to as the critical micelle concentration (CMC). Beyond this concentration, surfactant molecules assemble into aggregates that are known as micelles. The critical micelle concentration (CMC) refers to the concentration at which surfactants start to form micelles (Elraies *et al.*, 2011).

Depending on the nature of the hydrophilic group (head group), the surfactants are classified as:

- **Anionic** - the surface-active part of the molecule carries a negative charge (for instance  $\text{RC}_6\text{H}_4\text{SO}_3\text{Na}^+$ , alkyl benzene sulfonates, sodium dodecyl benzene sulfonate, phosphates). They are commonly used in a variety of industrial processes, for instance in the production of soaps and detergents (alkyl benzene sulfonates), wetting agents (di-alkyl sulfosuccinate), and foaming agents (lauryl sulphate). In general, they are the most used in EOR due to their ability to achieve ultra-low IFT, relative stability, relatively low adsorption onto reservoir rock in comparison to cationic surfactants and low cost of production (Wu *et al.*, 2005). Anionic surfactants can dissociate in water and generate an amphiphilic anion and a cation which would typically be an alkaline metal such as potassium ( $\text{K}^+$ ) or sodium ( $\text{Na}^+$ ). Wu *et al.* (2005) investigated a number of branched alcohol propoxylate sulfate surfactants for usage in EOR. Their results showed that the number of propoxylate groups has a considerable impact on the adsorption, IFT and the

optimal salinity. As the number of propoxy groups increased, the adsorption and optimal salinity decreased. In the study, the tests were performed at diluted surfactant concentrations, both in the presence or absence of co-surfactants. The loss of surfactants to the reservoir due to trapping, adsorption or any other occurrence is found to be minimal.

- **Cationic** – in this case, the surface-active part of the molecule carries a positive charge (for example  $\text{RNH}_3^+\text{Cl}^-$ , salt of a long chain amine, pyriminium, piperidinium). Cationic surfactants dissociate in water to form an amphiphilic cation and anion, normally a halide ( $\text{Cl}^-$ ,  $\text{Br}^-$ ) (Rosen & Kunjappu, 2012). During production, they are subjected to high pressure hydrogenation which makes them generally more costly compared to anionic surfactants and less used in comparison to nonionic and anionic surfactants. However, cationic surfactants are used to enhance the spontaneous rate of imbibition of water in oil-wet carbonate at concentrations higher than their critical micelle concentration (Standnes & Austad, 2000; Standnes *et al.*, 2002; Seethepalli *et al.*, 2004; Fletcher & Morrison, 2008). These surfactants are prone to dissolve in the oil phase as aggregates between the carboxylates and surfactant, under creation of ions pairs. Consequently, the surface turns more water-wet and the material that was adsorbed on the rock wall is removed making the surface less oil-wet (Seethepalli *et al.*, 2004). Cationic surfactants are also used as bactericides and disinfectants but principally utilized as fabric conditioners.

- **Zwitterionic or Amphoteric** - both positive and negative charges are present in the surface-active part (for instance  $\text{RN}^+\text{H}_2\text{CH}_2\text{COO}^-$ , long chain amino acid like amino carboxylic acid) (Rosen & Kunjappu, 2012). These surfactants are a mixture of cationic, anionic and others and have not been used in oil recovery.

- **Nonionic** - the surface-active part carries no visible ionic charge (for example  $\text{RCOOCH}_2\text{CHOHCH}_2\text{OH}$ , monoglyceride of long chain fatty acid). Nonionic surfactants include ethers, phenols, alcohols, amides or esters. They are mainly used as co-surfactants for CEOR (Gupta & Mohanty, 2010) and they can withstand high salinity. Their hydrophilic group is of a non-dissociating type and does not ionize in aqueous solutions (Wu *et al.*, 2005). However, their properties are not as good as anionics and their capacity to decrease the IFT is usually lower comparing to ionic surfactants. Various nonionic surfactants with different degree of ethoxylation were studied by Curbelo *et al.* (2007). They investigated the surfactant adsorption in sandstone core. It was observed that with higher degree of ethoxylation, the surfactant has a larger polar chain and in consequence a higher solubility in the direction of the aqueous phase. Hence, higher amounts of surfactant are needed to guarantee micelles formation. It was concluded that the adsorption to sandstone core is higher when the ethoxylation degree

is lower, which should not happen in surfactant CEOR flooding. In petroleum industry, the most common of these surfactants used is petroleum sulfonates manufactured by sulfonating a pure organic chemical, an intermediate molecular weight refinery stream or crude oil (Lake, 2011).

#### **2.2.4 Selection of Surfactants for Surfactant Flooding**

Selecting the appropriate surfactant is one of the major issues for chemical EOR application. The surfactant must be stable under reservoir conditions to cause an ultra-low IFT. Wangqi and Dave (2004) carried out extensive screening studies of various types of surfactants using core flood tests. The core flood tests showed that 11.2 % of the OOIP could be recovered once the appropriate surfactant type and concentration are mixed with polymer and alkali. Surfactants which contain large hydrophobes have been categorized as being extremely efficient when it comes to achieving very low interfacial tension (IFT) for heavy oils (Zhao *et al.*, 2015). The search for these kinds of surfactants, capable of achieving ultra-low IFT while presenting great tolerance to salinity, hardness and temperatures is attracting more efforts, as a result of the constantly growing number of reservoirs with harsh conditions.

It was demonstrated that high-performance and economical, surfactants can be manufactured in the form of Guerbet Alkoxy Sulfate surfactants (GAS) that exhibited good performance with difficult oils (Adkins *et al.*, 2010). The high performance anionic surfactants were produced by alkoxylation of the Guerbet alcohol containing various ethylene oxide (EO) and propylene oxide (PO) units, and subsequent followed by sulfation. This is a lower cost option to the more complex sulfonation method. Moreover, these sulfates can be formulated to exhibit variety of hydrophobicities by altering the number of ethylene oxide (EO) and propylene oxide (PO) groups, as required to satisfy the needs of different reservoir conditions. However, GAS is not very chemically stable at temperature higher than 50 °C except if the pH is kept high, between 10 and 11 using an alkali. Puerto (2010) found ether sulfonate surfactants (for instance alkoxy glycidyl sulfonates) to be more tolerant to high temperatures. But, ether sulfonates are quite expensive and are not readily available. Additionally, they generally present high hydrophilicity and short hydrophobes are not very efficient when used in crude oils with high alkane carbon number. Others chemically and thermally stable as well as economical surfactants are required for such conditions.

Experiments to formulate anionic surfactants for application in chemical flooding at extreme reservoir conditions (up to 150 °C) were performed by Barnes *et al.* (2003). They came to the conclusion that the ability of a particular surfactant is depended on reservoir characteristics such as temperature, the composition of water and crude oil type. Therefore, so as to obtain an ultra-low IFT during flooding, the surfactant's composition

has to be adapted to such conditions. Tests were performed using two types of surfactant, both manufactured by Shell, Internal olefin sulfonates (IOS) and the branched C<sub>16</sub>, C<sub>17</sub> alcohol-based anionic surfactants. The IOS surfactants demonstrated little sensitivity towards temperature, which could be advantageous to reservoirs with temperature gradients. When these surfactants were combined with normal alkalis, they gave excellent performance (Elraies *et al.*, 2011). Both were able to function under extreme temperatures, high salinity reservoirs and showed great potential for low cost and high efficiency CEOR processes (Levitt, 2006; Flaaten *et al.*, 2008). The results indicated that about 100% of the residual crude oil was recovered with an extremely low surfactant adsorption.

In their work, Puerto *et al.* (2010) noticed that many reservoirs have high temperatures (up to 120 °C), high salinities, and total dissolved solids content up to 200 g/L. All of these conditions may cause precipitation of injected surfactant or other unwanted phase separation. During tests, they came to the conclusion that blends of Alkoxylated glycidyl sulfonates (AGS) and Internal Olefin Sulfonates (IOS) have great possibility of given ultra-low IFT necessary to mobilize crude oil in addition to being suitable for high temperatures and optimal salinities reservoirs. For a successful EOR by surfactant flooding, a low interfacial tension (IFT) between oil and water is of great importance. The surfactant solution when injected into the oil/water system mobilizes oil droplets by reducing the IFT between oil and water (which in turn decreases the capillary forces in water-oil interfaces) and banks the oil until all the surfactant is diluted or lost due to adsorption onto the reservoir rock. Surfactants are able to reduce the IFT from about 20-30 mN/m to 0.001-0.01 mN/m, thereby achieving low residual oil saturations (Schramm, 2000; Zhang *et al.*, 2005). For this reason, the correct surfactant must be selected and evaluated at the right cost-effective concentrations.

According to Chan and Shah (n.d.) when the surfactant concentration is varied, the IFT between oil and water can also vary. They proposed a molecular mechanism to explain the observed ultra-low IFT curves obtained with dilute solutions of petroleum sulfonates. It was concluded that the minimum in IFT happens when the amount of surfactant monomers in the aqueous phase (water) is at its maximum. They also noticed that the minimum surfactant IFT corresponds to the CMC in the equilibrated aqueous phases. During the displacement process a critical challenge is to maintain surfactant concentration that will give a low IFT, due to dilution and adsorption inside the reservoir (Zhang *et al.*, 2005). Since oil displacement efficiency will be reduced by a change in surfactant concentration from the static equilibrium value (Rosen *et al.*, 2005).

Ben Shiau *et al.* (2010) investigated the possibility of designing an alcohol-free surfactant for CEOR. They employed a binary anionic surfactant combination consisting

of a branched-tail primary surfactant (dioctyl sulphosuccinate) and a low sorption, high performance surfactant (sodium linear alkyl diphenyloxide disulfonates). This mixture is reported to produce ultra-low IFT. Bryan & Kantzas (2007) performed a study on alkali-surfactants for surfactant flooding of heavy oils. Their work demonstrated that alkali-surfactant flooding is a promising process for non-thermal heavy oil recovery, as the addition of alkali-surfactants lowered the IFT between oil and water and to an extent that creation of emulsions was possible. Wang & Wang (2010) proposed a mechanism to achieve ultra-low IFT with no alkali, salts, alcohol, co-surfactants and solvents in the system. They identified that some sort of amphoteric surfactants such as the betaine surfactant is capable of reaching an ultra-low IFT at very low concentrations even in high salinities and high temperature surroundings.

Much attention is being given to oleochemicals (agricultural products) as substitute feedstock, in an attempt to produce cheaper surfactants (Gregorio, 2005a). A variety of surfactants have been manufactured from natural vegetable oils for CEOR purposes (Wuest *et al.*, 1994; Li *et al.*, 2000). According to Hill (2001) the mostly used feedstock are coconut and soybean oils, which are utilized to generate oleochemical feedstock, for instance fatty alcohol and esters. However, these surfactants are derived from edible vegetable oils and in the long run will compete with the food supply. In recent years, the demand and cost of edible vegetable oils has increased annually, which make their derived surfactants more costly (Gregorio, 2005a). Hence, there is incentive for the production of surfactants from cheaper non-edible or waste oils since for a successful surfactant flooding, factors such as availability, oil prices in the market, and cost of surfactants plays a huge role.

### **2.2.5 Effect of Surfactant on Wettability Alteration**

Wettability greatly effects oil and/or gas production during primary recovery and residual oil saturation left after water-flooding (Spinler *et al.*, 2002). The wettability of a reservoir rock is affected by brine composition, surface roughness, oil composition and the use of surfactants. Wettability can be reversed by the use of surfactants. Surfactant flooding schemes are used to alter the reservoir rock wettability and recovery oil more efficiently. Changes in wettability and adsorption are determined mainly by the surfactant structure, the oil and reservoir fluids compositions, the rock surface properties, pH level, temperature and salinity (Schramm, 2000).

Seethepalli *et al.* (2004) studied alteration of wettability of calcite plate by utilizing anionic surfactant and alkali substances. Studies have shown that the wettability alteration is achieved by the effect of anionic ion instead of alkali chemical. The alkali substance assists the anionic ion to reduce surfactant adsorption onto the carbonate surface. Anionic surfactant reduces the IFT and consecutively releases oil and absorbed

molecules in form of droplets or emulsion. However, in some reports, anionic surfactant was considered to alter wettability by the effect of formation of bilayer. The collaboration between alkali and anionic surfactant can alter the oil-wet surface to intermediate water condition. Wu *et al* (2005) performed studies on the wetting behaviour and surfactant in enhanced oil recovery within carbonates. The schemes of wettability reversal by the use on cationic and anionic surfactants were demonstrated.

Cationic surfactants altered the reservoir rock wettability by generating the ion-pairs with the dissociated adsorbed anion materials in aqueous phase, resulting in the removal of adsorbed material, giving the surface less oil-wet. However, anionic and nonionic surfactants were not able to remove the adsorbed molecules, on contrary they co-absorbed on the carbonate surface. Other researchers also utilized cationic surfactants to alter wettability of carbonate formations to more water-wet conditions (Standnes & Austad, 2000; Standnes *et al.*, 2002; Xie *et al.*, 2004). Xie *et al.* (2004) also applied a cationic surfactant and anionic surfactant to more than 50 cores from three dolomitic Class II reservoirs and the additional oil recovery varied from 5-10% OOIP. Change in wettability was identified as the principal factor. The recovery rate with the use of nonionic surfactant was found to be faster in comparison with that the cationic surfactant since the previous had higher interfacial tension.

According to Mohan (2009) wettability alteration can be considered more important on the secondary recovery than in the tertiary due to the fact that the recovery from oil-wet reservoirs is enhanced by a change of wettability to more water-wet by the addition of surfactants and other substances. This change can decrease the amount of macroscopic bypassing which improves the overall recovery (Yang, 2000). Most researches are conducted in the area of surfactant's ability to lower IFT and its usage for IFT reduction requires large amount of chemicals which renders this process alone uneconomical. Conversely, altering wettability can be done by using less costly surfactants at very reasonable concentrations. Thus, combining both (the effects of reduction in IFT and more favourable wetting conditions) would make surfactant flooding a more cost effective process. Moreover, the most important is that surfactants effect on wettability not only depends on how much surfactant is adsorbed but also on how they adsorb on the reservoir rock (Rao *et al.*, 2006).

### **2.2.6 Temperature and Pressure**

It is well known that temperature affects a number of crucial parameters for EOR processes, for instance IFT, wettability, rates of imbibition and the viscosity of the oil, in addition to having a significant impact on the phase behavior of oil/surfactant/water systems. An increase in temperature causes an increase in salinity (Skauge & Fotland,

1990). For most surfactants at higher temperatures, the optimal salinity reduced or stayed the same (Gupta & Mohanty, 2010). These ambiguous examples demonstrate the intricacy of surfactant systems where the phase behavior is dependent on both composition and component.

Although, many studies have been conducted on the effect of pressure on the phase behavior of microemulsions, still there is no lucid opinion as to when pressure has a considerable impact on the phase behavior or not. An increase in pressure causes a change in phase behavior in the direction of a lower phase microemulsion (Skauge & Fotland, 1990). During experimental tests on secondary alkane sulfonates, it was detected that an increase in pressure also causes an increase in the optimal salinity (Skauge & Fotland, 1990; Spildo *et al.*, 2014). The pressure dependence has a connection with optimal salinity. Numerous water/oil/surfactant systems has been studied, with the objective of experimentally verify the impact of pressure on their phase behavior as well as to obtain a thermodynamic model that can explain this influence (Sassen *et al.*, 1989; Sassen, 1991; Sassen *et al.*, 1992). It was concluded that the pressure has a significant influence on the phase behavior of oil/surfactant/water systems for both anionic and nonionic surfactant systems.

### **2.2.7 Surfactant Retention**

Controlling surfactant retention in the reservoir is one of the key parameters in determining the effectiveness of surfactant flooding (Liu *et al.*, 2008). Surfactants retention has been attributed to be due to any or combination of adsorption, precipitation, and phase trapping. All of these mechanisms cause retention of surfactant in the reservoir as well as deterioration of the chemical slug composition which leads to poor displacement efficiency. The retention of surfactant in the reservoir is dependent on the type of surfactant, concentration of surfactant, clay content, surfactant equivalent weight, rock minerals, flow rate of solution, pH and so on(Liu, 2008). In general, surfactant retention increases with an increase in the equivalent weight of the surfactant (Sheng, 2013). Petroleum sulfonates are broadly utilized in surfactant flooding process. The existence of divalent cations ( $\text{Ca}^{2+}$ ,  $\text{Mg}^{2+}$ ) in the solution results in the precipitation of the surfactant.

## **2.3 ALKALINE FLOODING**

Alkaline flooding is an EOR technique where an alkaline chemical is added to injected water (Pitts *et al.*, 2006). In some cases, the added alkaline chemical will react with the oil and form surfactants inside the reservoir. In due course, the surfactants play a big role by increasing oil recovery through reducing IFT between oil and water. The alkaline

agents displace the crude oil by raising the pH of the flooding water and also by altering the reservoir rock wettability. The reaction that occurs between the acidic components in crude oil and the injected alkali forms *in-situ* surfactant to overcome the depletion of surfactant in the liquid phases as a result of retention (Liu *et al.*, 2008). The formed mixture mobilizes the crude oil from the pore spaces in the reservoir. Adding an alkali can be beneficial in reducing the adsorption of surfactant, and thus the quantity of surfactant needed for injection, and consequently the lower the costs (Seethepalli *et al.*, 2004). ShamsiJazeyi *et al.* (2014) observed that anionic surfactants demonstrate minimal adsorption when  $\text{Na}_2\text{CO}_3$  is used in comparison to NaOH.

The mostly used alkali are sodium hydroxide (NaOH), sodium orthosilicate or sodium carbonate ( $\text{Na}_2\text{CO}_3$ ), ammonium hydroxide ( $\text{NH}_4\text{OH}$ ), potassium hydroxide (KOH), and trisodium phosphate (Li *et al.*, 2000). Sodium orthosilicate and sodium hydroxide are the most efficient in increasing the additional oil recovery. Sodium hydroxide can increase the pH to very high values; though a pH higher than 12 has been found to be detrimental, as it can accelerate the alkali consumption (Pitts *et al.*, 2006). According to Yuan *et al.* (2015) NaOH solutions at temperatures above 85 °C strongly interacts with sandstone leading to sandstone weight loss and increased porosity. The effects of temperature on reaction rates depends on the amount of caustic, rock minerals, and contact time. The loss of caustic caused by NaOH dissolution of silicates minerals can be considerably detrimental during field application (Yuan *et al.*, 2015).

French & Burchfield (1990) studied the IFT of a large variety of crude oil samples using NaOH solutions at various concentrations. The pendant drop method was used at ambient temperature. They found that in spite of a few oil samples only causing a small change in IFT, many samples demonstrated an ultra-low IFT at only one alkali concentration, whereas others showed very low IFT over a wide series of alkali concentrations. The use of sodium carbonate ( $\text{Na}_2\text{CO}_3$ ) is quite limited due to the fact that in the presence of calcium and other divalent ions, it precipitates unless soft brine is utilized. Recent studies have reported the utilization of sodium metaborate ( $\text{NaBO}_2$ ) as a substitute for  $\text{Na}_2\text{CO}_3$  (Liu *et al.*, 2008; Flaaten *et al.*, 2008). This alkali presented pH values of approximately 11 at 1wt. % alkali amount and produced soap when crude oils were used. The main advantage of  $\text{NaBO}_2$  is the fact that it is tolerant to divalent cations.

Usually, alkaline flooding is used only in reservoirs that contain specific types of highly acidic crude oils. Jackson (2006) studied the effects of  $\text{Na}_2\text{CO}_3$  on the phase behavior of surfactants, utilizing crude oil with small amount or no acid. It was noticed that the equilibration time was faster for the sample with the larger concentration of  $\text{Na}_2\text{CO}_3$ . Moreover, when  $\text{Na}_2\text{CO}_3$  was used the time needed for the mixture to coalesce to a



microemulsion was shortened. Due to the high cost of chemicals, silicates can be added to alkaline flooding as an enhancement to the process. The addition of silicates have two main purposes: it works as a buffer which maintains a steady high pH level and produces a lower IFT as well as it promotes high surfactant efficiency by removing hardness ions from reservoir brines, hence helping to reduce adsorption of surfactants on rock surfaces (Zhang *et al.*, 2005).

For a number of systems with low interfacial tension, the IFT value was noticed to be smaller than 0.001mN/m. The IFT between oil and water was found to be very sensitive to both salinity and NaOH concentration, and the minimum IFT can be achieved in the concentration range of 0.01-0.1wt% NaOH (Ramakrishnan & Wasan, 1983). Qutubuddin *et al.* (1985) observed that the ultra-low IFTs were obtained with the right NaOH concentration which comprises the electrolyte strength and high pH. Falls *et al.* (1992) found that key factor of alkaline-surfactant process lies on the interaction between synthetic surfactant and the soap generated *in-situ*. Synthetic surfactant is required to adjust the best possible salinity. In 1984, Nelson *et al.* (1984) came up with this idea and called it “Co-Surfactant Enhanced Alkaline Flooding”. Recently, the mixture of synthetic surfactant and alkali is typically called alkaline-surfactant process and approximately all alkali processes employ surfactants.

As stated earlier, wettability is a key factor in crude oil recovery. Reversal of wettability will create fluid relocation in the pore space, which is considered to be beneficial for the recovery of crude oil (Morrow, 1990). In the original wetting state of the medium, the wetting phase inhabits the small pores and the non-wetting phase inhabits big pores. If the wettability of a medium is reversed, the wettability of big pores modifies from oil-wet to water-wet (Wagner & Leach, 1959; Emery *et al.*, 1970; Ehrlich & Wygal, 1977; Olsen *et al.*, 1990). Basically, the main goal of alkaline flooding is to reduce adsorption of anionic surfactants while lowering the IFT. Right alkali is selected based on various parameters. These include, cost and availability at the flooding area, the temperature and mineralogy of the reservoir, the pH level and composition of the mixed water (Mohan, 2009).

### **2.3.1 Mechanisms of Alkaline Flooding**

The use of alkaline chemicals causes formation of emulsions which improve oil recovery. In this process, emulsification happens immediately, and the emulsions are considered to be very stable. Mostly, emulsification depends on the IFT between water/oil (Mohan, 2009). The lower the IFT, the more rapidly emulsification takes place. Emulsion stability depends on the film of the water/oil interface (Zhang *et al.*, 2005). Crude oil usually contains acidic compounds which makes emulsification to occur more easily, while the

asphaltenes are able to adsorb on the interface thereby enhancing emulsion stability and making the film stronger.

Alkaline flooding can enhance oil recovery through four mechanisms (Pingping *et al.*, 2009):

- Emulsification and entrainment where the injected alkali entrains the oil in the reservoir.
- Wettability reversal (from oil-wet to water-wet) in which a change in wettability have an effect on the permeability change which causes an increase in oil production.
- Wettability reversal (water-wet to oil-wet) where low residual oil saturation through low IFT is achieved.

Emulsification and entrapment where movement of emulsified oil enhances sweep efficiency. The hydroxide ion reacts with a pseudo-acid component (in the crude) to form a surfactant via the hydrolysis reaction (Reaction 1) (Li *et al.*, 2000). Surfactant is produced when pseudo-acid is present in the crude oil in reasonable quantities.



The reaction occurs at the water/oil interface and is strongly dependent on the aqueous solution pH. With the addition of an alkali agent, a portion of organic acids in oil become ionized, while the other portions remain electronically neutral. Between the ionized and neutral acids, there is a hydrogen-bonding interaction which leads to the formation of a complex called acid soap (Zhang *et al.*, 2005). In Reaction (2) this is then decomposed into a distribution of the molecular acid between the oleic and aqueous phases, and an aqueous hydrolysis (Zhang *et al.*, 2005).



where, HA represents a single acid species, A symbolizes an anionic surfactant, and the subscripts w and o denote aqueous phases and oleic respectively. That is HA<sub>o</sub> means the acid in oil phase, and HA<sub>w</sub> the acid in aqueous phase (Reaction 3).

The model illustrated in Figure 6 was first proposed by DeZabala (1982). Other numerous researchers have suggested chemical representations for the alkali-oil-rock chemistry.

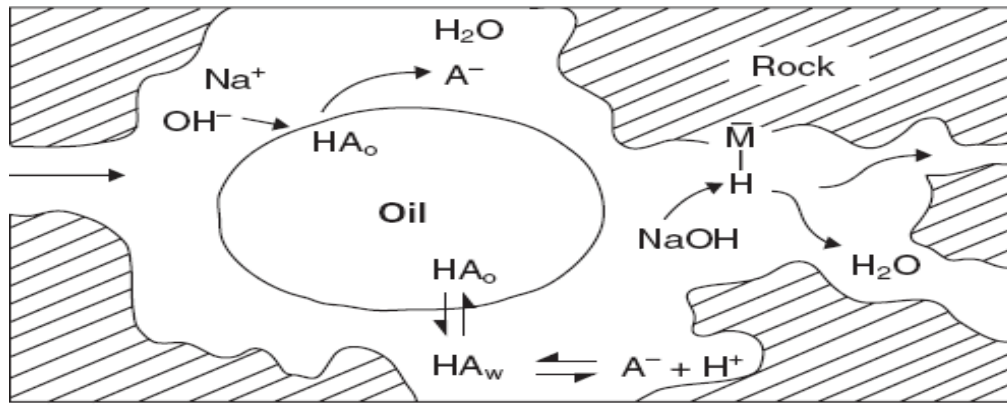


**Figure 6:** Schematic Alkaline process (Zhang *et al.*, 2005)

Various experimental outcomes performed by Ramakrishnan & Wasan (1983) sustained this alkali-oil chemistry model. The absence of hydrogen ions, which are consumed by the hydroxyl ions in the aqueous phase, will facilitate the production of soap ( $A_w^-$ ), which is a natural anionic surfactant other than artificial surfactant. The produced  $A_w^-$  ions will adsorb at oil/water interfaces to reduce the IFT.

## 2.4 POLYMER FLOODING

Polymer flooding is another CEOR method, introduced in the 1960s. This is a well-established CEOR technique and has shown its great potential in various field studies. Polymer flooding is the simplest and most widely used chemical EOR process for mobility control (Pope, 2011). During this process, a polymer (which is soluble in water) is usually added to the injected water containing surfactant to increase the viscosity of the injected water, decrease the Water/Oil (W/O) mobility ratio, diverting injected water from zones that have been swept and through the effects of polymers on fractional flow, thus increase oil recovery (Sadikhzadeh, 2006). This is illustrated in Figure 7.

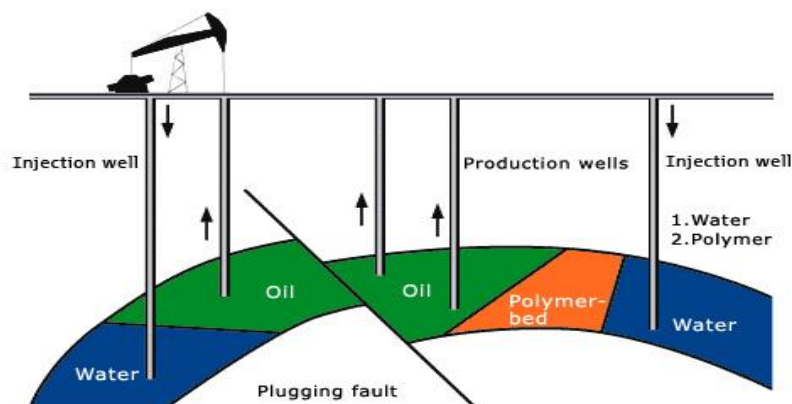


**Figure 7:** Schematic diagram of polymer flooding (Sadikhzadeh, 2006)

The effective permeability to water can be reduced to different degrees depending on the type of polymer used (Sydansk, 2006). Making use of the polymer flooding method is not a guarantee that the residual oil saturation ( $S_{or}$ ) will be reduced, but it is certainly a very efficient way to reach the  $S_{or}$  more rapidly or/and more cost-effectively (Sadikhzadeh, 2006). Adding a polymer to the water for flooding makes possible for the water to go through more of the reservoir rock which results in high amount of oil being recovered. Here, the volumetric sweep is also improved; hence more oil is effectively produced. Occasionally due to infectivity, the polymer solution used must be a non-Newtonian and shear thinning fluid; this is because the viscosity of the fluid decreases with increasing shear rate (Clara *et al.*, 2001). Its success depends on the reservoir temperature as well as reservoir water chemical properties (Clara *et al.*, 2001). This is attributed to the fact that at high salinity and high temperature it is very difficult to keep the polymer stable, and concentration significant quantity loses viscosity.

Polymer flooding can be implemented either on its own or utilized in combination with other chemicals such as surfactant (Alkaline-Surfactant-Polymer). The exceptional quality of polymer flooding is its large amount needed for mobility control, flow change or moving the surfactant front in the direction of the production wells, and back production of polymer is thus not inevitable; which makes handle of back produced polymer one of the biggest challenges for offshore CEOR. The most widely utilized polymers are hydrolyzed polyacrylamides (HPAM) and the biopolymer Xanthan. Usually low concentrations of polymer are utilized frequently in a range of 250 to 2 000 mg/L and the slug size of the polymer solution injected is typically between 15% and 25% of the reservoir pore volume (Sydansk, 2006). For extensive field projects, polymer solutions may be injected over a period of 1-2 year; after which the project goes back to a simple waterflood. For some field projects, the incremental oil recovery has been reported to be as high as 30% OOIP when polymer solution is injected for approximately one pore volume with values (Delshad *et al.*, 2013). The oil displacement is more efficient since less water is needed for injection and to produce a certain quantity of oil (Lyons & Plisga, 2005; Sydansk, 2006).

The performance of the mobility-control of any polymer flood inside the porous media is normally determined by the resistance factor, (RF), which compares the polymer solution resistance to dislocate throughout the porous media as compared to the mobility resistance of plain water. As demonstrated by Lyons & Plisga (2005), if a RF of 10 is noticed, it is 10 times more difficult for the polymer solution to move through the system, or the mobility of water is lowered to 10-fold. Since, water has a viscosity approximately of 1cP, the polymer solution, in this case, would flow through the porous media as though it had an effective viscosity of 10 cP, and although, a viscosity measured in a viscometer could be significantly lower. The current technological trends in polymer

flooding include the development of salinity and temperature resistant polymers (for instance hydrophobically modified polymers or associative polymers), high-molecular weight polymers, the injection in the reservoir of larger polymer concentrations, in addition to the injection of larger slugs of polymer solutions (Zaitoun & Potie, 1983; Aladasani & Bai, 2010; Dupuis *et al.*, 2010; Pope, 2011; Reichenbach-Klinke *et al.*, 2011; Seright *et al.*, 2011; Sheng, 2011; Singhal, 2011) among others.

#### 2.4.1 Polymers Used for EOR and Their Structure

Polymers are very long chains molecules which consist of repeating units (monomers) connected by covalent bonds (Sadikhzadeh, 2006). The mostly used types of polymers employed for effective reduction of mobility ratio in EOR include: polyacrylamides (PAM) or hydrolyzed polyacrilamide (HPAM) and biopolymers such as Xanthan and seleroglucan. These are polymers where the monomeric unit is acrylamide. The chemical structure of HPAM is shown in Figure 8:

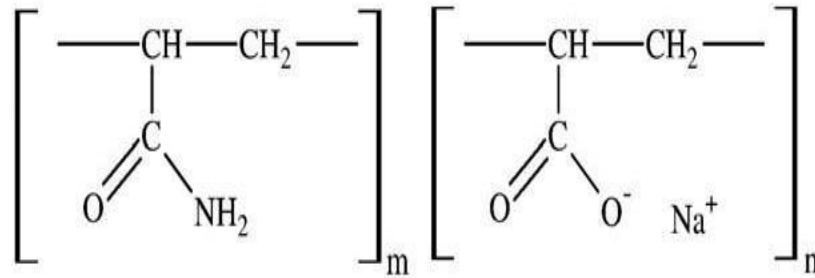


**Figure 8:** HPAM structure (Sadikhzadeh, 2006)

Polyacrylamides are able to adsorb on the rock surface to provide a long-term permeability reduction (Li *et al.*, 2000). They are reasonably cheaper and in fresh waters are capable of developing good viscosities. At high flow rates, they tend to degrade due to shear and perform poorly in high salinity brine. Biopolymers are derived from polymerized saccharide molecules during the fermentation process. They have less viscosifying power in high salinity water when compared to polyacrylamides (Ivonete *et al.*, 2007). They also offer good resistance to shear degradation. Furthermore, they are not easily retained on the rock surface and as a result are able to propagate into the formation with high facility than polyacrylamide. Majority of the polymer producers develop a large variety of homologous polymers from diverse monomers: especially allylic, acryloyl and vinyl. These result in a broad range of structures and properties e.g. heat resistant, zwitterionic, hydrophobic, rod-like, associative, branched and sulfonated. In addition to molecular weight, polymer architecture and polymer solution formulations are extensive and diverse, hence claimed to suit all specific EOR needs. New polymerisation techniques for instance micellar polymerisation, macro-transfer and

macro-initiators agents have resulted in the manufacturing of new polymers with extremely high molecular weights, of up to 30 million g/mol (Manrique *et al.*, 2010).

Pye (1964) described the potential of hydrolyzed polyacrylamide (HPAM) polymer to improve water-flooding process as a mobility control agent. Both synthetic polymer (e.g. HPAM), and biopolymers (e.g. xanthan) have been utilized in polymer flooding. Seright & Henrici (2009) demonstrated that HPAM can be utilized in EOR processes at higher temperature, for example, at 120 °C in the absence of oxygen and divalent ions. Xanthan gum is a rigid double helix polysaccharide which does not shear easily, and is more divalent ions and salt bearable. However, the principal issues when using polymers are injectivity and biodegradation problems (Moorhouse *et al.*, 1977; Ryles, 1988; Seright & Henrici, 2009).

The other factors which may alter the rheological properties of the polymer are retention and adsorption. The physical interaction between the solid surface of porous medium and the polymer molecules will cause adsorption of polymer molecules on the rock interface (Dong *et al.*, 2008). Furthermore, polymer molecules are also entrapped in some of the small pore throat of the pores medium. Apart from that, retention is also a common problem of all polymers within porous medium. Loss of polymer owing to retention can cause lower fluid viscosity. The tendency to shear degrade at high flow rate and high adsorption levels on the rock surface are also other disadvantages (Zaitoun & Potie, 1983; Ryles, 1988; Han *et al.*, 2006).

## 2.5 ALKALINE-SURFACTANT-POLYMER FLOODING

Alkaline-Surfactant-Polymer (ASP) is believed to be one of the major and most common EOR methods that effectively produce light as well as medium oils left in the reservoir after primary and secondary recovery. ASP flooding seeks to improve microscopic displacement efficiency by causing a reduction in the interfacial tension (IFT) between the oil and water via the addition of a surfactant to the water, at the same time the polymer (usually polyacrylamides) increases the oil mobility and sweep efficiency by increasing the viscosity of the injected solution (Clara *et al.*, 2001). The alkali (NaOH,  $\text{Na}_4\text{O}_4\text{Si}$  or  $\text{Na}_2\text{CO}_3$ ) is added to reduce adsorption of the surfactant onto the pore walls and to ensure minimum IFT by controlling the local salinity and reverse the reservoir rock wettability (Pratap & Gauma, 2004). It is also used to convert acids in oil to soap which creates more favorable conditions for the formation of *in-situ* natural surfactants. The process is illustrated in Figure 9:

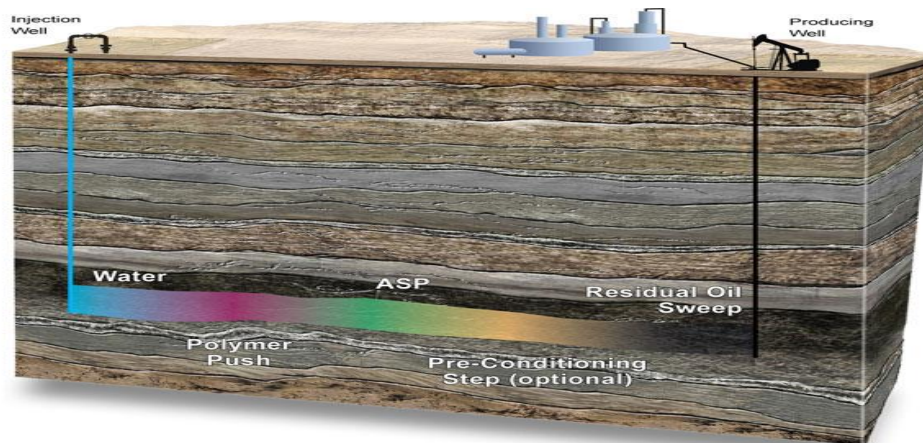


**Figure 9:** ASP flooding process (Gan-Zuo *et al.*, 2000)

Alkali-surfactant combinations have also been brought into play to improve macroscopic sweep during WAG (water alternating gas) process. In this process, the gas mobility is reduced by the addition of alkali and surfactant to the injected water and thus creating foam within the pore space (Liu, 2008). The ASP process is capable of recovering oil by using the benefits of the three flooding techniques: decrease IFT, improve the mobility ratio, increase the capillary number and enhance microscopic displacing effectiveness. Oil recovery is significantly improved by increasing the capillary number and enhancing the mobility ratio. The displacement mechanism of an ASP flood is quite similar to that of surfactant-polymer flooding apart from the fact that most of the surfactant is substituted by inexpensive alkali (Pitts *et al.*, 2006). Here, the overall cost is reduced although a larger chemical slug is used.

The chemical flooding techniques have been reported to result in the highest oil recovery rate (Pingping *et al.*, 2009). Unlike other EOR methods, ASP flooding can considerably improve recovery factors with additional costs estimated to be as low as US\$2.42 per additional barrel for an onshore field. However, like other chemical flooding techniques, there are currently numerous difficulties associated with this technique which have limited widespread field application, especially offshore (Pope, 2011). Among these difficulties, are the large quantities of chemicals that have to be transported to inaccessible locations and then stocked up on platforms where space is quite limited. Emulsions with droplets as small as 10  $\mu\text{m}$  in diameter are produced during ASP flooding, thus additional produced fluid processing is necessary. The fluids (containing the ASP chemicals) that are produced need to be disposed of without harming the environment. This method functions best with moderately low-salinity water, still, seawater is the only source of injection water, consequently desalination or substitute chemicals may be necessary (Li *et al.*, 2000). Formation damage due to the use of strong

base and scale build-up in the injection and production equipment are other technical issues related to this method.

ASP flooding was applied in the early 1980s onshore, when the crude oil price was very high. There has been recently increasing interest as crude oil prices have increased to the point where this method is once again financially viable, yielding an increase of above 20% in the recovery rates in a number of oil fields like Daqing oilfield in China and Oman, which is the most thriving case of this process in the world (Qiao *et al.*, 2000; Li *et al.*, 2000; Yang *et al.*, 2003; Chang *et al.*, 2006). Major developments have made ASP flooding a feasible option for field enhanced oil recovery and more attractive than polymer or micellar/polymer flooding (Wangqi & Dave, 2004; Wang *et al.*, 2006). Recently, apart from Daqing oil field in China, many field pilot tests using ASP flooding have been performed in USA, India and Venezuela showing an impressive recovery of about 21.4-23.24% (OOIP) over secondary recovery (water-flooding) (Clara *et al.*, 2001; Pratap & Gauma, 2004; Pitts *et al.*, 2006). This process is also being used in Russia where it is expected to prevent oil production decline and also increase the amounts of the Ugra oil and raise investment for a faster growth of the region's associated industries like as high-technology oilfield services and petrochemistry.

Nevertheless, even with all these advantages and the success of ASP projects, the process is associated with some disadvantages. The corrosion and scale problem that occurred during an ASP flooding in the Daqing field was recently addressed in a paper by Hou (2001). According to Pitts *et al.* (2006) strong alkali had detrimental effects on the performance of the polymer and in several cases more polymer was required to be added in order to achieve the viscosity desired. This makes, ASP flooding technique significantly more expensive. It is well known that, the mechanisms associated with ASP flooding are still not fully understood. The majority of researchers come to the agreement that the principal issues for the use of this technique are reduction of IFT at low surfactant concentration, reversal wettability, low surfactant adsorption by alkali along with mobility control (Liu *et al.*, 2008).

One of the most important factors when implementing ASP flooding for oil production is IFT reduction (Falls *et al.*, 1992; Arihara *et al.*, 1999). Krumrine *et al.* (1982) concluded that by using several alkaline chemicals in diluted surfactant systems, very low IFT could be achieved. By adding small amounts of surfactant to the alkaline solution, the IFT can be more rapidly reduced than if the surfactant or alkali were injected alone (Schramm, 2000). In 1983, Ramakrishnan and Wasan (Ramakrishnan & Wasan, 1983) suggested that the amount of organic acid in the crude oil has considerable effect on the reduction of IFT of AS-oil system. They observed that at low acid concentrations, adding an alkali to the surfactant solution would only cause an increase in the IFT. However, at



medium to high acid concentrations, adding an alkali can reduce IFT to ultra-low. Wanchao *et al.* (1995) also performed many studies related to ASP flooding in sandstone reservoir with oil containing high acid value.

The addition of alkali (sodium silicate, sodium carbonate and sodium hydroxide) helped to achieve the ultra-low IFT state at the interface. The existence of the alkali reduced the loss of the surfactant in the reservoir rock. Approximately 13.4% of the OOIP was recovered during the pilot tests performed in China, Shandong and Gudong fields. Nasr-El-Din *et al.* (1992) reported an exponential reduction in the viscosity of the combined ASP slug with the increase in amount of the alkali. Tests performed by Hirasaki & Zhang (2003) showed that there were optimal conditions for the reduction of IFT reduction by varying the amounts of surfactant and alkali. Alkaline-surfactant-polymer and alkaline-co-solvent-polymer formulations have also been currently developed for a small number of viscous oils (Liu *et al.*, 2008).

The typical alkali utilized for CEOR is sodium carbonate ( $\text{Na}_2\text{CO}_3$ ). But, in the presence of gypsum, the carbonate ion tends to precipitate. Sodium metaborate tetrahydrate ( $\text{NaBO}_2 \cdot 4\text{H}_2\text{O}$ ) is able to tolerate gypsum and divalent ions to certain extent and capable of providing high pH (~11) for 1000mg/L concentration, satisfactory for chemical flooding. It is also less adsorbed in the core compared to  $\text{Na}_2\text{CO}_3$ . Another significant characteristic of  $\text{NaBO}_2 \cdot 4\text{H}_2\text{O}$  alkali is its low cost which makes it feasible to employ in large scale oil production processes.

ASP process and surfactant process are quite different, in a sense that ASP contains two surfactants, the synthetic surfactant which is added and the natural (surfactant generated in-situ) created by the addition of an alkali. Owing to the diverse hydrophilic properties, these processes have different optimum salinities (Chang *et al.*, 2006). This is one of the key parameters of the process. Besides IFT reduction, wettability alteration is also taken into account as a significant factor for ASP recovery mechanism. The addition of alkali can result in wettability alteration (Li *et al.*, 2003). ASP process takes over this effect of alkaline flooding. Current successful imbibition studies demonstrated that alkali with dilute surfactant solution is able to alter the wettability (Xie & Morrow, 2001; Hirasaki & Zhang, 2003; Seethepalli *et al.*, 2004).

Alteration of wettability is crucial for alkaline-surfactant CEOR, particularly for the fractured, oil-wet reservoir. The presence of alkali also decreases surfactant consumption as well as its adsorption onto the reservoir rock. Several experimental tests showed mitigation of the surfactant adsorption by alkali (Hirasaki & Zhang, 2003). In the ASP process, the polymer will act as the mobility control agent. Surely, this process shows great potential since it presents the synergetic effect of alkali, surfactant and polymer.

The current trends in ASP flooding involve the use of alkali-resistant polymer to minimize costs; the development of weak-alkali ASP flooding system to ease problems associated with using strong base; the development of appropriate ASP flooding system for reservoirs with low to medium permeability. Field tests performed pointed out that hydrophobically modified associating polyacrylamide (HAPAM) can be a suitable flooding agent for high-temperature high-salinity reservoirs owing to its exceptional characteristics in temperature, salt, and shear resistance.

## **PRODUCTION OF FATTY ACID METHYL ESTERS FROM WASTE VEGETABLE OILS**

---

*This chapter focused on the choice of feedstock and solid catalysts for the production of fatty acid methyl ester (FAME) as well the process conditions to maximize the yield from the transesterification of waste vegetable oils. A review of the mechanisms of esterification and transesterification reaction for the production of fatty acid methyl ester (FAME) from natural and waste vegetable oils is discussed. The methods utilized to prepare and characterize catalysts used for transesterification reactions are highlighted. There is a need to utilize a method of catalyst preparation that is easily reproducible and which results in particles that are consistent and homogeneous in elemental composition. The experimental works carried out, including the formulation and characterisation of the bifunctional catalyst, and its use in the transesterification reaction of waste vegetable oils to produce the FAME, at optimum conditions is fully narrated here.*

### **3.1 OVERVIEW**

Fatty Acid Methyl Esters (FAME) can be produced from either edible or non-edible oils. Conventional feedstock for methyl esters production are natural vegetable oils from palm, sunflower, groundnut, soybean, cotton, coconut, rapeseed, palm kernel, olive and non-edible oils (for instance oil from *Jatropha*, sesame, rubber seed, tobacco seed, rice bran, camelina and karanja (Jacobson *et al.*, 2008). Other renewable resources such as oils from plant carbohydrates-sucrose, glucose, sorbitol, starches, animal fats-tallow and so on, have also been reported for FAME production (Babajide *et al.*, 2011). Waste or used vegetable oil is also a sort of non-edible oil which is available worldwide in large quantities. Its supply is expected to increase rapidly as a result of the massive growth in human population as well as an increase in food consumption (Yaakob, 2013).

These are produced locally wherever food is cooked or fried in oil. It is estimated that South Africa generates about 28 million tons of waste cooking oil per annum. Despite the fact that certain amounts of this waste vegetable oil is utilized in soap making, the larger volumes of it is still being illicitly dumped into landfills and rivers, thus leading to environmental pollution (Babajide *et al.*, 2011). Its disposal may impact negatively on human life and on the environment; hence a cost-effective and environmentally friendly

waste management approach is needed. Hence its choice as feedstock for the production of FAME (and or aviation fuel) which can be taken as renewable chemical intermediate for bio-surfactant production (Yaakob *et al.*, 2013).

### 3.2 CHARACTERISTICS OF FATTY ACID METHYL ESTERS

Triglycerides which serve as the starting material for FAME originate from various sources, including single fatty acids, vegetable oils and other edible oils (Demirbas, 2008, Babajide *et al.*, 2011). Waste vegetable oils and animal fats are cheap source of triglycerides and are readily available. However, their rather non-homogeneous composition makes their use challenging. In chemical terms, each oil type has particular fatty acids composition as presented in Figure 10.

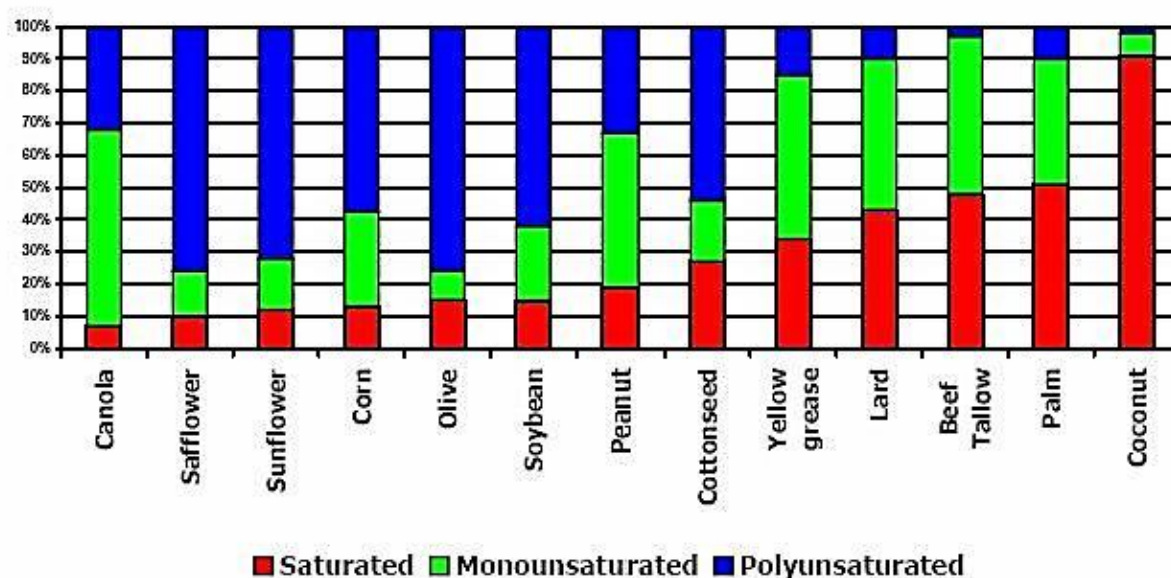
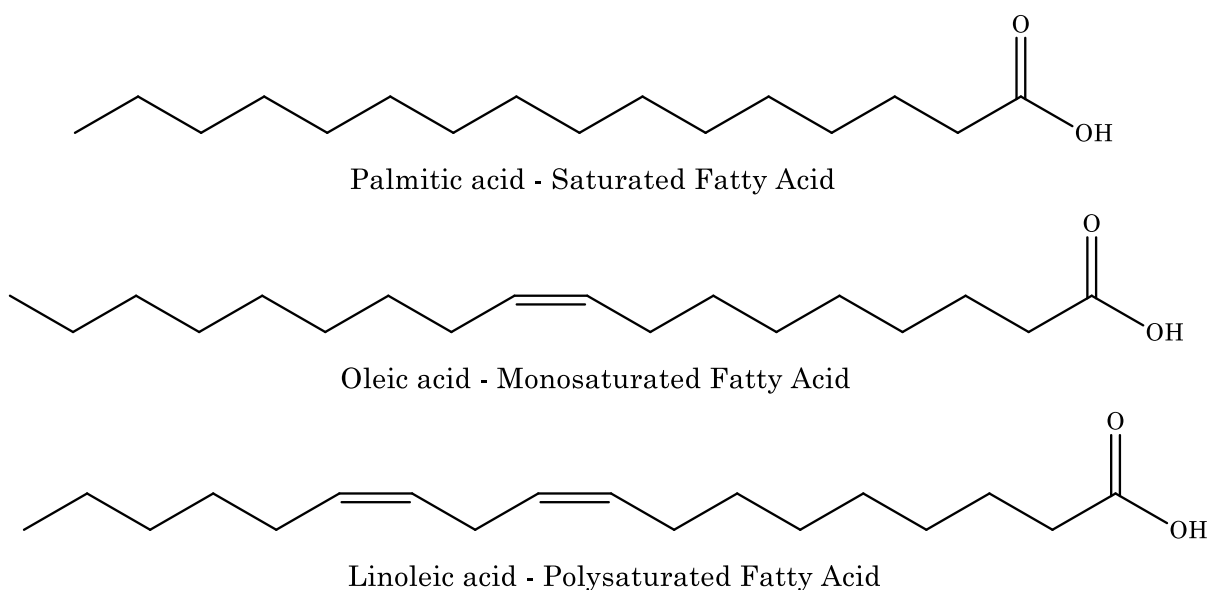


Figure 10: Fatty acid profile of diverse feedstock (Babajide *et al.*, 2011)

Typically, phospholipids or triglycerides contain fatty acids, which when not attached to other fragments, are identified as "free" fatty acids (FFAs). During transesterification reaction if the vegetable oil sample contains high amounts of FFAs, saponification reaction will occur which is undesirable in the FAME production. A triglyceride molecule comprises 3 fatty acid units which are attached to a three-carbon backbone (Solomon, 2002). If all carbon atoms of the free acid are attached to single bonds they are named saturated; a triglyceride molecule is considered to be mono-saturated only if it has one double bond and poly-saturated if it contains more than one double bonds as shown in Figure 11.



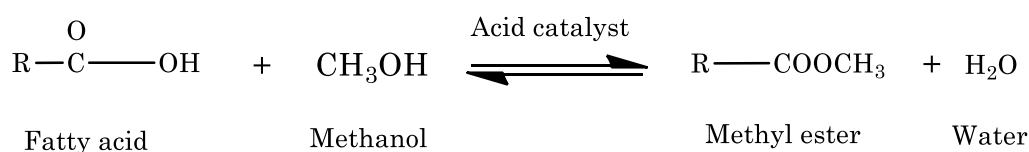
**Figure 11:** Typical composition of a triglyceride (Babajide *et al.*, 2011)

A fatty acid is a carboxylic acid containing a long unbranched aliphatic tail (chain of an even number of carbon atoms, from 4 to 28) which can be either saturated or unsaturated (Babajide *et al.*, 2011). The fatty acid composition of a specific oil sample is the sum of the various fatty acids existing in that sample and it can be utilized to predict both physical (extent of deterioration or its quality) and performance properties of the FAME product (Babajide *et al.*, 2011). The chemical structures of fatty acids are jointly defined by their carbon number and the extent of unsaturation. This imparts on reactivity toward the transesterification reaction as well as on the properties of the FAME produced (Babajide *et al.*, 2011). Since the FFAs content impacts on the yield potential and thereby on the economic feasibility of the feedstock, it is a crucial issue to characterize the oil sample before using it for FAME production (Mattingly *et al.*, 2004).

Very high FFA amounts in the base-catalyzed transesterification process reduces the FAME yield and generates by-products such as soap and water as illustrated in Reaction 4. The choice of the catalyst is a key factor when producing biodiesel via catalytic transesterification, which is also dependent on the FFA existent in the oil (Helwani *et al.*, 2009). For natural or waste vegetable oils with a lower FFAs content, base-catalyzed reaction gives a significant conversion in a reasonably short time whereas for oils containing higher FFAs stock, acid-catalyzed esterification followed by transesterification is the best option (Schuchardta *et al.*, 1998) to prevent hydrolysis of the final ester product.

### 3.3 ESTERIFICATION REACTION

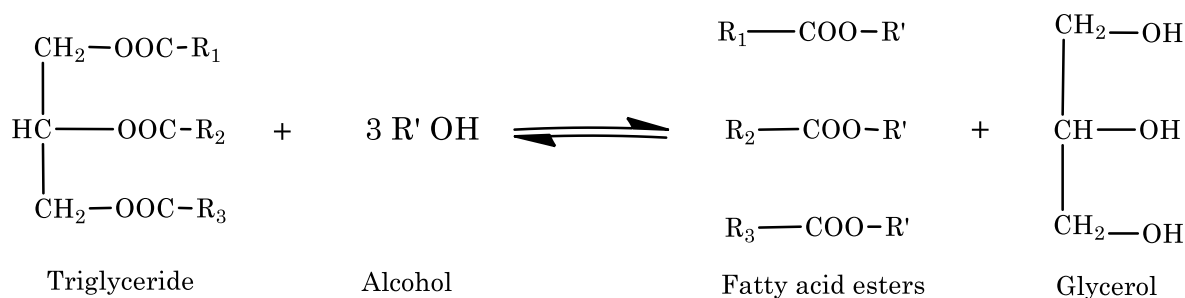
To cut down on the cost of FAME production one alternative would be to use low quality feedstock, as 70-80% of the cost of FAME is mostly dependent on the price of feedstock alone (Babajide *et al.*, 2011). Low cost and quality feedstock which is characterized by high amounts of free fatty acids (FFAs) include waste cooking oils, animal fats, grease as well as non-edible vegetable oils. Esterification is a slow, acid catalyzed reaction and is typically used when the FFAs concentrations are greater than 1% (Solomon, 2002). It is used as a pre-treatment process to prevent the saponification of FFAs by the alkali catalyst from occurring. Sulfuric acid is mostly employed as the catalyst. The esterification reaction is illustrated in Reaction 4.



**Reaction 4:** Esterification of free fatty acid reaction (Babajide *et al.*, 2011)

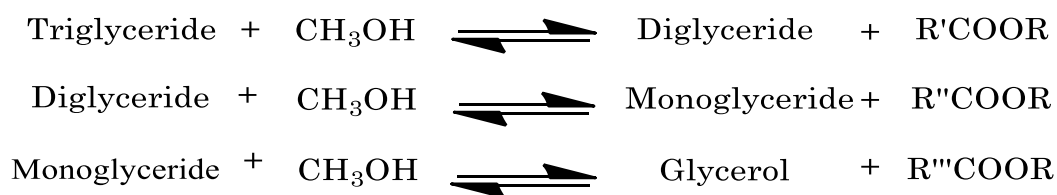
### 3.4 TRANSESTERIFICATION REACTION

Transesterification is the reaction between triglycerides molecules in vegetable oils or animal fat and alcohol to produce esters and glycerol as a by-product (Highina *et al.* (2011). Stoichiometrically, when the reaction occurs, for every 1 mole of triglycerides, three moles of alcohol are utilized (Reaction 5):



**Reaction 5:** Transesterification of triglyceride with alcohol (Fukuda, 2001)

Typically, a higher molar ratio of alcohol to triglyceride is utilized for optimal ester production (Sharma *et al.*, 2008). It is an equilibrium reaction which consists of many sequential steps, reversible reactions where triglyceride is converted stepwise to diglyceride (DG), monoglyceride (MG) and lastly glycerol (GL), yielding one methyl ester from each glyceride at each stage. The basic mechanism is shown in Reaction 6:



**Reaction 6:** General equation for transesterification of triglyceride (Enweremadu & Mbarawa, 2009)

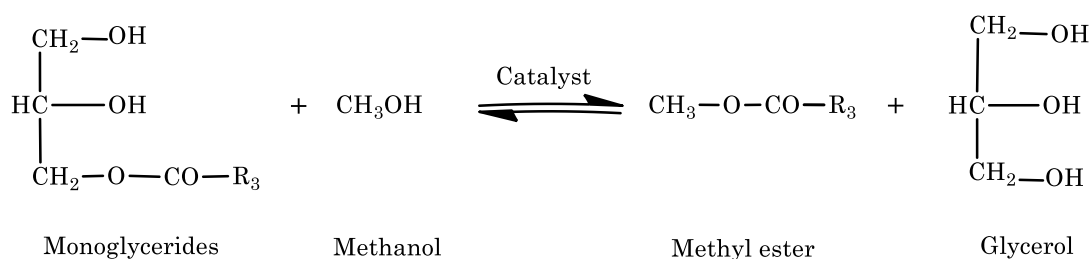
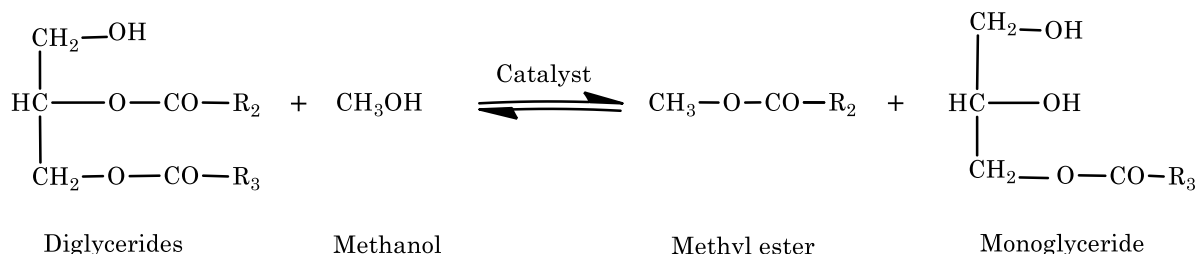
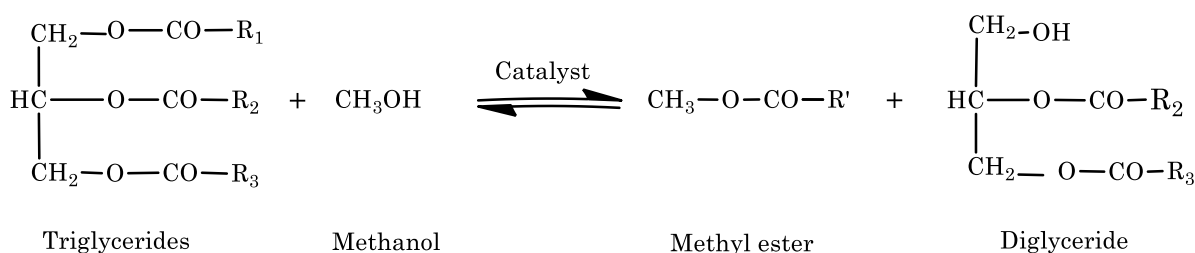
$R_1$ ,  $R_2$  and  $R_3$  are long chain hydrocarbons; at times they are also identified as fatty acids. In the presence of a catalyst, the alcohol molecule will be capable of breaking the fatty acid chains, which results in two distinct products, glycerol and mixture of fatty acid esters (Dennis *et al.*, 2010).

### 3.4.1 Reagents

As illustrated in the reaction above, two reagents are required, oil and an alcohol. The choice of oil and alcohol depend on various criteria. In both cases, availability is critical. Methanol ( $\text{CH}_3\text{OH}$ ), ethanol ( $\text{C}_2\text{H}_5\text{OH}$ ), propanol ( $\text{C}_3\text{H}_7\text{OH}$ ) and butanol ( $\text{C}_4\text{H}_9\text{OH}$ ) are some of the different alcohols used during transesterification reaction to produce FAME (commonly refer to as biodiesel). However, the most commonly used production is methanol (Reaction 7). This is attributed to its availability, high reaction rate and low-cost in comparison to other commercially available alcohols.

Even though ethanol is more soluble in oil than methanol, which improves mass transfer during the transesterification reaction, it is not typically utilized due to the high cost involved in the removal of the water content. Furthermore, methanol can also react with triglycerides more rapidly and easily dissolve the alkali catalyst. In addition, the ester generated from ethanol (fatty acid ethyl ester, FAEE) presents lower pour and cloud points compared to that produced from methanol, which increases the storage facility of FAME (Yaakob *et al.*, 2013). Dennis *et al.* (2010) showed that a methyl ester and ethyl ester have close heat content but the former is considerably less viscous.

When using low cost non-edible oils such as jatropha, pongamia, karanja, waste cooking oil and animal fats, there is a process challenge, owing to high FFA content, which will promote the undesirable saponification reaction (Kemp, 2006). The soap formed may cause problems during the reaction as well as separation of the products. So, pretreatment has to be performed in order to eliminate these FFAs before the subsequent transesterification process. There are two aspects that need to be considered in terms of the production cost, the entire transesterification process and the recovery of glycerol.



**Reaction 7:** Scheme for the step-wise transesterification reaction of triglycerides with methanol

Another important factor to be considered is the type of process used. Transesterification can be performed discontinuously (batch) or continuously. Batch transesterification typically requires a larger reactor, longer reaction time along with extended separation time compared with continuous transesterification due to the fact that reaction stages are carried out in the same reactor. Conventional batch reactors have extensively been utilized except it requires longer times to achieve the full production capacity (Yaakob *et al.*, 2013).

### 3.4.2 Factors Affecting the Yield of Fatty Acid Methyl Esters

The transesterification reaction entails some important parameters which affect the final yield. These include molar ratio of alcohol to oil, reaction time, reaction temperature, catalyst type and concentration, and the amount of free fatty acid in the feedstock. These factors usually have different effects on the transesterification process depending on the technique utilized for the transesterification process, so it is crucial that these parameters are constantly optimized to circumvent incomplete reactions which lead to poor yields. Each of these factors are discussed in the following sections.



### 3.4.2.1 The Effect of Free Fatty Acids

The free fatty acid (FFA) content in the feedstock used for transesterification reaction is a crucial parameter. The content of FFA should be less than 1 % when the base catalyzed transesterification is being utilized (Meher *et al.*, 2006). Using vegetable oils with FFA content higher than 1% will produce lower FAME yields due to neutralization of the catalyst by the FFA. Increasing the catalyst amount increases the chance of saponification which makes ester glycerol separation difficult (Dorado *et al.*, 2003). Ma and Hanna (1999) studied the influence of FFA in the production of FAME. They noticed that the feedstock contained FFA content higher than 1 %, and then the FFA must be refined either through saponification or via a pre-esterification reaction with an acid catalyst.

### 3.4.2.2 Molar Ratio of Alcohol to Oil

This is the principal factor that affects the yield of FAME (Ma & Hanna, 1999; Zhang *et al.*, 2003; Marchetti *et al.*, 2007; Banerjee & Chakraborty, 2009). In transesterification reaction, stoichiometrically, 1 mole of triglyceride and 3 moles of alcohol are required to produce 3 moles of FAME and one mole of glycerol. Nevertheless, since the transesterification is a reversible reaction, an excess of alcohol is usually utilized to make sure that the oil is totally converted into ester owing to the fact that the forward reaction is more favored and in a shorter reaction time. A study by Agarwal *et al.* (2012) on transesterification of waste cooking oil in the presence of homogeneous catalyst using an optimum alcohol to oil molar of 6:1, resulted in a FAME yield of 98 %. On the other hand, transesterification of the same oil using heterogeneous catalyst required a 9:1 alcohol to oil molar ratio resulting in a 96 % yield.

Other researchers also revealed that molar ratio of alcohol to oil from 5:1 (Yaakob *et al.*, 2013), 8:1 (Farooq *et al.*, 2013), 9:1 (Sahoo & Das, 2009), 12:1 (Meher *et al.*, 2006), and higher could also be utilized as the optimum molar ratio of methanol to oil, depending on the quality of feedstock and technique of the transesterification process employed. Additional increase in the amount of alcohol is not favorable to improve the yield of FAME, owing to the fact that it does increase the production cost because of the high amount of energy needed to recover it (Leung *et al.*, 2010). However, the ratio of alcohol/oil can be much higher, up to 15:1, 20:1 or 24:1 when the amount of free fatty acid (FFA) in the oil is very high and an acid catalyzed pre-esterification reaction is employed (Leung *et al.*, 2010; Zhang *et al.*, 2003).

### 3.4.2.3 Reaction Time

The reaction time evidently have an impact on the outcome of the reaction, given that the the conversion rate increases as the reaction time increases (Fan, 2008; Sahoo & Das, 2009). During the transesterification reaction to attain perfect contact between the reagents and the vegetable oil, they should be mixed well at steady rate. The transesterification reaction is usually very slow at the start owing to the immiscibility of the alcohol and oil (Ma & Hanna, 1999). During the course of the reaction, conversion reaches the point where all reagents are miscible, and the reaction goes on very rapidly and normally takes 1 to 2 h to complete (Ma & Hanna, 1999). If the reaction time is not long enough the ester yield will be considerably low, as a result, part of the oil will not react. When using base catalysts, the methyl ester yield achieves maximum at 120 min or less of reaction time (Berchmans & Hirata, 2008; Sahoo & Das, 2009; Berchmans *et al.*, 2010). Peanut oils was transesterified under conditions of methanol/oil molar ratio of 6:1, 0.5% sodium methoxide catalyst and 60 °C in a study by Freedman *et al.* (1984). It was shown that the conversion of the oil to methyl ester was approximately 98% after 1 h of reaction time. In case of acid catalysts, the transesterification reaction requires an even longer reaction time in comparison to the base-catalyzed reaction. This is because base catalysts normally exhibit a higher reactivity than acid catalysts (Georgogianni *et al.*, 2009).

A longer reaction time can cause a decrease in the final methyl ester yield as a result of the backward reaction of transesterification, which eventually leads to more fatty acids to generate soaps (Leung *et al.*, 2010). Thus, optimization of reaction time is also indispensable.

### 3.4.2.4 Reaction Temperature

The temperature of reaction has a strong impact on the rate and yield of FAME (Rashid & Anwar, 2008). High reaction temperature can reduce the viscosities of oils and cause an increase in reaction rate since more energy is being employed for the reaction to take place. Hence, the methyl ester yield is improved. However, saponification of triglyceride is likely to occur if the reaction is conducted above the optimum operating temperature (Leung *et al.*, 2010). In most cases, the temperature ranges between 50-65 °C, but usually a temperature of 60 °C is utilized (Dennis *et al.*, 2010). This is because it is just slightly below the boiling point of methanol, which is 64.7 °C. Thus, at temperatures higher than 64.7 °C, methanol will evaporate causing a decrease in the yield of FAME (Sharma *et al.*, 2008; Hayyan *et al.*, 2010). Depending on the kinds of oil, maximum yields are obtained at temperatures ranging from 60 to 80 °C (Barnwal & Sharma, 2005; Leung *et al.*, 2010).

### **3.4.2.5 Catalyst Weight**

The amount of catalyst used during the transesterification reaction has an effect on the final yield of FAME, depending of the type of oil utilized in process and the type of catalyst utilized.

As the catalyst concentration increases, the conversion of triglycerides and the yield of methyl ester also increases (Demirbas, 2007). This is attributed to the availability of more active sites by the additions of larger quantities of catalyst during the transesterification process. Ma & Hanna, (1999) reported that a concentration of NaOH of 0.3-0.5% gave maximum activity during the transesterification of beef tallow. However, at very high catalyst concentration (more than 5 wt. %), the yield of methyl ester reduced owing to direct saponification of triglycerides. From an economic viewpoint, larger quantities of catalyst may not be cost-effective owing to cost of the catalyst (Elvera *et al.*, 2009; Leung *et al.*, 2010). In addition, at high catalyst concentration, the reaction mixture becomes very viscous when heterogeneous catalysts are employed. Consequently, poor mixing is obtained. Some amount of the catalyst may remain unused owing to mass transfer limitation and also FAME may get adsorbed on the surface of the catalyst, thus, causing a reduction in the yield of alkyl esters (Fan, 2008). Therefore, optimization of the transesterification process is crucial to determine the optimum concentration of catalyst needed during the transesterification reaction.

### **3.4.2.6 The Effect of Mixing**

Vegetables oils and fats do not mix with alcohol, these rather result in a two-phase mixture (Elvera *et al.*, 2009). During the first stages of the reaction, the rate is diffusion controlled and a low rate is a result of poor diffusion between the two phases. As methyl esters are formed, they behave as solvent for both alcohol and oil to create a single phase system. Once the completely mixed single phase system is created, additional mixing becomes insignificant when homogeneous catalysts are utilized.

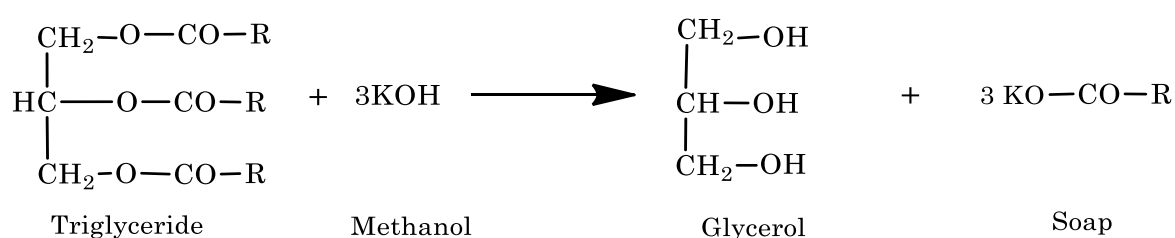
### **3.4.3 Transesterification using Homogeneous Catalysts**

During transesterification reaction, catalysts are used to increase the rate of reaction and the yield of FAME. Catalysts can be homogenous or heterogeneous. Homogeneous catalysts act in the same liquid phase as the reaction mixture, whereas heterogeneous act in a different phase from the reaction mixture, generally as a solid (Borges *et al.*, 2011). Homogeneous (base and acid) catalysts are widely used owing to their simplicity to apply, good performance, cost effectiveness and shorter reaction time for oil conversion in methyl ester production.

### 3.4.3.1 Homogeneous Alkali-Catalysis

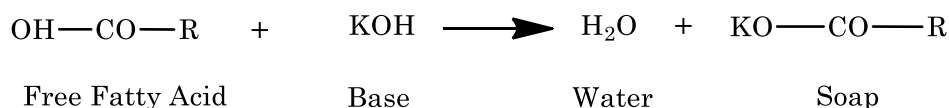
The mostly utilized alkaline catalysts are KOH and NaOH, which are highly soluble in methanol (forming potassium and sodium methoxide [KCH<sub>3</sub>O and CH<sub>3</sub>NaO]) but require several hours to complete the reaction. Sodium or potassium carbonates and alkoxides can also be used. This process is very advantageous due of the fact that very high yield of methyl ester is obtained under mild conditions (Math *et al.*, 2010). Basic catalysts are generally preferred to acid catalysts since they show higher reactivity and lower process temperature are required (Rashid & Anwar, 2008). According to Freedman *et al.* (1984) the alkali-catalyzed transesterification is faster than the acid-catalyzed reaction. In their study, it was observed that sodium methoxide (CH<sub>3</sub>NaO) was more effective than NaOH because some water was discharged in the mixing of methanol and NaOH which led to hydrolysis. However, NaOH is more economical than CH<sub>3</sub>NaO. These alkaline catalysts give good performance when feedstock with high quality (FFA < 1 wt. % and moisture < 0.5 wt. %) are utilized (Helwani *et al.*, 2009). Sivakumar *et al.* (2011) generated methyl ester from dairy waste scum and achieved 96.7% of FAME under optimal conditions of molar ratio of methanol to oil 6:1, 1.2 wt. % of KOH; reaction temperature 75 °C; reaction time 30 min at 350 rpm.

Vicente *et al.* (2004) also investigated the use of sodium and potassium hydroxides and methoxides as catalysts in the transesterification of sunflower oil utilizing a methanol/oil molar ratio of 6:1 and 1wt. % catalyst load. The yields of esters obtained were 85.9 and 91.67 wt. % for the sodium and potassium and 98% for the methoxide catalyst correspondingly. Undesired saponification (Reaction 8) when using KOH and NaOH resulted in significant yield reduction.



**Reaction 8:** Saponification of triglycerides (Vicente *et al.*, 2004)

One of the drawbacks of transesterification mediated by alkaline catalysts is that, triglycerides and the alcohol need to be anhydrous, as well as a low content of FFA, as these are able to react with the basic catalyst and generate soaps and water (Reaction 9) (Borges *et al.*, 2011).



**Reaction 9:** Free fatty acids saponification (Borges *et al.*, 2011)

The formation of soap during reaction causes catalyst consumption, reduction in ester yield and prevents the separation of glycerol from methyl ester (Verziu *et al.*, 2011). Homogeneous catalyzed transesterification reaction demonstrates major disadvantages for large scale methyl ester production. The production costs involved are high as the process includes washing/purification stages so as to meet the specified methyl ester quality requirements. It is reasonably difficult to remove Na/K traces from the methyl ester product, separation process of glycerol necessitates upgrading and large amounts of alcohol is required (Liu *et al.*, 2007). In addition, large amounts of water are needed in the washing process and consequently treatment of the effluent which contributes to the overall cost.

### 3.4.3.2 Homogeneous Acid-Catalysis

On the other hand, with feedstock such as *jatropha curcas*, waste cooking, tobacco oils, rubber. which contain a high content of FFA, typically a strong acid-catalyst such as hydrochloric, sulfuric or phosphoric acid, is better suited in comparison to a base-catalyst since the reaction does not generate soap (Kulkarni & Dalai, 2006; Canakci & Gerpen, 2003). Nevertheless, acid-catalyst is very susceptible to the amount of water in the feedstock. According to Canakci & Gerpen (2003) in order to achieve a good FAME conversion, the acid catalyst also requires water content lower than 0.5%, which is approximately the same for alkaline reaction. Whereas only 0.1% of water in the reaction medium is enough to result in some decrease of the methyl ester yield and water composition of 5 wt. %, completely represses the reaction. Freedman *et al.* (1984) studied the transesterification of soybean oil in the presence of 1% H<sub>2</sub>SO<sub>4</sub> with a methanol/oil molar ratio of 30:1, at a reaction temperature of 65 °C for 50 h. A methyl ester yield of over 99% was obtained.

Simultaneous esterification and transesterification reactions using acid catalysts under the reaction conditions of temperature 60 °C; molar ratio of methanol/oil 6:1; H<sub>2</sub>SO<sub>4</sub> 3.0 wt. %, and reaction time of 96 h was performed (Canakci & Gerpen, 1999). The yield of FAME attained was more than 90% with a moisture content of 0.5 wt. %. Various feedstock, including waste cooking oil and rice bran oil have been successfully transesterified using methanol in the presence of H<sub>2</sub>SO<sub>4</sub> at a temperature range of 60-80 °C (Zullaikah *et al.*, 2005; Zheng *et al.*, 2006). Zullaikah *et al.* (2005) reported studies on the acid catalyzed methanolysis of dewaxed rice bran oil with variation in the FFA content (20-80%) at atmospheric pressure using a methanol/oil molar ratio of 1:10 at 60

°C and with 2 wt. % H<sub>2</sub>SO<sub>4</sub> as catalyst. The rate of methanolysis and the final methyl ester content in the product were influenced by the initial FFA content of the feedstock. A FAME content of approximately 96% was attained in 8 h for rice bran oil containing an initial FFA content of 76%. Constant residual acid content (2-3 wt. %) was observed owing to the presence of tocopherols, oryzanol and/or other negligible components in the rice bran oil. Acid-catalyzed alcoholysis of triglycerides is a slow reaction, even after 24 h, a substantial amount of unreacted triglyceride was detected if the initial oil had more than 20% FFA content (Zullaikah *et al.*, 2005).

The use of homogeneous acid catalysts has various disadvantages, including a longer reaction time, higher temperature (above 100 °C) and equipment corrosion. Furthermore, to increase triglyceride conversion, an excessive quantity of methanol, for example, molar ratio of methanol/oil > 12:1 is required (Meher *et al.*, 2006). In order to reduce the reaction time, acid-catalysis is employed as a pre-treatment stage to convert FFA to esters, and is followed by the addition of a base-catalyst for the transesterification step to convert triglyceride into esters.

#### **3.4.4 Transesterification using Heterogeneous Catalysts**

Due to the difficulties associated with homogeneous catalyzed transesterification, heterogeneous catalyzed transesterification methods have been extensively applied for methyl ester production (Arzamendi *et al.*, 2007; Di Serio *et al.*, 2008; Hara, 2009; Zabeti *et al.*, 2009; Janaun & Ellis, 2010; Borges *et al.*, 2011). This process requires no neutralization and simple purification steps are required. Moreover, heterogeneous catalysts are more environmentally friendly and correspond to a more sustainable form of resource management. Heterogeneous catalytic conversion effectiveness depends on the solid catalyst's activity (Liu *et al.*, 2007). There are three types of inorganic solid catalysts that can be utilized for transesterification reaction namely: basic, acidic and bifunctional.

Heterogeneous bifunctional catalysts are able to mediate esterification and transesterification simultaneously (Janaun & Ellis, 2010; Borges *et al.*, 2011). Heterogeneous catalysts can be recycled, reused and regenerated. Their use is associated with less energy consumption, no saponification reaction; simplified glycerol purification better FAME yields in shorter reaction time (Liu *et al.*, 2007). Additionally, they are more tolerant to FFAs and water content in the feedstock. In spite of these merits, heterogeneous catalysts usually require elevated reaction conditions in comparison to homogeneous catalysts (Sharma *et al.*, 2011). These include high temperatures and pressures, high alcohol/oil molar ratio, longer reaction time owing to mass transfer limitation of oil-alcohol-heterogeneous catalyst (three-phase system) (Hara, 2009; Sharma *et al.*, 2011).

There are still improvements to be made on the formulations as to allow their higher natural efficiency in this reaction. Solid-alkaline catalysts are more attractive than solid-acidic catalysts, owing to the fact that relatively shorter reaction times and lower reaction temperatures are required (Dorado *et al.*, 2003). However, solid-acidic catalysts are less sensitive to FFA and water, they do not dissolve in the feedstock and alcohol, and therefore they can be easily separated through filtration and can be used again. Such catalysts are efficient for the esterification of FFA and transesterification of triglycerides (Peterson & Scarrah, 1984; Hara, 2009).

The most studied solid heterogeneous catalysts are metal oxides of alkaline earth metals (such as Mg, Ca, Be, Ba, Sr), mixed oxides, zeolites,  $\gamma$ -alumina as well as hydrotalcites. These catalysts can be simply separated from the reaction mixture and reused. The majority of these catalysts are alkaline/alkali oxides impregnated on substances with large surface areas. CaO and MgO are rich in nature and extensively utilized among alkaline earth metals (Demirbas, 2007; Sharma *et al.*, 2011). The order of activity of the alkaline earth oxide catalysts is BaO > SrO > CaO > MgO. CaO is mostly utilized owing to its characteristic advantages including low cost, high activity and long catalyst life. Its use involves mild reaction conditions, hence, less environmental impacts (Math *et al.*, 2010). There are a number of readily available calcium sources such as mollusk shells and egg shells. These shells are made up of calcium carbonates which can be calcined to calcium oxide for FAME production (Viriya-empikul *et al.*, 2010; Cho & Seo, 2010).

Hawash *et al.* (2011) used 1.5 wt % calcium oxide to optimize the production of methyl ester from *Jatropha oil* via transesterification, where 95% methyl ester yield was achieved at 70 °C for 3 h and with a methanol/oil molar ratio of 12:1. Van Isahak *et al.* (2010) reported the use of bulk calcium oxide and nano-calcium oxide catalysts in transesterification of palm oil with 2.5 % catalysts w/w of oil, reaction temperature of 65 °C for 150 minutes, methanol/oil molar ratio of 15:1 achieving a conversion of 90-94% of methyl ester. Ngamcharussrivichai *et al.* (2010) calcined dolomite (mainly MgCO<sub>3</sub> and CaCO<sub>3</sub>) at a temperature of 800 °C for 2 h to prepare MgO and CaO catalysts for palm kernel oil transesterification. It gives a FAME yield of 98% at a molar ratio of methanol/oil of 30:1; reaction temperature of 60 °C, amount of catalyst of 6 wt. %, and reaction time of 3 h. Subsequent to each run, the catalyst was separated by means of centrifuge and rinsed with methanol, and utilized for other runs. The results obtained demonstrated that the FAME yield was more than 90% after up to the 7<sup>th</sup> use.

Di Serio *et al.* (2005) and Di Serio *et al.* (2008) used MgO catalyst, and obtained 92% FAME yield using 12:1 methanol/oil molar ratio with 5.0 wt. % of the catalyst in 1 h reaction time. Dossin *et al.* (2006) observed that MgO works efficiently in batch reactor at ambient temperature in the transesterification reaction with a production capacity

500 tonnes of biodiesel. Liu *et al.* (2007) studied SrO for the transesterification of soybean oil. A yield of 95% was obtained at 65 °C with catalyst loading of 3 wt. % and methanol/oil molar ratio of 12:1 within reaction time of 30 min. A considerable reduction in the yield of methyl ester was noticed when the SrO catalyst was reused for 10 cycles.

Lingfeng *et al.* (2007) performed the transesterification of cottonseed oil with methanol utilizing KF/ $\gamma$ -Al<sub>2</sub>O<sub>3</sub> as heterogeneous catalysts. The reaction parameters used were methanol/oil molar ratio (6:1-18:1), temperature (50-68 °C) and catalyst amount (1-5 wt. %). The methyl ester with the most favorable properties was attained using a catalyst concentration of 4 wt. %, methanol/oil molar ratio of 12:1, reaction temperature of 65 °C and reaction time of 3 h and with the catalyst (KF/ $\gamma$ -Al<sub>2</sub>O<sub>3</sub>) mass ratio of 50.36%.

Wen *et al.* (2010) utilized mixed oxides of TiO<sub>2</sub>-MgO generated via the sol-gel method to convert waste cooking oil into methyl ester. The most favorable catalyst was MT-1-923 having a Mg/Ti molar ratio of 1 and calcined at a temperature of 650 °C. The maximum yield of FAME achieved was 92.3% which was obtained with catalyst amount of 10 wt. %; methanol to oil of 50:1; reaction temperature of 160 °C and reaction time of 6 h. They noticed that the catalytic activity of MT-1-923 reduced very slowly during the recycle process. To recover the catalytic activity, a two-step washing technique (the catalyst was cleaned using methanol four times and afterward with n-hexane one time prior to undergoing drying at 120 °C). The yield of FAME increased slightly to 93.8% in comparison with the 92.8% obtained with the fresh catalyst, this was due to an increase in the average pore diameter and specific surface area. TiO<sub>2</sub>-MgO exhibited great potential in large-scale FAME production from waste cooking oil.

Lingfeng *et al.* (2007) investigated methyl ester production using palm oil with methanol over a KF/Al<sub>2</sub>O<sub>3</sub> heterogeneous base catalyst. The methyl ester yield reached its maximum value of over 90% at the most advantageous condition, when the molar ratio of methanol/oil was 12:1 with a load ratio of KF/Al<sub>2</sub>O<sub>3</sub> of 0.331 (wt./wt.) and a KF/Al<sub>2</sub>O<sub>3</sub> catalyst amount of 4 wt.% of oil, a reaction temperature was 65 °C and a reaction time of 3 h. Teng *et al.* (2009) also studied and reported the transesterification of soybean oil for methyl ester production using KF/ $\gamma$ -Al<sub>2</sub>O<sub>3</sub> as an active catalyst. The most favorable conditions for the reaction were as followed: the load ratio of KF to  $\gamma$ -Al<sub>2</sub>O<sub>3</sub> was 72.68% (wt/wt), methanol/oil molar ratio of 12:1, catalyst concentration of 2 wt.% of oil, reaction temperature of 65 °C for 3 h. Under these conditions, the methyl ester yield reached over 99%.

Other currently developed catalysts for the production of methyl esters are biomass pyrolysis by-products which includes biochar, flyash, sugars, etc. (Toda *et al.*, 2005; Kotwal *et al.*, 2009). Natural products such as sugars, starch or cellulose were sulfonated



by Toda *et al.* (2005). These materials were incompletely carbonized which resulted in a rigid solid carbon substance; which was then used as a catalyst to produce high-grade methyl ester. The obtained results showed that these acid catalysts are more effective than other conventional solid acid-catalysts. Moreover, during the process there was no loss of activity or leaching of  $-\text{SO}_3\text{H}$  group. Additionally, the utilization of biomass materials is cost-effective and environmentally friendly. Zong *et al.* (2007) effectively performed the esterification of FFAs such as palmitic, stearic and oleic acids using  $\text{CH}_3\text{OH}$  in the presence of a D-glucose-derived catalyst. More than 95 % of FAME yield was achieved under the reaction conditions of 100 mmol methanol, 0.14 g sugar catalyst, 10 mmol FFA and a reaction temperature of 80 °C.

In general, the main issue related to heterogeneous catalysts is their deactivation with time due to various possible phenomena, for instance, coking, sintering, poisoning as well as leaching (Mazzocchia *et al.*, 2004). Poisoning is evident when the process involves used oils. While catalyst leaching not only increases the operational cost on account of substituting the catalyst but also leads to contamination of the product (Mazzocchia *et al.*, 2004; Barbosa *et al.*, 2006). Also, heterogeneous catalysts form three phases with alcohol and oil leading to diffusion drawbacks hence lowering the reaction rate (Enweremadu & Mbarawa, 2009). The mass transfer problem in heterogeneous catalysis can be fixed by making use of structure promoters or catalysts supports which are capable of providing more specific surface area and pores for active species where they can react with large triglycerides molecules (Zabeti *et al.*, 2009).

For that matter, alumina has been extensively utilized as a support in catalysis processes due to its exceptionally thermal resistance, mechanical stability, high specific surface area, high porosity, large pore size and pore volume, low density and transition crystalline phase existed in a wide-range of temperatures (Sharma *et al.*, 2010). Moreover, it serves as carrier with both solid base as well as acid. The majority of the super basicity sources can be well dispersed on the  $\text{Al}_2\text{O}_3$  support in the form of a monolayer at a low loading (Zabeti *et al.*, 2009). Additionally, alumina is believed to be more resistant comparing to other supports (for example: calcium oxide, silica, and zeolite) for alkali species.

### **3.4.5 Catalysts for Simultaneous Esterification and Transesterification**

Low cost feedstock contains high amounts of FFA's (free fatty acids) and water which lowers yield of the esters. For instance, Teng *et al.* (2009) reported the effect of the presence of water on rapeseed oil transesterification. Conversion decreased from 95 % to 86 % as the weight percentage of water increased from 1.0% to 4.0% (in relation to the weight of rapeseed oil), in comparison to the conversion of 98 % observed in the absence of water. The negative impact on conversion can be attributed to hydrolysis reaction in

the presence of water. This also causes serious separation and emulsification problems. To avoid this, a two-stage catalytic process has been developed. Firstly, the feedstock needs to be pre-treated, to reduce the content of FFA present. It is achieved by the use of catalysts such as ferric sulfate or Iron (III) sulfate [ $\text{Fe}_2(\text{SO}_4)_3$ ] and sulfuric acid ( $\text{H}_2\text{SO}_4$ ) then followed by the use of a basic catalyst to generate methyl esters (Hayyan *et al.*, 2010). Patil *et al.* (2010) studied a two-step process for the production of FAME so as to convert waste cooking oil to methyl esters. The process included esterification reaction for the conversion of FFA to FAME by Iron (III) sulfate subsequent transesterification for the conversion of triglycerides to FAME using KOH. Nevertheless, the two-stage process still faces the issue of catalyst removal in both steps. In the first step, the catalyst removal issue can be prevented by acid catalyst neutralization, using high quantities of alkaline catalyst in the second step (Liu *et al.*, 2007). Using extra catalyst adds additional costs to methyl ester production. Both catalysts should always be removed from the methyl ester once the reaction has gone to completion.

Bifunctional catalysts, possessing both basic and acidic sites can be employed for simultaneous esterification and transesterification reactions for methyl ester production (Salinas *et al.*, 2010). Tests on the catalytic activity of Quintinite-3T as bifunctional heterogeneous catalyst capable of converting FFA and triglycerides into FAME at the same time were reported by Kondamudi *et al.* (2011). The catalyst was produced via the sol-gel method and tested for canola, soy, coffee, in addition to waste vegetable oils with variable FFA contents (0-30 wt.%). Using canola oil, a yield of FAME of 97.28% was obtained under the optimum conditions of 12:1 methanol/oil molar ratio, reaction temperature of 75 °C, a catalyst loading of 10 wt. % in 2 h. Coffee oil (33 wt. % FFA) gave a yield of FAME of 96.6% under the operation conditions of 12:1 methanol/oil molar ratio, reaction temperature of 75 °C, a catalyst loading of 10 wt. % in 4 h. But when utilizing waste vegetable oil (15 wt.% FFA) the highest FAME yield of 97.72% was obtained, under reaction time of 6h at reaction temperature of 75 °C, with a methanol/oil molar ratio of 12:1 and a catalyst amount of 10 wt.%.

A mixed oxide catalysts of  $\text{MgO}/\text{TiO}_2$  prepared by the sol-gel method was used by Wen *et al.* (2010) for large-scale production of methyl ester from waste cooking oil (containing 3 wt. % FFA). It gave a yield of FAME of 91.6% under the operation conditions of 50:1 methanol/oil molar ratio, reaction temperature of 170 °C, a catalyst amount of 10 wt. % in 6 h. Amin & Omar (2011) reported transesterification of waste palm oil (5.08 wt. % FFA) to methyl ester over  $\text{Sr}/\text{ZrO}_2$  catalyst. When strontium metal was doped on catalyst, it increased the amphoteric nature of zirconia which contained acid and basic sites. A FAME yield of 79.7% was obtained, under reaction time of 87 min at reaction temperature of 115.5 °C, with a methanol/oil molar ratio of 29:1 and a catalyst amount of 2.7 wt.%. The presence of acid and basic sites in  $\text{Sr}/\text{ZrO}_2$  makes simultaneous

esterification and transesterification reactions much easier. Farooqa *et al.* (2013) investigated several bifunctional heterogeneous catalysts for methyl ester production from waste cooking oil. The Mo–Mn/ $\gamma$ -Al<sub>2</sub>O<sub>3</sub>-15wt. % MgO catalyst gave the highest FAME yield of 91.4%, under reaction time of 4 h at reaction temperature of 100 °C, with a methanol/oil molar ratio of 27:1. Furthermore, the bifunctional heterogeneous catalyst showed substantial chemical stability and could be used again for at least 8 times with minor losses in its catalytic activity.

### 3.4.6 Enzymatic Transesterification

Enzymatic catalysts (particularly lipase) have shown various advantages such as less energy due to the fact that reactions occur at room temperature, insensitive to FFA, the catalyst and glycerol are easily recovered, and the water-washing step is kept to a minimum hence reducing wastewater treatment. *Pseudomonas cepacia* (PS 30), *Mucor miehei* (Lipozym IM 60), *Bacillus subtilis* and Novozym 435 are some examples of enzyme preparations that have demonstrated good catalytic activity in the mediation of transesterification reaction. Additionally, enzymatic catalysts have been improved with the introduction of immobilization technology (Hsu *et al.*, 2004). The intention of immobilization is to provide a more rigid external backbone for lipase so that it can sustain high stability, be easily recycled and reused for multiple reactions (Shah *et al.*, 2004).

In transesterification using enzymatic catalyst, solvent is added into the reaction media to ensure homogeneity between the oil and alcohol (reducing mass transfer drawback) and therefore improving lipase catalytic activity (Du *et al.*, 2003). In general, n-hexane has a preference because of its low cost and its easy market availability. On the other hand, it was found that the solubility of methanol and glycerol in n-hexane is low and this leads to lipase deactivation (Shah *et al.*, 2004; Kumari *et al.*, 2007). After years of research, it was found that *tert*-butanol was a superior solvent comparing to n-hexane. Methanol and glycerol can easily be dissolved in *tert*-butanol which reduces the contamination rate caused by methanol and minimizes the deposition of glycerol on the immobilized lipase (Kumari & Gupta, 2007). Royon *et al.* (2007) added *tert*-butanol into the reaction mixture and observed that the catalytic activity of Novozym 435 increased by approximately 358%.

Nielsen *et al.* (2008) also noticed the same during the transesterification of waste cooking palm oil when Novozym 435 was utilized. However, a number of issues must still be dealt with due to the use of solvent in the transesterification catalyst, such as: (1) extra reactor volume to accommodate the additional volume of solvent, (2) plant safety requirement (toxicity of solvent) (3) high production cost (additional solvent recovery steps) (Du *et al.*, 2003; Shah *et al.*, 2004). Unlike chemical catalysts, enzymatic

transesterification needs certain quantity of water in the reaction media to preserve the enzyme catalytic activity. Commonly, the availability of interfacial area is one of the parameters that has an impact on the catalytic activity (Shah *et al.*, 2004). However, the use of this catalyst has limitations due to the high cost of lipase and slow reaction rate (Kumari *et al.*, 2007).

### 3.4.7 Non-catalytic transesterification

Owing to the drawbacks of most of the catalysts (chemicals and enzymes), a non-catalytic process with supercritical alcohol (commonly methanol) has been developed (Xin *et al.*, 2008; Saka & Isayama, 2009). Transesterification with no catalyst is the application of alcohols in the supercritical state that is heated above the critical temperature. Demirbas (2007) studied the transesterification of sunflower oil under supercritical condition at a lower temperature for methyl ester production. The reaction was carried out with methanol in the presence of CaO as catalyst and the results showed that the transesterification reaction was completed within 6 min using a molar ratio of methanol/oil of 41:1, 3 wt. % of CaO catalyst at reaction temperature of 251.85 °C as opposed to a temperature of more than 326.85 °C in the case without catalyst. Varma & Madras (2007) synthesized methyl ester from castor oil with methanol and ethanol in the presence of Novozym 435 in supercritical CO<sub>2</sub>.

Supercritical methanol method has been reported to be advantageous over the traditional process regarding the elimination of catalysts, simple separation of products, quicker reaction rate and thus, has a higher possibility to produce methyl ester on a continuous basis, elimination of soap formation, removal of FFA and water contents on the ester yield, no further purification step (water washing) needed, reduced wastewater treatment (Campanelli *et al.*, 2010; Quesada-Medina & Olivares-Carrillo, 2011). Moreover, this process is very water-tolerant in comparison to the methods utilizing alkaline catalysts (Devanesan *et al.*, 2007; Kumari *et al.*, 2007). However, the supercritical methanol method has serious disadvantages due to the fact that it requires high temperature, high pressure, large quantities of alcohol (1:42 molar ratio of oil/alcohol), high energy consumption as well as high production cost (Saka *et al.*, 2010). Lee *et al.* (2012) also performed supercritical transesterification of canola oil and attained a yield of about 100% at 270 °C and 100 bar for 45 min with methanol/oil molar ratio of 2:1. Tan *et al.* (2011) used methyl acetate at 400 °C and 220 bar with methanol/oil ratio of 30:1 to conduct a supercritical transesterification of used oil where 99% of FAME yield was achieved within 1h.

## 3.5 SOLID CATALYSTS PREPARATION

A number of industrial heterogeneous catalysts are prepared through the fusion of mixtures of their individual oxidic or metallic precursors. The method utilized to prepare a catalyst has an impact on the catalyst's performance (Geus & van Veen, 1999). Typically, there are two major methods utilized for catalyst preparation; namely precipitation and impregnation. Ion exchange and vapour phase deposition techniques are other methods. Vapour phase deposition techniques have great potential, in the sense that high metal dispersion is attained without deactivation via strong metal support interaction (Zabeti *et al.*, 2009).

### 3.5.1 Impregnation

Impregnation is a typical method used to make supported catalysts (Chavali *et al.*, 2004). The incipient wetness (or dry) impregnation method involves the addition of a solution of the active precursor to the dry support powder until the mixture becomes viscous, demonstrating that the pores of the support are completely filled with the liquid (Haber *et al.*, 1995; Augustine, 1996; Satterfield, 1980). Subsequently, the liquid is also removed during the calcination step. This results in an oxidic catalyst precursor. The procedure is then repeated until the desired level of metal concentration on the support is obtained. When numerous precursors are present at the same time in the impregnating solution, the impregnation is referred to as co-impregnation. Here, three processes happen; transport of solute within the pore system of the support bodies, dispersion of solute within the pore system, uptake of solute by the pore wall.

Another method which can also be used is vacuum pore impregnation, where the support is first dried and subsequently placed under vacuum, infilling the pores of air. A volume of precursor solution corresponding to the pore volume is then combined with the support under vacuum. The solution is absorbed in the pores of the seemingly-dry powder. Very high concentrations of active material can be attained by drying the catalyst. This method is very advantageous due to the synthesis simplicity, no complex equipment is needed for the preparation of the catalyst, additionally, it functions with the use of any porous material and metal salt combination providing that a solvent compatible with both exists.

The simplicity of the preparation method allows large amounts of catalysts to be produced. However, this technique offers poor control over the distribution of metal particles in the pores and the surface. The activation steps for instance evaporation of the solvent needs particular attention as it may result into agglomeration of metal precursors and the creation of very large particles (Chavali *et al.*, 2004). Another issue is the incapability to produce highly dispersed catalysts at high metal weight loading.

### 3.5.2 Precipitation and Co-Precipitation

Precipitation methods are utilized for the production of many important catalysts and support materials such as alumina, silica, and the Cu/ZnO/Al<sub>2</sub>O<sub>3</sub> methanol synthesis catalyst. During this process, the objective is to obtain a reaction of the type (Hermans and Geus, 1979) as follows:



This method has been utilized to produce supported molybdenum, manganese, nickel, vanadium, iron, and copper catalysts with a homogenous distribution during the whole support. The chance of obtaining a highly pure final substances and the flexibility of the co-precipitation and precipitation process are the major attractions of this otherwise demanding method (Morikawa *et al.*, 1967; Augustine, 1996). Usually, a high dispersion of the metal components in the final product is acquired. In this instance, the soluble salts of the active phase (metals) normally nitrates, are dissolved in water or in an appropriate medium to create a homogeneous solution. Then, the solution undergoes pH adjustment with the addition of suitable precipitating agent to cause the precipitation of the desired metal ions, solid precursors of the wanted catalyst. The ether soluble salts are less favoured in comparison to nitrate salt. This is due to the fact that nitrate salt is most likely to be the least corrosive and in the course of filtration and afterwards calcinations, the remaining anion in the precipitate decomposes with no difficulty. Complex form of the active metal salts such as the metal formate, glycolate, oxalate or acetate, may in most cases be the preferred choice. Owing to environmental regulations, the disposal of the nitrate-rich filtrate might be a problem (Yermakov *et al.*, 1981).

Subsequently, washing of the solids is needed for complete removal of the mother liquor and to get rid of any dirty. When it comes to separate the solid phase from the mother fluid, this is quite easy in cases of crystalline precipitates, but difficult for flocculates and impossible for hydrogels. The separation method is chosen according to the solids particle size. The slurry is added to a large amount of deionized water and the suspension is meticulously blended, allowing for particles to settle down. Water is eliminated via decantation when a definite interface is visible and the process is done again until the wanted purity is attained. The washing and settling time should not take too long. As soon as washing is completed the solid is then filtered. If the particles are too small and take long to settle, filtration or centrifugation should be utilized. Washing may also be employed to remove certain unwanted or worthless ions for others that are simply decomposed through calcination. A suitable salt solution in water must be utilized as an alternative for deionized water. Elevated temperature for instance 100 °C can raise the efficiency of the exchange rate of Na<sup>+</sup> for NH<sub>4</sub><sup>+</sup> which is utilized to get the

ammonium form of a zeolite, which is converted into the acidic form via the calcination process (Mul & Hirschon, 2001).

One of the major challenges with the preparation of co-precipitated catalysts is with the drying and calcinations process (Teichner *et al.*, 1976). Drying involves the removal of the solvent (typically water) used in crystallization is eliminated from the solid pores. Usually, this is applied in crystalline solids, however becomes critical for flocculates and especially for hydrogels which presents up to 90% water content (Mul & Hirschon, 2001). Water removal may cause the collapse of the structure. If high porosity is desired, the drying operations should be properly controlled. Evaporation of the solvent generates a vapour-liquid interface within the pores of the solid. Water and other high surface tension solvent gives particles with lower surface area owing to partial collapse of the solid (Van Gorp, 1996). Since, the precursor ions are distributed within the volume of the support oxide and the pore structure of the finished catalyst is harder to control compared to starting from a separately produced carrier. The rate of water loss is constant and the mass transfer is controlled through relative humidity, flow rate of air over the surface, temperature and particle size. Drying is a very critical stage and may well determine the quality of the catalyst.

In general, the precipitation process is performed jointly with the promoter atoms precursors (Lee *et al.*, 2014). After drying and calcination, the obtained precipitate yields the oxidic catalyst precursors. The resultant powder morphology, pore structure, physical strength, texture and its performance (that is, stability, activity, and selectivity) is determined by the procedures and conditions of precipitation. In addition, the physical and chemical properties of the final particles are greatly influenced by the conditions under which the crystallites are formed. By varying the amount of the precursor salts and precipitating agents solutions, precipitation temperature, mixing intensity, technique of addition and pH, the crystallite size as well as the pore volume for instance can be optimized (Perego & Villa, 1997). In comparison with other methods, catalysts prepared by co-precipitation method, yields catalysts with more homogenous metal composition, excellent crystallite sizes, better dispersion (Hermans & Geus, 1979). It also makes possible for incorporation of higher loading of the active components all in one step production (Augustine, 1996). Precipitation is the favored deposition method for loading higher than 10-20% whereas below this value, impregnation is generally used.

**Calcination and Reduction** – The majority of the synthetic methods for catalysts preparation require further activation stages in order to generate a catalytically active disperse phase (Hattori, 2001). During the calcination process, reduction of the metal carbonates and other anions of the corresponding metal oxides occur. Calcination is an additional heat-treatment beyond drying at high temperatures (300-800 °C). A number

of processes arise in the course of calcination, including structure alteration, active phase generation, loss of CO<sub>2</sub> or the chemically bonded water, small particles or crystals tend to turn into bigger ones through sintering, and mechanical properties stabilization. A good example is alumina which shows all these characteristics. This process involves heating the catalysts in an oxidizing atmosphere at a typically higher temperature than that encountered during reaction (Hattori, 2001). The objective of calcination is to decompose (either in air or in a synthetic gas combination) the metal precursor (typically nitrates/carbonates) by forming an oxide and removing the gaseous products (usually water and CO<sub>2</sub>) as well as the cations/anions which have been formerly introduced. For instance calcination temperature of 550 °C was found to be optimum for CaO as catalyst to eliminate the poisoning substances (principally water and/or carbonate), since Ca(OH)<sub>2</sub> is dried out at 550 °C (Sharma *et al.*, 2010). Further increase in calcination temperature to 600-700 °C considerably decreased its catalytic activity. The catalyst calcined at 900 °C resulted in 0% yield of FAME. Apart from decomposition, during the calcination a sintering of the formed oxide or of the precursor and reaction of the formed oxide with the support may happen (Van Gorp, 1996). In actual fact, in case of alumina as the support, if calcination is carried out at temperatures in the region of 500-600 °C, it can give rise to a reaction with divalent metal (Ni, Co, Cu) oxides with consequent formation of metal aluminates which are more stable in comparison to the oxides (Pinna, 1998). In this case, higher temperatures of reduction are needed. To demonstrate this, Xie & Huang (2006); Xie & Li (2006) and Xie *et al.* (2006) performed extensive studies on the transesterification of vegetable oil using supported catalysts under different calcination temperatures. They concluded that optimization of the calcination temperature when preparing catalysts is crucial to reach high catalytic performance.

Catalysts calcined at 500-600 °C, for instance KI/Al<sub>2</sub>O<sub>3</sub> and KNO<sub>3</sub>/Al<sub>2</sub>O<sub>3</sub>, demonstrated very good performance during the transesterification of vegetable oil. Zabeti *et al.* (2009) have reported the temperature of 718 °C as the optimum calcination temperature for CaO/Al<sub>2</sub>O<sub>3</sub> in transesterification of palm oil. Sawangkeaw *et al.* (2012) also used 40 wt. % CaO/Al<sub>2</sub>O<sub>3</sub> for the transesterification of palm oil and calcined it at 500 °C for 2 h. While Galadima & Garba (2009) reported the transesterification of neem seed oil using 5wt% CaO/Al<sub>2</sub>O<sub>3</sub> calcined at 400 °C and a yield of 95.63 % was achieved. Yalman (2012) performed the transesterification of safflower and canola oils in the presence of CaO/Al<sub>2</sub>O<sub>3</sub> with loadings of 60, 70 and 80 wt. %. The Catalysts were calcined at various temperatures 400-700 °C. It was observed that 70% CaO/Al<sub>2</sub>O<sub>3</sub> catalyst when calcined at 700 °C had the highest catalytic activity resulting in a high FAME yield (~95%). Altering the calcination temperature even when phase transitions are avoided can have an effect on the pore size distribution (Perego & Villa, 1997). In contrast to drying, calcination can be placed before or after the catalyst synthesis step, in a controlled environment, so as to



avoid pore collapse. Further thermal treatments include reductions or sulfidations which are conducted in unique atmospheres.

### 3.6 CATALYST CHARACTERIZATION TECHNIQUES

Important catalyst parameters such as chemical surface and texture are determined to relate catalytic activity to characteristics. Thus, characterization of catalysts becomes a crucial point in any study. In the current study, BET, SEM-EDX and TEM analyses were employed to assess the surface area, particle size, particle size distribution, pore size, the pore volume distribution, elemental composition and the elemental distribution. The bulk phases present were studied using XRD whereas the reducibility and the maximum degree of reduction of the metal oxides were studied by means of the TGA method. All techniques are described below.

#### 3.6.1 Thermo-Gravimetric Analysis (TGA)

Thermo-gravimetry analysis continuously measures the quantity (or mass) and rate of change in the weight of a sample subjected to a steady increase in temperature in a controlled atmosphere; so as to compute reactions involving gaseous emissions. A TGA run of a sample will usually exhibit weight-loss steps corresponding to various stages in the degradation of the original substance. Weight losses correspond to secondary reactions of the initial degradation steps. Basically, measurements are performed to determine the composition of substances and to predict their thermal stability at very high temperatures (up to 1200 °C). The technique is able to characterize substances that show weight loss or gain caused by oxidation, decomposition, oxidation, or dehydration.

#### 3.6.2 X-Ray Diffraction (XRD)

X-ray diffraction (XRD) analysis is used to evaluate metal oxide (or bulk) phases present in the calcined test samples in addition to obtain the average particle sizes. It is a fast, non-destructive, multi-elemental and cost-effective method. In addition, XRD gives a fairly consistent detection limit across a large section of the periodic table and is valid to a broad range of concentrations, from 100 % to few parts per million (ppm) (Cullity, 1978). The shortcoming of this method is that its analyses are normally limited to components heavier than fluorine and that a large sample is needed (Guidotti *et al.*, 2007). The average crystallite sizes, dc-XRD were obtained from the peak width at half-height by means of *Debye-Scherrer* Equation (7):

$$d_{\text{XRD}} = K\lambda / \beta \cos\theta \quad (7)$$

where  $k$  is the shape factor taken as 0.9;  $\beta$  is the line width at half-maximum (FWHM) in radian and  $\lambda$  is the X-Ray wavelength of 0.154nm.

### 3.6.3 Brunauer-Emmett-Teller (BET) Characterization

BET surface area analysis is employed to attain a rough estimate of the average crystallite size of the bulk catalysts and the mineral clay material used in adsorption experiment. It is believed that the crystallites are spherical and are present as CaO and Al<sub>2</sub>O<sub>3</sub> following calcination. The Equation used is:

$$d_{\text{BET}} = \frac{6}{\rho_{\text{catalyst}} \cdot S_g} \quad (8)$$

where  $\rho_{\text{catalyst}}$  is the density of the catalyst,  $S_g$  is the BET surface area in cm<sup>2</sup>/g and  $d_{\text{BET}}$  is the average crystallite diameter equivalent to the volume-weighted average.

Although BET test has become an extremely popular method for obtaining the surface area of absorbents for over the past 60 years; it has limitations and is applicable in a restricted  $p/p^0$  range (normally between (0.05-0.3)).

### 3.6.4 Scanning Electron Microscopy and Energy Dispersive X-ray Spectroscopy

Scanning Electron Microscopy/Energy Dispersive X-ray Spectroscopy (SEM/EDS) is extremely useful when it comes to obtaining fast qualitative and quantitative elemental analysis of an unidentified test sample in both physical and biological sciences (Gai, 2003). The diagram is presented in Fig 12.

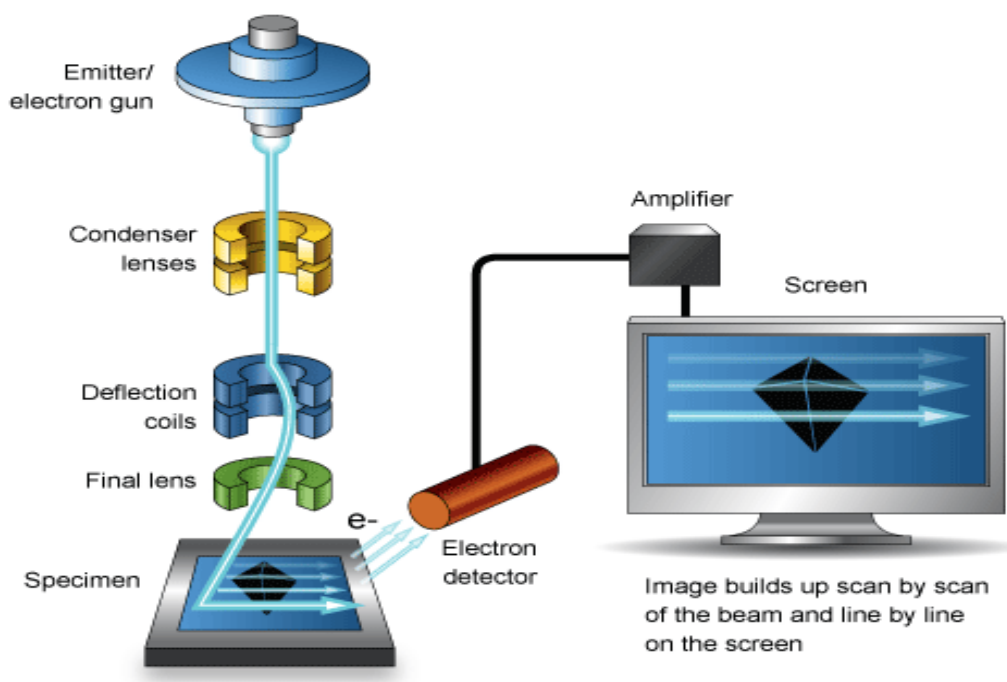


**Figure 12:** SEM layout and function (Goodhew *et al.*, 2001)

SEM is able to produce magnifications up to 2 million times in comparison to 2000 times maximum for regular light microscopes. In the SEM/EDS, the specimen surface is scanned by means of a focused electron beam producing different signals which are detected and translated into an image (Gai, 2003). Secondary electrons, emitted from the outmost atoms of the surface, backscattered electrons (electrons returning from the sample), and X-rays are distinguished and evaluated using SEM and EDS. The SEM/EDS analysis depends on the samples consisting of conductive properties, if not, the samples might charge and cause abnormalities in the electron beam. Thus, biological samples with low conductivity often require to be coated with conductive materials such as carbon or gold. The X-ray emissions, coming from the shell transitions induced by the atom interactions with the electron beam, are sensed with the EDS. The emanated X-ray allows elemental analysis as the energy of the X-rays varies between elements.

### 3.6.5 Transmission Electron Microscopy (TEM)

The internal structure of solids and their microstructural and ultra-structural feature are able to be investigated by transmission electron microscopy (TEM) which offers to this analytical technique a wide use in the field of heterogeneous catalysis. The formation of images is quite similar to that of an optical microscope but it makes use of electrons in the place of light. At the top of the microscope, an electron gun emits the electrons that travel through the vacuum of the microscope column. Commonly, the acceleration voltage is between 100 and 200 kV, even though higher voltages are also offered by some commercial microscopes (Williams & Carter, 1996; Gai, 2003). An

arrangement of condenser lenses demagnifies the beam emitted by the gun and controls its diameter as it hits the test sample (catalyst). The test sample should be thin enough so as to transmit the beam. The lenses form a magnified image which is enlarged by the subsequent projector lenses on a fluorescent screen. The image can be visualized by the operator or photographed by camera (Imelik & Vedrine, 1994; Cahn FRS, 2005).

The major difference between SEM and TEM is that SEM sees contrast owing to the topology and composition of a surface, while the electron beam in TEM projects all information on the mass it comes across in a two-dimensional image, which, on the other hand, is of sub-nanometer resolution. TEM is one of the only catalyst characterization techniques which allows the determination of particle size distributions (Cahn FRS, 2005).

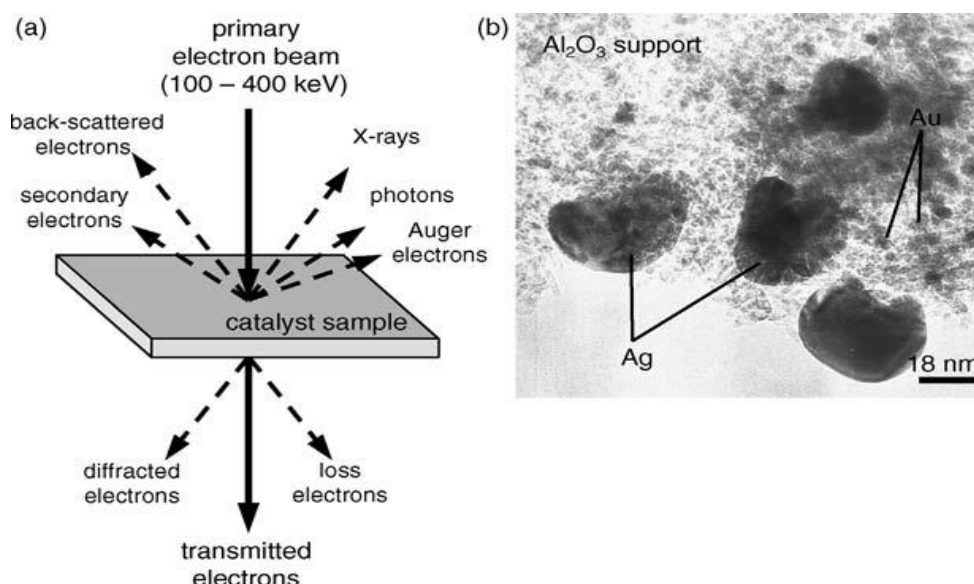


**Figure 13:** An electron beam hitting the catalyst surface begins various processes; the electrons that are transmitted by the sample test are used for generating the TEM image (demonstrating gold and silver nano-particles supported on g-alumina (Wang *et al.*, 2004).

### 3.7 EXPERIMENTALS

All chemicals utilized were of analytical grade (AR grade). Calcium nitrate  $\text{Ca}(\text{NO}_3)_2 \cdot 4\text{H}_2\text{O}$  (Merck, 99%), sodium hydroxide pellets (Merck, 98%) and aluminium nitrate,  $\text{Al}(\text{NO}_3)_3 \cdot 9\text{H}_2\text{O}$ , (Kimix, 98 %) were used as starting materials. Deionized water was used as the solvent. These reagents were used without further purification for catalyst synthesis. The transesterification reaction was carried out using waste palm oil and waste sunflower oil (collected from Suppa Oil Company, Cape Town) and methanol,  $\text{CH}_3\text{OH}$ , (Sigma Aldrich, 99.8%) in the presence of prepared calcium oxide on alumina

catalysts (60%, 70% and 80% CaO/Al<sub>2</sub>O<sub>3</sub>). In the batch process a 500 mL glass reactor was used in which waste vegetable oil was weighed and the desired quantity of methanol and the solid catalyst added. The reactor is maintained at a constant temperature with stirring at 700 rpm.

### 3.7.1 Preparation of Catalyst

A 80 CaO/20 Al<sub>2</sub>O<sub>3</sub> wt % catalyst was prepared via the method of co-precipitation. The CaO and Al<sub>2</sub>O<sub>3</sub> precursors were formed by using sodium hydroxide, NaOH to co-precipitate the respective oxyhydroxides from a solution containing the right proportion of the respective metal nitrates. The required amount of Al(NO<sub>3</sub>)<sub>3</sub>·9H<sub>2</sub>O (Kimix, 98%) and Ca(NO<sub>3</sub>)<sub>2</sub>·4H<sub>2</sub>O (Merck, 99%) to give a CaO/Al<sub>2</sub>O<sub>3</sub> ratio of 80%CaO/20%Al<sub>2</sub>O<sub>3</sub> (on weight basis) were introduced into a 2L flask. Just enough deionized water to dissolve the salts but to avoid splashing of the solutions during the vigorous stirring was added. The solution was heated to boiling point over a Heidolph MR 3001K hot plate fitted with a thermocouple (Heidolph EKT 3001) to control the temperature. The flask placed on the hot plate was fitted with Dragon Lab OS20-S overhead stirrer.

A required amount of the boiling precipitating NaOH solution (Merck 98%, 4 M) at just below 80 °C was added to the boiling nitrate solutions with continuous stirring. The milky suspension/solution is maintained at 100 °C and stirred continuously for about 30 minutes to promote the nucleation-dissolution processes. The stirrer speed was initially set at 1000 rpm and increased gradually to 2200 rpm as the solution viscosity increased due to nucleation. The stirrer used was Dragon Lab OS20-S overhead stirrer. The precipitate and solution was allowed to cool down for 20 minutes. This was then transferred into a Buckner filter set-up and filtered. The precipitates (Ca(OH)<sub>2</sub> and Al(OH)<sub>3</sub>) is washed with boiling distilled water (about 2L each time) until the filtrates were free of nitrate (NaNO<sub>3</sub>). The clean precipitate is scooped into a flat plate and placed in an electrically heating oven and dried overnight at a temperature of 100 °C. The dried cake was crushed into desired particles sizes using pestle and mortar.

Prior to testing the solid catalyst, an appropriate pre-treatment was employed since H<sub>2</sub>O and CO<sub>2</sub> must be removed to reveal basic sites and this depends on treatment temperature (Tanabe *et al.*, 1989). Hence, the calcination temperature required to remove H<sub>2</sub>O and CO<sub>2</sub> was determined using TGA. The dried particles were calcined using a fluidized bed reactor (Fig. 14) at 750 °C for 6 h at a heating rate of 10 °C/ min in air flowing at 80 ml/min (NTP). During calcination calcium and aluminium hydroxides are reduced to calcium and aluminium oxides (CaO/Al<sub>2</sub>O<sub>3</sub>) powder.

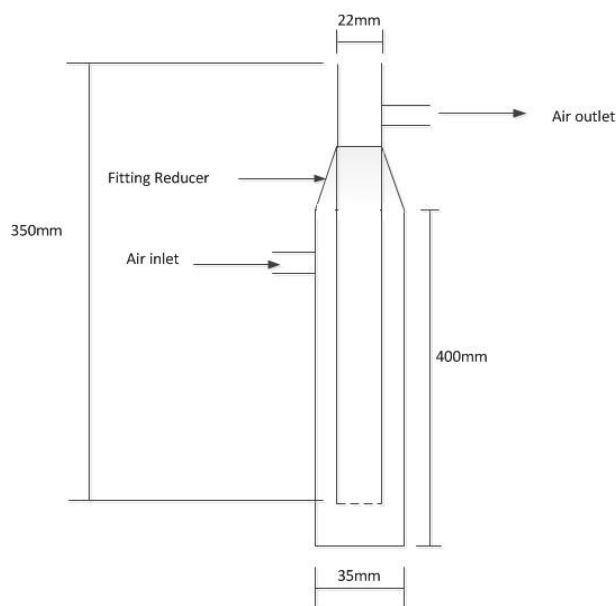
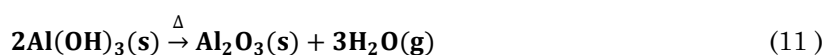
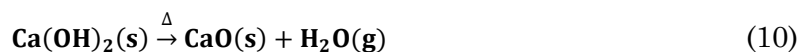


**Figure 14:** Reactor used for the calcination of the catalysts

### 3.7.2 Catalyst Characterization

#### a) Thermal Reduction Behavior

The thermal behavior of the catalyst was evaluated using a Perkin Elmer TGA7 bench model thermo-gravimeter analyzer (TGA). The sample (20g) was heated from room temperature to 900 °C in high flow of nitrogen (100 ml/min) with a ramp of 20 °C per minute. The weight change was recorded as related to water removal, possible carbon burning and metal oxidation (Reactions 10 and 11).



#### b) Scanning Electron Microscopy (SEM)

A high resolution conventional scanning electron microscope was used in this test, Hitachi S-3000N Standard VP-SEM (Hitachi High Technologies, USA) equipped with a four quadrant solid state Back Scatter Electron Detector (BSED) and a thermo-ionic electron source, which allows for imaging in the compositional, 3D and topographic modes by manipulating from each segment of the detector. The S-3000N with the PCI Data Management Interface and the patented Hitachi dual-bias system permits easy attainment of high-resolution images down to 300 volts. This is shown in Figure 12.

The S-3000N contained an energy dispersive x-ray spectroscopy detector (ISIS 300 EDX) which facilitated the investigation of the macroscopic distribution of the oxides

crystallites and the determination of the actual amount of the metals in the prepared catalysts. The preparation of the catalyst samples involved pressing dry powder of the sample on an aluminium sample holder coated with graphite glue. The graphite was utilized to conduct electrons thus stopping charge build up. A Denton vacuum desk II cold sputtering unit (Denton Vacuum, USA) fitted with a gold sputter cathode was used to clean the surface of the sample and to deposit an ultra-thin layer of a heavy metal conductive coating, Au in this case. The SEM analysis was conducted at room temperature with accelerating voltage of 20 kV to characterize the morphology and homogeneity of the catalysts.

#### **c) Transmission Electron Microscopy (TEM)**

The measurements were performed using a Hitachi kF-3300 Standard TEM microscope operated at 300 kV. The solid catalyst was homogeneously dispersed in pure acetone using a hot water bath. Then it was deposited in copper grid and afterwards the solvent was allowed to evaporate under atmospheric air before analysis.

#### **d) Brunauer-Emmett-Teller (BET) Characterization**

The BET surface area and pore volume, of the catalysts were determined using a Gemini 2375 adsorption equipment (Micromeritics ASAP 2000 analyzer, Instruments Corp., USA) at liquid nitrogen temperature after pre-treating the catalysts at 100 °C under the flow of helium for 1 h.

#### **e) X-ray Diffraction (XRD)**

X-ray diffraction measurements were performed on a Rigaku Multiflex X-ray diffractometer (Rigaku America Corporation, USA) using Cu-K $\alpha$  radiation with a wavelength of 1.540 Å at 40 kV and 20 mA. The scan range was 15°- 85° at a scanning rate of 1 °/min. All diffraction patterns were recorded in the continuous scan mode utilizing a sampling width of 0.04 °. Diffraction peaks of crystalline phases were contrasted with those of standard compounds reported in the ICDD PDF data file making use of the JADE 7.0 software.

### **3.7.3 Fatty Acids Methyl Esters Production**

#### **a) Feedstock Pre-Treatment**

Prior to the solid basic-acid catalyzed transesterifications of the WVOs (waste vegetable oils), it was firstly vacuum-filtered using a filter paper to remove all the suspended solid materials, phospholipids and other impurities. The filtered oils is put into an oven set to

a temperature of 110 °C for 30 min so as to evaporate the water (Sabudak, 2010). This is necessary to avoid saponification, formation of gels, foam as well as to ease glycerol and catalyst separation (Demirbas, 2008).

### **b) Determination of the Free Fatty Acid Content**

The free fatty acid (FFA) content in the oils was determined using the method of titration. The first step was to prepare the standard solution that was used for the titration. The standard solution consisted of 1 g KOH or NaOH diluted in 1 L of distilled water. Then, a burette was filled with the prepared standard solution and an Erlenmeyer flask containing 10 mL of isopropyl alcohol and four drops of phenolphthalein was prepared. The standard solution was added slowly until the solution turned pink. At this point the volume of standard solution ( $V_1$ ) was recorded. Subsequently, 1 mL of oil is incorporated and standard solution is added again till the solution turned pink. The new volume of standard solution was recorded ( $V_2$ ). The free fatty acids content in oil was determined by using the following Equation (9) (Buhain & Guo, 2007):

$$\text{FFA} = (V_2 - V_1) \times \frac{1.4}{\rho_{\text{oil}}} \quad (9)$$

### **c) Production of Fatty Acid Methyl Esters**

50 mL of waste palm oil was put into a 500 mL capacity batch round-bottom flask immersed in a water bath maintained at a constant temperature of 65 °C. The reactor is equipped with mechanical agitator set at an agitation speed of 700 rpm. Connected to the mouth of the reactor vessel was a condenser, which was cooled using circulating cooling water. An illustration of the experimental set-up is shown in Figure 15.



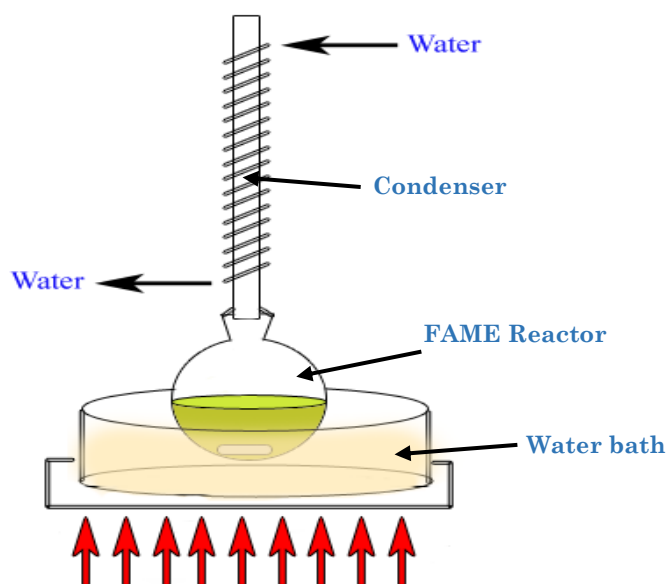


**Figure 15:** Simultaneous esterification and transesterification set-up

The desired amount of the  $\text{CaO}/\text{Al}_2\text{O}_3$  catalyst to give a catalyst/solution of 4 wt % is added to 450 mL methanol (to give a methanol/oil ratio of 9:1) and the mixture carefully added to the waste palm oil in the glass reactor. The reaction was timed once the catalyst/methanol solution was added to the reactor and allowed to react for 4 hours. Upon completion, the reactor's content was allowed to cool at room temperature and then the mixture was transferred to a separating funnel where the glycerol plus catalyst was separated from the solution by gravity overnight. This was to facilitate the separation of FAME and glycerol/solid catalyst phase. The glycerol phase (bottom layer) was removed and put in a separate container. After removing the glycerol phase, the methyl ester phase (upper layer) was washed with two volumes of water to remove the methanol, catalyst and glycerol vestiges.

The procedure was repeated for waste cooking oil at different combinations of  $\text{CaO}/\text{Alumina}$  ratios of 70% and 60%. Methanol to oil molar ratio of 9:1 was kept constant. The weight concentration of catalyst based on the oil used was 4% by weight. The same procedure was repeated when using waste sunflower oil. The methyl esters phase was weighed and analyzed using a gas chromatography coupled to a mass spectrometry (GC-MS) after separation to determine the oil conversion and FAME yield.

### 3.7.4 Products Analyses

Given FAME is produced via the transesterification reaction of the waste vegetable oils (WVOs) with methanol in the presence of a catalyst (in this case a bifunctional heterogeneous catalyst) to form methyl esters of the triglycerides. The product stream will contain FAME, unreacted feedstock (triglycerides) and traces of methanol. Residual

glycerol, obtained as a by-product and separated from FAME in the production process, can also be found in the final mixture. The composition and quantity of fatty acids (FAs) in the WVOs and in the synthesized FAME samples from WSO (waste sunflower oil) and WPO (waste palm oil) were identified and determined using two methods: Gas Chromatograph with a Flame Ionization Detector (GC-FID) and Gas Chromatograph-Mass Spectrometry (GC-MS).

#### a. Analysis of Fatty Acids Contents

The fatty acids (FAs) profiles of WVOs and in the synthesized FAME samples determined by a Gas Chromatograph with a flame ionization detector (GC-FID). The column type was HP88, (100 mm × 250 µm, 0.250 µm). Nitrogen was utilized as the carrier gas and also as a supplementary gas for the FID at flow rate of 1.0 ml/min. With the initial oven temperature set at 50 °C held up for 2 min and afterward raised at 5 °C/min to 250 °C (hold for 15 min). Temperatures injector was set at 250 °C. Undecanoic acid (C<sub>11</sub>) was used as the internal standard. In every run one micro-liter (1µL) of sample was injected into the GC using a 7980B Agilent Technologies Injector and FAME yield was calculated. The experiment was conducted for 65 minutes.

#### b. Conversion and FAME Yield

The products samples were analyzed using a gas chromatograph-mass spectrometry (GC-MS) technique on an Agilent 6890N with CTC CombiPAL Auto-sampler and Agilent 5975B mass spectrometer. The capillary column was a 30 m ZB-5MS Guardian with 0.25 mm internal diameter (ID) and carrier gas was helium at a flow rate of 1ml/min. The oven temperature was similar to that used for the epoxy FAME profiling given in details in section 4.3.3 and was: 100 °C for 1min, 25 °C/min to 180 °C for 2 min, 4 °C/min to 200 °C, maintained for 5 min, 8 °C/min to 280 °C for 3 min and 4 °C/min to 320 °C and kept for 10 min. Heptadecanoic acid (C<sub>17:0</sub>; 50 µl) was used as the internal standard

The comparative fractions of each FA were determined from the fraction of the total peak area attributed to each by the mass spectrum libraries given with the GC-MS and normalized to the heptadecanoic acid methyl ester peak. In calculating the fatty acid methyl esters mass produced, the concentration of the internal standard was multiplied by the ratio of the peak of the fatty acid methyl ester and the peak of the internal standard. Yield of FAME was expressed as illustrated in Equation (10) (Mohadesi *et al.*, 2014):

$$\text{FAME Yield (\%)} = \frac{\text{Weight of FAME produced (g)}}{\text{Weight of oil used (g)}} \times 100 \quad (10)$$

where the weight of oil is 50 g and the FAME produced from each run was acquired from the GC-MS results.

The fatty acid profile was compared with the literature values to authenticate the determination. This proved to be a reliable technique as heptadecanoic acid methyl ester is a saturated ester and does not participate in either reaction.

### **3.7.5 Catalyst Reusability**

The reusability of the solid catalysts which represents its ability to conduct the similar catalytic activity was assessed by means of performing experimental runs right after the first batch at the conditions attained for maximum FAME yield. The solid catalyst after the first reaction was recovered and washed using n-hexane and methanol to get rid of any remains of oil and/or glycerol that is adsorbed to the surface of the catalyst. Afterwards, it was filtered and dried in an electric oven for 12 h. The catalyst was then used for second consecutive runs to obtain FAME using WSO and WPO. The continued utilization of the catalyst to appraise its impact and viability for industrial use was revised.

## **3.8 RESULTS**

### **3.8.1 Catalyst Characterization**

#### **a) TGA**

Thermal-Gravimetric Analysis was performed to obtain the optimum calcination temperature. Before analysis, the heterogeneous catalysts were pre-treated, in order to remove the poisoning species mainly H<sub>2</sub>O and carbonate as well as to expose basic sites (Tanabe, 1989). Hence, the temperature of calcination required to get rid of H<sub>2</sub>O was determined by making use of TGA. The TGA profile is shown in Figure 16:

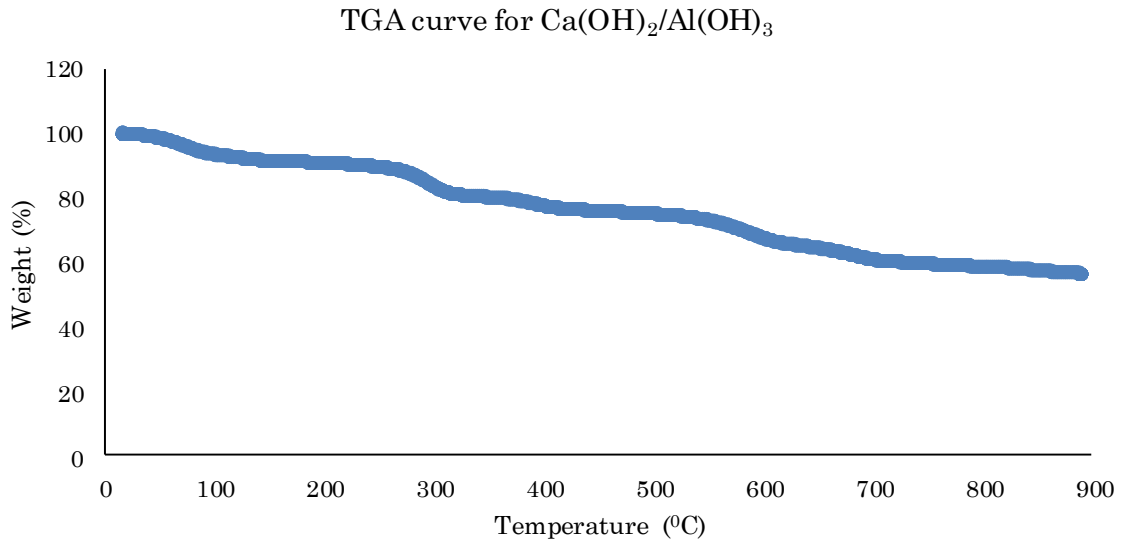


**Figure 16:** Thermal-gravimetric analysis of 80% Ca/ 20% Al filtrate

It was observed that there was minimal weight loss until 300 °C. The decrease noticed between 300 °C and 500 °C can be attributed to the removal of  $\text{H}_2\text{O}$  (Figure 16 and 17). The 40% reduction in weight at 750-900 °C (Figure 16 and 17) is as a result of the generation of calcium and aluminium oxides owing to the surface hydroxides decomposition (Tanabe 1989). Thus, 750 °C is selected as the calcination temperature for this study.

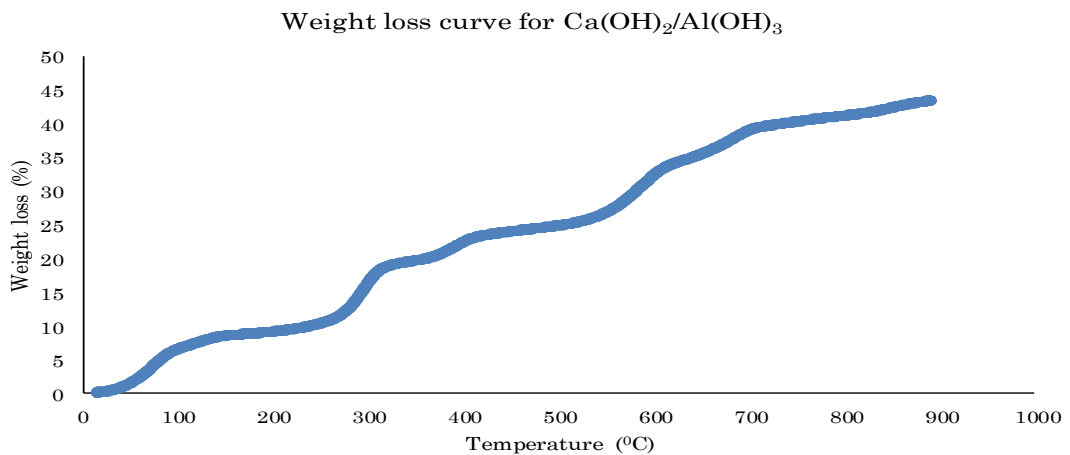


**Figure 17:** Weight loss vs Temperature curve for 80% Ca/ 20% Al filtrate

## b) Scanning Electron Microscopy Analysis

After calcination, the morphology of the catalyst was studied with SEM as shown in Figure 18 and 19 in addition Table 2. The calcined sample (750 °C) demonstrated formation of aggregated (interconnected) particles.

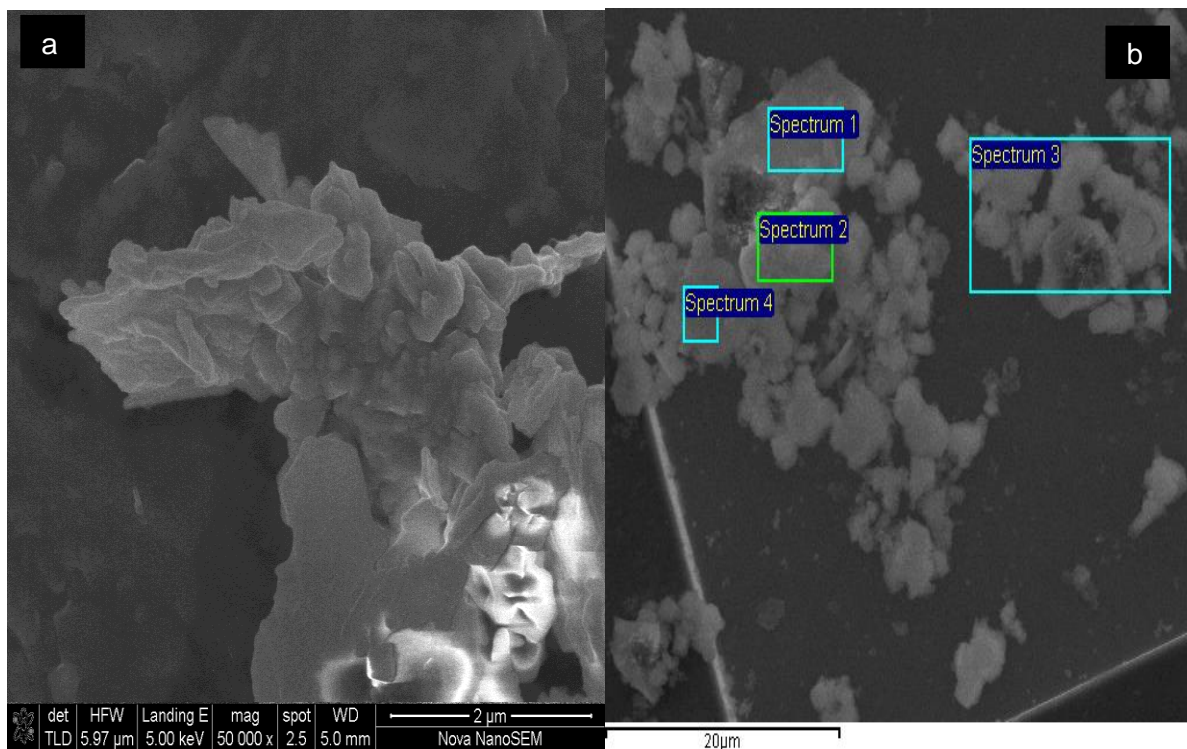


**Figure 18:** SEM-EDX micrograph of (a) the 80 CaO/20 Al<sub>2</sub>O<sub>3</sub> and (b) showing the areas chosen for EDX analysis at different magnifications.

Table 2 and Figure 19 show the elemental composition of areas examined (determined by 4 replicates of EDX) on each catalyst sample. The SEM-EDX analysis of the catalyst confirmed the presence of Ca (CaO) and Al (Al<sub>2</sub>O<sub>3</sub>). The elemental composition of the 80CaO/20 Al<sub>2</sub>O<sub>3</sub> revealed that Ca (41.41 wt. %) and O (49.62 wt. %) are present in large percentage with Al (8.97 wt. %). All of the supported catalysts demonstrated analogous morphology and there is no specific shape that can be originated from the image except for the rough surfaces of the solid materials (Fig. 18). The image in Figure 19 also shows Ca particles were well distributed on Al regardless of the 4.6:1 ratio obtained instead of 4:1 which could have been caused by discrepancies in the equipment used as well as the high level of impurities of the aluminium nitrate used. Hence, it can be concluded that the presence of Al<sub>2</sub>O<sub>3</sub> contributed significantly to the high catalytic activity during the transesterification of WPO and WSO. It also showed a significant homogeneity of the CaO/Al<sub>2</sub>O<sub>3</sub> catalyst which was visible in the value of Al and Ca acquired from the EDX analysis.

**Table 2:** EDX analysis of the selected areas (weight %) of 80 CaO/20 Al<sub>2</sub>O<sub>3</sub>

<b>Samples</b>	<b>Al</b>	<b>Ca</b>	<b>O</b>
<b>Sample 1</b>	10.73	36.33	52.94
<b>Sample 2</b>	8.38	40.32	51.31
<b>Sample 3</b>	9.06	46.54	44.4
<b>Sample 4</b>	8.04	45.76	46.2
<b>Sample 5</b>	10.05	33.68	56.27
<b>Sample 6</b>	10	38.29	51.71
<b>Sample 7</b>	7.8	41.35	50.85
<b>Sample 8</b>	8.63	32.28	59.09
<b>Sample 9</b>	10.36	45.8	43.84
<b>Sample 10</b>	6.7	53.73	39.57
<b>Minimum</b>	6.7	32.28	39.57
<b>Maximum</b>	10.73	59.09	53.73
<b>Std. Dev.</b>	1.3	6.63	6.03
<b>Mean</b>	<b>8.97</b>	<b>41.41</b>	<b>49.62</b>

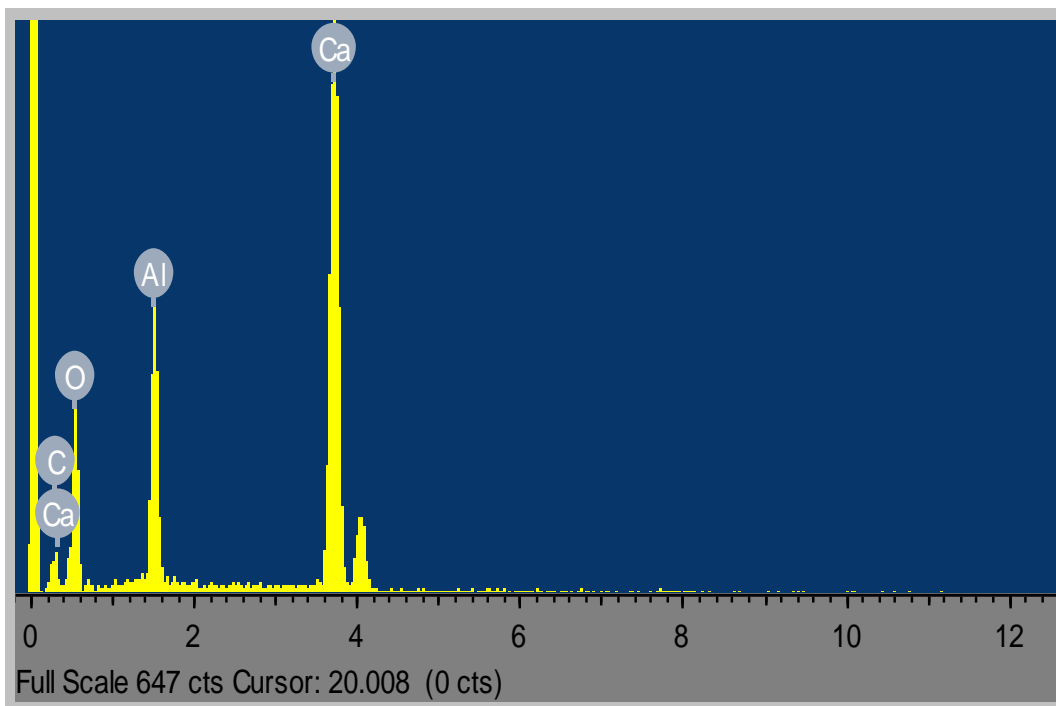


**Figure 19:** 80%CaO/Al<sub>2</sub>O<sub>3</sub> EDX Spectrum

### c) Transmission Electron Microscopy (TEM)

The morphology of the particles of the 80%CaO/Al<sub>2</sub>O<sub>3</sub> catalyst was studied from the transmission electron morphology (TEM) image as depicted in Figure 20.

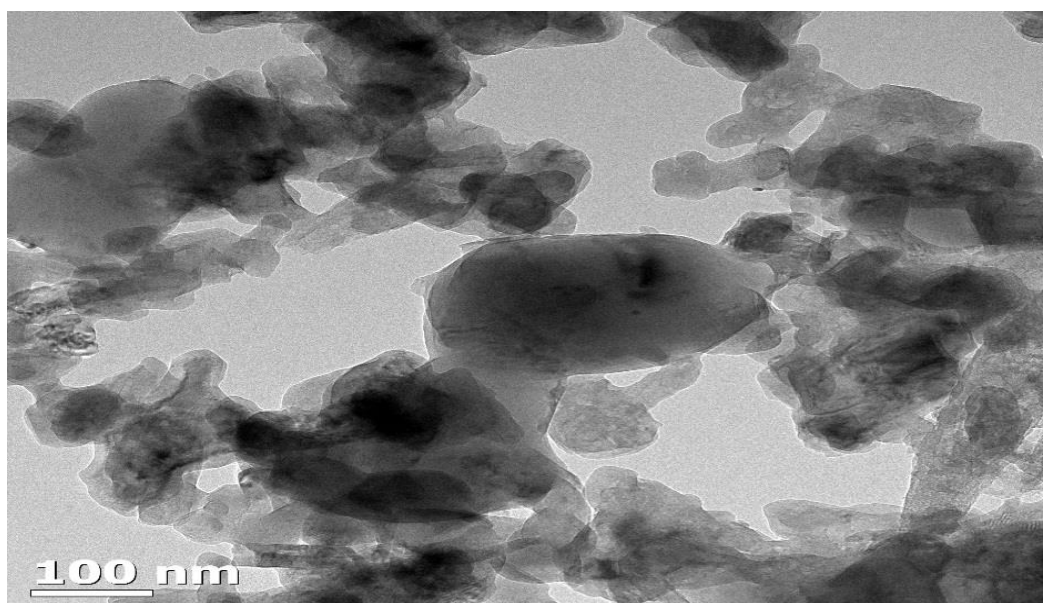


**Figure 20:** TEM images and structural information of 80%CaO/Al<sub>2</sub>O<sub>3</sub> catalyst

Figure 20 shows the micrograph of 80%CaO/Al<sub>2</sub>O<sub>3</sub> particles synthesized by co-precipitation method. Most of the particles were in the range of 10-100 nm. The porosity

of the catalyst particles were confirmed by TEM and most of the crystal particles were in rectangular shape; which goes in accordance with the study performed by Yalman (2012) The catalyst particles exhibited high efficacy during transesterification of triglyceride, irrespective of the free fatty acids present in the WPO and WSO.

#### f) Brunauer-Emmett-Teller (BET) Characterization

The textural properties of the solid base-acid catalysts at calcination temperature of 750 °C were determined through BET measurement (Table 3). Results showed that BET surface area of pure CaO and Al<sub>2</sub>O<sub>3</sub> are 3.8624 m<sup>2</sup>/g and 539.2541, respectively. However, the surface area of the CaO/Al<sub>2</sub>O<sub>3</sub> catalyst was increased to 8.5683 m<sup>2</sup>/g after its preparation via co-precipitation and thermal activation. Nevertheless, a significant reduction of pore volume of Al<sub>2</sub>O<sub>3</sub> was observed. Calcination at high temperature is necessary to thermally activate metal hydroxides to active metal oxides catalyst for transesterification reaction (Lee *et al.*, 2014).

**Table 3:** Catalysts Morphological Properties

Parameters	CaO	Al <sub>2</sub> O <sub>3</sub>	80CaO/20 Al <sub>2</sub> O <sub>3</sub>
Area, m <sup>2</sup> /g	3.8624	539.2541	8.5683
Total pore volume, cm <sup>3</sup> /g	0.019392	1.297447	0.045008
Average Pore size, Å	200.8361	96.2401	210.1157

#### g) Bulk Phase of Catalyst

The qualitative and quantitative X-ray diffraction spectra XRD patterns of the 60%, 70% and 80% CaO on Al<sub>2</sub>O<sub>3</sub> used in this study are shown in Figure 21. The XRD of the catalysts showed familiar peaks. A broad reflection of the CaO crystalline phases was clearly observed at 2θ range of 20.0-40.0° for 60%, 70% and 80% CaO/Al<sub>2</sub>O<sub>3</sub> which, supports the presence of highly dispersed CaO particles in all CaO on Al<sub>2</sub>O<sub>3</sub> catalysts. Pasupulety *et al.* (2013) observed peaks characteristic of crystalline CaO phase at 2θ range of 30.0-37.0° for 20% CaO/Al<sub>2</sub>O<sub>3</sub>. This disparity in the location of the peaks could be attributed to the equipment settings and/or catalyst preparation technique used in this study.

There were also some diffraction peaks detected at ~51 and 68° 2θ angles which did not correspond to CaO crystalline phases but were identified as hydrated calcium aluminate and alumina crystalline phases. The formation of these phases is expected due to the adsorption of water and CO<sub>2</sub> from air which must have occurred during the XRD analysis (Balakrishnan *et al.*, 2013). In fact, the samples were open to atmosphere prior to and also during the XRD measurements. From these results, it can be concluded that



high dispersion of CaO on Al<sub>2</sub>O<sub>3</sub> give rise to high activity and bulk particle formation by crystallization of CaO which may cause the decrease of active sites leading to the reduction of activity.

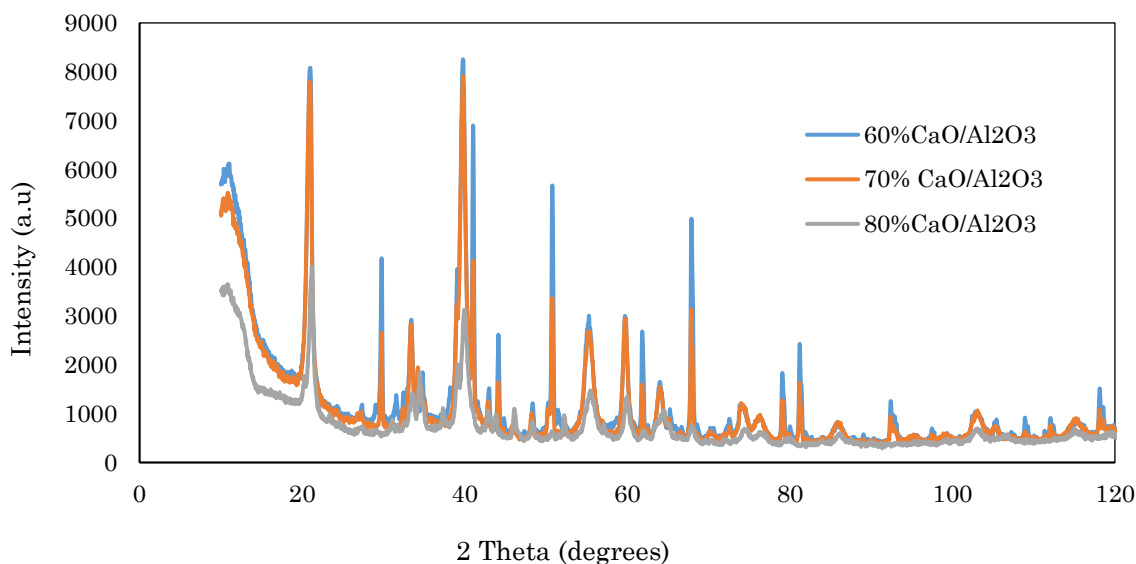


**Figure 21:** XRD pattern of 60%, 70% and 80% CaO on Al<sub>2</sub>O<sub>3</sub> catalysts

### 3.8.2 Fatty Acid Profiles of Oil Samples

FFA is a major concern during the transesterification of glycerides with alcohol in the presence of a catalyst (Mushtaq *et al.*, 2011). This is due to the fact that the high FFA content (>1%w/w) can cause saponification and products separation will be challenging, and consequently, low yield of FAME would be achieved. It is crucial to first determine the FFA content of the oil being used. The waste vegetable oil samples used to produce the FAME in this study were evaluated to determine the fatty acid composition present in the oils. It was achieved with the use of a Gas Chromatograph-Flame Ionization Detector (GC-FID) and a Gas Chromatograph-Mass Spectrometer (GC-MS). The findings are summarized in Tables 4 to 6.

Any kind of vegetable oils (used or not) present diverse composition of fatty acids (FAs) and consequently this may lead to distinct activities during the transesterification reactions (Babajide *et al.*, 2011). The waste vegetable oil samples were composed mostly of four kinds of fatty acid triglycerides including Palmitic acid, Stearic acid, Linoleic acid and Oleic acid triglycerides. The waste oils show a high degree of unsaturation specifically oleic and linoleic fatty acids (Table 4). Table 4 indicates that the waste palm oil contains 18.68% of saturated FAs and 17.52 % of unsaturated FAs. It was found that waste palm oil has the highest quantity of short carbon chains of Palmitic acids (16.56%)

and Oleic acid (14.11%). However, waste sunflower oil consisted mostly of Oleic (17.04%) and Stearic (5.93%) acids (Table 5). This is in accordance with the findings reported by Saifuddin *et al.* (2014) where the major FAs present in the waste oils are palmitoleic, palmitic, linoleic, oleic and stearic acid.

**Table 4:** Analysis of fatty acid content of the waste oils

<b>Fatty Acids</b>	<b>WSO (mass basis, wt. %)</b>	<b>WPO (mass basis, wt. %)</b>
Palmitic acid (C16:0)	5.99	16.56
Stearic acid (C18:0)	5.93	1.91
Arachidic acid (C20:0)	0.22	0.21
Lignoceric acid (C24:0)	0	0
Palmitoleic (C16:1)	0	0
Oleic acid (C18:1c)	17.04	14.11
Linoleic acid (C18:2c)	0	3.41

**Table 5:** Analysis of fatty acid content of waste sunflower oil

<b>Fatty Acids</b>	<b>Wt. %</b>
Heptane, 2,2,4,6,6-pentamethyl	0.1808
4-Methyldecane	0.277
Hexane, 3,3-dimethyl	0.4396
3,6-Dimethyldecane	0.2217
Octane, 5-ethyl-2-methyl	0.1093
Dodecane, 2-phenyl	0.3037
Indanol-5	0.3677
2,4-Dimethylheptane	0.2818
Pentadecane	0.3578
Diethyl Phtalate	0.6016
Nonadecane	0.2484
Phenol, 2,4-bis(1,1-dimethylethyl)	1.4815
n-Pentacosane	0.3449
Triacontane	0.2417
Hexadecanoic acid or Palmitic acid	7.6173

Table 5 contd:

<b>Fatty Acids</b>	<b>Wt. %</b>
Heptadecanoic acid or Margaric acid	0.8198
9,12-Octadecadienoic acid or Linolelaidic acid	48.5629
9-Octadecenoic acid or Oleic acid	25.6451
Octadecanoic acid or Stearic acid	7.6528
Linoleic acid	1.0534
5-Dodecyne	0.2022
Eicosanoic acid or Arachidic acid	0.2815
Docosanoic acid or Behenic acid	1.4139
Hexadecadienoic acid	1.2934

**Table 6:** Analysis of fatty acid content of waste palm oil

<b>Fatty Acids</b>	<b>wt %</b>
2,2,4,6,6-Pentamethylheptane	0.223
n-Nonadecane	0.3331
S-Butylbenzene	0.2269
n-Octadecane	0.4567
2,4-Di-tert-butylphenol	1.9877
n-Docosane	0.4907
Hexadecanoic acid or Palmitic acid	40.5223
Heptadecanoic acid or Margaric acid	0.8483
11,14-Octadecadienoic acid or Linoleic acid	7.689
8-Octadecenoic acid or Oleic acid	40.8909
Octadecanoic acid or Stearic acid	6.3312

The analysis of WSO indicated the presence of nine types of FA namely Palmitic acid, Margaric acid, Linolelaidic acid, oleic acid, Stearic acid, Linoleic acid, Arachidic acid, Behenic acid and Hexadecadienoic acid; with Linolelaidic acid being present in significant amounts (48.56%) followed by Oleic acid (25.64%) (Table 5). Whereas for waste palm oil, the GC-MS was able to identify only four FA types, Oleic acid, Stearic acid, Palmitic acid, and Linoleic acid. WPO showed high levels of Palmitic acid (40.52%) and Oleic acid (40.89%) (Table 6). Waste sunflower oil presented a total FAs content of 29.18% which is quite low in comparison to waste palm oil which showed a total FAs

content of 36.2% (Table 5); thus waste sunflower oil has better potential as a feedstock for FAME production due to the low content of FFAs compared to waste palm oil.

### 3.8.3 Yield of Fatty Acid Methyl Esters

The use of waste vegetable oils originating from restaurants and households as raw material in the production of FAME is motivated by economics due to its low price and availability. However, these low quality vegetable oils characteristically have high content of impurities including water and free fatty acids. The suitable catalyst therefore, must be capable of promoting simultaneous esterification and transesterification reactions, thus eliminating the pre-treatment step of removing the FFA content. The WSO and WPO oil samples having free fatty acid contents of 0.3825 mg/g and 76.96 mg/g respectively were transesterified with a methanol to oil molar ratio of 9:1 and at reaction temperature 65 °C for 4h. According to a previous studies, a methanol to oil molar ratio of 9:1 is satisfactory for a high yield, and complete conversion of triglycerides to methyl esters (Hindryawati *et al.*, 2014; Saifuddin *et al.*, 2014). With higher ratios only a minor enhancement in FAME yield can be achieved. With the aim of making the production of FAME more economically sustainable, a maximum methanol to oil molar ratio of 9:1 was used.

The optimum catalyst loading selected for the transesterification of both waste oils was 4 wt. %. Farooqa *et al.* (2013) and Kim *et al.* (2004) reported that the yield of FAME decreases with an increase in catalyst loading above 5 wt. %. Catalyst loading above 5 wt. % leads to an increase in the mixture viscosity, thus resulting in mass transfer problems during mixing. The effect of catalyst ratio on the yield of FAME was investigated by varying the catalyst ratio at a range of 60% to 80%. The compositions of fatty acids were determined using gas chromatography after being converted into their equivalent methyl esters (FAME). The use of mass spectrometer would reduce any uncertainties regarding the nature of eluting materials as mass spectra unique to individual compounds would be acquired. The results of the transesterification reactions are presented in Figure 22.

It is apparent from Table 31-36 in the *Appendix A* that the purification process was effective as no traces of glycerol was seen in the FAMEs produced. At catalyst (CaO/Al<sub>2</sub>O<sub>3</sub>) ratios of 60%, 70% and 80%, the yield of the produced FAME using WSO, were 54.3%, 74.7% and 97.5%, respectively (Figure 22). For WPO at catalyst (CaO/Al<sub>2</sub>O<sub>3</sub>) ratios of 60%, 70% and 80% FAME yields were 89.1%, 61.4% and 55.1%, respectively. This is a clear indication that all the catalysts prepared in this study were highly active. The maximum FAME yield, ~97.5%, was achieved at 80% CaO/Al<sub>2</sub>O<sub>3</sub> when WSO was used, however in the case of WPO the maximum yield of ~89.1% was obtained at 60%

CaO/Al<sub>2</sub>O<sub>3</sub> at the same reaction time of 4 h. Remarkably, when WPO was used, a high CaO loading (80 wt%) did not lead to a higher FAME yield. This could be attributed to the fact that WPO consisted a higher amount of FFAs (76.96 mg/g) compared to WSO (0.3825 mg/g) (*Appendix A*). It required high quantities of acidic sites (Al<sub>2</sub>O<sub>3</sub>) to esterify the FFAs and facilitate the conversion of triglycerides to FAME in conjunction with the basic sites (CaO) and thus achieve a high FAME yield. This could also be an indication of the impact of external mass transfer constraints originated by the generation of products, for instance FAME and the by-product glycerol.

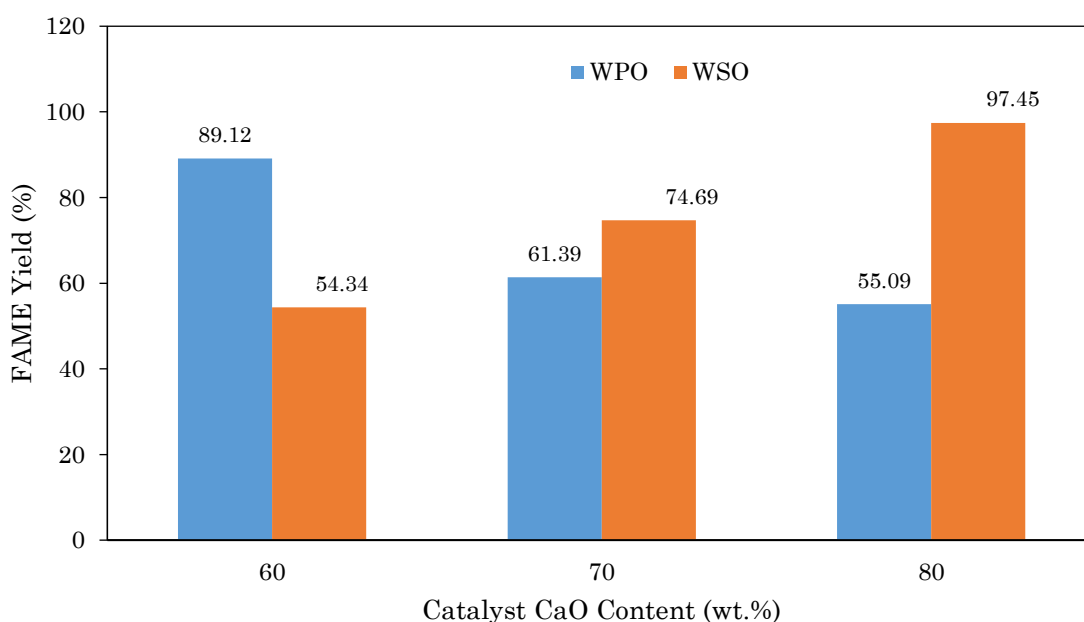


**Figure 22:** Fatty acid methyl ester yield versus catalyst ratio (60%, 70% and 80% CaO/Al<sub>2</sub>O<sub>3</sub> catalysts for 4 h of reaction time and methanol to oil molar ratio of 9:1

According to Yalman (2012) such constraints are only avoidable at higher stirring speed of approximately 1300 rpm and thus improving the FAME yield. Inopportunately, there was no stirrer with the capability of more than 1000 rpm readily available for use. Additionally, Furthermore, the partial blockage of active sites at higher loadings (80 wt. %) decreases the basicity of the catalyst and lowers its activity (Saifuddin *et al.*, 2014). This decrease in yield could also be attributed to the variation in the particle size of the CaO/Al<sub>2</sub>O<sub>3</sub> catalysts, which might have caused a decrease in its catalytic activity during the reaction systems. Lee *et al.* (2014) reported that the activity of a catalyst is dependent on the particle size. Thus, smaller catalyst particles are supposed to demonstrate higher reaction rate owing to an increase in the external surface available. On the other hand, the bigger the particle size of a solid, the smaller the surface area available for reaction to take place, also it reduces the number of collisions between the molecules (solid-liquid phase) during the reaction. The further increase in CaO load had a small change on the yield of FAME from 61.4% (catalyst ratio was 70 wt. %) to 55.1%

(catalyst ratio was 80 wt. %). This can be attributed to the fact that the solubility of methanol in waste oil is partial and when the amount of  $\text{Al}_2\text{O}_3$  load decreased, less FFAs were esterified, which led to the decrease in the yield of FAME. Thus, the appropriate CaO loading on  $\text{Al}_2\text{O}_3$  for transesterification of waste palm oil was considered to be around 60 wt. %.

From Figure 22 can also be observed that in the case of WSO as the CaO loading is increased the FAME yield tends to increase at the same reaction conditions. The steep increase in the yield of WSO from ~54.3 to ~97.5 at catalyst ratio of 60 to 80 wt. % could be because of the increase in the basic sites, more specifically CaO load. As a matter of fact, basic catalysts are well recognized for the capacity of reaction completion at higher rate and higher conversion efficiency concerning low FFA feedstock. Consequently, the appropriate CaO loading on  $\text{Al}_2\text{O}_3$  for the different waste oils should be taking into consideration when conducting transesterification reactions. Therefore, it is safe to say that CaO presence contributed to the high catalytic activity in the transesterification of waste sunflower oil.

#### **3.8.4 Catalyst Reusability**

The economic potential of  $\text{CaO}/\text{Al}_2\text{O}_3$  catalyst was evaluated via the reusability tests (which represents its capacity to perform the same catalytic activity) conducted on WSO and WPO. After the washing step the solid catalysts were collected by means of filtration and washed with methanol for a number of times, followed by calcination in air at 750 °C and used for transesterification in a new reaction cycle at the same conditions. The reaction conditions at which the highest FAME yield was achieved were utilized, that is, 9:1 methanol to oil molar ratio, 4 wt. % catalyst loading at 65 °C for 4 h. Figure 23 shows the reusability of the  $\text{CaO}/\text{Al}_2\text{O}_3$  catalysts. The GC-MS results of the FAMEs are shown in Tables 37 and 38 in *Appendix A*.

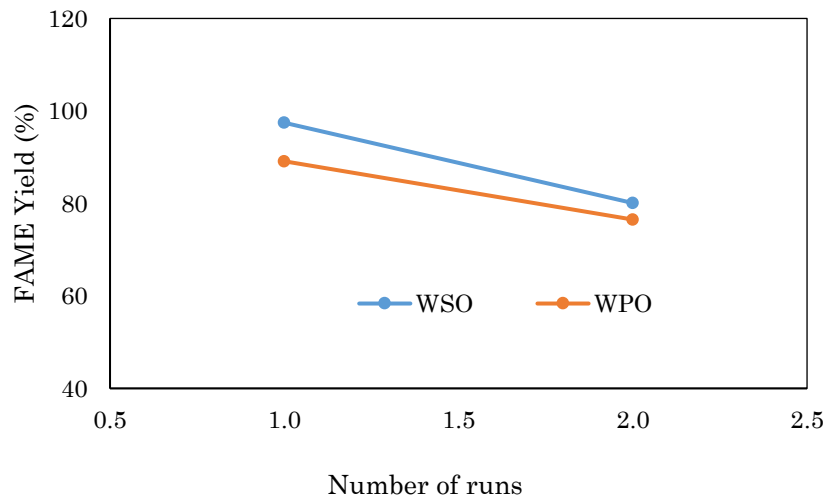


**Figure 23:** Reusability of CaO/Al<sub>2</sub>O<sub>3</sub> catalysts at optimum reaction conditions (60% and 80% CaO/Al<sub>2</sub>O<sub>3</sub>, 9:1 methanol to oil molar ratio, 4 wt. % catalyst loading at 65 °C for 4 h)

It was noticed that FAME yield displayed a descending trend which implies the influence of deactivation of the catalyst active sites which is the main issue when using heterogeneous catalysts. Their deactivation with time is due to various possible phenomena, for instance, coking, sintering, poisoning as well as leaching (Mazzocchia *et al.*, 2004). In the case of WSO for the 1<sup>st</sup> run, a maximum FAME yield of 97.45% FAME yield was attained, 80.09% yield for the second run. For WPO the 1<sup>st</sup> run, a maximum yield of 89.12% was obtained, 76.51% FAME yield for the 2<sup>nd</sup> run. The decrease in the catalytic activity of the CaO/Al<sub>2</sub>O<sub>3</sub> suggests that the active sites of the catalyst pores were blocked by large oil particles, a number of contaminants as well as certain impurities that were present in WSO and WPO. Poisoning is evident when the process involves used oils. These impurities can be in the form of pigments, food debris, oxidized fats, non-hydratable lecithins and various other non-lipid substances (Balakrishnan *et al.*, 2013). Loss of catalytic activity can also be attributed to leaching during the process which not only increases the operational cost on account of substituting the catalyst but also leads to contamination of the product (Mazzocchia *et al.*, 2004; Barbosa *et al.*, 2006). The substantial loss in the catalytic activity in the second reuse could also be due to decrease in the number of active sites on the catalyst surface or reduction in the weight of the catalyst as a result of process operations.

### 3.9 SUMMARY

The CaO/Al<sub>2</sub>O<sub>3</sub> has been used as a catalyst in the FAME production process in several studies. The catalysts synthesized by the co-precipitation method exhibited high dispersion of the Ca and Al particles (also aided by the continuous stirring). This was

apparent in results obtained in the SEM, TEM and XRD analysis. Furthermore, the results of the specific surface area of BET showed that there was an increase in the catalyst specific surface area after thermal activation which contributed to higher reaction rate, hence leading to higher FAME yield in some reaction systems. The optimum reaction conditions for the production of fatty acid methyl esters via simultaneous esterification and transesterification reaction by means of the batch process with the waste vegetable oil samples (WSO and WPO) were found to be as follows: a reaction time of 4h at 65 °C with a methanol: oil ratio of 9:1 and 4 wt.% catalyst amount.

A 60% CaO/ 40% Al<sub>2</sub>O<sub>3</sub> basic to acidic oxides ratio was found to be the optimum for waste palm oil; whereas the optimum catalyst ratio for the waste sunflower oil was 80% CaO/ 20% Al<sub>2</sub>O<sub>3</sub> at the same reaction conditions. It is evident from this study that WPO showed a decrease trend in FAME yield when the catalyst ratio was increased from 60-80%. The contrary was observed when WSO was used, an increasing pattern in the FAME yield was observed. There was an evidence to suggest that the different trends reported in this study, with the two types of oil used, is due to the fact that WPO presented higher amount of FFAs compared to WSO, and hence requires more acidic sites on the catalyst to esterify the FFA to triglyceride before it is converted by the basic sites to FAME. It may also be a partial indication of the impact of external mass transfer constraints due to higher viscosity in addition to the partial blockage of active sites at higher loadings. The catalysts with optimum ratios were reused and the results showed that the catalytic efficiency of the CaO/Al<sub>2</sub>O<sub>3</sub> catalysts lowered with reusability. This could be due to deactivation with time as a result of coking, sintering, poisoning as well as leaching, which led to contamination of the product and subsequent decrease in the FAME yield (Mazzocchia *et al.*, 2004; Barbosa *et al.*, 2006). The high yield of FAME obtained despite the low quality of the oils used demonstrated that the use of a bifunctional catalyst will provide an opportunity to lower the cost of production as well as assist in disposal of the waste vegetable oils.



## METHLY ESTERS EPOXIDATION AND SULFONATION

---

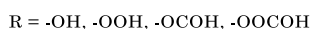
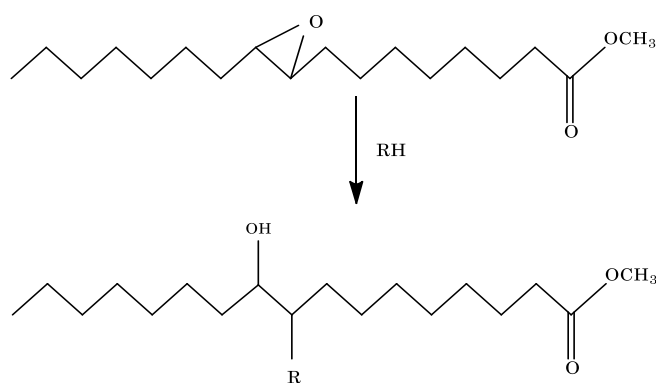
*The majority of vegetable oils and the methyl esters synthesised therefrom contain high contents of unsaturated fatty acids (Aluyor et al., 2009). Thus in this chapter a review on the various epoxidation processes (conventional, catalytic and chemo-enzymatic) used to convert the unsaturated fatty acids present in the FAME produced into epoxy fatty acids is presented. The epoxidation reaction is performed by adding a solution of formic acid ( $\text{CH}_2\text{O}_2$ ) and hydrogen peroxide ( $\text{H}_2\text{O}_2$ ) to the FAME produced in Chapter 3. Hydrogen peroxide and formic acid react to produce performic acid in-situ, which in turn reacts with the double bond to form the epoxide and formic acid. The epoxidation of the FAME in the absence and presence of different solvents (toluene, n-hexane and propan-2-ol) at temperatures ranging from 25 °C to 50 °C and analyses of the epoxy products obtained are presented. The epoxidized FAME is then subjected to the sulfonation reaction to produce the surfactant. A concise review of the sulfonation reaction and the sulfonating agents used during reaction is described in this chapter. The epoxidized esters are reacted with chlorosulfonic acid ( $\text{HSO}_3\text{Cl}$ ) in a solution of pyridine ( $\text{C}_5\text{H}_5\text{N}$ ) to obtain the SEMES surfactant. Whereas various sulfonating agents have been used, chlorosulfonic acid was chosen in this study owing to its simplicity of the process. For example, sulfuric acid has been reported to cause the formation of sulfonated polymers while sulfur trioxide and sulfur trioxide complexes require special handling. Moreover, there is no need for further preparation when chlorosulfonic acid is used. The subsequent findings for the epoxidation and sulfonation of methyl esters are also given.*

### 4.1 EPOXIDATION OF FATTY ACID METHYL ESTERS

Epoxidized oil and its epoxidized methyl esters are manufactured on an industrial basis mostly from vegetable oils such as linseed and soybean oils to meet the high demand. Various researchers have studied the production of epoxidized oils using other natural oils: cottonseed, safflower, cottonseed, canola and olive (Akintayo, 2006; Scala & Wool, 2002), rubber seed oil and sunflower (Okieimen *et al.*, 2002). However, very few studies have reported the use of waste vegetable oils. Fatty acids like linoleic, oleic and linolenic esters can be transformed into mono-, di- and tri-epoxy esters. Nevertheless according to Akintayo (2006) there has been very little effort to evaluate the products of epoxidation

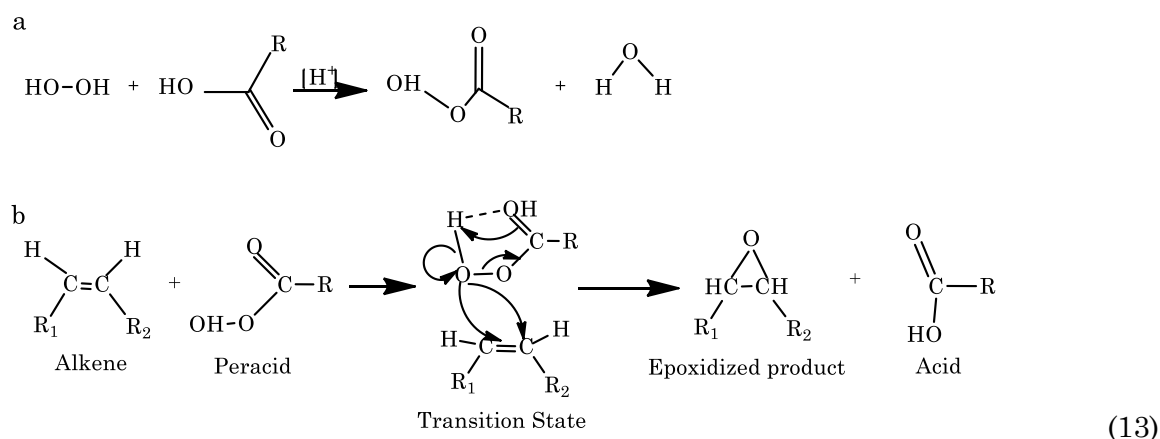
in terms of their different epoxy acids. Epoxidized methyl ester is readily converted into surfactants, fuel additives, and other industrial products.

Epoxidation of vegetable oils is the reaction between a double bond with an active oxygen, resulting in the addition of a single oxygen atom to each unsaturation (carbon-carbon double bond) in the fatty acid chain using organic and inorganic peroxides or percarboxylic acids as oxidizing agents (Gamage *et al.*, 2009). The initial unsaturation is thereby converted into a three-membered ring structure called oxirane ring or epoxy group (Espinoza Perez *et al.*, 2009). Reaction 12 present the main degradation reactions of the oxirane ring. The more the degree of unsaturation in the vegetable oil or from the obtained fatty acid methyl esters the faster is the epoxidation reaction.



(12)

Epoxy groups are more reactive compared to other ethers; this is because of their highly strained ring structure, which makes them essential intermediates for numerous products (Goud *et al.*, 2006). The epoxidation of vegetable oils and methyl esters can be efficiently achieved with a peracid or peroxyacid (normally peracetic acid or performic acid as the peroxygen carrier). These are usually produced *in-situ* with hydrogen peroxide ( $H_2O_2$ ) as oxygen donor (Reaction 13a) (French, 1971; Aluyor *et al.*, 2009). Perbenzoic acid can also be used (Gamage *et al.*, 2009). Findlay *et al.* (1945) was the first to report the production of epoxy esters utilizing peracid. Peracetic acid (or performic acid) has been extensively utilized as oxidizing agents during conventional chemical epoxidation (Swern, 1947). However, with  $H_2O_2$  and acetic acid ( $CH_3COOH$ ), the process typically requires making use of an acid catalyst which can be homogeneous or heterogeneous. The mechanism for the generation of peracetic acid obtained from the reaction of hydrogen peroxide with acetic acid during acid catalyst epoxidation and acid catalyst epoxidation is shown in figure 13 (Chua & Guo, 2012).



Homogeneous catalysts such as the inorganic  $\text{H}_2\text{SO}_4$  and  $\text{HNO}_3$  are less costly, but then again they are not so easy to reuse and recycle and their side reactions lead to the degradation of the epoxy-group (particularly to hydroxyl groups). On the other hand, heterogeneous catalysts can be easily separated from the final product, regenerated and reused, therefore reducing the environmental impact as well as the cost of production. Heterogeneous catalysts, such as strong cation exchange resins, also decrease the formation of side reaction, reduce the degradation of epoxy group which are necessary steps to speed up the peracid formation, whereas the production of performic acid does not require the presence of a strong acid (Gunstone, 1997; Hang & Yang, 1999; Campanella *et al.*, 2008). Mineral acid are rarely applied owing to the fact that their usage prevents the attainment of high yields, due to the opening of the oxirane ring throughout the course of the major reaction (Gan *et al.*, 1992; Rangarajan *et al.*, 1995; Campanella & Baltanas, 2006).

A number of kinetic studies on the epoxidation of various vegetable oils and FAME with peracetic acid and performic acid produced *in-situ* using homogeneous catalysts, have been reported (Gan *et al.*, 1992; Goud *et al.*, 2006). It was found that the rate-determining step in the epoxidation is at all times the peracid production. The detailed epoxidation reaction mechanism with performic acid (PFA) and concentrated  $\text{H}_2\text{O}_2$ , is depicted in Figure 24. PFA is formed in the aqueous phase from  $\text{H}_2\text{O}_2$  and FA, then PFA and FA “shuttle” between both phases during the reaction. Once the PFA is generated in the aqueous phase, it is transported into the organic phase, where it reacts with the C=C bonds, to form Epoxidized Fatty Acid Methyl Ester (EFAME) (Rangarajan *et al.*, 1995; Campanella *et al.*, 2008). At that time the FA is transferred to the aqueous phase, where it reacts with  $\text{H}_2\text{O}_2$ , once more to form PFA, which then starts again the reaction cycle.

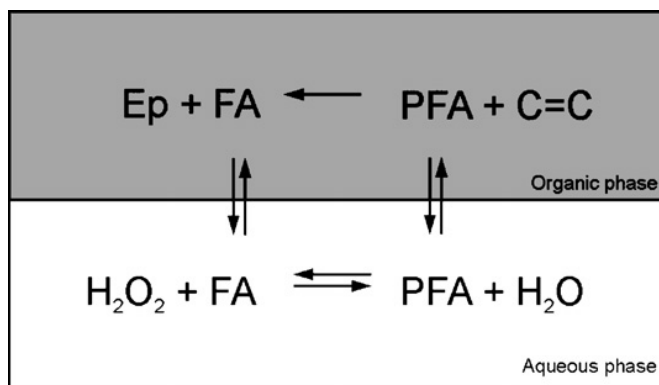


**Figure 24:** Epoxidation reaction of double bonds in the organic phase, using PFA generated in the aqueous (polar) phase from hydrogen peroxide (Campanella *et al.*, 2008)

Dinda *et al.* (2008) also studied the kinetics of epoxidation of cottonseed oil using peroxyacetic acid produced *in-situ* from glacial acetic acid and  $\text{H}_2\text{O}_2$  using liquid inorganic acid as a catalyst. A yield of 78% relative conversion of oxirane ring was obtained but with oxirane cleavage using the *in-situ* method. The order of effectiveness of catalysts was sulfuric acid > phosphoric acid > nitric acid > hydrochloric acid. In the *in-situ* cottonseed oil epoxidation, the acetic acid was found to be more efficient than formic acid. Comparing all the liquid inorganic acids studied,  $\text{H}_2\text{SO}_4$  was noticed to be the most effective. Higher acid amounts and higher temperatures decreased the reaction time required to reach the maximum conversion to oxirane value. However, it increases the extent of oxirane ring cleavage to glycol. Maximum yield of oxirane ring with insignificant amount of oxirane cleavage could be reached if the epoxidation step is performed at optimum conditions. These conditions include temperature ranging from 50 to 60 °C, acetic acid-to-unsaturation mole ratio of approximately 0.5,  $\text{H}_2\text{SO}_4$  loading of about 2 wt.% of aqueous phase and  $\text{H}_2\text{O}_2$ -to-unsaturation mole ratio ranging from 1.5 to 2.0 (Abdullah & Salimon, 2010).

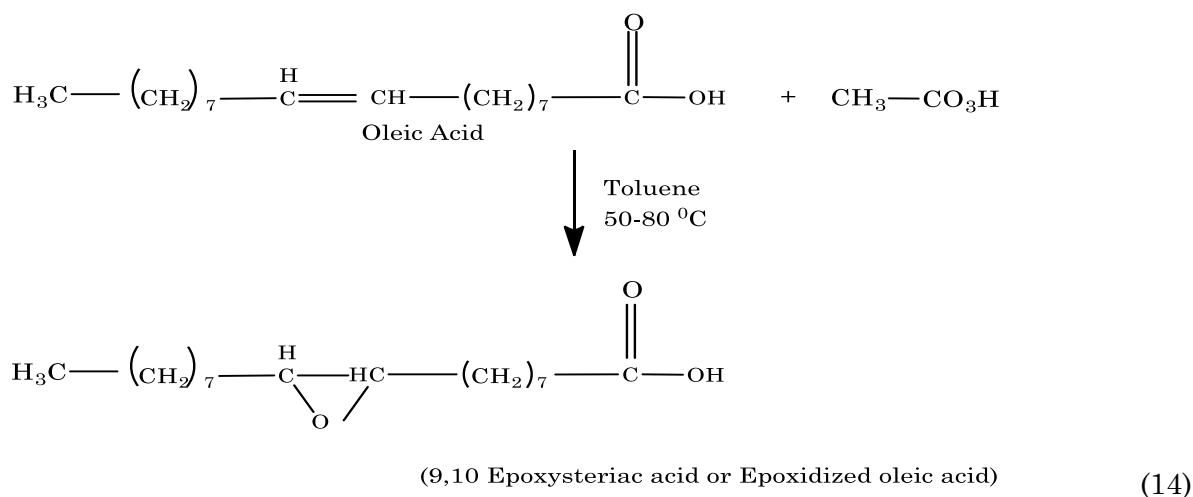
To obtain a high yield of epoxy Campanella *et al.* (2008) studied in detail the effect of the significant process factors on the epoxidation reaction of soybean oil FAMES using PFA generated *in-situ* with  $\text{H}_2\text{O}_2$  (up to 60 wt.%). The effects of temperature, intensity of mixing, reactants molar ratios, concentration and usage of diluents were studied. Increase in temperature is considered to be unfavorable for attaining high oxirane numbers. This is because the selectivity to ring-opening reactions tends to increase as well. Therefore, it is best to perform epoxidation reaction at moderate temperatures and low concentrations of formic acid (FA). Very high amounts of either  $\text{H}_2\text{O}_2$  or formic acid are also detrimental (mainly the carboxylic acid) however far less comparing to temperature. A less than stoichiometric quantity of formic acid can be utilized since it is not consumed in the reaction. Alternative processes that employ reasonable temperature (up to 40 °C) with concentrated  $\text{H}_2\text{O}_2$  are proposed, which in comparison with the conventional process (which is conducted at 60 °C using 30 wt. %  $\text{H}_2\text{O}_2$ ) are also able to

achieve very high double bond conversion together with high epoxide productivity and excellent selectivity. Therefore, it is crucial to use the right molar ratios amounts of formic acid and H<sub>2</sub>O<sub>2</sub> plus temperature of reaction for attaining high epoxy yield.

Another important factor which governs the reaction progress both in ring opening and epoxidation period is reaction time. According to Campanella *et al.* (2008) longer reaction times (of more than 20 h) have been utilized for the epoxidation reaction with low temperature of reaction. Goud *et al.* (2006) also studied the epoxidation of mahua oil (*Madhumica indica*) using H<sub>2</sub>O<sub>2</sub>. The mahua oil was epoxidized *in-situ* using H<sub>2</sub>O<sub>2</sub> as oxygen donor and glacial acetic acid as active oxygen carrier in the presence of inorganic acid as a catalyst. The loading of two acids, H<sub>2</sub>SO<sub>4</sub> and HNO<sub>3</sub> were studied. Sulfuric acid was found to be more effective in terms of oxirane conversion. Comparative conversion data revealed that epoxidation of mahua oil by *in-situ* produced peracetic acid is best carried out at temperatures ranging from 55 to 65 ° C and at stirring speeds >1500 rev/min. Nevertheless, the presence of H<sub>2</sub>SO<sub>4</sub> as acid catalyst may lead to several side reactions for instance hydroxyl esters, oxirane ring opening to diols, estelloids as well as the formation of dimer (Lathi & Mattiasson, 2007). Moreover, it leads to poor selectivity, very high concentrations of H<sub>2</sub>O<sub>2</sub> are used and it is environmentally unfriendly. During commercial production of fatty epoxide, the presence of these side reactions reduces their attraction as a raw material for additional elaboration, as producers could need costly purification (Piazza *et al.*, 1998).

Several kinetics studies concluded that by diluting the organic phase with a solvent reduces the rate of opening oxirane caused by the production of side reactions. Furthermore, it also reduces the degradation of the epoxy-group and simplifies the product purification which increases the conversion efficiency. Organic solvents such as heptane, hexane, toluene, chloroform and benzene are utilized during the epoxidation of vegetable oils (Goud *et al.*, 2007, Campanella & Baltanas, 2006). Degradation of the oxirane product has long been identified as a serious concern in most epoxidation processes (Akintayo, 2006). Findlay *et al.* (1945) observed that the rate of ring opening of 9,10-epoxystearic acid was 1% per hour at 25 °C and 100% at 65-100 °C in 1-4 h and recommended that the formation of by-product could be minimized via the use of an appropriate solvent (such as toluene or heptane) at low temperatures. Peracid epoxidation of oleic acid using toluene as a solvent can be represented by reaction 14 (Deshpande, 2013).

Gan *et al.* (1992) also noticed that the presence of organic solvents seemed to have some stabilizing influence on oxirane produced by the epoxidation of oils using peroxyacids. Thus, conducting epoxidation reactions using organic solvent at room temperature minimizes side and by-products formation and ring opening reactions particularly to hydroxyl compounds (Pages & Alfos, 2001).



Epoxidation with solvent simplified product handling, thus reducing filtration losses which led to more product being recovered. The solvent commonly use is n-hexane due to its relatively lower toxicity, lower boiling point in addition to ease of evaporation from the final product comparing to benzene and toluene. The use of such solvents present some disadvantages however which includes: health hazards, the cost of organic solvent usage, increased time, solvent recovery as well as reduction of the rate of oxiranes opening which causes a decrease in the conversion efficiency. Mushtaq *et al.* (2011) studied the expoxidation of fatty methyl esters (FAMEs) from transesterification of *Jatropha* oil using both bifunctional catalyst. The FAMEs were epoxidized with peroxyacetic acid and peroxyformic acid, generated *in-situ* with H<sub>2</sub>O<sub>2</sub> in the presence and absence of a n-hexane as the solvent. With formic acid without a solvent, the conversion was found to be 79% and with solvent was 83% obtained at 60 °C. Besides improving the reaction yield, the use of solvent favours the reaction rate that suppresses dihydroxylation. Formic acid was found to be quite effective at a temperature of 69 °C in solvent.

#### 4.1.1 Enzymatic Epoxidation

To prevent the side reactions and to make the process more eco-friendly, enzyme catalyst such as immobilized *Candida antarctica* lipase has been employed for epoxidation (Tornvall *et al.*, 2007). Enzyme catalysts for epoxidation are by far the best substitute to chemical treatment. The epoxidation reaction can be enhanced by the addition of the lipase step by step. However the principal issue related with the use of this catalyst is its low stability under the reaction conditions (Suarez *et al.*, 2009). Tornvall *et al.* (2007) investigated the factors that most significantly affect the activity and operational lifetime of lipase during chemo-enzymatic epoxidation of fatty acids. It was observed that during bio-catalyzed reactions, enzymatic activity can be lost at very high concentrations of H<sub>2</sub>O<sub>2</sub> and temperature. However, a number of studies have demonstrated that

*Candida antarctica* B lipase kept its activity at temperatures above 50 °C, even though this was unfavorable, mostly because of the H<sub>2</sub>O<sub>2</sub> decomposition. Moreover, at elevated temperatures, the enzyme attains a more open structure, which leads to reduction of its catalytic activity.

Orellana-Coca *et al.* (2005) also studied the effect of reaction factors on lipase-mediated chemo-enzymatic linoleic acid epoxidation. H<sub>2</sub>O<sub>2</sub> was observed to have great effect on the rate of reaction as well as the degree of epoxidation. So as to achieve total conversion at short reaction time, excessive amounts of H<sub>2</sub>O<sub>2</sub> (with regard to the quantity of double bonds) as well as temperatures above 50 °C (to compensate for the breakdown of H<sub>2</sub>O<sub>2</sub>) are required. However, long incubation periods with high amounts of H<sub>2</sub>O<sub>2</sub> may cause peracid to accumulate in the final product. Even though increasing H<sub>2</sub>O<sub>2</sub> concentration (between 10 and 50 wt. %) increases the reaction rate, it causes enzyme inactivation. Additionally, when toluene (at a concentration of 0.5-2 M and temperature of 30 °C) was mixed with the linoleic acid, it was epoxidized fully, whereas in the absence of a solvent, the reaction was incomplete owing to the generation of a solid substance or an extremely viscous oily phase, which in turn promoted mass transfer resistance. By raising the temperature up to 60 °C the rate of epoxide formation is improved.

Sun *et al.* (2011) studied the epoxidation of *Sapindus mukorossi* seed oil using enzymes, with stearic acid as active oxygen carrier and H<sub>2</sub>O<sub>2</sub> as oxygen donor and immobilized *Candida antarctica* lipase B as the catalyst. The effects of the concentration of stearic acid, temperature and enzyme amount on the epoxidation reaction were investigated. It was observed that the amount of enzyme had considerable effects on the epoxidation and the enzyme activity was affected negatively at higher temperatures. Klass & Warwel (n.d.) used lipase-catalyzed perhydrolysis to study the complete and partial epoxidation of plant oils, sunflower, soybean, rapeseed and linseed oils. They noticed that the epoxidation using immobilized lipase biocatalyst exceeded the epoxidation conversion rate up to 90%.

The use of immobilized enzymes has various other advantages. They can be easily separated via filtration and they are reused without significant loss of activity. Nonetheless, the main disadvantage of such process is that the enzyme is very sensitive to the type of substrate used and as a result it can be unsuitable with some specific oleochemical (Guidotti *et al.*, 2007).

#### **4.1.2 Epoxidation using Heterogeneous Catalysts**

The use of *in-situ* peracid produced when a carboxylic acid (typically acetic acid) is reacted with H<sub>2</sub>O<sub>2</sub> in the presence of a mineral acid as the catalyst, is used for the epoxidation reaction, comes with a number of challenges. These include the need for

the acidic by-products separation (whose presence is disadvantageous for additional use), the selectivity to epoxidized products is low owing to acid catalyzed oxirane ring-opening; and the management of highly concentrated H<sub>2</sub>O<sub>2</sub> and strong acids is risky and can cause deterioration to equipment (Aluyor *et al.*, 2009). Hence, there is intensive search for new techniques and development of catalytic processes to overcome such.

Suarez *et al.* (2009) investigated the use of H<sub>2</sub>O<sub>2</sub> with Lewis acid metals (Sn, Ti, Zn, and Zr) doped on Alumina. The maximum yield obtained was 54% which was not promising. Even though the yield was improved by increasing the catalyst load, the trend was not linear. Utilizing a heterogeneous catalyst, such as ion exchange resins has been investigated (Sinadinovic-Fiser *et al.*, 2001; Campanella & Baltanas, 2006). Goud *et al.* (2007) and Dinda *et al.* (2008) utilized organic acids and H<sub>2</sub>O<sub>2</sub> in the presence of ion exchange resins for the epoxidation reaction with and without toluene as a solvent. The performic acid was found to be more effective in comparison with peracetic acid. The maximum yield was reported to be 88%.

Many other studies have reported the importance of utilizing solid catalysts for epoxidation reaction. Campanella *et al.* (2004) studied the epoxidation of soybean oil and soybean FAMEs using a dilute solution of H<sub>2</sub>O<sub>2</sub> (6 wt. %) with an amorphous heterogeneous Ti/SiO<sub>2</sub> catalyst in the presence of *tert*-butyl alcohol as a solvent. The highest yields of epoxidized olefins were achieved upon utilizing a substrate molar ratio: H<sub>2</sub>O<sub>2</sub> of 1:1.1. When higher ratios were used, the reaction rate was slow and no degradation of the oxirane ring occurred. It was concluded that, increase in temperature was detrimental for achieving high yields, and high concentrations of either H<sub>2</sub>O<sub>2</sub> or formic acid were significantly harmful but much less compared to increased temperature. Du *et al.* (2004) studied the epoxidation of methyl linoleate over transition metal complexes as catalysts. With 4 mol% of methyltrioxorhenium and pyridine, methyl linoleate was fully epoxidized by aqueous H<sub>2</sub>O<sub>2</sub> in 4 h.

Sepulveda *et al.* (2007) performed the epoxidation of unsaturated fatty esters using aqueous H<sub>2</sub>O<sub>2</sub> as an oxidant in the presence of aluminas and ethyl acetate was used as the solvent. The commercial alumina demonstrated excellent catalytic activity in addition to good selectivity toward the formation of epoxides. The alumina produced from the sol-gel process showed high activity and when using aqueous H<sub>2</sub>O<sub>2</sub>, could be recycled and reused many times. This catalyst is cost-effective and showed excellent activity during the methyl oleate and soybean oil methyl esters epoxidation. A conversion of approximately 95% as well as a selectivity of more than 97% for the oxirane were achieved in 24 h. A conversion of 87% was attained after the catalyst was re-used four times. The results obtained showed that alumina (via the sol-gel) is a great catalyst for vegetable oils epoxidation. Similarly, tungsten-based, amorphous Ti/SiO<sub>2</sub> or



rhenum catalysts were employed by Salles *et al.* (2000) and Goud *et al.* (2007). A high yield and selectivity were achieved.

However, the solid catalysts reported are expensive, therefore unsuitable for large-scale production. An alternative route that utilize performic acid (PFA) as a substitute for peracetic acid (PAA), and requires no catalyst has been proposed (Hang & Yang, 1999; Campanella *et al.*, 2004). Also, it was found that the degradation reactions are much lower when the reaction is conducted under isothermal conditions.

## 4.2 SULFONATION OF FATTY ACID METHYL ESTERS

Sodium Methyl Ester Sulfonates (SMES) are anionic surfactants produced via the sulfonation reaction from saturated fatty acid methyl esters obtained from vegetable oils (Inagaki, 2001). These are widely used in the chemical industries as detergents, additives in drilling mud formulation, biotechnology, magnetic recording, high-tech electronic printing, pharmaceuticals industries and for enhanced oil recovery. Different methods have been utilized in the preparation of different kinds of sulfonated fatty acid esters (Hovda, 1996; Foster & Hovda, 1997). The main process involves the sulfation step to form an oxygen-sulphur bond. Usually, sulphating agents used include fuming sulphuric, concentrated sulphuric acid ( $H_2SO_4$ ) and sulphuric anhydride. However, making use of such agents have some implications (Sosis & Dringoli, 1970). For example, fuming sulfuric acid or sulfuric acid will result in water produced as a by-product lowering conversion. To avoid this, an excess of sulfonating agent must be used, consequently large amounts of waste acid is generated. The resulting surfactant via this process is quite expensive making it unsuitable for EOR project.

SMES is also synthesized from epoxidized sodium methyl ester using chlorosulfonic acid as sulfonating agents, with little or no waste acid produced. Verma (2010) synthesized an anionic surfactant, sodium octadecyl sulfate using non-toxic n-octadecanol in the presence of chlorosulfonic as the sulfating agent. A yield of about 80% is obtained and the purity of the synthesized product was found to be very high. Sulfate-based surfactants can also be generated via sulfonation which produces a carbon-sulfur bond. The direct sulfonation of long-chain fatty acids using sulfur trioxide ( $SO_3$ ) was firstly introduced by Weil *et al.* (1953). Sulfonation reaction refers to the addition of sulfur trioxide ( $SO_3$ ) into an organic compound. It can be achieved by reacting the organic compound with chlorosulfonic acid, oleum or pure  $SO_3$ . The main issue related with direct sulfonation is that it can only be performed under extreme conditions in the presence of strong sulfonating agents. This is because the hydrogen in the  $\alpha$ -position is only weakly activated by the nearest ester group. These strong conditions lead to side

reactions, so that the products obtained are of poor quality (Elraies *et al.*, 2008). Furthermore, low yield is obtained which causes the production of low quality sulfonate surfactants product. The above methods present numerous issues, which include: high corrosion rate, high operating cost, high cost of maintenance, low yield of reaction and it is not eco-friendly.

To cut down the cost of production of surfactants, much interest is being focused on oleochemicals, derived from agricultural materials, as substitute feedstock. Surfactants from renewable raw materials are typically environmentally friendly, biodegradable, very low or non-toxic and harmless on human health (Gregorio, 2005b). A number of surfactants have been manufactured from natural vegetable oils to suit EOR requirements (Willi, 1994, Gan-Zuo *et al.*, 2000; Qiang *et al.*, 2006). Commonly, coconut and soybean oils are the most used raw materials to obtain oleochemical feedstock, for instance fatty acids alcohol and esters (Karlheinz, 2000). However, the down side of these surfactants is the utilization of edible vegetable oils that will compete with the food market on the long run. The growing demand for vegetable oils has led to a rise in its price. The surfactant therefrom produced tends to be more costly as the price of these oils increase (Gregorio, 2005b). Thus, it has become imperative to look for alternative feedstock for surfactant production. Waste vegetable and non-edible oils are being considered as feedstock for surfactant production.

A number of different methods for the preparation of sulfonated fatty acid esters from oleochemicals can be found in literatures. The sulfonation reaction of fatty acid methyl esters using  $\text{SO}_3$  was studied in detail by Stein & Baumann (1975), and products with distinct carbon chains which have great properties for surfactant applications were obtained. Triglycerides with the required number of carbon chains can be found in coconut oil (~ 48%  $\text{C}_{12}$ , 17%  $\text{C}_{14}$ ), palm oil (~ 46%  $\text{C}_{16}$  palm kernel oil (~ 50%  $\text{C}_{12}$ , 17%  $\text{C}_{14}$ ) and tallow (~ 26%  $\text{C}_{16}$ , 23%  $\text{C}_{18}$ ) (Kaufmam, 1990; Barnes *et al.*, 2003). In general, unsaturated esters contained in vegetable oils and tallow (comprising approximately 43% oleic acid) result in the bad color of the ester sulfonates. Thus, the esters must be hydrogenated or distilled before sulfonation so that their iodine number is less than 0.5 (Inagaki, 2001).

#### 4.2.1 Sulfonating Agents

A number of sulfonating agents have been utilized in the sulfonation of fatty acid and their corresponding esters, such as  $\text{SO}_3$  vapor, stabilized liquid  $\text{SO}_3$  and dioxane-sulfur trioxide complex. Weil *et al.* (1953) reported that liquid  $\text{SO}_3$  was the best choice owing to the fast adsorptive behavior of  $\text{SO}_3$  in the ME (methyl ester) liquid film. Ishiguro *et al.* (1965) added  $\text{SO}_3$  drop-by-drop to fatty acids dissolved in tetrachloroethylene, carbon

tetrachloride or chloroform. In the last stage of sulfonation, the reaction temperature was raised to 65 °C, the molar ratio of SO<sub>3</sub>/fatty acid was 1.5-1.7 and the obtained yield was 75%-85% of the dark sulfonated acid. In each case the free sulfonic acid served as its own catalyst, or with the monosodium salt and a mineral catalyst.

Fatty acid esters and vaporized SO<sub>3</sub> diluted with air was used by Neth (1964) in a cascade-type reactor comprising of five vessels and in each vessel peroxide was added before neutralization. The concentration of H<sub>2</sub>O<sub>2</sub> plays a special function in the bleaching process and was found to depend on the fatty ester quality (between 1.5 - 3.5 % of the sulfonated product. There is a relationship between the concentration of H<sub>2</sub>SO<sub>4</sub> (formed during the reaction of excess SO<sub>3</sub> contained in the sulfonated product with the water in the H<sub>2</sub>O<sub>2</sub>) and the bleaching effect. If the amount of H<sub>2</sub>SO<sub>4</sub> is too low, hydrolytic cleavage of the ester may take place and if the amount of H<sub>2</sub>SO<sub>4</sub> is too high, the color is undesirable.

For safety reasons, a number of sulfonate reagents have been developed to decrease the SO<sub>3</sub> reactivity in the sulfonation process including sulfamic acid, sodium bisulfite and chlorosulfonic acid. Elraies *et al.* (2009) synthesized sodium methyl ester sulfonate from FAME using chlorosulphonic acid in the presence of pyridine and the product extracted into n-butanol. The fatty acid methyl ester was produced via esterification and transesterification of non-edible *Jatropha* oil. Babu *et al.* (2015) synthesized SMES for enhanced oil recovery application using chlorosulfonic acid and ricinoleic acid methyl ester obtained from castor oil. They use the methodology described by Elraies *et al.* (2009). The SMES showed good surface activity in decreasing the IFT up to 38.4 mN/m and 27.6 mN/m in the absence and presence NaCl respectively. The thermal analysis revealed that the SMES about 30 % of its mass as temperature increased in the range 70 °C to 500 °C. Zhang *et al.* (2015) also converted waste cooking oil to bio-based zwitterionic surfactants with exceptional surface and interfacial behavior. The IFT between crude oil and water could attain ultra-low value (as low as 0.0016mNm<sup>-1</sup>) at a low dosage (0.100g/L) of the biobased surfactant without the use of an alkali. It demonstrated an excellent interfacial activity as well as very good potential for application in various industrial fields, particularly, its use in CEOR processes.

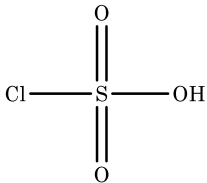
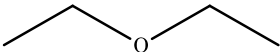
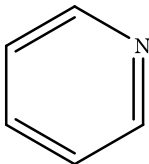
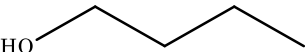
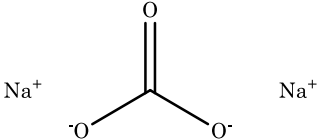
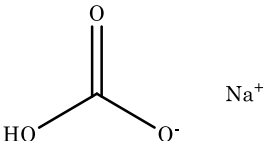
### 4.3 EXPERIMENTALS

The experimental works involve two stages, the epoxidation of the FAME produced from waste oils as earlier reported in Chapter 3 to form epoxidized FAME (EFAME). This was then sulphonated to produce the surfactant.

### 4.3.1 Production of Epoxidized Fatty Acid Methyl Esters

The chemicals utilized for the epoxidation of methyl esters are formic acid (99.81% CH<sub>2</sub>O<sub>2</sub>), sodium bicarbonate (7.5% aqueous NaHCO<sub>3</sub>), sodium chloride (ACS reagent, ≥99.0% NaCl), hydrogen peroxide (30 % aqueous H<sub>2</sub>O<sub>2</sub>), diethyl ether (≥99.0% CH<sub>3</sub>CH<sub>2</sub>)<sub>2</sub>O), toluene (anhydrous, 99.8% C<sub>7</sub>H<sub>8</sub>), n-hexane (anhydrous, 95% C<sub>6</sub>H<sub>14</sub>) and propan-2-ol (anhydrous, 99.5% CH<sub>3</sub>CHOHCH<sub>3</sub>). These were purchased from Sigma Aldrich. For surfactant synthesis, chlorosulfonic acid (97% HSO<sub>3</sub>Cl), pyridine (99.5% C<sub>5</sub>H<sub>5</sub>N), sodium carbonate (99.5% Na<sub>2</sub>CO<sub>3</sub>), sodium bicarbonate (7.5% aqueous solution of NaHCO<sub>3</sub>), n-butanol (99.5% C<sub>4</sub>H<sub>9</sub>OH) and diethyl ether [(C<sub>2</sub>H<sub>5</sub>)<sub>2</sub>O] were purchased from Sigma Aldrich. The chemicals properties and their structures are tabulated in Table 7.

**Table 7:** Chemicals properties and their structures

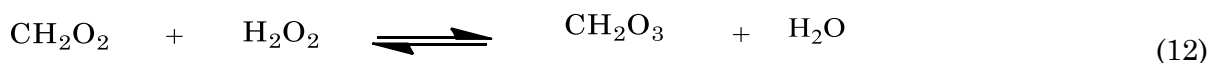
Chemicals	Structure	Molecular formula	M <sub>w</sub> (g/mole)
Chlorosulfonic acid		HSO <sub>3</sub> Cl	116.52
Diethyl ether		(C <sub>2</sub> H <sub>5</sub> ) <sub>2</sub> O	74.12
Pyridine		C <sub>5</sub> H <sub>5</sub> N	79.1
n-butanol		C <sub>4</sub> H <sub>9</sub> OH	74.12
Sodium carbonate		Na <sub>2</sub> CO <sub>3</sub>	105.9888
Sodium bicarbonate		NaHCO <sub>3</sub>	84.0066

To reduce the saturated fatty acids contents and to epoxidize the unsaturated fatty acids a detailed investigation regarding the effects of solvent-free and solvent in the

epoxidation reaction at 25 °C, 30 °C and 50 °C using 4 moles of formic acid at reaction time of 4 hours was conducted. The reaction conditions were identical to those proposed by Campanella *et al.* (2008) and Akintayo *et al.* (2006). Formic acid was utilized in this study owing to the fact that the performic acid formation rate is superior in comparison to that of peracetic acid and the formic acid method is well-known to progress at a faster rate (Scala & Wool, 2002; Campanella *et al.*, 2008). Moreover to generate peracetic acid in high concentrations, the use of a catalyst is required (Campanella *et al.*, 2008). Because the mass of catalyst added to the reaction is very small, random error in the catalyst mass is significant and can have a large effect on the peracid concentration. The formation of performic acid requires no catalyst and is therefore easier to produce with a specific concentration, however it offers an environment more favourable for the hydrolysis of oxirane to generate by-products; particularly in the presence of aqueous hydrogen peroxide (Smith *et al.*, 2009).

#### 4.3.2 Epoxidation with no solvent

The epoxidation reaction was performed in a temperature controlled batch reactor as described in Figure 15. About 10.7 g of CH<sub>2</sub>O<sub>2</sub> and 100 g of FAME is added to the reaction vessel. The vessel is connected to a condenser and placed in a water bath maintained at 25 °C. 58.8 g of H<sub>2</sub>O<sub>2</sub> was added drop-wise to the vessel through the top of the condenser which then formed peroxyformic acid by reacting with the formic acid (Reaction 12) and allowed to stand for 4 hours.



The principal product is epoxidized methyl ester (EFAME) with oxirane rings at the position of double bonds. Possible by-products include keto compounds due to the redistribution of oxirane group or vicinal di-hydroxy because of oxirane hydrolysis.

**Epoxidized FAME purification** step was carried out to purify the EFAME by removing the H<sub>2</sub>O<sub>2</sub> and the excess acid. About 20 ml of diethyl ether (99.9%, Sigma Aldrich) is added to the EFAME in a 250ml separation funnel and stirred well. First, the EFAME/ether solution is washed 3 times with de-ionized H<sub>2</sub>O to get rid of the excess acid. Then, the product was washed again with about 10 ml of aqueous sodium bicarbonate solution (5 g NaHCO<sub>3</sub>/100 g H<sub>2</sub>O), which neutralized the residual acid and peroxide. As the bicarbonate solution was added to react with the rest of the acid and slowly agitated, the stopper of the separating funnel was pointed away and into the fume hood and occasionally opened to allow produced gasses to be discharged safely from the funnel. This was repeated until pH paper indicated that it was neutral, showing that the only components remaining in the organic layer was the epoxidized methyl esters. If the

solution was too basic, it was rinsed again with water, if it was too acidic, it was rinsed again with NaHCO<sub>3</sub> solution.

Then about 10 ml of sodium chloride solution (5 g NaCl/100 g H<sub>2</sub>O) is added to separate any remaining H<sub>2</sub>O from the organic phase. The aqueous layer was decanted from the reaction system and disposed of. The organic layer was moved to a round bottom flask and attached to a rotary evaporator (Buchi Rota vapour Model R-205 equipped with a Buchi controller V-800 and a water bath) and was evaporated for at least 30 minutes at 80 °C to evaporate both the ether and any residual H<sub>2</sub>O from the organic phase. The produced epoxy fatty acid methyl esters are analysed using a GC-MS to detect and determine the different epoxy acids present. Afterwards, it was utilized for the surfactant synthesis process.

#### **4.3.3 Epoxidation with solvent**

In this thesis the process for synthesis of EFAME from FAME described by Akintayo *et al.* (2006) was used. 100 g of FAME was dissolved in 50 mL of toluene and 4 moles of CH<sub>2</sub>O<sub>2</sub> added at temperature of 25 °C while stirring. Hydrogen peroxide (100 ml) was then added while keeping the temperature constant. Afterwards the reaction was allowed to continue for 4 hours. Reaction mixture was then allowed to settle and the aqueous layer removed using a separating funnel. The organic layer was repeatedly rinsed with warm H<sub>2</sub>O until free of acid. The residual toluene and H<sub>2</sub>O were removed under reduced pressure in the Buchi rotary evaporator at 100 °C. The same procedure was repeated using n-hexane and propan-2-ol at 30 °C and at 50 °C.

#### **4.3.4 Analyses of Epoxy Fatty Acid Methyl Esters**

A gas chromatography coupled with an electron impact mass spectrometry was selected for the analysis of Epoxy FAME due to its capacity to concurrently determine and identify the constituents. The GC-MS is fitted with a capillary column of 30 m ZB-5MS Guardian with 0.25 mm internal diameter and with a film thickness of 0.25 µm (Table 8). 0.1 g of the sample was diluted in 10 ml of hexane. 1 ml of the mixture was transferred into a Teflon-lined screw glass tube. 1ml of 2.5% (v/v) sulfuric acid in methanol was added into the tube. The mixture was incubated in the oven and maintained at temperature of 80 °C for 1h. After incubation, the mixture was allowed to cool to room temperature and 1.5 ml of 1% (w/v) NaCl was added to it to extract the fatty acid methyl esters. The sample was centrifuged at 200 rpm to facilitate phase separation.

The upper hexane phase (pentane containing FAMEs) was transferred to a GC vial. Some of the hexane was evaporated using dry nitrogen so as to improve GC sensitivity.

In every run one micro-liter (1 $\mu$ L) of sample was injected using a 7980B Agilent Technologies Injector with CTC CombiPAL Autosampler and Agilent 5975B Mass Spectrophotometer (mass selective detector) used to identify the fraction of the total peak areas attributed to each by the mass spectrum libraries provided with the GC-MS software. Heptadecanoic acid (C17:0; C<sub>17</sub>H<sub>34</sub>O<sub>2</sub> or margaric acid) was used as the internal standard. The GC-MS specification and oven temperature program are described in Tables 8-10.

**Table 8:** GC-MS Specifications

<b>Instrument Settings</b>	<b>Parameters Used</b>
Injector temperature	280 °C
Injection volume	1 $\mu$ l
Injection mode	Split
Slit ratio	5:1
Carrier gas	Helium
Flow rate	1 ml/min
MS mode	El+
Scanning mass range	40 to 550 m/z
Scan Time	0.15 min
Inter-scan delay	0.05 min

**Table 9:** Oven Temperature Program

<b>Oven Ramp</b>	<b>°C/min</b>	<b>Temperature (°C)</b>	<b>Hold (min)</b>
Initial		100	1
Ramp 1	25	180	3
Ramp 2	4	200	5
Ramp 3	8	280	3
Ramp 4	4	320	10

#### 4.3.5 Sulfonation of the Epoxidized Methyl Esters for Surfactant Production

About 2.63 g of chlorosulfonic acid (HSO<sub>3</sub>Cl) was added very slowly while stirring (at 800 ppm) to 15 ml of pyridine (C<sub>5</sub>H<sub>5</sub>N) in a 500 ml round bottom flask placed in ice-cooled

water bath for 15 min. 2.60 g of the epoxidized fatty acid methyl ester solution obtained above was introduced slowly to the round bottom flask with continuous stirring, for another 30 min. The reactor and its contents were afterwards heated to a temperature of 65 °C in a water bath until the solution turned clear. For the second step, the reaction was quenched and the solution is poured into an ice-cooled 500ml flask containing 33 g in 300 ml solution of sodium carbonate ( $\text{Na}_2\text{CO}_3$ ) and enough (approximately 30 g) solid sodium bicarbonate ( $\text{NaHCO}_3$ ) to keep the solution saturated with inorganic sodium salts. The sulfonated product, was extracted into 40 ml of n-butanol ( $\text{C}_4\text{H}_9\text{OH}$ ) using a separating funnel. The solvent was removed from the crude product via drying with a rotary evaporator. The powder obtained is re-dissolved in 200 ml of water. Then, the organic impurities were eliminated from the aqueous solution of methyl ester sulfonate (SEMES) via extraction with 50 ml of diethyl ether. The crude product is concentrated and dried under vacuum for 24 h. Since  $\text{C}_4\text{H}_9\text{OH}$  and  $\text{Na}_2\text{CO}_3$  are typically utilized in CEOR as co-solvent and alkali correspondingly, the SEMES produced was analyzed without further purification so as to reduce the cost of surfactant manufacturing (Elraies *et al.*, 2008). The schematic illustration of the proposed chemical reaction for SMES surfactant is shown in Figure 25.

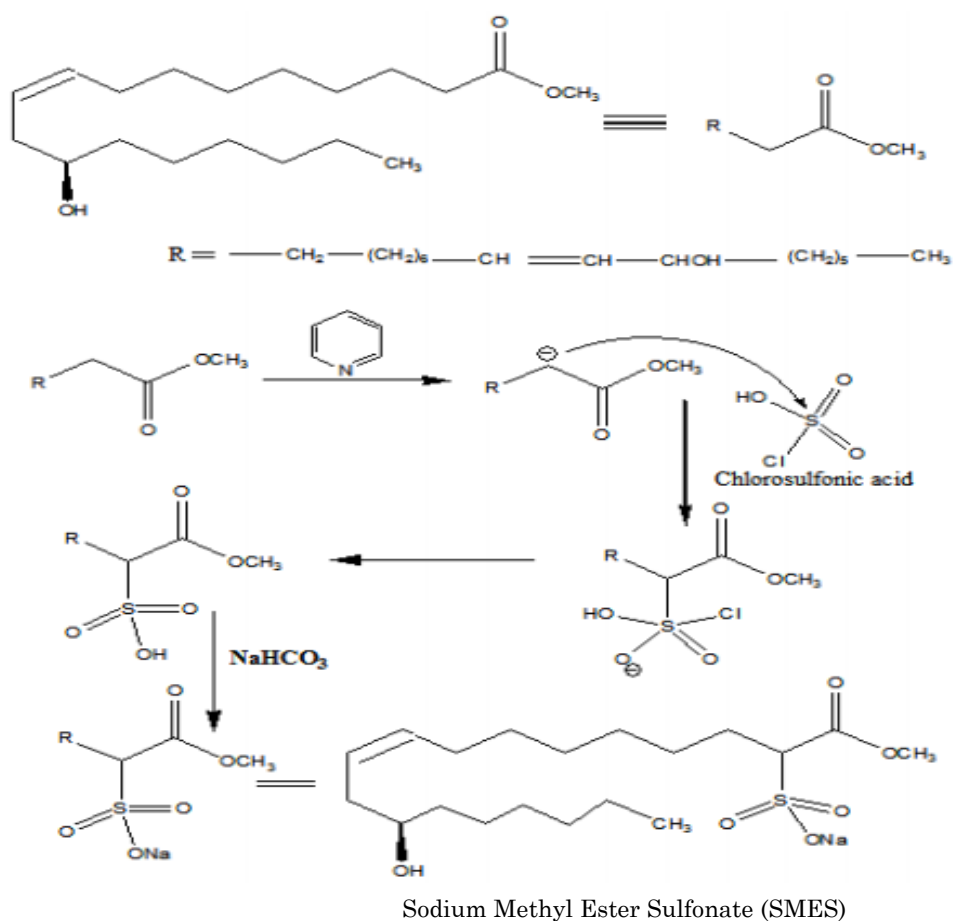


**Figure 25:** Schematic illustration of proposed chemical reaction for Sodium Methyl Ester Sulfonate surfactant (Babu *et al.*, 2015)



### 4.3.6 Surfactants Analysis

A Fourier Transform Infrared (FTIR) spectrophotometer was utilized to give information on the molecular structure of the synthesized and synthetic surfactants. Different functional groups are prone to absorb specific frequencies of IR radiation (Elraies and Tan, 2013). The synthesized (SEMES) and two commercial (SDS and CTAB) surfactants were grinded with potassium bromide (KBr) to obtain a fine powder. The powder was then compressed into a thin pallet for analysis. About 15 mg of this pallet in each case was put on the Attenuated Total Reflectance (ATR) sample holder of a Perkin Elmer spectrum 100 FTIR spectrometer (model JASCO FT/IR-4100). The sample was recorded in the range of 4000-500 cm<sup>-1</sup>, baseline was corrected and the spectra smoothed. The utilization of diamond cells consisting of a beam condenser and a microscope made possible the adjustment of the thickness of the sample by squeezing, which permitted the analysis of µg samples to be conducted. The FTIR spectrophotometer was used to determine the chemical functional group present in the surfactants.

## 4.4 RESULTS AND DISCUSSIONS

### 4.4.1 Epoxidation of FAME

The fatty acid composition of the FAME used in this study is analysed using a Gas Chromatography Mass Spectrometry (GC-MS). The results are presented in Table 10, while the spectra are shown in Figures 26 and 27.

**Table 10:** Percentage composition of Fatty acid methyl esters

FAME	Area (%)
9-Hexadecenoic acid, methyl ester, (Z)-	0.2635
Hexadecanoic acid, methyl ester	12.1634
10,13-Octadecadienoic acid, methyl ester	47.9177
15-Octadecenoic acid, methyl ester	29.1843
Octadecanoic acid, methyl ester	7.6116
11-Eicosenoic acid, methyl ester	0.789
Eicosanoic acid, methyl ester	0.7046
Docosanoic acid, methyl ester	1.0874
Heneicosanoic acid, methyl ester	0.2784

The GC-MS of fatty acid methyl esters confirmed the presence of the following: saturated fatty acids, Palmitic acid (C16:0), Stearic acid (18:0), arachidic acid (C20:0), Heneicosylic acid (21:0), Behenic acid (C22:0), Palmitoleic acid (C16:1). The mono-unsaturated FA include Gadoleic acid (C20:1), Oleic acid (C18:1c) while the polyunsaturated FA is Linoleic acid (C18:2c) and oleic acid. The content of saturated fatty acids (16:0, 18:0, 20:0 and 24:0) was 19.95% which is considered to be quite high. According to Perez *et al.* (2009) saturated fatty acids cannot be epoxidized; consequently, they cannot take part in cross linking during the preparation of polymers which makes the attainment of epoxy group a challenge.

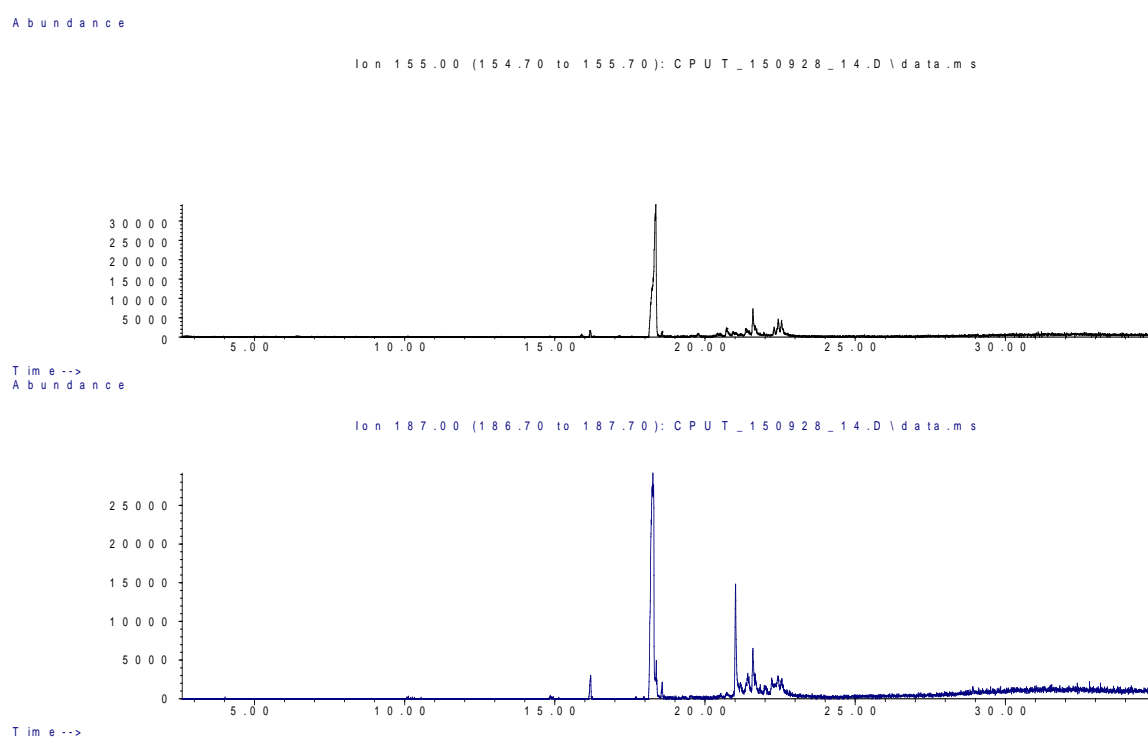


**Figure 26:** Mass spectrum of fatty acid methyl esters

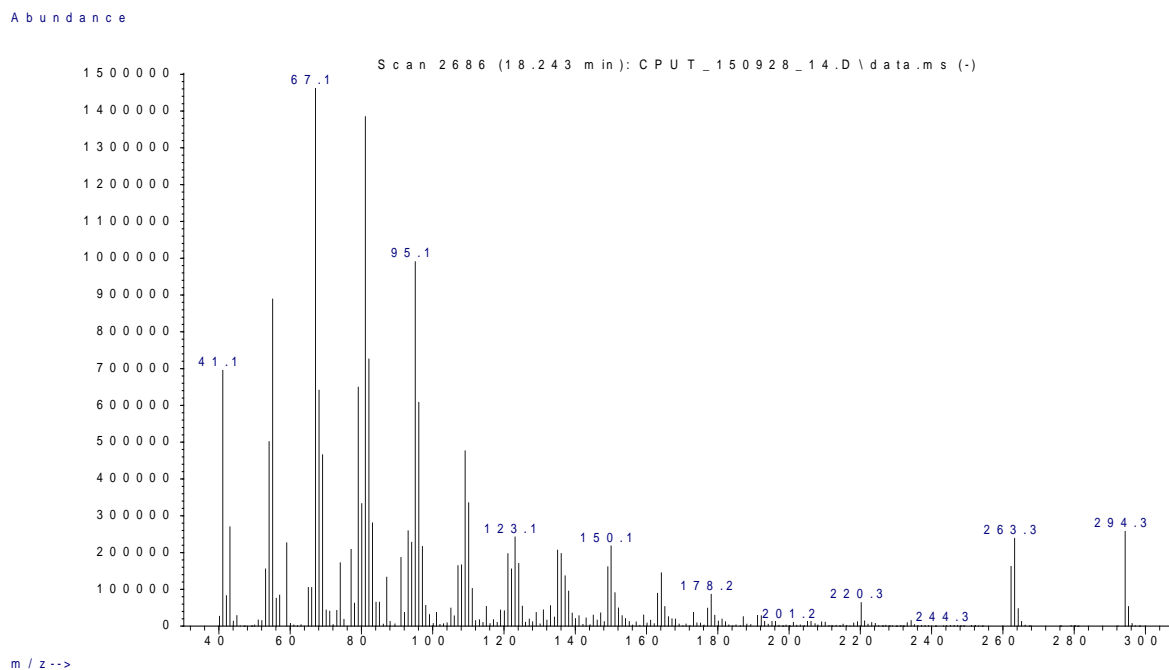
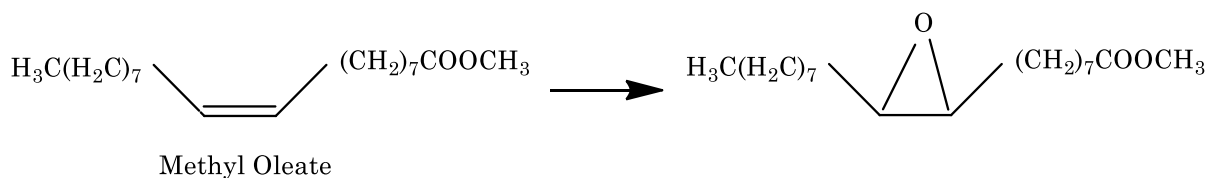
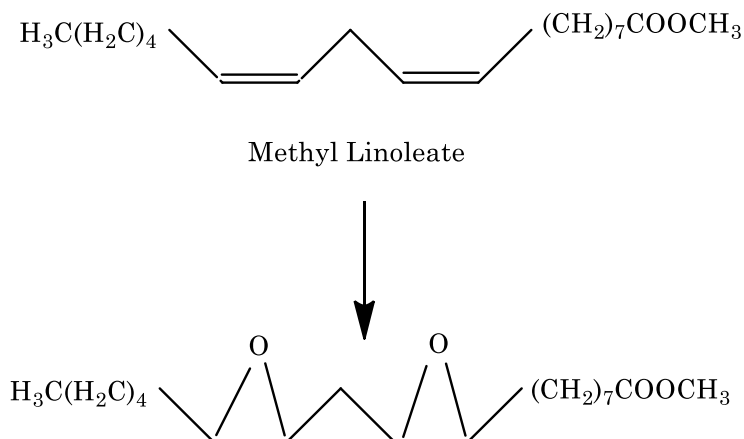


**Figure 27:** Chromatogram from the GC-MS of the Fatty acid methyl esters

For a FAME containing oleic, linoleic methyl esters, different products are possible during epoxidation reaction. Possible epoxy products obtainable are presented in Schemes 1 and 2 displaying some potential epoxy compounds from oleate and linoleate.



**Scheme 1:** Conversion of methyl oleate to mono-epoxy compound



**Scheme 2:** Conversion of methyl linoleate to di-epoxy compound

The percentage compositions of the EFAMES produced under different conditions are presented in Tables 11 to 18. The mass spectrum of the epoxy FAMES are illustrated in *Appendix B*. The GC-MS was able to determine the degree of conversion of FAMES to epoxy FAMES by the reduction in the area of the peaks. However, it was not able to accurately identify more product peaks as epoxy FAMES. Furthermore, there are no commercially available reference standards for epoxy fatty acid methyl esters. To make it more complicated, FAME produced from WVO is an intricate combination of various different fatty esters with many reaction sites (double bonds). Hence, there are several possible products that may not be fully determined via the GC technique.

**Table 11:** Composition of solvent-free epoxidized fatty acid methyl esters at 25 °C

EFAME	Area (%)
Methyl tetradecanoate	0.1373
9-Hexadecenoic acid, methyl ester, (Z)	0.1
Hexadecanoic acid, methyl ester	10.143
Heptadecanoic acid, methyl ester	3.022
11,14-Octadecadienoic acid, methyl ester	14.0976
9-Octadecenoic acid, methyl ester, (E)	17.4806
Octadecanoic acid, methyl ester	6.5219
cis, 6-Octadecenoic acid, trimethylsilyl ester	0.1773
2(5H)-Furanone, 4-hydroxy-3-(2-quinolinyl)	0.0972
3-Cyclopentylpropionic acid, hex-4-yn-3-yl ester	0.147
11-Eicosenoic acid, methyl ester	0.2659
Octadecanoic acid, 10-oxo-, methyl ester	0.5909
Benzylamine, .alpha.-methyl-m-nitro-	0.3667
Eicosanoic acid, methyl ester	1.0987
3-Chloropropionic acid, 2-tetrahydrofurylmethyl ester	0.2289
Benzoyl chloride, 3-(fluorosulfonyl)	1.389
2,2'-Dimethoxy-biphenyl-4,4'-diamine	0.5398
9-Octadecenoic acid, 13-hydroxy-12-methoxy-, methyl ester	3.4982
2-Naphthylthioacetonitrile	9.8107
Nitrobenzene, 3,4,5-trimethoxy-	7.6367
p-Cyanophenyl trifluoromethyl ether	14.8596
Methyl ricinoleate	0.9084
5,8-Methano-4H-3,1-benzoxazine-2-thione, 1,2,4a-rel,5-cis,8-cis,8a-cis-hexahydro	0.1815
3-Amino-3-(4-chloro-3-nitro-phenyl)-propionic acid	1.2765
Octadecanoic acid, 9,10-dihydroxy-, methyl ester	1.9885

1-Propene, 1-methoxy	0.5422
8-Hydroxy-3-methyl-1,5-dioxaspiro[5.5]undecane-3-carboxylic acid	0.9114
Docosanoic acid, methyl ester	1.4065
3-Amino-5-chloro-benzofuran-2-carboxylic acid methyl ester	0.1293
4,7,7-Trimethyl-6-thiabicyclo[3.2.1]octane	0.286
Butanoyl fluoride, heptafluoro-	0.1605

**Table 12:** Composition of epoxidized fatty acid methyl esters produced with toluene at 25 °C

<b>EFAME</b>	<b>Area (%)</b>
Decanal dimethyl acetal	0.1057
Nonanal dimethyl acetal	0.5946
Octanoic acid, 6,6-dimethoxy-, methyl ester	0.8604
Methyl tetradecanoate	0.2011
Hexadecanoic acid, methyl ester	14.2891
Heptadecanoic acid, methyl ester	4.7313
Octadecanoic acid, methyl ester	8.759
Octadecanoic acid, 10-oxo-, methyl ester	0.8891
4-Methoxyformanilide	0.7245
Eicosanoic acid, methyl ester	1.39
Tetrahydrofuran, 2-hexyl-	1.0829
Borane, diethyl[1-ethyl-2-(methoxymethyl)-1-butenyl]-, (Z)-	0.6352
Butanoic acid, 2-propenyl ester	0.6678
Benzidine, 3,3'-dimethoxy-	3.8359
Cyclohexane-1,3-dione,5,5-dimethyl-2-[1-[2-(4-(1-oxopentyl)-1-piperazinyl)ethylamino]ethylidene]-	0.253
p-Cyanophenyl trifluoromethyl ether	24.9375
1,4-Dioxaspiro[4,5]decane-7,9-dipropionic acid, 8-oxo-, dimethyl ester	0.9995
2,8-Diazaspiro[4,5]decane-1,3-dione, 8-(2-chloroethyl)-2-isopropyl-	0.3824
Octadecanoic acid, 9,10-dihydroxy-, methyl ester	8.2822
Trimethylamine, compd. with borane (1:1)	0.972
Benzene, 1-isocyanato-3-(trifluoromethyl)-	1.6101
Docosanoic acid, methyl ester	1.921
Thiocyanic acid, o-anilinophenyl ester	4.3757
1,4-Dioxaspiro[4,5]decane-7-ethanol, 10-methyl-.beta.-methylene-	5.8127
2-Methyl-4-triisobutylsilyloxyoct-5-yne	4.5458
4,7,7-Trimethyl-6-thiabicyclo[3.2.1]octane	6.624

**Table 13:** Composition of epoxidized fatty acid methyl esters produced with propan-2-ol at 30 °C

<b>EFAME</b>	<b>Area (%)</b>
9-Hexadecenoic acid, methyl ester, (Z)-	0.2245
Hexadecanoic acid, methyl ester	11.6522
Heptadecanoic acid, methyl ester	3.989
8,11-Octadecadienoic acid, methyl ester	44.6752
9-Octadecenoic acid, methyl ester	27.8692
1,3-Cyclooctadiene	0.3675
Octadecanoic acid, methyl ester	7.3216
9,12-Octadecadienoic acid, methyl ester, (E,E)-	0.0869
Oleic acid, trimethylsilyl ester	0.0783
11-Eicosenoic acid, methyl ester	0.6758
Eicosanoic acid, methyl ester	0.6905
3-Methoxyhex-1-ene	0.0966
2-Ethyl-1-cyclohexyldimethylsilyloxyhexane	0.3448
6-Methyl-hept-2-en-4-ol	0.1497
2,2'-Dimthoxy-biphenyl-4,4'-diamine	0.2798
9-Octadecenoic acid, 12-hydroxy-13-methoxy-, methyl ester	0.1318
2(3H)-Benzothiazolethione, 5-chloro	0.1739
2-Octen-1-ol, 3,7-dimethyl	0.1281
Docosanoic acid, methyl ester	1.0646

**Table 14:** Composition of epoxidized fatty acid methyl esters produced with n-hexane at 30 °C

<b>EFAME</b>	<b>Area (%)</b>
9-Hexadecenoic acid, methyl ester, (Z)	0.2573
Hexadecanoic acid, methyl ester	11.5649
Heptadecanoic acid, methyl ester	5.1701
8,11-Octadecadienoic acid, methyl ester	44.2539
9-Octadecenoic acid (Z)-, methyl ester	28.3584
9,12,15-Octadecatrienoic acid, methyl ester, (Z,Z,Z)	0.3647
Octadecanoic acid, methyl ester	7.1854
9,12-Octadecadienoic acid, methyl ester, (E,E)	0.0848
11-Eicosenoic acid, methyl ester	0.662
Eicosanoic acid, methyl ester	0.6713
1,3-Difluoro-5-octyldimethylsilyloxybenzene	0.158
Benzidine, 3,3'-dimethoxy-	0.1441

1H-Indene, 5-(1,1-dimethylethyl)-2,3-dihydro-1,1-dimethyl	0.096
Docosanoic acid, methyl ester	1.029

**Table 15:** Composition of epoxidized fatty acid methyl esters produced with toluene at 30 °C

EFAME	Area (%)
9-Hexadecenoic acid, methyl ester, (Z)	0.2155
Hexadecanoic acid, methyl ester	11.618
Heptadecanoic acid, methyl ester	4.0293
8,11-Octadecadienoic acid, methyl ester	43.7705
9-Octadecenoic acid, methyl ester, (E)	30.9394
Methyl trans-9,10-epoxyoctadecanoate	7.1318
11-Eicosenoic acid, methyl ester	0.626
Eicosanoic acid, methyl ester	0.6372
Methyl (11R,12R,13S)-(Z)-12,13-epoxy-11-methoxy-9-octadecenoate	0.0417
Docosanoic acid, methyl ester	0.9904

**Table 16:** Composition of epoxidized fatty acid methyl esters produced with n-hexane at 50 °C

EFAME	Area (%)
Hexanal dimethyl acetal	0.2333
Decanal dimethyl acetal	0.3113
9-Hexadecenoic acid, methyl ester	0.2538
Hexadecanoic acid, methyl ester	12.0481
Heptadecanoic acid, methyl ester	2.8101
8,11-Octadecadienoic acid, methyl ester	45.2527
16-Octadecenoic acid, methyl ester	27.9275
Octadecanoic acid, methyl ester	7.628
11-Eicosenoic acid, methyl ester	0.6808
Eicosanoic acid, methyl ester	0.8134
Phenol, 4-chloro-2-(1-methylethyl)	0.3445
2-Propenoic acid, 3-(2-thienyl)	0.1987
Docosanoic acid, methyl ester	1.1996
Tetracosanoic acid, methyl ester	0.2982

**Table 17:** Composition of epoxidized fatty acid methyl esters produced with propan-2-ol at 50 °C

EFAME	Area (%)
-------	----------

9-Hexadecenoic acid, methyl ester	0.2526
Hexadecanoic acid, methyl ester	11.8677
Heptadecanoic acid, methyl ester	3.5445
8,11-Octadecadienoic acid, methyl ester	45.1697
9-Octadecenoic acid, methyl ester	28.2422
Octadecanoic acid, methyl ester	7.4033
11-Eicosenoic acid, methyl ester	0.7529
Eicosanoic acid, methyl ester	0.6994
Ether, 1-hexadecenyl methyl	0.3669
Tetrahydrofurfuryl bromide	0.3382
Docosanoic acid, methyl ester	1.0873
Tetracosanoic acid, methyl ester	0.2753

Table 18: Composition of epoxidized fatty acid methyl esters with toluene at 50 °C

<b>EFAME</b>	<b>Area (%)</b>
Hexadecanoic acid, methyl ester	11.4337
Heptadecanoic acid, methyl ester	4.3919
10,13-Octadecadienoic acid, methyl ester	43.3259
9-Octadecenoic acid, methyl ester	31.5094
Octadecanoic acid, methyl ester	7.0059
11-Eicosenoic acid, methyl ester	0.6583
Eicosanoic acid, methyl ester	0.5946
3-Quinazolineacetamide, N-(2-chlorophenyl)-3,4-dihydro-4-oxo	0.1553
Docosanoic acid, methyl ester	0.925

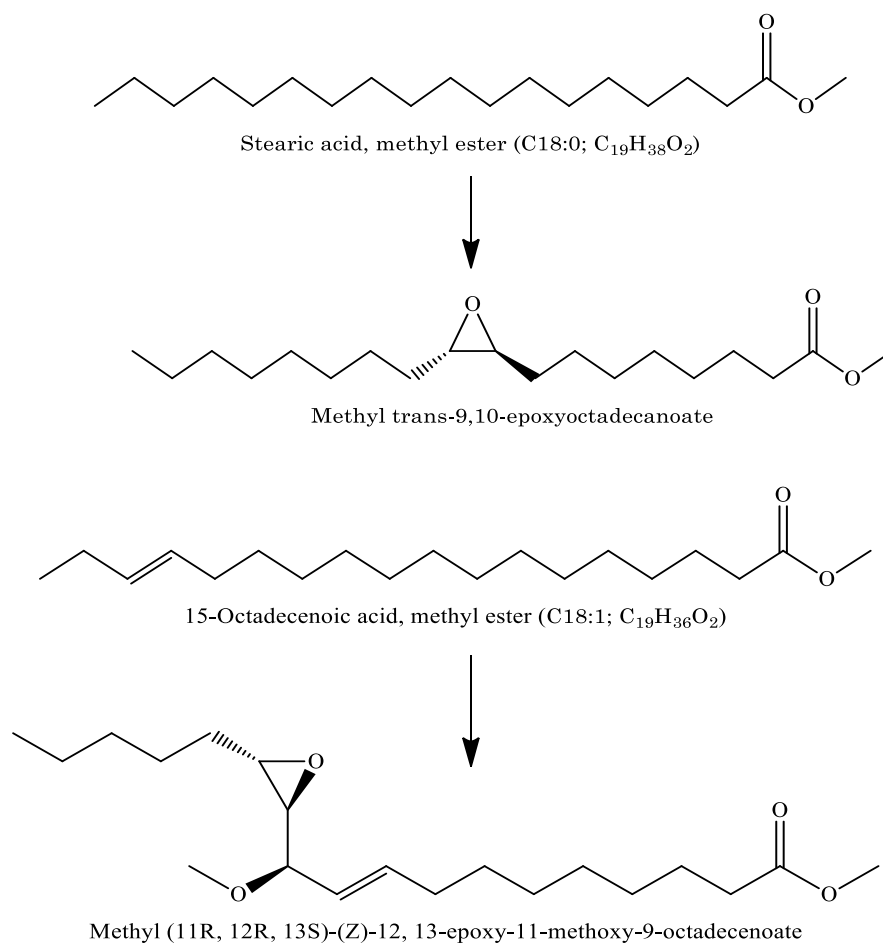
The idea of carrying out epoxidation reaction at lower temperatures and in the presence of organic solvents was informed by the number of studies that reported that the use of a solvent have been reported to minimize oxirane degradation and by-products formation (Akintayo, 2006; Goud *et al.*, 2007; Espinoza Perez *et al.*, 2009). For instance, because hydrogen peroxide presents a higher solubility in organic solvent compared to water, the generation of carboxylic acids, a side reaction product, is eliminated (Espinoza Perez *et al.*, 2009; Goud *et al.*, 2007). The presence of organic solvents seems to have some stabilizing effect on the oxirane formed during the peroxyformic or peroxyacids epoxidation of oils and FAMEs (Espinoza Perez *et al.*, 2009). Moreover solvent can control the temperature increase during reaction by adsorbing the heat released to



provide the solvent's heat of vaporization, hence preventing the rise in temperature beyond the boiling temperature of the selected solvent, thus reducing the adverse temperature effects (Mushtaq *et al.*, 2011). Solvent use also offers good solubilization for all inorganic and organic substances thus promotes good mass transfer.

The epoxidation reactions were conducted in the presence and absence of organic solvents (toluene, n-hexane and propan-2-ol) at 25 °C, 30 °C and 50 °C. From Tables 13 to 18 it can be observed that performing epoxidation reactions at 30 °C and 50 °C and in presence of organic solvents minimized to a very high extent side- and by-products formation and ring opening reactions especially to hydroxyl compounds. Since the epoxidation is an exothermic reaction, a poor control of temperature could cause and increase significantly the formation of undesired di-hydroxy groups. According to Deshpande (2013) the presence of an inert solvent like toluene in the epoxidation reaction stabilizes the epoxide product and reduced the adjacent reactions, for instance the opening of the epoxy ring; which is in agreement with the results obtained in the current study. When toluene was used at reaction temperature of 30 °C for 4 hours the first traces of epoxy fatty acid methyl esters were produced. Moreover, epoxidation reactions in the presence of solvents simplified sample handling, thus reducing filtration losses as well as giving higher sample recoveries.

Reaction at lower temperature of 25 °C showed lower rate of epoxidation but high rate of hydrolysis of the product. Tables 15 and 16 clearly demonstrates that there was indeed formation of various by-products due to hydrolysis, for instance *9-Octadecenoic acid*, *13-hydroxy-12-methoxy-, methyl ester*, *Octadecanoic acid*, *9,10-dihydroxy-, methyl ester*. When the temperature was increased from 30 °C to 50 °C, a change in the composition of the fatty acid methyl esters and a decrease in side reactions and by-products were observed. As stated earlier, in the presence of toluene and at 30 °C, *Methyl (11R, 12R, 13S)-(Z)-12, 13-epoxy-11-methoxy-9-octadecenoate and Octadecanoic acid, 9,10-epoxy-, methyl ester, trans* were produced. The mechanism is presented in Scheme 3 and the mass spectrum as shown in Fig. 28. This implied that moderate temperatures of 30 °C were more suitable for epoxidation of oleic acid with PFA generated *in-situ* for optimum oxirane levels and hydrolysis rate reduction. However, very low yield of epoxy products was achieved; this is attributed to the fact that the double bonds on the methyl linoleate and methyl oleate are less reactive if one were to compare them with the double bonds of the linoleic and oleic acids (Deshpande, 2013). As a result, structural arrangement of the methyl linoleate and methyl oleate may have caused a reduction in the reactivity of the unsaturated sites.



**Scheme 3:** Reaction scheme for the epoxidation of FAME in the presence of toluene at 30 °C including the main products: *Methyl (11R, 12R, 13S)-(Z)-12, 13-epoxy-11-methoxy-9-octadecenoate and Octadecanoic acid, 9, 10-epoxy-, methyl ester, trans*

Here solvent is used to mitigate the possible effect caused by the energy released from the epoxidation reaction. The results obtained at higher reaction temperature (50 °C) in combination with the use of a solvent (Tables 16 to 18) , suggest simultaneous decrease in the side reactions that open the epoxy ring in addition to minimization of the rate of hydrolysis (oxirane cleavage) of the product, which is in agreement with a previous report (Mushtaq *et al.*, 2011). At 50 °C and in the presence of a solvent, the epoxidized FAME showed very low or no hydroxyl formation compared to the solvent-free epoxidation and at 25 °C. This goes in accordance with the literature reported by Espinoza Perez *et al.* (2009) and Smith *et al.* (2009) where di-hydroxy (glycol) formation greatly influenced by the increase in temperature. Furthermore, increasing temperature demonstrated a favorable influence on the formation of performic acid (Espinoza Perez *et al.*, 2009). The results further show substantial reduction in the percentage composition of saturated and unsaturated fatty acids in product composition for epoxidation reactions carried out at higher temperatures.

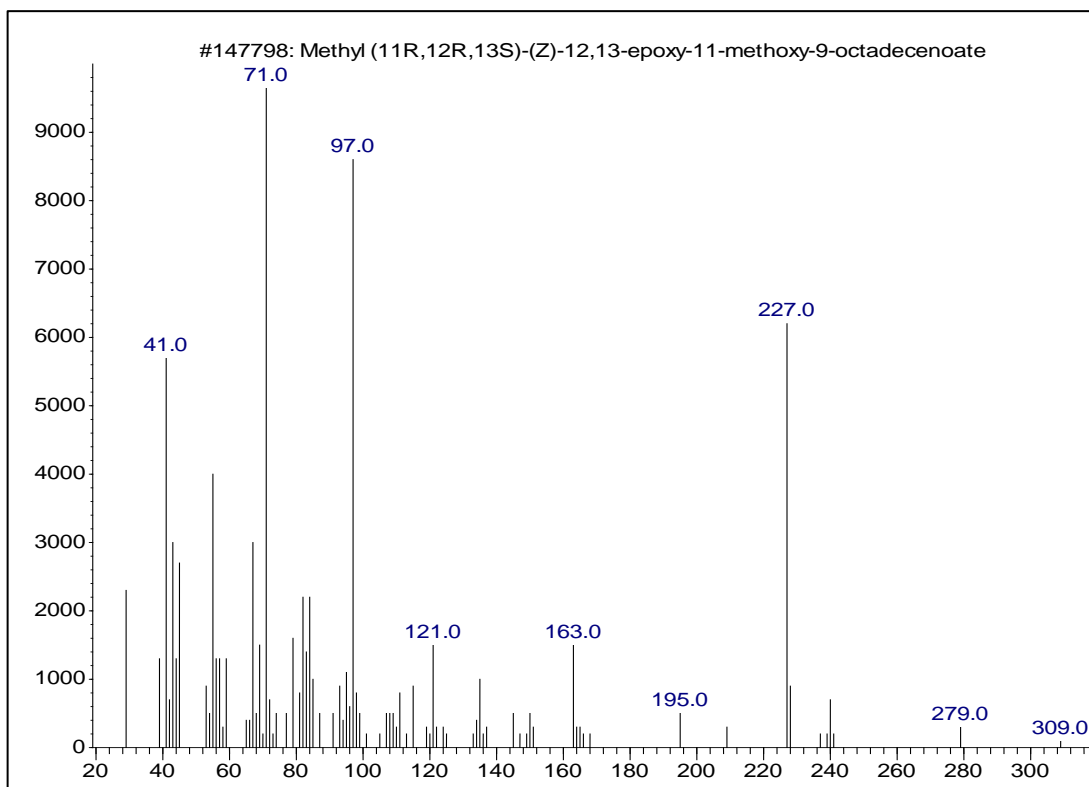


**Figure 28:** Mass spectrum of FAME derivatives: *Methyl (11R, 12R, 13S)-(Z)-12, 13-epoxy-11-methoxy-9-octadecenoate*

#### 4.4.2 Thermo-gravimetric Analysis of FAME and EFAME

The epoxidation reaction results in the replacement of the unsaturated double-bonds by the epoxy group which results in the reduction of unsaturation in the FAME. The existence of various functional groups, -unsaturated, epoxidized as well as hydroxyl-methyl esters could enable a closer packing arrangement (Kongyai, 2013). This promotes the side-by-side parallel packing of the particles, thus resulting in an increase in both flash point in addition to the oxidation stability of epoxy FAME (Carmona, 2014). The thermo-gravimetric method was used to assess the change in weight of FAME and epoxidized FAME as a function of temperature. In this study, the approach of Borugadda & Goud (2014) was used to evaluate the thermo-oxidative stability of FAME and its epoxide. The temperature was varied from ambient to 700 °C. The analysis was performed in Perkin Elmer TGA7 bench model thermo-gravimeter analyzer. To obtain the thermal oxidative stability, samples were heated in oxygen atmosphere at constant heating rate of 10 °C/min. TG curves and its derivative curves were utilized to analyze the oxidative behavior of the FAME and its epoxide. The TGA curve of both FAME and EFAME sample are shown in Figure 29.

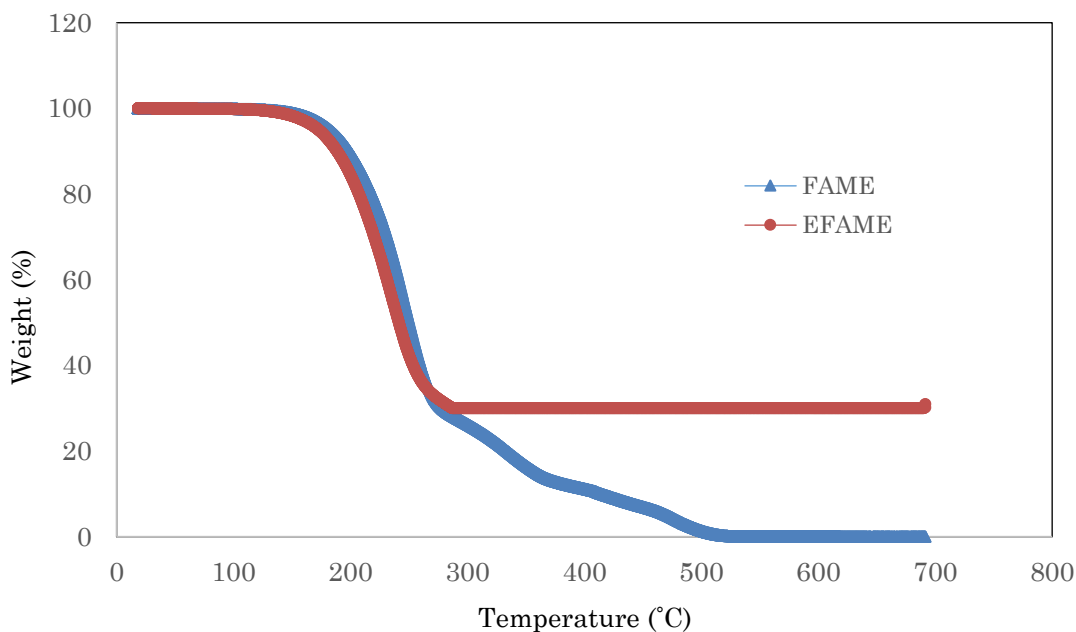


**Figure 29:** TGA curve of FAME and epoxidized FAME in O<sub>2</sub>

From the figure, it can be observed that FAME and EFAME were stable up to 167 and 152 °C respectively. However, beyond the oxidative temperature substantial loss in weight was detected. From the TGA curves of epoxy FAME and FAME, it is evident that decomposition process of FAME was at a faster rate than that of epoxy FAME. On the other hand, the decomposition of Epoxy FAME stabilized at temperature of 289.26 °C and it remained approximately 30 % of its mass at temperature of 700 °C. The thermo-oxidative behavior of the EFAME was found to be lower in comparison to FAME (Borugadda & Goud, 2014). A previous study reported that vegetable oil esters with high saturated and mono-unsaturated fatty acids content are more thermally and oxidatively stable compared to the esters with poly-unsaturation content.

#### 4.4.3 Surfactant Analyses

Fourier Transform Infrared spectrophotometer was utilized to evaluate the chemical functional groups present in the product after the sulfonation of the epoxidized FAME, that is, the yield of the targeted sulfonated surfactants. According to Elraies & Tan (2003) different functional groups are prone to absorb specific frequencies of IR radiation. Figure 30 to 32 illustrate the FTIR spectra in the range of 500-4000 cm<sup>-1</sup> of SEMES, SDS as well as CTAB using Microsoft Excel. All the IR absorption bands were investigated with respect to the spectrometric identification of organic compounds by Silverstein *et al.* (2005). The IR spectrum of SEMES is shown in Figure 30.

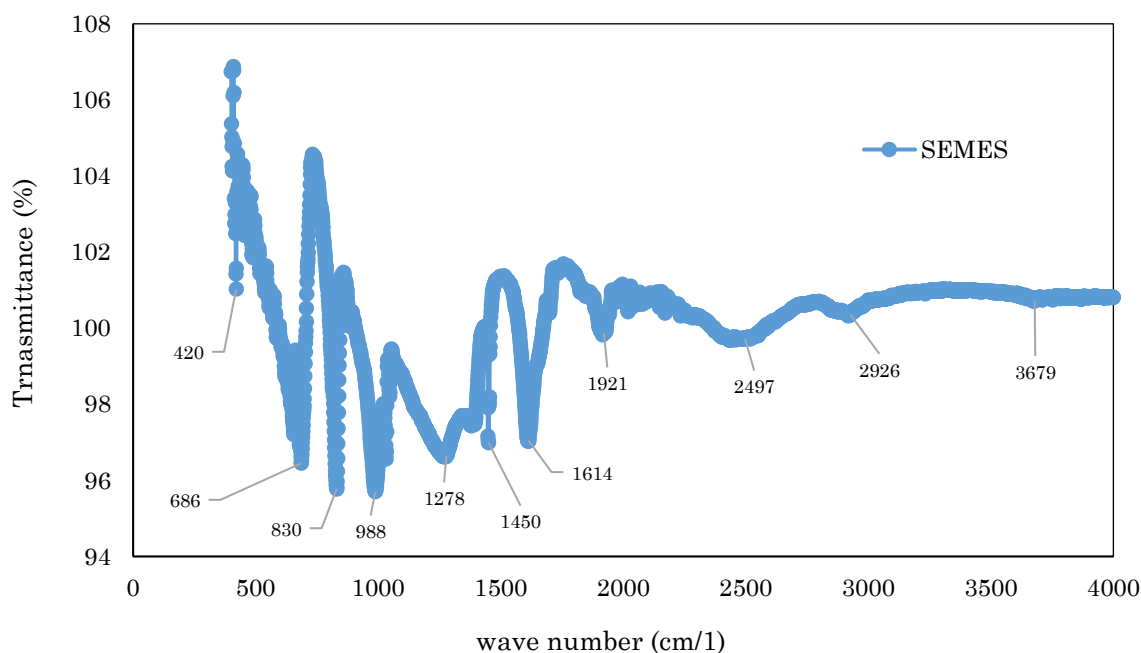


**Figure 30:** FTIR spectrum of SEMES

The peak at 1450 cm<sup>-1</sup> is typically assigned to the disproportion stretching vibration band of methyl group (C-H). Elraies *et al.* (2008) obtained a similar peak for epoxidized methyl ester sulfonate from jatropha oil. The symmetric and asymmetric C-H stretching vibration of the -CH<sub>3</sub> group appears at 2497 and 2926 cm<sup>-1</sup> (Figure 30). Similar peaks between 2473 and 2955 cm<sup>-1</sup> were reported by Babu *et al.* (2015) in a study where SMES was synthesized from castor oil and the ricinoleic acid methyl ester was sulfonated without the epoxidation step. The peak at 3679 cm<sup>-1</sup> in the SEMES is attributed to the OH stretching of the sorbed water (Figure 30). This sorbed water vibration band suggests that the surface property of SEMES changed from hydrophobic to hydrophilic (Hongping *et al.*, 2004; Babu *et al.*, 2015). Existence of the epoxy ring in the SEMES was shown by the presence of C-O stretching absorption band in the area of 988-830 cm<sup>-1</sup>.

However Elraies *et al.* (2008) observed the same peaks between 950 and 810 cm<sup>-1</sup>. These discrepancies in the results could be attributed to the type of vegetable oil as well as to the different procedures used to synthesize the surfactant. The strong vibration (absorbance) peak at 1614 cm<sup>-1</sup> corresponds to the existence of sulfonate group due to S=O stretching which is also an indication of the presence of esters (Silverstein *et al.*, 2005, Awang & Seng, 2008). These results clearly indicate that the substance synthesized must be sodium epoxidized methyl ester sulfonate. For a better understanding the structural arrangement of the surfactants investigated in this study, commercial anionic, SDS, and cationic, CTAB surfactants were also characterized by Fourier transform infrared spectroscopy. The characteristic FTIR spectra of pure SDS and CTAB are illustrated in Figure. 31 and 32.

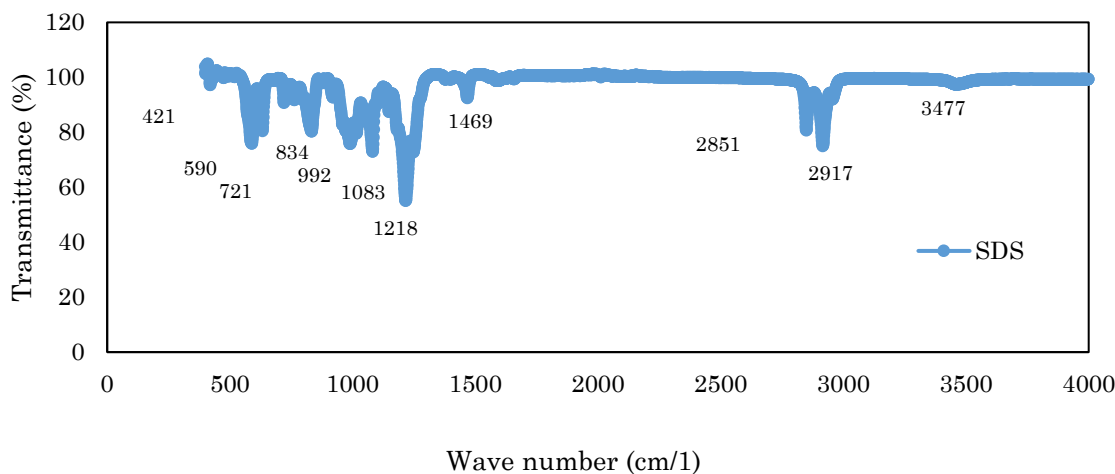


**Figure 31:** Infrared Spectrum of SDS

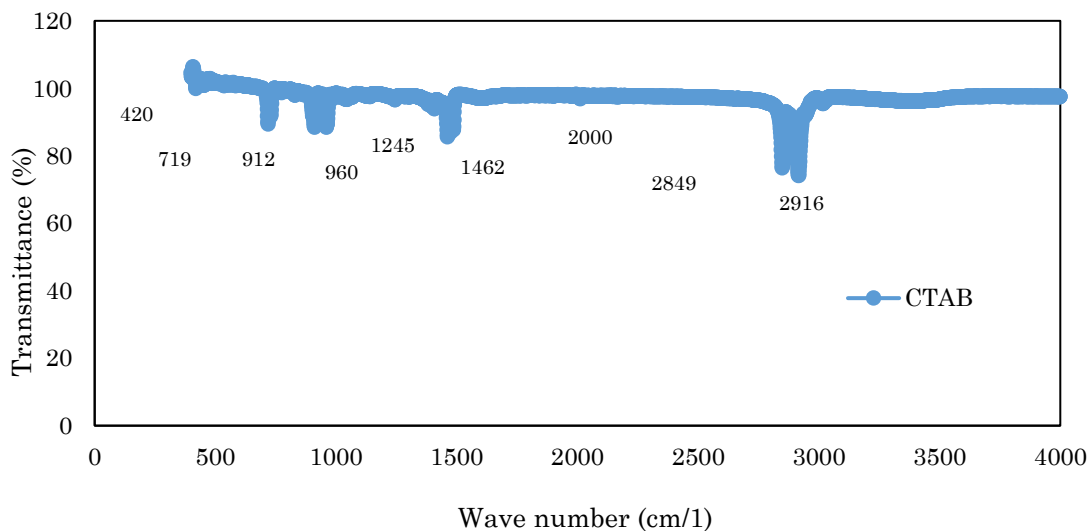


**Figure 32:** Infrared Spectrum of CTAB

The spectrum of SDS shows peaks at 1218 and 1083.0 cm<sup>-1</sup> (Figure 31), which according to Mehta *et al.* (2007) are attributed to  $\nu$ -S=O stretching vibrational band of SO<sub>4</sub> in the SDS molecule. This in agreement with the values found for C-H stretching vibrations which are similar to the values obtained by Mehta *et al.* (2007) where these peaks are shown at 1219.6 and 1083.0 cm<sup>-1</sup> correspondingly. The peak at 1469 cm<sup>-1</sup> corresponds to C=C/C=N stretching vibrations of pyridine ring. The peak between 2851 and 2917 cm<sup>-1</sup> is attributed to the C-H stretching modes of methyl group which is quite similar to the values of 2850.4 and 2918.9 cm<sup>-1</sup> obtained by Mehta *et al.* (2007) and Li (2004). The soft peak at 3477 cm<sup>-1</sup> corresponds to water O-H stretching vibration. In the case of CTAB, the bands characteristic of the [N<sup>+</sup>(CH<sub>3</sub>)<sub>3</sub>] head group, namely  $\nu$ (CN<sup>+</sup>), stretching vibrations at 912 and 960 cm<sup>-1</sup> (Figure 32), with the former peak being much higher

compared with the peaks at 912 and 904 cm<sup>-1</sup> obtained by (Baran *et al.*, 2014). A strong C-CH<sub>2</sub> stretching vibration bands at 2849 and 2916 cm<sup>-1</sup> was observed in the CTAB amphiphilic particles which is in agreement with previous reports. Li (2004) reported similar peak at 2849 and 2922 cm<sup>-1</sup> precisely in the methylene chains. The IR spectrums depicted different pattern/shape between the anionic SDS and the cationic CTAB however SDS showed similar pattern if compared with the synthesized SEMES but the percentage of transmission were different as a result of the discrepancy in their relative molecular mass. Parameters such as improper handling of the instrument may have contributed to other inconsistencies in the results. However, the results clearly indicate that the formulated surfactant resembles an anionic surfactant rather than a cationic surfactant.

#### 4.5 SUMMARY

It evident that the saturated fatty acids contents of the fatty acid methyl esters subjected to epoxidation reaction in the presence and absence of a solvent at 25 °C, 30 °C and 50 °C were reduced while promoting desired conversion of the unsaturated fatty acid methyl esters to epoxy esters (with oxirane groups). Linoleic acid methyl ester (LAME) and oleic acid methyl ester (OAME) were found to be the most abundant in the FAME, 48% and 29%, respectively. Reaction at lower temperature of 25 °C exhibited lower rate of epoxidation but high rate of hydrolysis of the epoxy product. The results obtained at reaction temperature of 50 °C in combination with the use of a solvent also suggested simultaneous decrease in the side reactions and minimization of the rate of oxirane bond cleavage of the product. These results are consistent with published works. The FAME was readily converted to epoxy compounds which were *Methyl (11R, 12R, 13S) - (Z)-12, 13-epoxy-11-methoxy-9-octadecenoate* and *Octadecanoic acid, 9, 10-epoxy-, methyl ester, trans*.

It can be inferred from the results presented herein therefore, that moderate temperatures of 30 °C were more suitable for epoxidation of oleic acid with PFA generated *in-situ* for optimum oxirane levels and hydrolysis rate diminishment. Additionally, the thermal degradation behaviour of the FAME and EFAME showed that the decomposition process of FAME was at a faster rate comparing to that of epoxy FAME which was a result of the high content of poly-unsaturated esters. The EFAME was consequently sulfonated to produce the Sodium Epoxidized Methyl Ester Sulfonate (SEMES) surfactant which was then compared to the synthetic SDS and CTAB surfactants. The identified FTIR spectrum of SEMES was similar to that of SDS which indicated that the formulated SEMES is an anionic surfactant. The same result have been reported (Elraies & Tan, 2003; Silverstein *et al.*, 2005).

## CHARACTERIZATION OF THE SURFACTANTS

---

*In this chapter, the adsorption behaviour of the formulated SEMES and that of commercial anionic and cationic surfactants were investigated and presented. This is carried out to estimate the degree of loss of the formulated surfactant that will result from adsorption to the reservoir surface when employed for flooding; and compare that to commercial surfactants. The tendency of ionic surfactants to adsorb onto and influence the wettability of reservoir rock and solid surfaces is described. Anionic surfactants exhibit lower loss via adsorption and hence greater potential for use in CEOR processes. The adsorption characteristics of three different surfactants namely anionic, SDS, cationic, CTAB, and the synthesized SEMES on diverse reservoir materials including alumina, silica and kaolin (forms of clay found in reservoirs all over the world) were investigated. This was carried out at different reservoir condition of salinity and pH. Additionally, the adsorption tendency on the emerging drilling mud weighing agent, ilmenite was also assessed. The equilibrium surfactant concentrations for the three surfactants were evaluated so as to determine the maximum quantity of surfactant adsorbed onto the various reservoir materials. The stability and hence performance of the surfactant during flooding into high temperature reservoir is also investigated. This was carried out by studying the thermal behavior via the TGA. The findings on epoxidation and thermal behaviour of the surfactants studied are also presented.*

### 5.1 INTRODUCTION

Surfactant flooding is widely employed to manipulate the phase behavior of the reservoir fluids to counteract the high capillary force trapping oil in the pores of the reservoir during EOR (Zargartalebi *et al.*, 2015; Kamari *et al.*, 2015; Babu *et al.*, 2015). The surface active chemical promote the formation of microemulsions at the crude oil and the displacing fluid (mostly water) interface (Ahmadi & Shadizadeh, 2015; Spildo *et al.*, 2014), thus causing a significant lowering of the fluids interfacial tension (IFT). This is required to efficiently mobilize a substantial percentage of the residual oil towards the production wells to enhance overall crude recovery (Lu *et al.*, 2014). The major problem that affects the efficiency of tertiary oil recovery during micellar flooding, steam-surfactant flooding, alkaline-surfactant (AS), surfactant-polymer (SP) or alkaline-



surfactant-polymer (ASP) is the loss of surfactant through interaction with reservoir rock (Ponce *et al.*, 2014), along with surfactant partitioning into the oil interface (Bera *et al.*, 2013). The loss of injected chemical(s) in the reservoir during injection due to the adsorption of the surfactant (and co-surfactants) onto the rock materials weighs heavily on the economics and environmental footprint of the process and remains a focus of research attention.

Surfactants loss on account of their interactions with crude oil and reservoir rocks surface are perhaps the most significant parameters that can define the effectiveness of a micellar flooding method (Somasundaran and Huang, 2000). It is necessary that the surfactant loss in the reservoir during injection is minimized to improve on the process economics and ensure its wider application. In a CEOR process, the surfactant adsorption is strongly dependent on the nature of the crude oil as well as geologic of the flow field (Bera *et al.*, 2013). As soon as the surfactant mixture is introduced, it is segregated into the crude oil and the water and reduces the IFT between the crude oil and the water thus causing an increase in the capillary number and mobilization of the trapped motionless crude oil (Kamari *et al.*, 2015). Simultaneously, an emulsion between the crude oil and water is created. This leads to an enhancement in the actual mobility ratio (Romero-Zerón & Kittisrisawai, 2015). The surfactant injected carries on mobilizing the crude oil, until the surfactant is diluted or lost owing to adsorption by the reservoir rock, hence can no longer be available to lower the IFT between the oil and the water and mobilize residual oil anymore (Berger and Lee, 2006). At that point, the process is reverted into a simple water flooding. Hereafter, to plan a surfactant flooding for EOR, it is crucial to have a broad understanding of adsorption of the particular surfactant on the rock material under the specific reservoir conditions.

This chapter present the findings of the investigation into the adsorption characteristics of the sodium epoxidized methyl ester sulfonate (SEMES), formulated from waste vegetable oil and that of two commercial surfactants, onto common reservoir rock materials is investigated at various concentrations, salinity and pH. The indirect method of residual equilibrium concentration measurement was employed to obtain the adsorption isotherm of SEMES, cetyltrimethyl ammonium bromide (CTAB) and sodium dodecyl sulfate (SDS) on kaolin, silica, alumina and a drilling mud weighing agent, ilmenite. Adsorption density and modelling of the equilibria of adsorption processes on the mentioned materials is investigated. Langmuir and Freundlich equations were utilized to evaluate the isotherm which gives the best correlation with experimental data.

## 5.2 SURFACTANT ADSORPTION ON RESERVOIR ROCKS

In surfactant-water-solid systems, the quantity of surfactant adsorbed depends on the rock properties (surface charge), the character of the surfactant (the kind of surfactant, the chain structure), temperature, salinity and pH (Qiao *et al.*, 2012; Sheng *et al.*, 2011). pH change affects the surface charge consequently altering the adsorption quantity. Salinity may alter the electrical potential of surface sites for the adsorption (Wesson and Harwell, 2010). Other mechanisms that may cause surfactant losses include precipitation of surfactant when in the presence of electrolyte ions and surfactant diffusion into dead-end pores (Tichelkamp *et al.*, 2015; ShamsiJazeyi *et al.*, 2014). High adsorption of surfactants onto the reservoir rock causes surfactant chromatographic retardation while they are carried through a reservoir formation, thus turning the EOR project unproductive and economically not viable (Ma *et al.*, 2013). Dynamic and balanced surfactants adsorption at the solid/liquid interface is mainly dependent on the surfactants nature as well as the nature of the reservoir rock surface (Hosna Talebian *et al.*, 2015; (Romero-Zerón & Kittisrisawai, 2015; Zhang & Somasundaran, 2006).

Depending on the rock formation, oil reservoirs are typically categorized into two types: carbonate and sandstone (Dandekar, 2013; Lashkarbolooki *et al.*, 2014). Anionic surfactants are generally preferred in sandstone reservoir formations owing to the fact that they are relatively less adsorbed in comparison to other surfactants (nonionics, cationics as well as zwitterionics) (Ma *et al.*, 2013). Usually, sandstone reservoirs comprise of huge quantities of quartz (silica) and less of silicate and carbonate rock crystals. The arrangement is dependent on the sedimentology of the reservoir formation (Ma *et al.*, 2013).

Owing to this unusual mineralogy, the majority of solid surfaces of reservoir rocks are charged, for instance silica is predominantly negatively charged, clay, calcite, alumina and dolomite may be positively charged at neutral pH (Yoshihara, 1996; Cappelletti *et al.*, 2006). Taking that into consideration three sorts of interactions are usually implicated during surfactant adsorption at solid-liquid interface. The repulsive or attractive forces of interaction among the hydrophilic head-group and the solid surface, the attractive forces of interaction between the hydrophobic head-group and the solid surface and the adjacent interactions taking place amongst adsorbed surfactants (Muherei, 2009) are the most significant interactions occurring between the hydrophilic head-group of surfactants and the solid surface (Paria *et al.*, 2004; Zhang & Somasundaran, 2006).

In case of ionic (anionic and cationic) surfactants, they adsorb onto solid surfaces due to repulsive and electrostatic forces (Ahmadi & Shadizadeh, 2015; Zhao, 2014). If the

surfactant being injected and the reservoir material (adsorbent) have different charges, the degree of adsorption is very rapid and equilibrium time is reduced (Muherei, 2009). In contrast, if the surfactant and the reservoir material have the same charge, repulsive interaction occur which results in negligible adsorption (Wesson & Harwell, 2010). On the other hand, some clay minerals (principally illite and kaolinite) in sandstone cause small quantities of anionic surfactants to be adsorbed due to the heterogeneous surface charge in clay minerals (Ma, 2013). Here, the adsorption depends on the dispersion of the clay minerals spread over the surface of sandstone. In the case of carbonate reservoirs, the complexity of its surface charge imposes certain difficulty to evaluate whether cationic or anionic surfactants have to be utilized to reduce electrostatic interactions between the formation surface and the surfactant (Lu *et al.*, 2014).

### 5.2.1 Selection of Surfactants for Micellar Flooding

Tabatabal *et al.* (1993) used natural dolomite and synthetic calcite powder to conduct a static adsorption study so as to relate the adsorption characteristics of anionic and cationic surfactants on carbonate formations. Sodium dodecyl sulfate (SDS), as the anionic surfactant, and cetylpyridinium chloride (CPC), as the cationic surfactant, were used. The results obtained demonstrated that the cationic surfactants were less adsorbed on both calcite and dolomite in comparison to the anionic surfactant with no pH adjustment. Similar observations were later reported by Kamari *et al.* (2015), Lu *et al.* (2014), Sheng (2013) and Ma *et al.* (2013). Surfactant adsorption has been found to increase as the surface charge of the reservoir rock increases in the direction of the more positive charges (Pei *et al.*, 2014), which is in accordance with the mechanism of electrostatic attraction. Alumina showed higher aggregation number and the negatively charged SDS surfactant was strongly adsorbed on positively charged alumina at pH of 6.5 (Muherei, 2009).

The adsorption of CTAB onto carbonate rocks was investigated by Salari *et al.* (2011) studied and found that maximum adsorption density of 1.891 mg/g at 350 ppm of surfactant concentration. They came to the conclusion that the adsorption rate depends on the surfactant availability in the system. It was also established that surfactant adsorption increases with increasing concentration of surfactant. Surfactant adsorption increases as the surface charge of the reservoir rock increases in the direction of the more positive charges, which is in accordance with the mechanism of electrostatic.

More studies have demonstrated the benefit of utilizing anionic surfactants instead of cationic surfactants in carbonates reservoirs. In a study conducted by Ivanova *et al.* (1995) cetyltrimethylammonium bromide (cationic surfactant, CTAB) exhibited an adsorption plateau of 2.51 mg/m<sup>2</sup> on limestone (comprising of 99% CaCO<sub>3</sub>). It was more

adsorbed in comparison to alkyl aryl ethoxylated sulfonated phenol and alkyl aryl ethoxylated sulfonate (anionic surfactants) with an adsorption plateau 0.9 mg/m<sup>2</sup> and 1.3 mg/m<sup>2</sup>, respectively (Seethepalli *et al.*, 2004). A report by Bastrzyk *et al.* (2012) showed that CTAB exhibited higher adsorption relative to SDS on both natural dolomite (from old quarry Kletno) and natural magnesite (from magnesite mine Grochow) in a low-salinity solution consisting of 10<sup>-4</sup> M of sodium chloride. Taking into account the isotherms shown in their study, CTAB adsorption plateaus on magnesite (pH of 8.5) and dolomite (pH of 10.4) were 6.9 and 5.8 mg/m<sup>2</sup>, correspondingly. While for SDS plateaus of 1.1 and 2.2 mg/m<sup>2</sup> on dolomite (containing 98% of carbonates) and magnesite (containing 88% of carbonates) respectively were observed.

Sanchez-Martin *et al.* (2008) also observed that octadecyl trimethylammonium bromide (a cationic surfactant) showed higher adsorption plateau in comparison to SDS on a number of clay minerals (for example, illite and montmorillonite). Significant adsorption of cationic surfactants may be expected to occur if the carbonate formation is rich in clay and/or silica (Ma *et al.*, 2013). Ma *et al.* (2013) studied the adsorption of anionic and cationic surfactants using natural and synthetic carbonate materials. Likely impurities in natural carbonate, for example clay and silica, were also investigated. Sodium dodecyl sulfate (SDS) and cetylpyridinium chloride (CPC) were selected as the cationic and anionic surfactants respectively. CPC showed insignificant adsorption when synthetic calcite was used but then again quite high adsorption on a number of natural carbonates. It was observed that the adsorption plateau of CPC on carbonates was highly dependent on the composition of silicon in the carbonate samples as a result of the strong electrostatic interaction between CPC and the negative binding sites in clay and/or silica. It was concluded that the low adsorption of CPC on carbonate formations is only effective if the composition of silica is low, this relating to the adsorption of SDS.

Upadhyaya *et al.* (2007) evaluated the adsorption of anionic and cationic surfactant mixtures on alumina and silica surfaces. Two anionic surfactants, namely, sodium dodecyl sulfate and sodium dihexyl sulfosuccinate and two cationic surfactants, dodecyl pyridinium chloride and benzethonium chloride were used. It was found that for an anionic-rich surfactant mixture below the Critical Micelle Concentration (CMC), the adsorption of anionic surfactant increased considerably by adding low mole fractions of cationic surfactant. Whereas cationic surfactants were found to co-adsorb with anionic surfactants on positively charged surfaces (for instance alumina), the isotherm plateau of the adsorption of the anionic surfactant at or above the CMC did not present any significant changes in the case of anionic–cationic surfactant mixtures. Conversely, the adsorption of anionic surfactants on alumina showed a radical decrease in the presence of a cationic-rich surfactant mixture and the cationic surfactants adsorption onto silica was substantively diminished when present in anionic-rich micelles. As a consequence,

surfactant adsorption can either be boosted or prevented with mixed anionic–cationic surfactant schemes by changing the amount and composition.

### 5.2.2 Effect of pH and Salinity on Surfactants Adsorption

The effect of alkalinity and salinity on the adsorption of surfactants have been investigated by a number of researchers (for instance Yuan *et al.*, 2015; Olajire, 2014; Ma *et al.*, 2013; Delshad *et al.*, 2013; Sheng, 2011; Maheshwari, 2011). Zhou & Liu (2005) studied the influence of salinity and alkalinity on surfactant adsorption onto sand and oil-water interface in heavy oil/water/sand systems. It was concluded that by adding an alkali, the adsorption reduced while, adding an electrolyte (NaCl) (that is, increasing salinity) caused an increase in the adsorption. Elraies and Tan (2011) also investigated the static adsorption of a new polymeric methyl ester sulfonate on sandstone in the presence and absence of different alkali ( $\text{NaCO}_3$ ) concentrations. The adsorption was determined by making a comparison between the acquired refractive index before and after equilibrium. It was concluded that adsorption increased as the concentration of surfactant increased. It was found that the addition of the alkali decreased the adsorption of the anionic surfactant significantly.

Tabatabal *et al.* (1993) also used divalent ions for instance  $\text{Mg}^{2+}$  and  $\text{Ca}^{2+}$  to assess the adsorption of the cationic surfactants on carbonates at different salinity level. When using calcite, the presence of 0.05 M  $\text{MgCl}_2$  or  $\text{CaCl}_2$  made the adsorption of CPC to be negative and on synthetic calcite powder CPC exhibited negligible adsorption compared with SDS. These divalent ions turned the carbonates surface highly charged with positive ions, and the columbic interactions repelled the cationic surfactant (CPC) from the interfacial region, thus causing a reduction in the adsorption of the cationic surfactant (Ma *et al.*, 2013). Adding salts of multivalent cations can cause a significant increase in the adsorption of anionic surfactants (Salari *et al.*, 2011). However, it can considerably cause a decrease in the adsorption of cationic surfactants. This is attributed to the fact that the added cations, lattice ions of the reservoir material, have an impact on the material surface charge which in turn increase the adsorption of the anionic surfactant while decreasing the adsorption of the cationic surfactant (Tabatabal *et al.*, 1993).

The pH and salinity of brine have a strong impact on the rock surface charge (Bera *et al.*, 2013). For instance, when the effects of brine chemistry are eradicated, silica have a tendency to adsorb simple organic bases (cationic surfactants), whereas the carbonates are likely to adsorb simple organic acids (anionic surfactants). This happens due to the fact that silica usually takes a negatively-charged weak acidic surface in water, close to a neutral pH, whereas the carbonates present positively-charged weak basic surfaces.

### 5.2.3 Thermal Stability of Surfactants

Chemicals need to be stable at reservoir conditions during the entire flooding process. A study of the effect of temperature on the surfactant degradation is crucial. The majority of the commercial surfactants have been produced to suit the prevailing reservoir conditions rather than the very high temperatures (or steam injection conditions). Al-Khafaji *et al.* (1982) tested a number of experimental surfactants for their capacity to withstand steam injection conditions.

Some surfactants tend to be temperature resistant, whereas others degrade more rapidly at high reservoir temperatures; due to that thermal analysis are performed. Thermogravimetric analysis (TGA) is a thermal analysis technique which determines the amount of rate of change in the weight of a material as a function of temperature or time in a controlled atmosphere (Piispanen, 2002). TGA analysis is utilized principally to measure the surfactant composition and to calculate their thermal stability up to extreme temperatures. It is normally conducted for temperature range of 30 °C to 500 °C with increments of 30 °C/min (Elraies *et al.*, 2008). The results obtained from this analysis are usually presented in the form of curves relating the mass lost from the surfactant against temperature, as water is lost from the surface.

## 5.3 TECHNIQUES TO DETERMINE ADSORPTION

During a surfactant core flood, surfactant lost through adsorption onto the porous medium (Green & Willhite, 1998) is experimentally studied to evaluate the performance of the surfactants produced. In certain cases, kaolinite clay is utilized to create the porous medium, which corresponds to the worst case scenario as clays are able to adsorb more owing to their larger surface area comparing to bulk rock substances. In general, the most commonly used technique to determine adsorption is the method of depletion, where the change in the amount of surfactant after it comes in contact with adsorbents is registered and said to be adsorbed. The results obtained from determining the adsorption experimentally are usually represented as adsorption isotherms, where the quantity of surfactant adsorbed is given as a function of equilibrium concentrations (Paria *et al.*, 2004; Salari *et al.*, 2011; Bera *et al.*, 2013). Adsorption isotherms are determined by maintaining solution environment states, for instance pH, temperature and ionic strength constant (Touhami *et al.*, 2001).

When determining surfactant adsorption in dispersed systems, a known quantity of surfactant is added to the system and allowed to reach equilibrium. Afterwards, the

dispersed solids (clay or rock materials) are separated and the surfactant concentration in the solution is measured (Salari *et al.*, 2011). Surfactant adsorption is given by the relationship:

$$\Gamma = \left( \frac{(C_i - C_e) \times M_s}{M_c} \right) \times 10^{-3} \quad (11)$$

where,  $\Gamma$  is the adsorption density (mg/g),  $C_i$  is the initial surfactant concentration (ppm),  $C_e$  is the equilibrium surfactant concentration in solution (ppm),  $M_s$  is the mass of the surfactant solution (g) and  $M_c$  is the mass of the dry adsorbents (g).

There are many ways to determine the concentration of surfactant in the solution after maximum adsorption separation which include: refractive index, ion-selective electrodes or conductivity, UV/vis spectroscopy, titration, surface tension and chromatography (Somasundaran *et al.*, 2000). In this study the conductivity method was employed. Using this technique, a decrease in surfactant initial concentration would show surfactant loss to the clay or rock material. Salari *et al.* (2011) investigated the adsorption of a cationic surfactant onto carbonate rocks and made use of a conductivity meter to obtain the surfactant concentration after equilibrium.

Adsorption models are usually needed to estimate the loading on the adsorption medium at a certain concentration of the element being studied. The two most commonly used adsorption isotherms which can be utilized to define the equilibrium adsorption relation are the monolayer Langmuir and empirical Freundlich models (Salari *et al.*, 2011). These isotherms are represented in a diagram of surfactant adsorbed quantity per quantity of adsorbent against concentration of surfactant. They are graphically illustrated in the linear-linear or the linear-log plots or log-log scale. In these adsorption isotherms, sudden variations in the gradient can normally be observed if plotted in a series of concentrations (Behrens, 2013). A diagram of a usual four region isotherm for a monoisomeric anionic surfactant is presented in Figure 33:

A scheme of the mechanisms for the four different regions is as follows:

**I:** At very low concentrations of surfactant the adsorption performance is consistent and there is no surfactant-surfactant or surfactant-solvent contact. The surfactant molecules are adsorbed as single unimers with no contact between adsorbed particles. In case of non-ionic surfactants, the synergy comprises of H<sub>2</sub> bonding among the head-group and surface. However, for ionic surfactants the dynamic force is electrostatic interactions among the charged sites at the mineral surface and the head-groups.

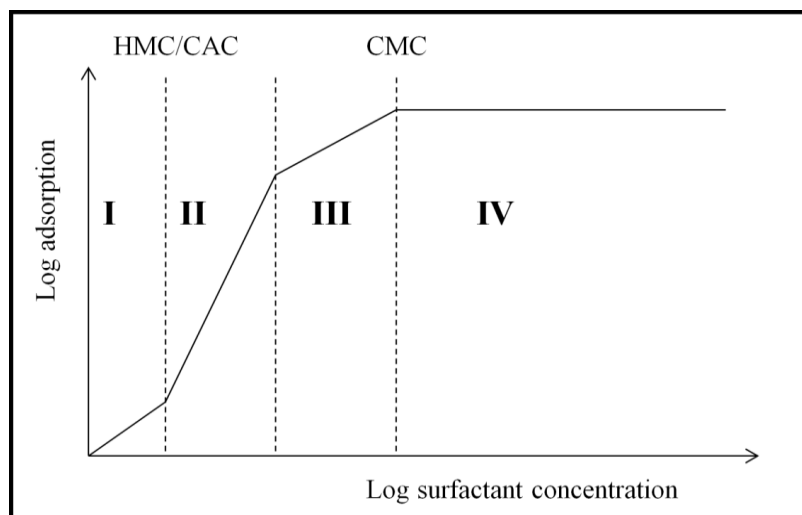


**Figure 33:** Diagram of a typical four region isotherm (Behrens, 2013)

**II:** In the 1<sup>st</sup> region of the isotherm, the adsorption is carried out through a mechanism where the molecules of the surfactant do not come into contact with one another, the 2<sup>nd</sup> region of the isotherm will certainly be at the concentration where there is contact between the surfactant particles. The disruption between the 1<sup>st</sup> and 2<sup>nd</sup> region is denoted as the Hemimicelle Concentration (HMC) or the Critical Micelle Concentration (CAC) (Salari *et al.*, 2011; Behrens, 2013). This is referred to as the concentration where the 1<sup>st</sup> agglomeration of surfactant molecules is formed at the surface of the mineral material. The HMC or CAC fluctuate in the same way as the CMC. Raising the chain length of the surfactant tail will significantly decrease the HMC/CAC (Behrens, 2013). A similar pattern occurs if an electrolyte is introduced into the system that consists of ionic surfactants. A suggested concept for why this region presents a higher gradient/slope number comparing to the 1<sup>st</sup> region is the fact the hydrophobic tail-tail contact stimulates adsorption.

**III:** There are a number of theories which describe the adsorption scheme in the 3<sup>rd</sup> region of the isotherm. Somasundaran *et al.* (2000) and Schramm (2000) described the reduction in slope to be caused by having a surface filled with micelles. Then, the adsorption in the 3<sup>rd</sup> region would be a 2<sup>nd</sup> layer of surfactants, where the driving force for adsorption was an association of the hydrocarbon chains. It was also caused by a change in surface charge as ionic surfactants tend to be adsorbed to the surface. It was also suggested that a bi-layer was generated previously in the 2<sup>nd</sup> region and covered the 3<sup>rd</sup> region but then again at different proportions. Therefore, the variance in adsorption could be attributed to the absence of actively viable sites at the interface as it is regularly saturated.

**IV:** In the 4<sup>th</sup> region of the isotherm the critical micelle concentration has been achieved and no additional adsorption occurs. Subsequent to the critical micelle concentration



being reached, further addition of surfactant will reasonably generate micelles than being adsorbed to the surface. The phenomena in this region can still take place even deprived of a fully bi-layer of surfactants.

### 5.3.1 Langmuir Adsorption Isotherm

The Langmuir isotherm has been extensively used in various adsorption modelling. A wide range of experimental data for the adsorption of a solute from a liquid solution has been obtained with the use of the Langmuir isotherm (Paria & Khilar, 2004). The Langmuir theory works with the assumption that the sorption occurs at precise homogeneous sites in the adsorbent (Zhang & Somasundaran, 2006). Furthermore, when a site is saturated with a solute, no additional adsorption happens at that site.

The rate of adsorption to the surface is proportional to a driving force as well as area. The driving force being the concentration in the solution and the area is the quantity of plain surface. The Langmuir isotherm takes into consideration the solid-phase adsorbate amount to the equilibrium solvent concentration at a specific temperature (Zhang & Somasundaran, 2006). Irving Langmuir developed this equation in 1916 (Langmuir, 1916) which is described as follows (Salari *et al.*, 2011):

$$q_e = \frac{Q_o K C_e}{K C_e + 1} \quad (12)$$

where  $q_e$  is the quantity adsorbed per unit mass of adsorbent (wt/wt),  $C_e$  is the equilibrium concentration of adsorbate in solution after adsorption,  $Q_o$  and  $K$  are empirical constants. The constants  $Q_o$  and  $K$  can be obtained by plotting  $\frac{1}{q_e}$  vs.  $\frac{1}{C_e}$  and can be rewritten as Equation (13) (Salari *et al.*, 2011):

$$\frac{1}{q_e} = \frac{1}{Q_o K C_e} + \frac{1}{Q_o} \quad (13)$$

The adsorption data obtained was fitted to Langmuir models.

### 5.3.2 Freundlich Adsorption Isotherm

In 1906 Freundlich created an empirical equation to represent the adsorption process. A basic assumption of the Freundlich isotherm is that the adsorbent has a heterogeneous surface constituted of diverse classes of adsorption sites (Salari *et al.*, 2011). It was shown that at different solution concentrations, the ratio of the quantity of solute adsorbed onto a certain amount of an adsorbent (or porous) material to the concentration of the solute in the solution changes. This theory does not estimate any overload of the adsorbent material by the adsorbate. Hence, infinite surface coverage can be estimated

using mathematical terms, which indicates multilayer sorption of the surface (Rawajfih & Nsour, 2006). The Freundlich isotherm takes into account that if the amount of the solute in the solution at equilibrium,  $C_e$  is elevated to the power  $\frac{1}{n}$ , the quantity of solute adsorbed,  $q_e$ , the  $\frac{C_e^{\frac{1}{n}}}{q_e}$  is constant at a particular temperature (Salari *et al.*, 2011):

$$q_e = K_F C_e^{\frac{1}{n}} \quad (14)$$

where  $K_F$  and  $n$  are constants.  $K_F$  and  $\frac{1}{n}$  can be determined by plotting  $\log q_e$  against  $\log C_e$  (Mannhardt, 1988; Thomas, 1998; Salari *et al.*, 2011).

### 5.3.3 Critical Micelle Concentration

The Critical Micelle Concentration (CMC) is a very important parameter when characterizing surfactants. CMC is the concentration at which the surfactant solutions begin to aggregate to form micelles in large amounts (Touhami *et al.*, 2001). They begin to aggregate since they do not want the hydrophobic tails to come in contact with water. Hence, they form micelles with the hydrophilic head groups pointing outwards towards the water and the hydrophobic tails pointing inwards. In so doing, free energy is decreased. In general, the first formed aggregates are roughly spherical. A schematic illustration of a spherical micelle is shown in Figure 34:

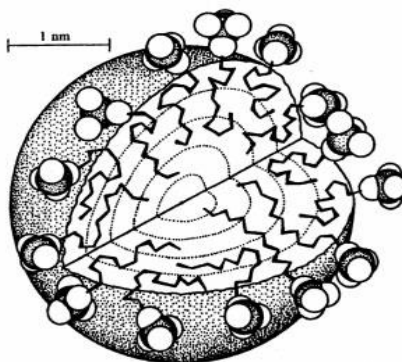


**Figure 34:** A typical illustration of a spherical micelle (Holmberg *et al.*, 2003)

The most common technique for determining the CMC of a surfactant is by measuring the surface tension, interfacial tension (IFT) and conductance. Surfactant is most effective on lowering the surface tension after it reaches the CMC. The surface tension of a surfactant solution decreases as the surfactant concentration increases until CMC is attained (Wesson & Harwell, 2010). In the plot of interfacial tension versus concentration of a surfactant solution, a curve break occurs at CMC, after which it remains practically steady with additional increases in concentration (Fig. 35). Other

methods such as measurement of solubility, fluorescence spectroscopy, self-diffusion measurements and nuclear magnetic resonance (NMR) can be applied.

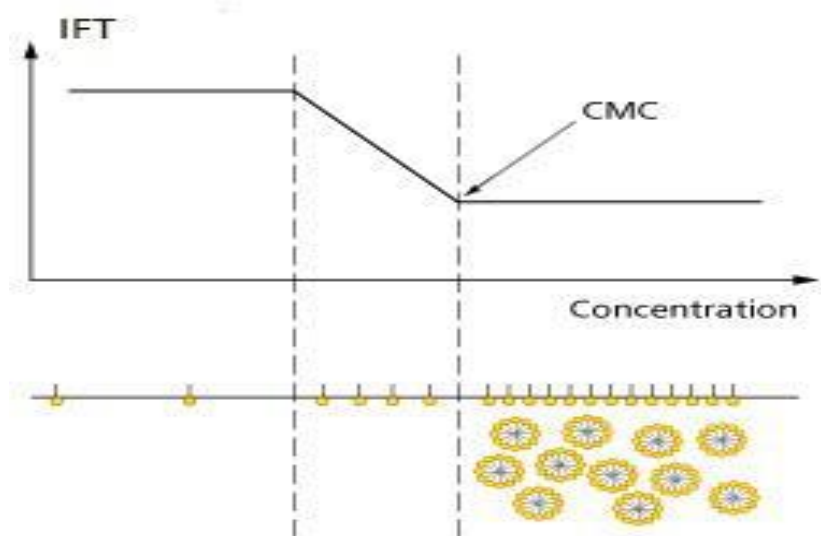


**Figure 35:** IFT variation with surfactant concentration

Salari *et al.* (2011) determined the CMC of CTAB at different surfactant concentrations using the conductance method. A graph of conductivity in terms of CTAB solutions was drawn. The CMC was reached at a surfactant concentration of 370 ppm. They noticed that as the concentration of surfactant solution increased, its molecules/ions started an association reaction, and formed micelles, therefore a sharp change in trend of the curve was observed. By making use of these various techniques to attain the CMC of a surfactant, the values obtained would certainly diverge to a certain extent from one another. Consequently, the CMC can be taken as series of concentrations instead of just one particular point of concentration (Behrens, 2013).

## 5.4 EXPERIMENTALS

An anionic surfactant, sodium dodecyl sulfate, SDS (Sigma Aldrich, 98%), cationic surfactant, cetyltrimethylammonium bromide, CTAB (Sigma Aldrich, 98%) and the synthesized sodium epoxidized methyl ester sulfonate (SEMES) were employed. pH was adjusted with NaOH (Sigma Alrich, 97%) while NaCl (Sigma Alrich, 99%) was used to prepare the synthetic brine solution for salinity adjustment. In this study four types of adsorbent materials (to represent reservoir rock materials) were used: alumina powder (Sigma Aldrich, 99.5% metals basis), fine silica (Sigma Aldrich, 99.8 %), kaolin clay ( $\text{Al}_2\text{Si}_2\text{O}_5(\text{OH})_4$ ) (Sigma-Aldrich, 98%) and ilmenite ( $\text{FeTiO}_3$ ) obtained from South Africa ore was used as typical drilling fluid weighing agent. The adsorbents were dried in a convection electric oven at 120 °C overnight to eliminate water and any other adsorbed

substances. The various reservoir materials were characterized using inductively coupled plasma optical emission spectrometer.

#### 5.4.1 Static Adsorption Experiments

Static adsorption experiments were run to analyze the adsorption characteristics of SDS and CTAB surfactants from aqueous solution onto synthetic kaolin clay, silica, alumina and ilmenite surfaces. Initial surfactants concentrations prepared from a 30 mL surfactant solution in 2 vol. % NaCl ranged from 50 to 600 ppm (Table 43-59 in the *Appendix C*) and methodically measured so as to maximize precision. The absorbent-dispersed surfactant solution samples were combined at a mass (solid-liquid) ratio of 1:20 in 500 mL glass bottles and shaken at 240 rpm for 24 h at a temperature of  $25 \pm 2$  °C using a temperature controller horizontal electrical shaker machine. To ensure equilibrium, the absorbent-surfactant solution mixtures were agitated for 24 h at room temperature and ambient pressure. After adsorption, the surfactant-solid system was separated by means of filtration using a vacuum pump. Surfactant sample aliquots were taken for determination of surfactant concentration before and after adsorption. The equilibrium surfactant concentrations of both surfactants were evaluated so as to determine the maximum quantity of surfactant adsorbed onto reservoir material.

The effects of pH and NaCl concentration on the adsorption capacity of the adsorbent (kaolin clay) to the anionic and cationic surfactants were investigated. To adjust the required pH values of the maximum adsorption of the surfactant solutions were considered and NaOH (0.2 M) solutions ranging from 0 wt. % to 1 wt. % were used. The salinity of the solution was altered with NaCl (0.2 M) solutions from 0-5 wt. %. The adsorption behavior of an equimolar (50:50) mixture of anionic and cationic surfactants on silica mineral surface was also evaluated at constant salinity so as to assess the synergistic interaction between these surfactants. The surfactant concentrations were selected below the CMC of the individual surfactant systems. This is because in anionic-cationic mixtures there is a propensity for the formation of precipitates and this could be prevented by working below the CMC (Paria *et al.*, 2004). A conductivity meter (Mi 170 Bench Meter, EC/TDS/NaCl/Temperature) from Martini Instruments was used to obtain the residual surfactant concentration before and after contact with the reservoir materials. The amount of surfactant adsorbed (adsorption density) was expressed as the unit of mass of surfactant adsorbed per 1 gram of solid absorbent (mg/g). Adsorption density on reservoir materials was determined by using the expression in Equation (25).

A number of adsorption studies have applied similar technique with the obtained results being presented by means of isotherms which are graphical representation of the amount of surfactant adsorbed/g of solid against the equilibrium surfactant concentration at a constant temperature (Elraies *et al.*, 2011; Salari *et al.*, 2011). These graphs are

generally utilized to acquire data over an extensive range of surfactant concentrations, and they usually consist of four regions with evident gradient alterations as surfactant concentration is increased (Paria & Khilar, 2004). Adsorption data for reservoir have been evaluated by fitting with Langmuir and Freundlich isotherm models.

#### 5.4.2 Thermal Stability test

The thermal degradation of the synthetic and formulated surfactants was measured using Perkin Elmer TGA7 bench model thermo-gravimeter analyzer (TGA). The TGA is used to determine changes of weight loss of substance against temperature. This test will be conducted for temperature range of 30 °C to 500 °C with increments of 30 °C/min.

### 5.5 RESULTS

#### 5.5.1 Analyses of Reservoir Rock Materials

The results from BET analysis of the kaolin clay powder and ilmenite measured using a Quantachrome Autosorb-3b BET Surface Analyser are presented in Table 19. The data obtained for the aluminium (Al), iron (Fe) and titanium (Ti) analysis on the ICP-OES is given in Table 20, respectively. Oxygen (O<sub>2</sub>) is also observed in these reservoir materials, however, it is not presented in Table 20 as it has no ostensible influence to the anionic SDS and the cationic CTAB adsorption, since they predominantly interact with Al, Fe Si, and Ti more willingly than O<sub>2</sub>.

**Table 19:** BET characterization

Parameter	Kaolin	Ilmenite
Area, m <sup>2</sup> /g	14.9086	1.7714 m <sup>2</sup> /g
Total pore volume, cm <sup>3</sup> /g	0.082731	0.002447
Average Pore size, Å	221.9684	55.2565

**Table 20:** Atomic surface composition for the reservoir materials using ICP-OES analysis

Samples	Mass (mg)	Volume (l)	% Al	% Fe	% Ti
Kaolin clay	50.9	0.1	13.78	-	-

Ilmenite	50.6	0.1	-	28.89	24.09
Alumina	53.3	0.1	17.73	-	-

Fe and Ti are observed in ilmenite mineral but not in kaolin or alumina (Table 20). A significant amount of Al is observed in kaolin clay and alumina but not in ilmenite (Table 20). These observations are all in accordance with the characteristic chemical compositions of these rock crystals.

XRD test was used to confirm the minerals and phases present in the reservoir materials which may contribute to the significant differences in adsorption behavior of the ionic surfactants. Figures 36 to 39 illustrate the X-ray diffraction patterns of the four reservoir materials used in this study. In Fig. 36, a reference pattern of SiO<sub>2</sub> normalized by the highest peak with the equivalent angle at  $2\theta = 23^\circ$  was recorded. This finding is in accordance with literature. Prepared SiO<sub>2</sub> by (Martínez *et al.*, 2009) also presented an amorphous peak at  $2\theta = 23^\circ$ .

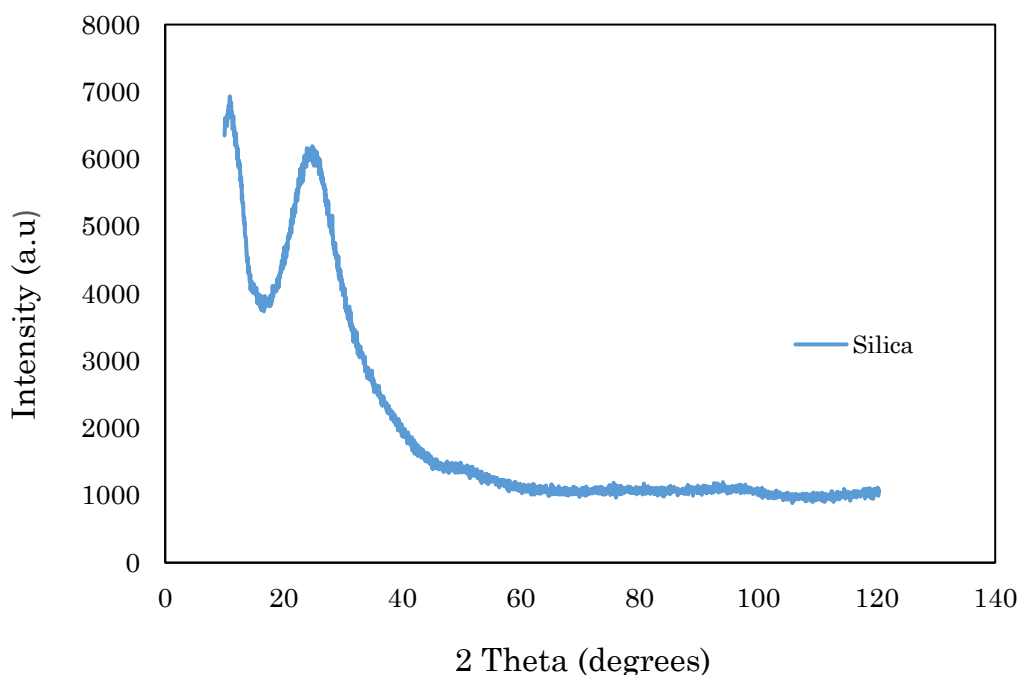


**Figure 36:** XRD spectrum of silica

In Fig. 37 a broadened XRD peak for kaolin clay centered at a  $2\theta$  of  $14.3^\circ$  was detected and corresponded to the SiO<sub>2</sub> peak and the other peak at  $2\theta$  of  $\sim 29^\circ$  was related to the alumina since kaolin clay material is a mixture of both.

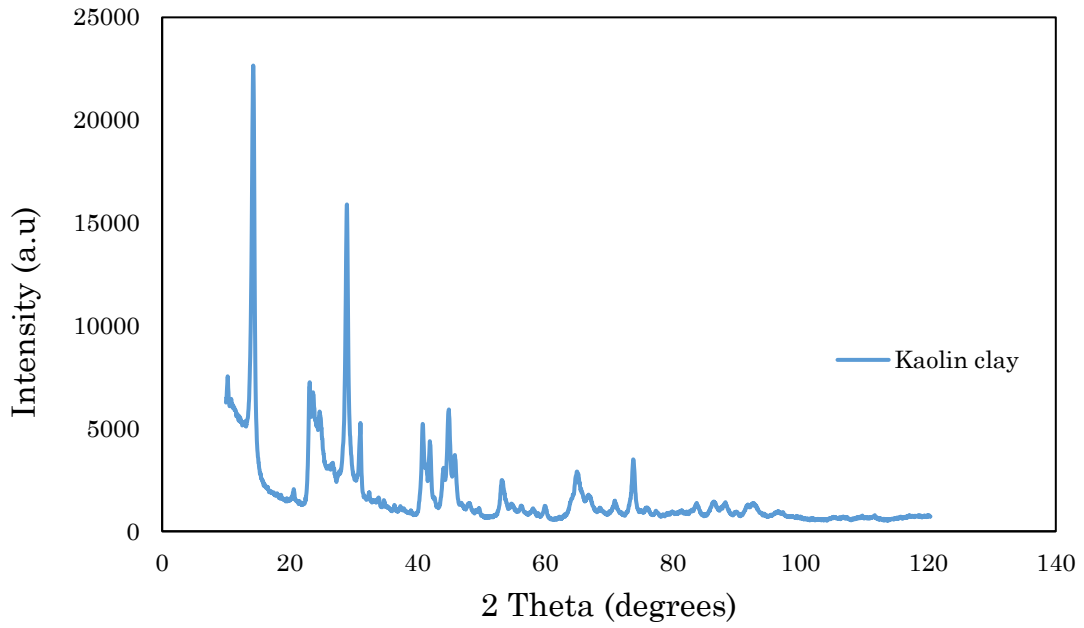


**Figure 37:** XRD spectrum of kaolin clay

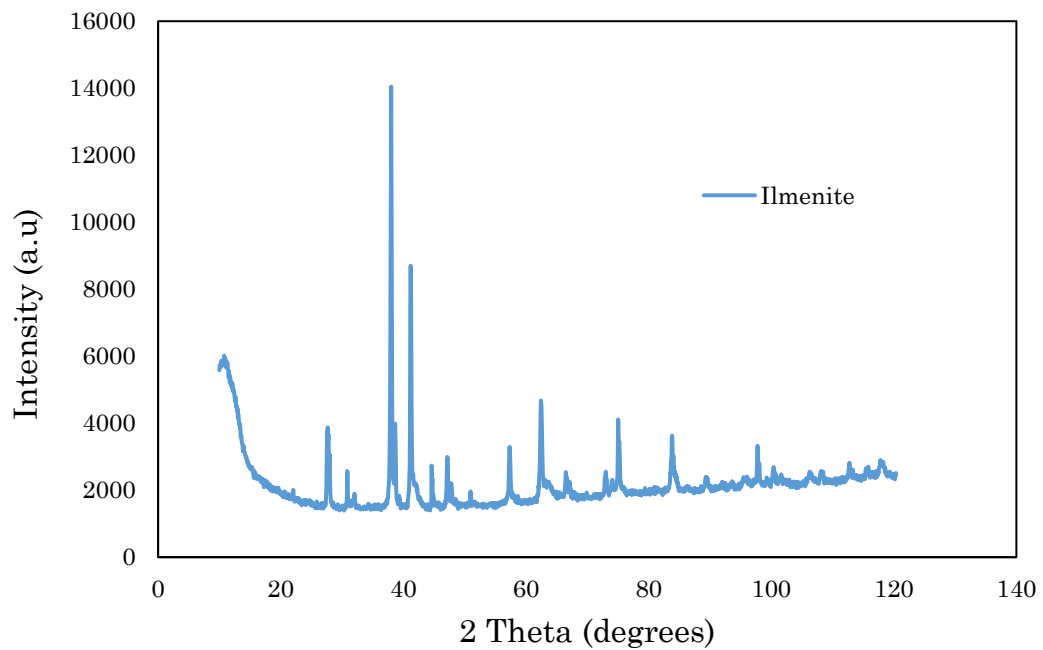


**Figure 38:** XRD spectrum of synthetic ilmenite

The X-ray diffraction pattern in Fig. 38 reveals the presence of ilmenite and suggests that it is in form of  $\text{FeTiO}_3$  which is represented by the angle  $2\theta = \sim 38^\circ$  and  $41^\circ$ . The other minor peaks confirms the existence of  $\text{Fe}^{++}$  ions (Zhao & Shadman, 1993).

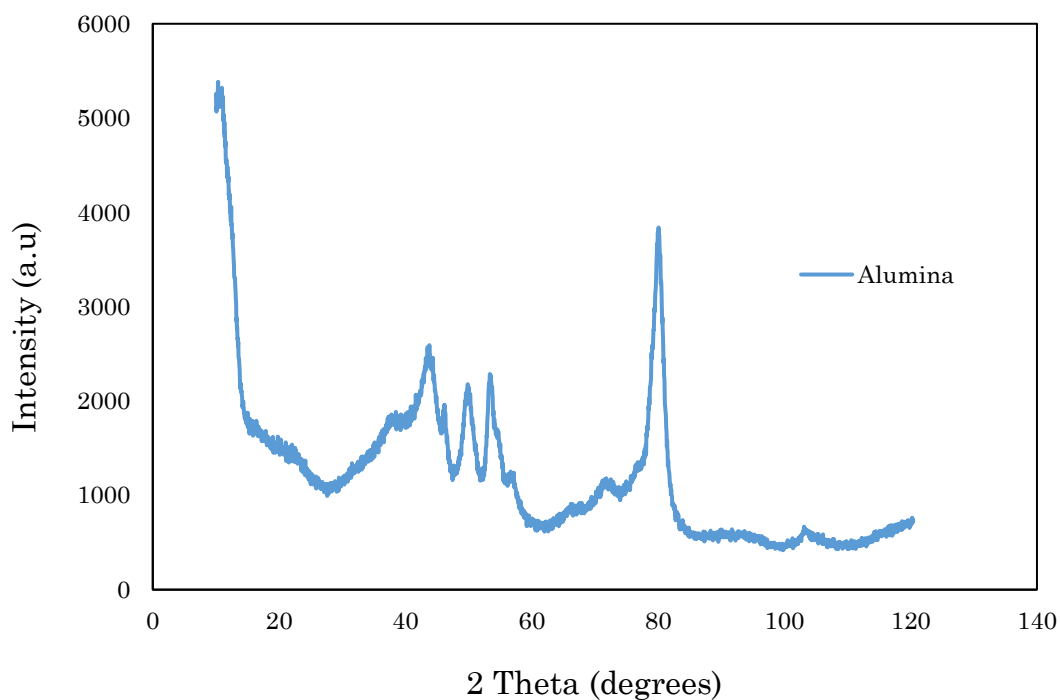


**Figure 39:** XRD spectrum of alumina

As aluminium is also found in natural reservoir minerals it was also analysed. The 2 $\theta$  peaks, which indicated that aluminium oxide were present at angles of  $\sim 12^\circ$  and  $\sim 80^\circ$ . (Fig. 39). The XRD results do not show that the samples contained other impurities.

### 5.5.2 Adsorption of Surfactants at Constant Salinity

Figures 40-43 illustrate the adsorption isotherm for SDS, CTAB and SEMES on the representative reservoir rock materials (synthetic kaolin powder, alumina and silica) and the weighing agent (ilmenite) at ambient temperature and constant pH of 6.0. The solution salinity was kept constant with 2 vol % NaCl solution. The anionic SDS, cationic CTAB and the synthesized SEMES surfactants adsorb onto kaolin clay powder (Fig. 40). This is due to the presence of both negative and positive binding sites on this mineral surface at the prevailing pH. This was reported to be the case in other published works (Xu *et al.* (1991); Zhou & Gunter (1992); Jiang *et al.* (2010); Ma *et al.* (2013)). Similar phenomenon was observed when ilmenite was used (Figure 41) as its surface is more negatively charged.

With an increase of surfactant concentration, the SDS adsorption density increased from 0.3960 mg/g at 50 ppm to 1.170 mg/g at surfactant concentration of 250 ppm when kaolin clay was used (Fig. 40) whereas in case of ilmenite a very small increase in the adsorption of SDS was observed from 0.27 mg/g to 0.99 mg/g in the range of 50 to 300 ppm (Fig. 41). At low surfactant concentration, adsorption takes places mostly because of



individual ion interchange without contact between the adsorbed molecules (Tichelkamp *et al.*, 2015). It seems that SDS and SEMES can be adsorbed by kaolin clay as well as on ilmenite as an anion due to the capability of the minerals to generate a variable charge and to adsorb totally disassociated anions by means of ligand exchange (Sastry *et al.*, 1995; Ko *et al.*, 1998).

An increase of surfactant monomer adsorption happens for all the rock crystals as soon as the surfactant concentration in solution rises up to a point when the surfactant concentration in the equilibrium solution attains a value near to or somewhat higher than the CMC (Figures 40 to 43 ) (Liljeblad, 2006). Initially, SMES and SDS adsorptions occur through scatter interactions between the hydrophobic kaolin surface and the non-polar hydrocarbon chain of the probe particle. As the SDS concentration exceeded 250 ppm and SEMES concentration surpass 200 ppm, the adsorption became more stabilized with the escalation in the amount of surfactant. This shows that the adsorption has to surpass the electrostatic repulsion between the anionic heads groups of the SDS and SEMES and the like charges existing on the edge surface of the kaolin clay and ilmenite mineral until saturation adsorption is attained (Figures 40 and 41).

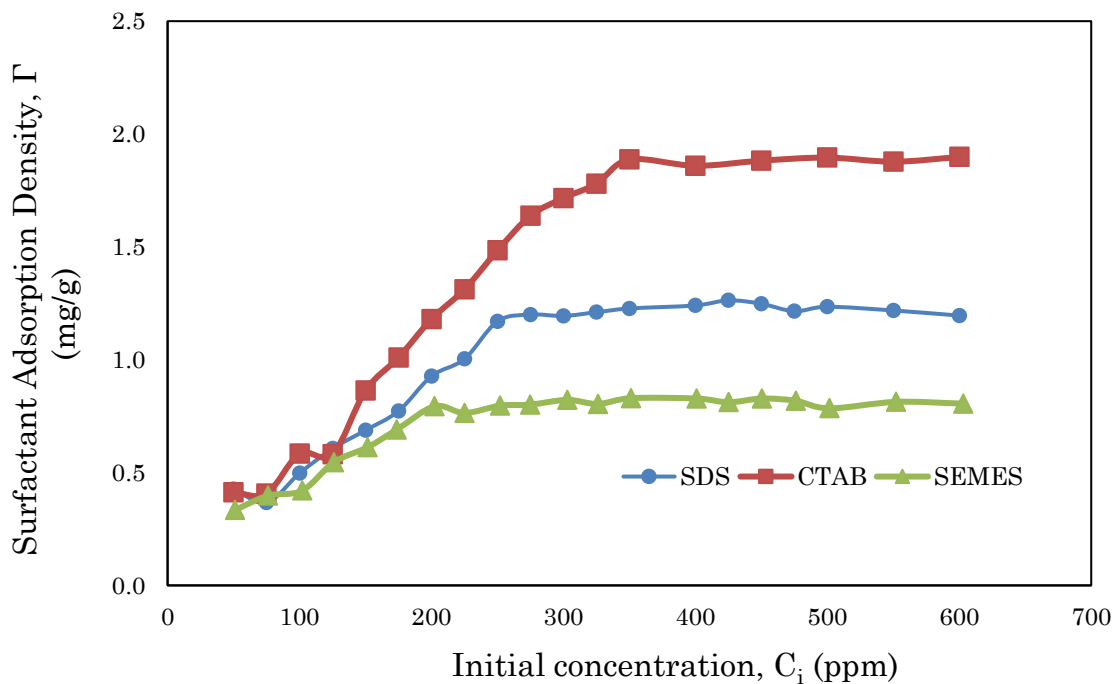


**Figure 40:** Static adsorption of SDS, CTAB and SEMES onto synthetic kaolin clay

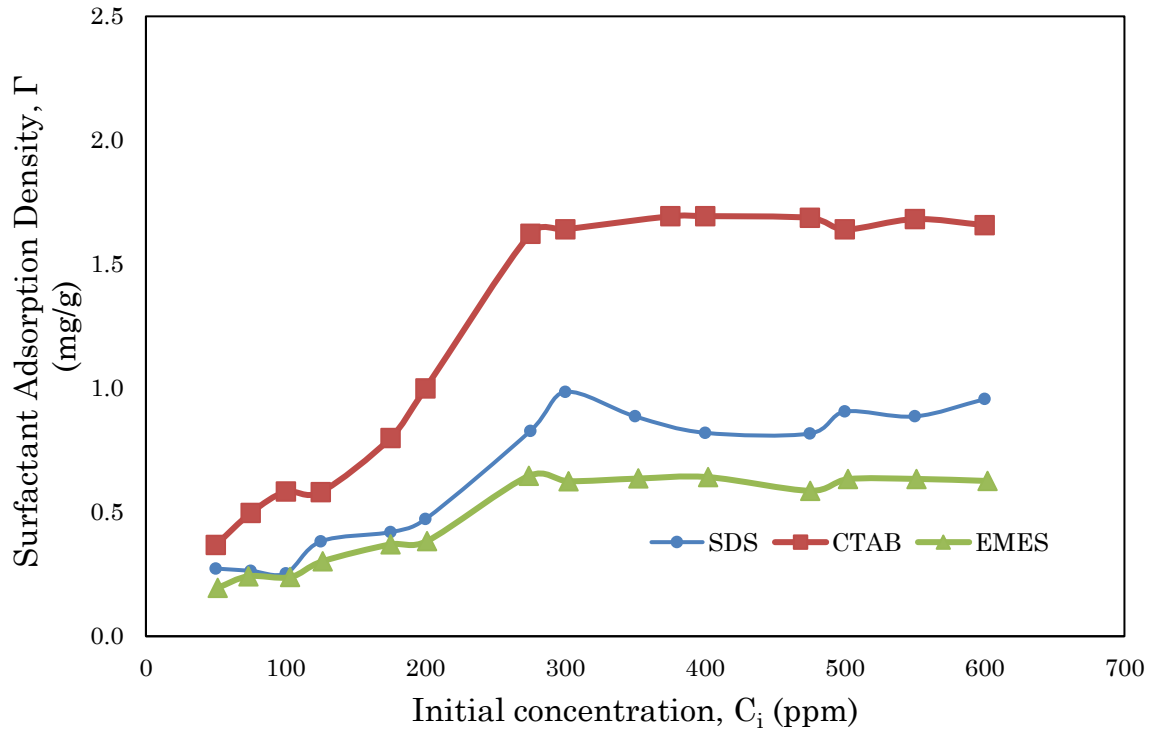


**Figure 41:** Static adsorption of SDS, CTAB and SEMES onto ilmenite

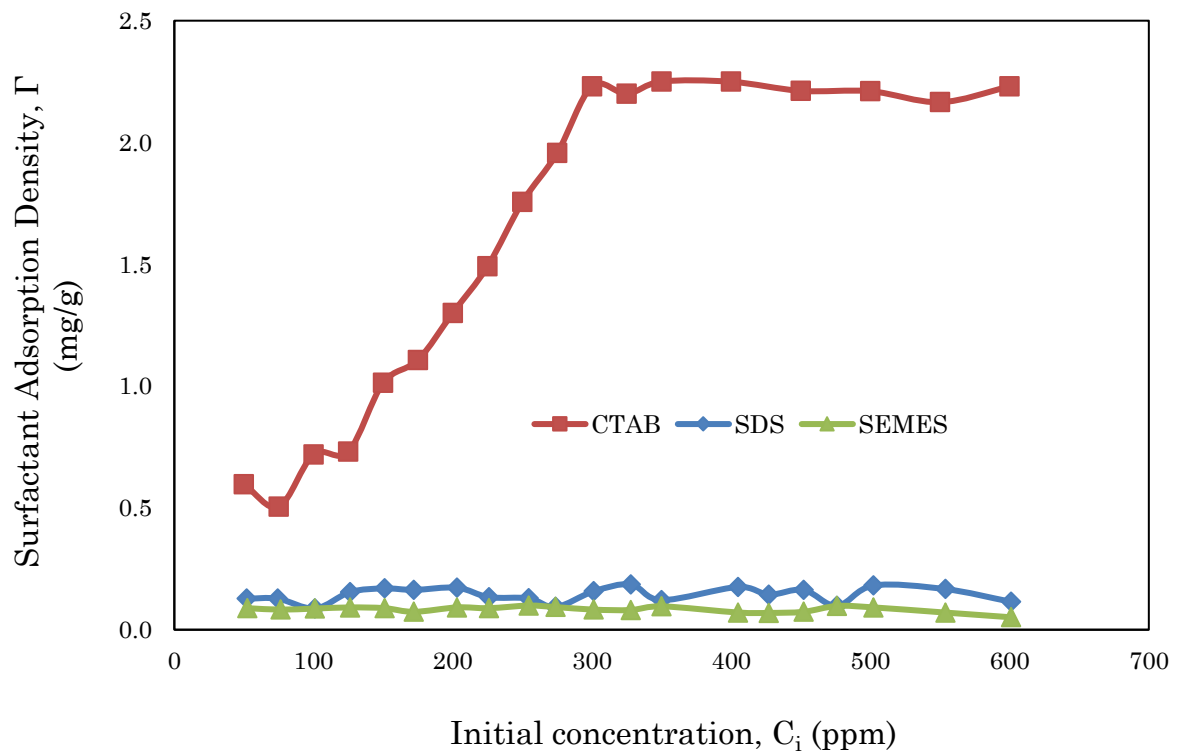


**Figure 42:** Static adsorption of SDS, CTAB and SEMES on silica

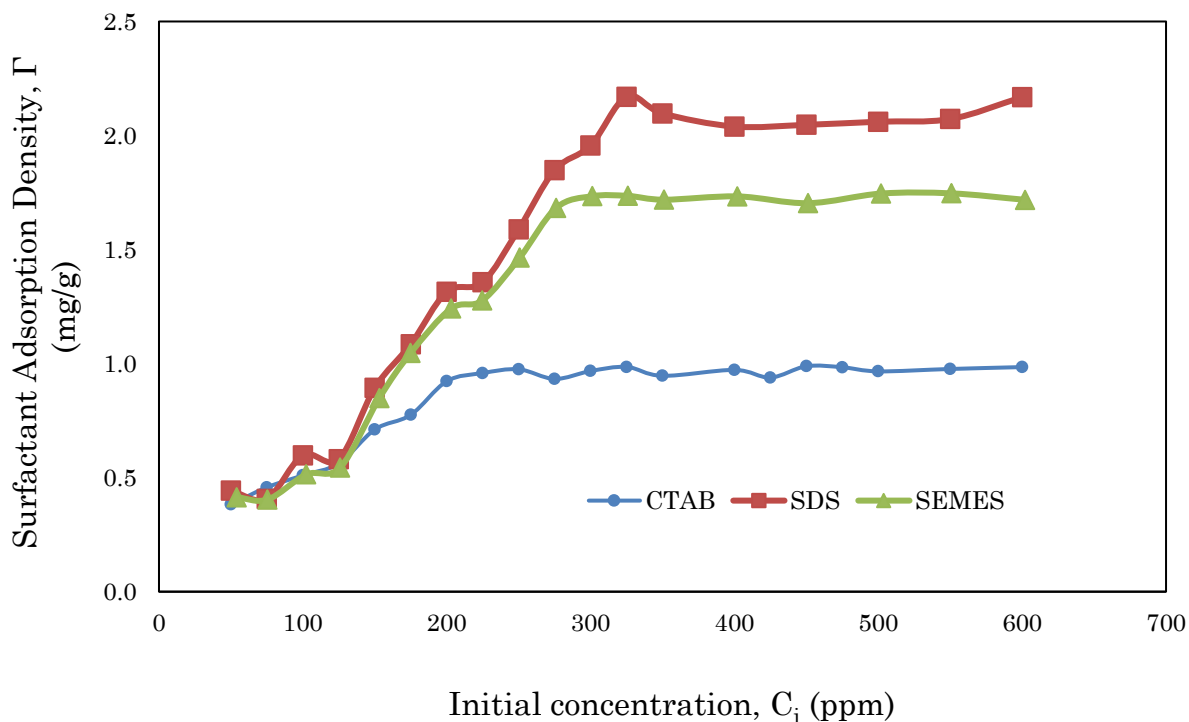


**Figure 43:** Comparison of static adsorption of SDS, CTAB and SEMES on alumina

The adsorption isotherm also indicates that once the SEMES and SDS surfactant concentrations reach 600 ppm, the volume adsorbed peaked and stabilized (Figures 40 and 41). However, SDS and SEMES exhibited a lower adsorption plateau compared to CTAB, which is most probably because of the strong electrostatic repulsion between the anionic SDS and SEMES and the negatively-charged kaolin ions. The maximum amount of SDS surfactant adsorbed on the kaolin clay and ilmenite surfaces was found to be 1.17 mg/g at concentration of 250 ppm and 0.99 mg/g at concentration of 300 ppm, respectively. The SEMES demonstrated a behavior similar to SDS when adsorbed onto kaolin clay and ilmenite. Nevertheless, a lower adsorption plateau was observed. When adsorbed on kaolin clay the SEMES adsorption density increased from 0.3345 mg/g at 50 ppm to 0.7935 mg/g at surfactant concentration of 200 ppm but in case of ilmenite a slight rise in the adsorption of SEMES was observed from 0.195 mg/g to 0.6465 mg/g in the range of 50 to 275 ppm (Figures 41 and 42). In case of CTAB, a higher and substantial increase in adsorption density with surfactant concentration in contrast to SDS was observed from 0.3975 mg/g to 1.8249 mg/g on kaolin while on ilmenite was 0.3675mg/g to 1.6233 mg/g at concentrations of 50 ppm to 275 ppm (Figures 41 and 42)

The basal planes of kaolin clay, ilmenite as well as silica are negatively charged, which causes a significant adsorption of CTAB (Ma *et al.*, 2013) as presented in Figures 40, 41 and 42. The CTAB adsorption occurs mostly due to the presence of some charged components of kaolin and ilmenite particles such as silica (on kaolin) and TiO<sub>2</sub> (on ilmenite) which are negative in nature at neutral pH or in water. Salari *et al.* (2011) also

noticed the same pattern where the CTAB adsorption density increases with surfactant concentration on carbonate material. According to Ma *et al.* (2013) if kaolin is present as a contaminant in natural carbonate material, its negative binding sites possibly will cause substantial CTAB adsorption particularly in alkaline systems. When lower concentrations are used, the accessibility of surfactant in the reservoir is not sufficient to attain a steady adsorption. Thus, adsorption density onto kaolin clay, silica and ilmenite presented a significant increase with the availability of CTAB surfactant. Here, the adsorption occurs via electrostatic interaction between the positively charged CTAB head groups and the negatively charged kaolin surfaces. This attraction comply with Henry's law which states that the adsorption increases linearly with concentration (Paria & Khilar, 2004).

CTAB adsorption attains its maximum and equilibrium state at 350 ppm and 275 ppm with an adsorption density of 1.8871 mg/g-kaolin and 1.6233 mg/g-ilmenite, respectively (Figures 40 and 41). It can be said that the adsorption density in this system is a function of the amount and availability of CTAB, as well as kaolin clay and ilmenite to surfactant solution proportion (Salari *et al.*, 2011). As the hydrophobic mass increases, the hydrophobic attraction between the surfactant and the absorbent molecules increases which in turn also causes an increase in the adsorption density. Here, increasing the surfactant concentrations appears to also cause an increase in the quantity of surfactant adsorbed. As the CMC is attained, the adsorption density stabilizes (or saturates) owing to the surfactant ions having filled all of the kaolin surface sites as well as the chemical potential of the surfactant monomers present in solution are practically steady beyond the CMC (Liljeblad, 2006). In this region, as additional surfactant is injected beyond the CMC, a slight or no increase in adsorption with increasing surfactant concentration is observed. The micelle concentration (MC) increases and begins to agglomerate in bulk solution but then again the concentration of monomer stays almost steady because these micelles act as a chemical potential sink for any additional surfactant introduced into the system.

The positively-charged CTAB is also strongly adsorbed onto synthetic silica whereas the negatively-charged SDS shows minor adsorption (Fig. 42). The SEMES exhibited very insignificant adsorption on silica surface in comparison to the anionic, SDS, surfactant. The high adsorption capacity of CTAB on silica particles can be described on grounds of electrostatic interaction which happens between the positively-charged head group of CTAB and the negatively-charged silica (Bera *et al.*, 2013). At that pH of 6 the surface of the silica is strongly negatively charged, which is in accordance with the report of Ma *et al.* (2013). Thus, the electrostatic repulsion among the formation containing silica material and the anionic surfactant constrains the adsorption.

The behavior of SDS and the SEMES is totally different when alumina is used as the solid material (Fig. 43). At low CTAB concentrations the surfactant adsorbs randomly, with no associated structure. As the surfactant concentration increases, the existence of hemimicelles on the surface is noticed. Consequently, if natural carbonates have a considerable quantity of silica, substantial adsorption of CTAB may be expected to take place. The adsorption plateau of CTAB is slightly similar to that exhibited on kaolin, however it is to some extent higher with an adsorption density of 2.2305 mg/g at surfactant concentration of 300 ppm and the maximum adsorption for SDS surfactant was 0.270 mg/g at 325 ppm. However, SDS and SEMES adsorption plateaus on synthetic alumina are much higher in comparison to that of CTAB as presented in Fig. 43, which is in agreement with previous studies (Waterman *et al.*, 1986; Paria and Khilar, 2004). However, the synthesized surfactant showed lower adsorption on alumina compared to SDS. Likewise, SEMES attained CMC at 275 ppm with an adsorption density of 1.683 mg/g (Fig. 50). This is because negatively charged surfactant strongly adsorbs on positively charged alumina at pH 6. The adsorption of CTAB on alumina is quite low due to the fact that its concentration in the vicinity of alumina surface is inferior to that in the bulk. This is probably attributed to the resilient electrostatic repulsion among the cationic CTAB surfactant and the positively-charged aluminium ions on alumina.

### **5.5.3 Effect of pH on the Surfactant Adsorption Isotherm**

The pH of the aqueous solution is one of the key controlling factors during surfactant adsorption to the reservoir rocks. In Fig. 44 the effect of pH on the adsorption isotherms of the two different surfactants (anionic and cationic) on synthetic kaolin clay surface is represented. Different sodium hydroxide concentrations (0 to 1 wt. %) were used in this study and measurement carried out at ambient temperature. The SDS, CTAB and the synthesized SEMES surfactant concentrations were kept constant at 250 ppm, 350 ppm and 200, correspondingly. These values were selected due to the fact that at these surfactant concentrations the adsorption plateau stabilized and reached critical micelle concentration (CMC) when kaolin was used as the reservoir material.

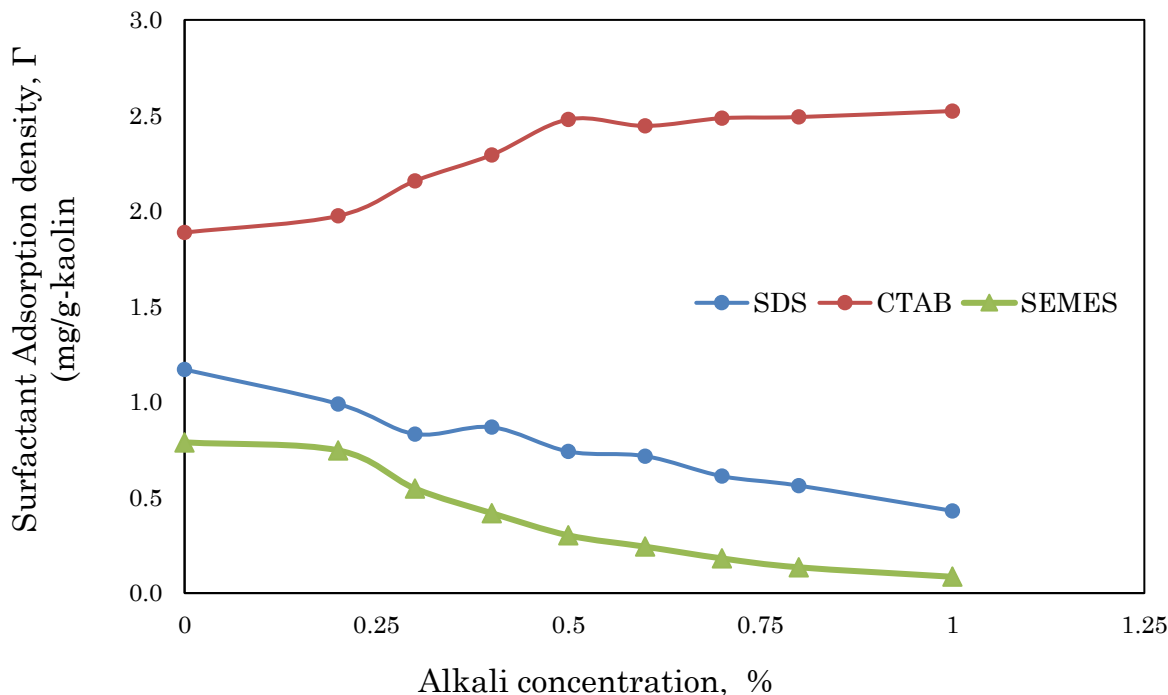


**Figure 44:** The effect of different alkali concentrations on the adsorption isotherms of SDS, CTAB and SEMES on kaolin at ambient temperature

The adsorption of anionic surfactant and the synthesized surfactant decreases with the increase in concentration of alkali (~pH 10-12). This makes the mineral surface (adsorbent) more negatively charged; which in turn repulses the anionic surfactant and drive more surfactant to the solution, causing a decrease in the adsorption. Fig 44 shows that at an alkali concentration of 0.2 wt. %, the SDS surfactant adsorption was instantly decreased from 1.17 mg/g-kaolin to 0.99 mg/g-kaolin. Then as the alkali concentration exceeded 0.6 wt. %, the adsorption of the surfactant on kaolin reached saturation and its maximum adsorption shown to be ~0.431 mg/g-kaolin (Fig. 44). Relative to the synthesized SEMES surfactant, the former showed similar adsorption characteristics to the synthetic anionic SDS with the addition of alkaline chemical but its adsorption plateau reduced significantly from 0.747 mg/g-kaolin to 0.086 mg/g-kaolin at NaOH concentrations of 0.2 to 1 wt.%. However, in case of CTAB, as the pH of the solution increased, the CTAB adsorption capacity also increased due to the fact that the cationic surfactant positively-charged head groups are strongly attracted at high pH with negatively-charged kaolin clay surface. Figure 44 shows that at alkali concentration of 0.2 wt. %, the CTAB surfactant adsorption increased from 1.887 mg/g-kaolin to 1.974 mg/g-kaolin. When the alkali concentration was raised to 0.6 wt. %, the adsorption of the cationic surfactant on kaolin clay attained equilibrium and its maximum adsorption observed to be ~2.523 mg/g-kaolin. Consequently, it can be concluded that ionic surfactant adsorption on mineral rock surfaces can be minimized or modified by

adjusting the pH of the solution which is crucial to the economic viability of surfactant use in EOR processes.

#### 5.5.4 Effect of Salinity on the Adsorption Isotherm of Surfactants

Generally, enhanced oil recovery (EOR) is carried out using brine injection or sea water which contains hard ions. In actual fact, nought concentration of divalent ions in a genuine application of an EOR process is very uncommon. Hence, it is essential to study the effect of divalent ions on surfactant adsorption. Adsorption isotherms for SDS, CTAB and SEMES surfactant solutions at different salinities on synthetic kaolin clay are presented in Figure 45.

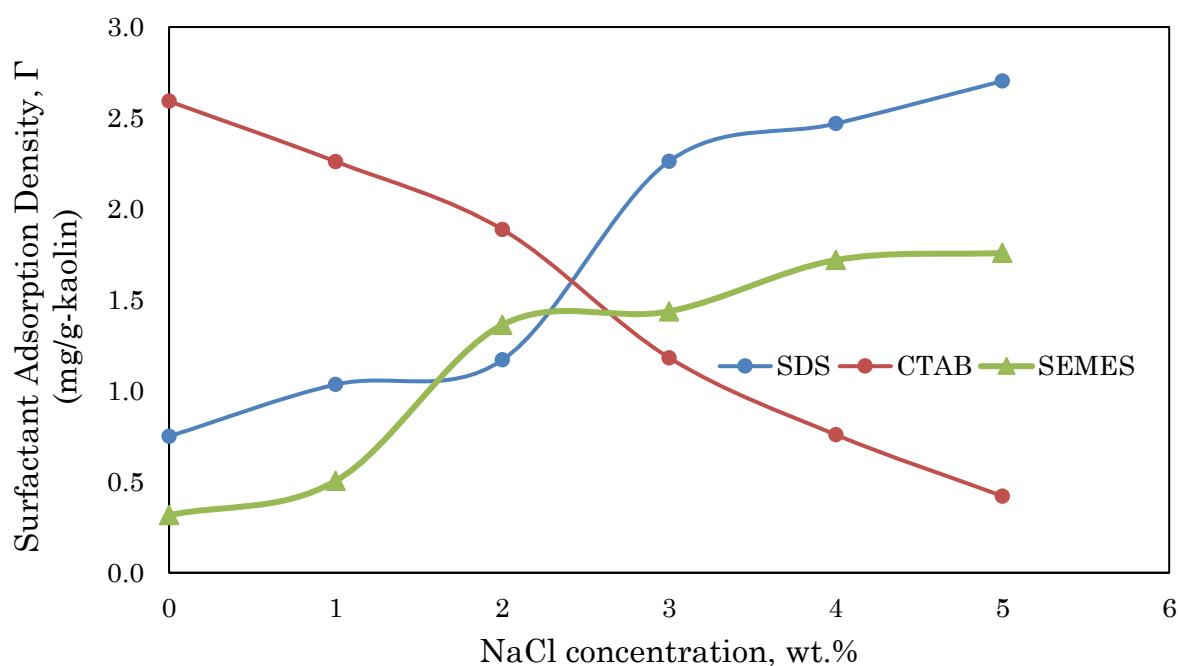


**Figure 45:** Adsorption Isotherm of SDS and CTAB at different NaCl salt concentrations at ambient temperature

An increase of the adsorption plateau of anionic surfactants (SDS and SEMES) with increase in the equilibrium amount of hard ions can be observed from Fig.45. The addition of salts of multivalent cations may in some instances result in a substantial increase in the anionic surfactants adsorption while causing a decrease in the adsorption capacity of cationic surfactants (Bera *et al.*, 2013). At the interface between surfactant and the kaolin particles, there is always an imbalanced dispersal of electrical charges. This uneven charge distribution contributes to the rise of a potential through the interface and creates a so-called electrical double layer (Pethkar and Paknikar, 1998).

When the concentration of NaCl is increased, the electrical double layer on the adsorbent's surface is compressed, thus causing a decrease in the electrostatic repulsion between the adsorbed surfactant species and the adsorbent. This results in an increase of adsorption capacity of anionic surfactants. Thus, there is a monotonic increase in the adsorption capacity of SDS and the synthesized surfactant SEMES as more NaCl solution is added. This is attributed to the fact that the concentration of divalent ions ( $\text{Na}^+$ ) in the solution increases with increase in the added quantity of sodium chloride. However, a different trend was observed with CTAB, increase in the NaCl salt concentration caused the electrostatic attraction between the adsorbed surfactant species to fall resulting in the decrease of the adsorption capacity for CTAB (Fig. 45). The surface of the kaolin clay became more positively-charged and as a result it repulsed the cationic surfactant, thus causing a decrease in its adsorption.

### 5.5.5 Adsorption of Mixed Anionic-Cationic Surfactants System

Anionic-cationic surfactants mixtures are well-known to show astonishing synergism, as confirmed by the ultra-low CMCs and IFT values generated by these arrangements (Nakama *et al.*, 1990; Upadhyaya *et al.*, 2007). Thus, this study investigates the adsorption of anionic-cationic mixtures using a ratio of 50:50 onto silica. Figure 46 shows the adsorption isotherm for anionic-cationic surfactant mixtures onto silica surface.

Despite the fact the anionic surfactant SDS does not adsorb on negatively charged silica as a single system, it does co-adsorb with the cationic surfactant CTAB. These cationic head groups offered a striking site for the co-adsorption of negative SDS head groups. According to Upadhyaya *et al.* (2007) besides the favorable electrostatic interactions between the positive and negatively charged head groups, there are also favourable hydrophobic interactions between the tails of the CTAB and SDS particles. All these interactions result in co-adsorption of cationic surfactant with SDS onto the silica mineral, and consequently raised packing density of surfactant on the interface. In the case of the synthesized SEMES+CTAB system its co-adsorption plateau was lower compared with the anionic SDS surfactant+CTAB cationic surfactant system. However, this enhancement in adsorption both in rate and amount of adsorption is lower compared with the amount of adsorption of CTAB alone on silica surface (Fig. 46).



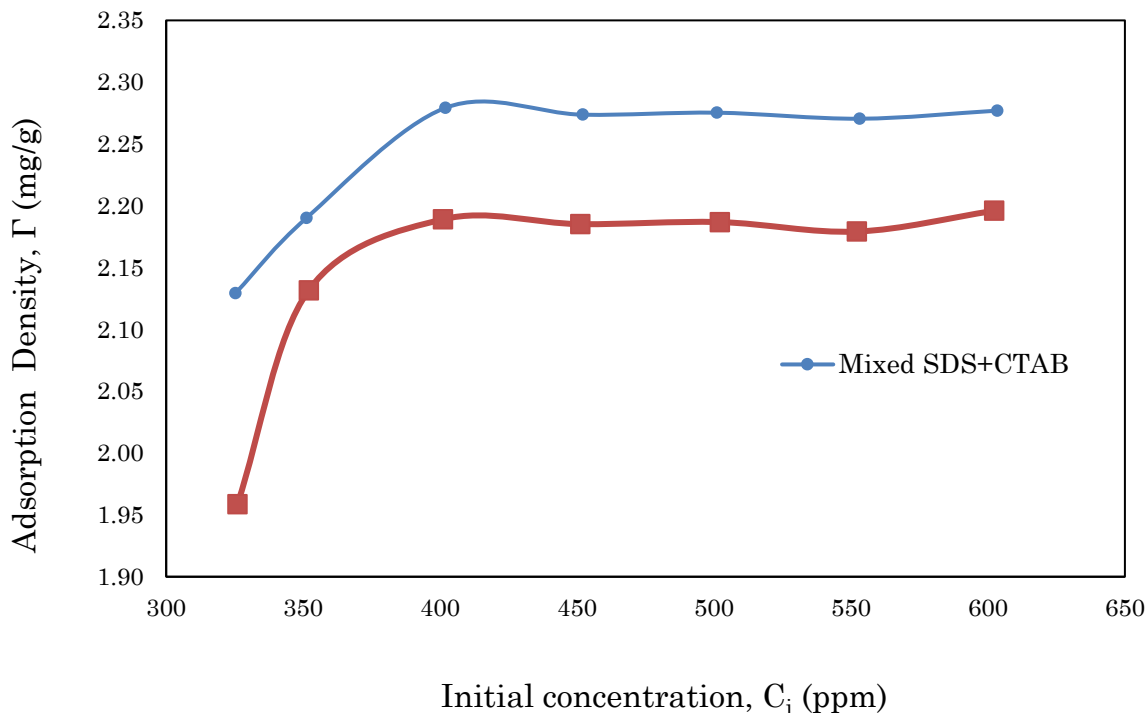


**Figure 46:** Adsorption isotherm of SDS+CTAB and SEMES+CTAB systems with fixed salinity at ambient temperature

The principal reason for this variance is because mixed cationic and anionic surfactants systems, tend to form an ion pair and thus behaving like surfactant with practically no apparent charge, hence presenting lower adsorption plateau in comparison to CTAB. These results also demonstrate the crucial importance of surfactant structural arrangement on the adsorption of mixed surfactant systems. It is vital to control the adsorption behavior of mixed surfactant schemes by means of regulating the comparative physical factors of surfactants, once the interactions between the different constituents are well understood.

### 5.5.6 Sub-CMC Adsorption Isotherms

Adsorption data obtained were fitted to Freundlich and Langmuir models and suitability of the isotherm equations were related by comparing the correlation coefficients,  $R^2$ . The best-fitted parameters in conjunction with the regression coefficients for the anionic and cationic-surfactant systems adsorbed in synthetic kaolin clay, silica, alumina and ilmenite are presented in Tables 21 to 28. Tables 21 to 24 demonstrate Langmuir-fitted equations, constants, and  $R^2$  whereas Tables 29 to 32 give the Freundlich-fitted equations, constants and  $R^2$  for the anionic, the synthesized SEMES and cationic-surfactant systems adsorbed onto synthetic kaolin clay, silica, alumina and ilmenite, correspondingly. The adsorption data acquired from the two synthetic surfactants (SDS and CTAB) and synthesized surfactant (SEMES) -systems were fitted to the Langmuir

model by plotting  $1/\Gamma$  against  $1/C_e$  which gives a slope of  $1/(\Gamma_{\max}K_L)$  and an intercept of  $1/\Gamma_{\max}$ . Langmuir isotherm makes possible to evaluate the adsorption grade through the aforementioned  $K_L$  and  $\Gamma_{\max}$  factors.  $K_L$  is a constant in the Langmuir model which shows the adsorption capability of the solid material to the corresponding solutes: the higher the  $K_F/K_L$  the higher the  $\Gamma$  value (Salari *et al.*, 2011).  $K_L$  values of SDS on alumina (0.0123 g/L) and CTAB (200.66 g/L) on kaolin are by far higher than those of SDS on silica (-253.21 g/L) and ilmenite (-2.355 g/L) and CTAB on the alumina surface (-11.2 g/L). However, in the case of SEMES,  $K_L$  value (0.193 g/L) on silica is higher in comparison to  $K_L$  values on alumina, ilmenite as well as kaolin clay (0.0123 g/L, 0.0113 g/L and 0.0253). This due to the fact that on these minerals their adsorption capacity is almost negligible; which is also the case of SEMES on silica material.

**Table 21:** Parameters for Langmuir model fitted to synthetic kaolin clay data

Surfactants	Fitted Langmuir Equation	$R_L^2$	$\Gamma_{\max}$ (mg/g)	$K_L$ (g/L)
SDS	$(1/\Gamma) = 52.397 \times 1/C_e + 0.7469$	0.7364	1.17	29.58
CTAB	$(1/\Gamma) = 59.754 \times 1/C_e + 0.426$	0.7957	1.89	200.66
SEMES	$(1/\Gamma) = 62.319 \times 1/C_e + 1.0526$	0.9127	0.79	0.0253

**Table 22:** Parameters for Langmuir model fitted to silica data

Surfactants	Fitted Langmuir Equation	$R_L^2$	$\Gamma_{\max}$ (mg/g)	$K_L$ (g/L)
SDS	$(1/\Gamma) = 61.109 \times 1/C_e + 6.9879$	0.0324	0.19	-253.21
CTAB	$(1/\Gamma) = 19.233 \times 1/C_e + 0.5654$	0.5031	2.23	187.70
SEMES	$(1/\Gamma) = -114.47 \times 1/C_e + 12.927$	0.0667	0.1	0.193

**Table 23:** Parameters for Langmuir model fitted to alumina data

Surfactants	Fitted Langmuir Equation	$R_L^2$	$\Gamma_{\max}$ (mg/g)	$K_L$ (g/L)
SDS	$(1/\Gamma) = 53.41 \times 1/C_e + 0.8787$	0.9191	2.17	214.51
CTAB	$(1/\Gamma) = 58.277 \times 1/C_e + 0.3687$	0.7461	0.92	-11.2
SEMES	$(1/\Gamma) = 67.875 \times 1/C_e + 0.4137$	0.7735	1.68	0.0123

**Table 24:** Parameters for Langmuir model fitted to ilmenite data

Surfactants	Fitted Langmuir Equation	$R_L^2$	$\Gamma_{\max}$ (mg/g)	$K_L$ (g/L)
SDS	$(1/\Gamma) = 121.69 \times 1/C_e + 1.0542$	0.715	0.99	-2.355
CTAB	$(1/\Gamma) = 64.109 \times 1/C_e + 0.4755$	0.9152	1.62	105.20
SEMES	$(1/\Gamma) = 164.42 \times 1/C_e + 1.3193$	0.8927	0.64	0.0113

The adsorption data was also fitted to the Freundlich isotherm by plotting a graph of  $\log \Gamma$  against  $\log C_e$  which yields a slope =  $1/n$  and an intercept =  $\log K_F$ .  $K_F$  is equivalent to  $K_L$  in the Langmuir model which is related to the bonding energy.  $K_F$  can be described as an adsorption coefficient plus it denotes the amount of adsorbate adsorbed on adsorbents for a unit equilibrium concentration. Similar to the Langmuir isotherm

model, from Tables 24 to 28, the  $K_F$  values of SDS on alumina (0.2698 L/Kg) (Table 27) and CTAB surfactants when adsorbed on silica (0.1648 L/Kg) (Table 26) are the highest.

**Table 25:** Parameters for Freundlich model fitted to synthetic kaolin clay data

Surfactants	Fitted Freundlich Equation	$R_F^2$	1/n	$K_F$ (L/Kg)
SDS	$\text{Log}(\Gamma) = 0.4488 \times \text{LogCe} - 1.0448$	0.8521	2.23	0.1157
CTAB	$\text{Log}(\Gamma) = 0.6406 \times \text{LogCe} - 1.3173$	0.862	1.56	0.0335
SEMES	$\text{Log}(\Gamma) = 0.3122 \times \text{LogCe} - 0.8762$	0.8162	3.20	0.3895

**Table 26:** Parameters for Freundlich model fitted to silica data

Surfactants	Fitted Freundlich Equation	$R_F^2$	1/n	$K_F$ (L/Kg)
SDS	$\text{Log}(\Gamma) = 0.056 \times \text{LogCe} - 0.9871$	0.0318	17.86	0.1377
CTAB	$\text{Log}(\Gamma) = 0.5191 \times \text{LogCe} - 0.9422$	0.7884	1.93	0.1648
SEMES	$\text{Log}(\Gamma) = -0.0854 \times \text{LogCe} - 0.8807$	0.1449	-11.71	$5.0297 \times 10^{11}$

**Table 27:** Parameters for Freundlich model fitted to alumina data

Surfactants	Fitted Freundlich Equation	$R_F^2$	1/n	$K_F$ (L/Kg)
SDS	$\text{Log}(\Gamma) = 0.3291 \times \text{LogCe} - 0.8389$	0.8286	3.04	0.2698
CTAB	$\text{Log}(\Gamma) = 0.6787 \times \text{LogCe} - 1.3523$	0.8253	1.47	0.0318
SEMES	$\text{Log}(\Gamma) = 0.6215 \times \text{LogCe} - 1.2982$	0.8027	1.61	0.0355

**Table 28:** Parameters for Freundlich model fitted to ilmenite data

Surfactants	Fitted Freundlich Equation	$R_F^2$	1/n	$K_F$ (L/Kg)
SDS	$\text{Log}(\Gamma) = 0.5686 \times \text{LogCe} - 1.5353$	0.8471	1.76	0.0444
CTAB	$\text{Log}(\Gamma) = 0.5803 \times \text{LogCe} - 1.2463$	0.8903	1.72	0.0823
SEMES	$\text{Log}(\Gamma) = 0.4993 \times \text{LogCe} - 1.5043$	0.8947	2.00	$7.329 \times 10^{-3}$

From the obtained results it can be noticed that there is a high adsorption capacity of alumina for the anionic surfactants in comparison to silica. On the other hand, for SEMES,  $K_F$  values for silica ( $5.0297 \times 10^{11}$  L/Kg) and kaolin minerals (0.3895 L/Kg) are quite high compared with the  $K_F$  values on alumina (0.0355 L/Kg) and ilmenite ( $7.329 \times 10^{-3}$  L/Kg). These discrepancies could be due to the difference in preparation techniques of the different surfactants.

The slope 1/n, starting from 0.8389 to 1.5353 is an indication of the surface heterogeneity and intensity of adsorption and as its value approximate to zero (Tables 24 to 28). According to Muherei (2009) if the value of 1/n is lower than 1, the Freundlich/Langmuir isotherm is considered to be normal whereas if it is above 1 means that there was cooperative adsorption. Moreover, a greater value of n (and considerably small slope) is an indication that the adsorption is good over the series of concentrations studied, but a low value of n (and sharp slope) reveals that the adsorption is good at high concentration but then again is considered to be much poorer at very low concentrations. From Table

28 it can be concluded that the adsorption of SDS and SEMES onto ilmenite ( $1/n=1.5353$  and  $1/n =1.5043$  respectively) involves cooperative adsorption ( $1/n=1.5353$ ). This also implies that SDS and SEMES possess similar adsorptive behavior.

The Langmuir constant,  $\Gamma_{\max}$ , is an indication of the highest amount of the surfactant adsorbed. As observed in Tables 25 to 28,  $\Gamma_{\max}$  values are higher for CTAB adsorbed on silica and SDS on alumina as well as slightly higher for SEMES adsorbed on alumina also which indicates silica and alumina higher capacity to adsorb cationic and anionic surfactants. Nevertheless, 'n' values of the Freundlich isotherm (Tables 25 to 28), the  $\Gamma_{\max}$  values of the surfactants are quite similar (Tables 25 to 28).

## 5.6 THERMAL STABILITY ANALYSIS

The thermal stability of sodium epoxidized methyl ester sulfonate (SEMES) and the synthetic surfactants, sodium dodecyl sulfate (SDS) and cetyltrimethylammonium bromide (CTAB) is illustrated in Figures 47 and 48. Three mass loss phases were noticed.

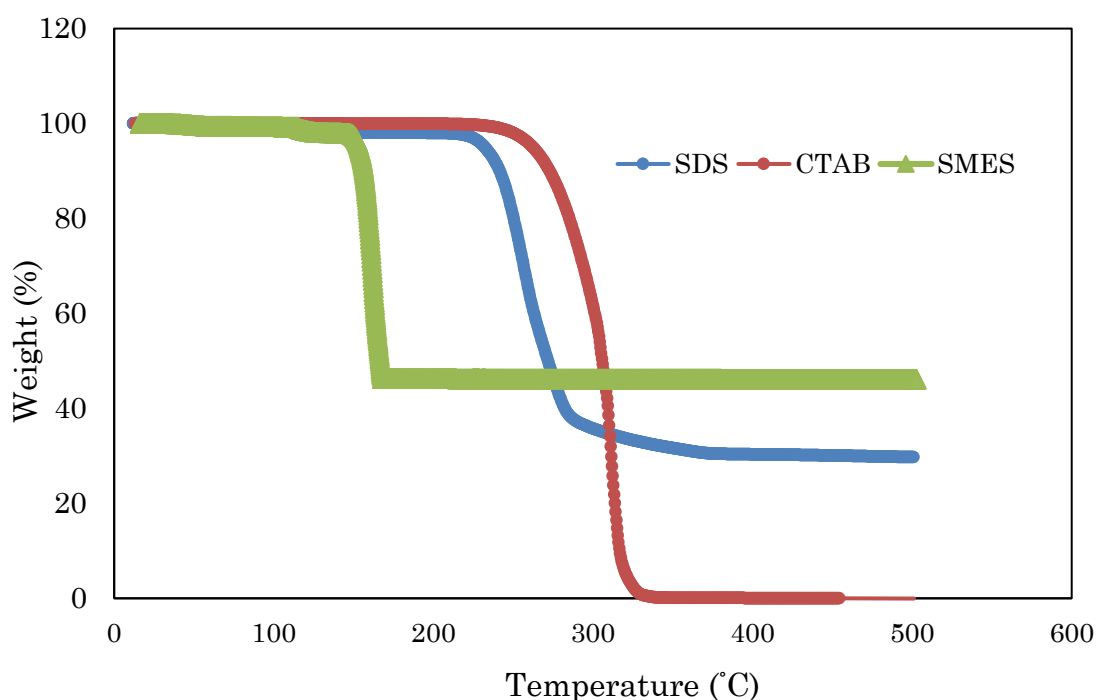


**Figure 47:** Thermal stability analysis for SDS and CTAB and SEMES as a function of temperature

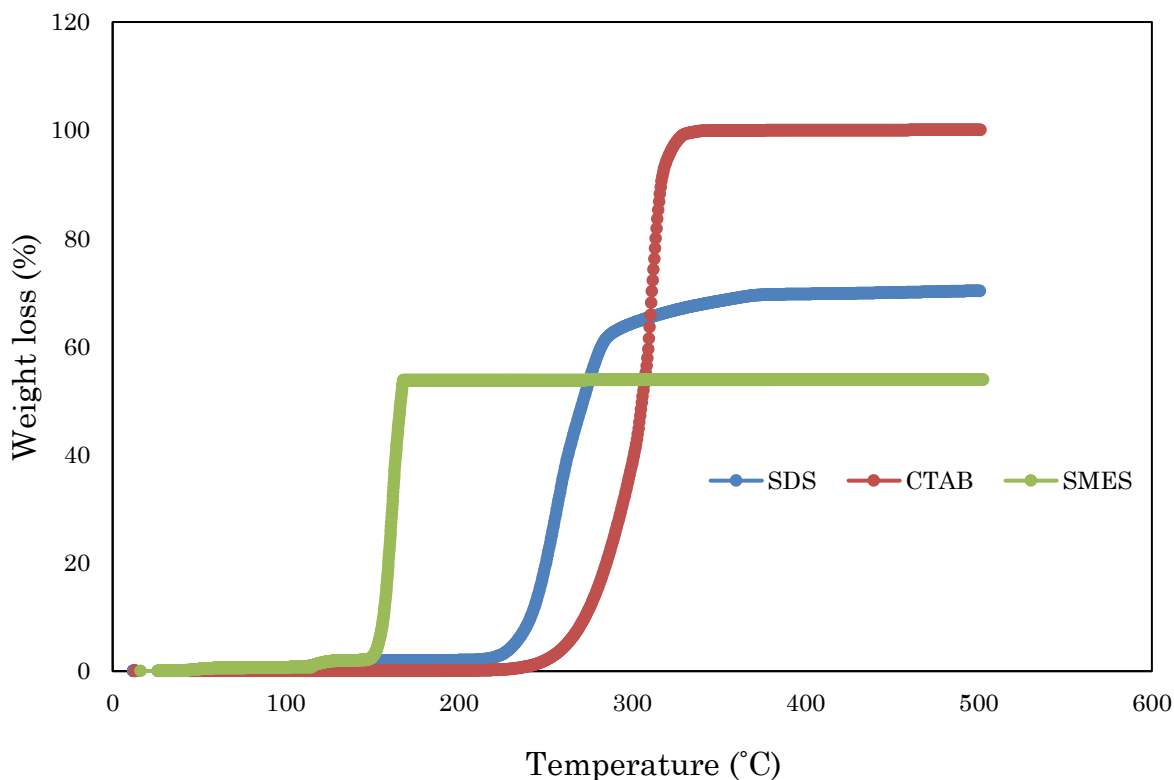


**Figure 48:** Weight loss of SDS, CTAB and SEMES as a function of temperature

The TGA profile of SDS shows that the first thermal degradation took place from 242 °C where ~5% weight loss was observed, then again approximately 62% weight loss occurred from 242 °C to 340 °C due to bound water (Fig. 48). These show that SDS molecules were thermally stable up to temperatures >242 °C. This is similar to the observation reported by Elraies *et al.* (2009) where it was observed that SDS started to degrade at 242 °C to 341 °C with a weight loss of 75% (Fig. 47 and 48). In the case of CTAB, around 6% weight loss was recorded at 259 °C. Then, 68% weight loss occurred from 259 °C to 353 °C. Beyond 353 °C, residual components of the CTAB were totally decomposed up to 500 °C (Fig. 47).

For the synthesized surfactant, SEMES, in the first region, a mass loss of 0.7% from ambient to 100 °C (Fig. 48) which could be attributed to the loss of weakly bonded water molecules (Babu *et al.*, 2015). Afterwards, a 22.9% mass loss occurred abruptly in the second region from 100 °C to 160 °C, which reveals that SEMES molecules begin to decompose at temperatures greater than 100 °C. The last region is the degradation region that starts from 160 °C to 500 °C, represent a multifaceted thermal breakdown of molecules which may have been caused by the addition of the sulfonate group (Fig. 47). The residual elements of SEMES surfactant were thermally stable up to 500 °C (Babu *et al.*, 2015; Elraies & Tan, 2003). Nevertheless, as the typical reservoir temperature varies from 50 °C to 120 °C, both surfactants SDS and the SEMES should be able to maintain an average of 84.89% and 97.7% respectively of their structural arrangement and mass

(Elraies *et al.*, 2011). In conclusion, these anionic surfactants have great thermal stability and can be efficiently used for EOR at the desired reservoir temperatures. Conversely, CTAB decomposes fully at temperatures beyond 329 °C.

## 5.7 SUMMARY

Although injection of surfactants in oil reservoirs often can lead to production of more oil, loss of surfactant due to adsorption on porous media can make this process economically unfeasible. This study showed that cationic surfactant (CTAB) adsorbed strongly onto all the tested reservoir rock materials in the order silica > kaolin > ilmenite, compared to the anionic (SDS) and the synthesized surfactants (SEMES), under the same conditions (constant salinity of 2 vol. %). The anionic surfactant adsorption on synthetic kaolin clay surface decreased due to an increase in the electrostatic repulsive forces among the adsorbent and the adsorbed surfactant molecules while the contrary occurred when cationic surfactant was utilized. The adsorption of anionic surfactants (SDS and SEMES) on synthetic kaolin clay surface increased as a result of the low electrostatic repulsion between the adsorbed surfactant species and the reservoir material surface. However, an opposite pattern was observed in the adsorption plateau of the cationic surfactant (CTAB).

These findings suggest that, the adsorption capacity of anionic surfactant is favored by increase in salinity while the adsorption capacity of cationic surfactant is favored by increase in alkalinity of the system at ambient temperature. It is evident that, anionic surfactants are preferred when it comes to reservoirs containing mineral surface with a net negative surface charge due to the fact that the electrostatic repulsion between the mineral surface and the surfactant head-group help to minimize adsorption. Cationic surfactants are preferred for use in reservoirs with a positive net surface charge.

The mixed equimolar surfactant systems demonstrated more complex behavior compared with single surfactant systems and resulted in co-adsorption of cationic surfactant with anionic surfactants onto the silica mineral. It can also be deduced from the results presented herein that, the sodium epoxidized methyl ester sulfonate demonstrated good surface thermal stability at reservoir temperature (500 °C), where approximately 10% mass loss was observed. The chapter highlights the advantages of the newly SEMES as opposed to anionic SDS and cationic CTAB during enhanced oil recovery processes and that waste vegetable oil can potentially be used for cost effective surfactant production.

## CONCLUSIONS AND RECOMMENDATIONS

---

### 6.1 GENERAL CONCLUSIONS

Taking into consideration the findings and results presented in this study, it can be concluded that the waste vegetable oil is a great source of sustainable resource and a suitable cost-effective substitute for petrochemical feedstock and other edible vegetable oils for the production of surfactants. Production of sodium epoxidized methyl ester sulfonate (SEMES) based on waste vegetable oil can fulfil EOR needs, since it is economical, less toxic, environmentally friendly, in addition to the fact that it is a renewable raw material for other processes. SEMES presents applicable surfactant characteristics at considerable cost, and for that reason it compromises a durable cost-effective inducement to substitute sodium dodecyl sulfate and other industrialized surfactants for EOR uses. SEMES was successfully synthesized from fatty acid methyl ester derived from waste sunflower oil. The experimental work started with the production of the methyl ester, followed by epoxidation of the poly-saturated fatty acids and sulfonation using chlorosulfonic acid.

The reaction conditions of temperature 65 °C, 1:9 oil to methanol molar ratio, 4 wt. % of catalyst/oil, and reaction time of 4h employed in the current study resulted in high FAME yield (89.1% for WPO and 97.5% for WSO). Results showed that 60% CaO/40% alumina by weight catalyst at 4% loading, effectively mediated the transesterification of waste palm oil ([FFA]=76.96 mg/g) given 89.1% FAME yield. However, due to the lower FFA content, a lower ratio of the acidic oxide was required, 80% CaO/20% alumina by weight catalyst at 4% loading to obtain same FAME yield from waste sunflower oil. As shown in this study; highly active catalyst with high CaO dispersion could be prepared via the co-precipitation method as confirmed by the SEM analysis. However, depending on the type of WVO and its FFAs content, the basic-acidic oxide ratio to be used will depend on the FFA content of the waste oil.

The epoxidation reactions with formic acid as an oxygen carrier, chosen for the higher reaction rate generated unacceptable high levels of vicinal di-hydroxy by-products. This highlighted the need to reduce by-product formation and was the drive for the use of a

suitable solvent at different temperatures. Epoxidation reactions under the conditions used resulted in the conversion of a high percentage of the unsaturated fraction. The use of solvent and at higher temperatures with formic acid was beneficial since the production of by-products and other side reactions was greatly minimized. The GC-MS method was effectively able to monitor the reactions progress and identify the epoxy FAME and also provided the facility to detect and identify the epoxidation by-products. Furthermore, it proved to be an efficient and a consistent qualitative and quantitative method for the determination and monitoring of transesterification and epoxidation reactions. Formic acid was found to be highly effective as a solvent at 30 °C.

The optimum reaction conditions for the epoxidation of waste sunflower oil derived FAME were hydrogen peroxide to FAME molar ratio of 1.73, formic acid to FAME molar ratio of 4, solvent (toluene) to formic acid/peroxide 0.54 ml, 4 h of reaction time at 30 °C giving epoxy products. In the attempt to minimize the formation of by-products by hydrolysis and side reactions, there was low conversion of FAME to epoxy FAME at the commercially considerable residence time of 4 h. Without solvent, the temperature at 25 °C had an effect on the oxirane ring opening reactions. Additionally, significant quantities of vicinal hydroxyl and di-hydroxy by-products were produced during the epoxidation with no solvent and at temperatures of 25 °C.

Sodium epoxidized methyl ester sulfonate was produced with the epoxidation followed by sulfonation of the methyl. FTIR results provided an insight into the dynamics of surfactants moiety and confirmed the presence of the sulfonate group (S=O) at 1614 cm<sup>-1</sup> which is an indication that this complex must be sodium epoxidized methyl ester sulfonate.

In summary, the results obtained from the adsorption tests revealed that the amount of adsorption in terms of mass per unit surface area varies with different reservoir minerals. From this study, it can be concluded that cationic surfactant (CTAB) have a tendency to be strongly adsorbed to silica > kaolin > ilmenite surfaces compared with the anionic (SDS) and the synthesized surfactants (SEMES). At low surfactant concentrations, the adsorption of cationic surfactants is induced by electrostatic forces of interaction on diaspore as well as ion exchange, thus making them to adsorb readily on kaolinite, silica and ilmenite mineral surfaces. With increase in the surfactant concentration, adsorption on the surface of reservoir materials particles increases until the saturation point is reached. With further increase in surfactant concentration, the adsorption is ascribed to the hydrophobic association of chain-chain interactions through van der Waals forces.



With increasing alkali concentration (pH) of the solution, the anionic surfactant adsorption on synthetic kaolin clay surface decreases on account of an increase in the electrostatic repulsive forces among the adsorbent and the adsorbed surfactant molecules whereas the contrary occurs when cationic surfactant is used.

With the addition of NaCl salt to the surfactant solution, the adsorption of anionic surfactants (SDS and SEMES) on synthetic kaolin clay surface increases owing to the low electrostatic repulsion between the adsorbed surfactant species and the reservoir material surface. While an opposite trend was observed in the adsorption plateau of the cationic surfactant (CTAB). Thus, these facts suggest that the adsorption capacity of anionic surfactant is favored by increase in salinity while the adsorption capacity of cationic surfactant is favored by increase in alkalinity of the system at ambient temperature.

In reservoirs or soils containing mineral surface with a net negative surface charge, anionic surfactants have a preference owing to the fact that the electrostatic repulsion between the mineral surface and the surfactant head-group help to reduce adsorption. In the same way, cationic surfactants are favored for use in reservoirs with a positive net surface charge. The mixed equimolar surfactant systems showed more complex behavior compared with single surfactant systems and resulted in co-adsorption of cationic with anionic surfactants onto the silica mineral. Crude oil reservoirs and aquifer soils are intrinsically multifaceted and comprise of diverse minerals which includes carbonates, silicates, aluminates, and different clays. The surface charge of all of these minerals differ with both hydrogen ion concentration and mineral type, which creates a substrate that has areas of positive charge and areas of negative charge. In these circumstances, it is challenging to avoid significant surfactant adsorption when utilizing either anionic or cationic surfactants.

The sodium epoxidized methyl ester sulfonate demonstrated good surface thermal stability at reservoir temperature (500 °C), with approximately only 10% mass loss recorded. Furthermore, the sodium epoxidized methyl ester demonstrated a comparable thermal stability at reservoir temperature compared to sodium dodecyl sulfate. The results obtained demonstrate the prospect of developing cheap surfactants from waste vegetable oils to replace petrochemical-based surfactants. The main attraction of the formulated sodium epoxidized methyl ester sulfonate (SEMES) is the low production cost in comparison to the commercial grade of methyl ester sulfonate and sodium dodecyl sulfate. SEMES is a potential candidate as a durable cost-effective inducement to substitute sodium dodecyl sulfate and other commercial surfactants for EOR uses.

## 6.2 RECOMMENDATIONS

Based on the general findings reported in the current study, investigations that would aid in the further improvement of the production of high performance surfactant from Sustainable Feedstock for Application in Alkaline-Surfactant-Polymer Flooding are highlighted in the following sections:

**1. Catalyst Reusability:** The data obtained from the current study demonstrated that the  $\text{CaO}/\text{Al}_2\text{O}_3$  catalyst can be successfully re-used with only minimal loss in activity. Evidence suggests that additional runs (tests) should be conducted to confirm that the catalyst does leach to the reaction mixture appreciably. Hence, there is a need for future work to investigate the re-usability of the solid catalyst to save cost.

**2. Investigation of the physical and chemical properties of the waste vegetable oils:** Results from this study indicated that the water content and viscosity of the WVO have a huge impact on the yield of FAME. Based on this, water content, viscosity, acid and saponification values should be determined and control to assure consistent quality of the oil feedstock.

**3. Adsorption of different anionic+cationic mixture ratios on other reservoir rock materials:** the co-adsorption experiment was limited to 50:50 anionic+cationic mixture on kaolin clay. The work need to be extended to adsorption of mixed surfactant systems at different molar ratios and on reservoir rock materials.

**4. Investigation of the interfacial tension (IFT) and critical micelle concentration of surfactants:** From the current study, it could be observed that when producing new surfactants, the determination of IFT and CMC are crucial factors. Further studies should consider the study of the capacity of the bio-based surfactant to decrease the IFT between crude oil and water during ASP flooding.

It is envisaged that this present research will open up new ways for production of bio-based surfactants and also provide a comprehensive insight into the management of these surfactants during chemical enhanced oil recovery processes. The inter-relatedness of the processes reported herein have potential for the production of a cost effective, nevertheless high performance surfactant for use in petroleum production industry.

## REFERENCES

- Abdallah, W., Buckley, J. S., Carnegie, A. and Edwards, J. (2007). Fundamentals of Wettability. *Oilfield Review*, 19, 2.
- Abdullah, B. M. and Salimon, J. (2010). Epoxidation of Vegetable Oils and Fatty Acids: Catalysts, Methods and advantages. *Journal of Applied Sciences*, 10, 1545–1553.
- Adkins, S., Liyanage, P.J., Arachchilage, G.W., Mudiyansele, T., Weerasooriya, U. and Pope, G. (2010). A New Process for Manufacturing and Stabilizing High Performance EOR Surfactants at Low Cost for High Temperature, High Salinity Oil Reservoirs. In *SPE Improved Recovery Symposium*. Tulsa, Oklahoma. Retrieved from SPE 129923
- Agarwal, M., Singh, K., Upadhyaya, S. and Chaurasia, S. P. (2012). Potential vegetable oils of Indian origin as biodiesel feedstock - An experimental study. *Journal of Scientific and Industrial Research*, 71(4), 285–289.
- Agbalaka, Chinedu, Dandekar, Abhijit, Patil, Shirish, Khataniar, Santanu and Hemsath, J. (2008). The Effect of Wettability on Oil Recovery: A Review. In *the SPE Asia & Gas Conference and Exhibition* (pp. 20–22). Perth, Australia: SPEJ. Retrieved from paper SPE 114496
- Ahmadi, M.A. and Shadizadeh, S. R. (2015). Experimental investigation of a natural surfactant adsorption on shale-sandstone reservoir rocks: Static and dynamic conditions. *Fuel*, 159, 15–26.  
<http://doi.org/http://dx.doi.org/10.1016/j.fuel.2015.06.035>
- Aladasani A. and Bai, B. (2010). Recent Developments and Updated Screening Criteria of Enhanced Oil Recovery Techniques." In *SPE 130726 presented at the CPS/SPE International Oil & Gas Conference and Exhibition*. (pp. 1–24). Beijing, China: Society of Petroleum Engineers.
- Al-Khafaji, A. H., Wang, F., Castanier, L. and Brigham, W. E. (1982). Steam Surfactant Systems at Reservoir Conditions. In *Paper SPE California Regional Meeting*. San Francisco, California.
- Akintayo, E. T. (2006). *Chemical Society of Ethiopia*, 20(1), 75–81.
- Aluyor, E. O., Obahiagbon, K. O. and Ori-jesu, M. (2009). Biodegradation of vegetable oils : A review. *Solutions*, 4(6), 543–548.
- Amin, N. A. S. A and Omar, W. N. N. W. (2011). Optimization of heterogeneous biodiesel production from waste cooking palm oil via response surface methodology. *Biomass and Bioenergy*, 35, 1329–38.
- Arihara, L., XiangGuo, Yoneyama, T. and Akita, Y. (1999). Oil Recovery Mechanisms of Alkali-Surfactant-Polymer Flooding. SPE, Waseda University, JNOC and Daqing Petroleum Institute.

- Arzamendi, G., Campoa, I., Arguinarena, E., Sanchez, M., Montes, M. and Gandia, L. M. (2007). Synthesis of biodiesel with heterogeneous NaOH/alumina catalysts: comparison with homogeneous NaOH. *Chemical Engineering Journal*, *134*, 123–130.
- Augustine, R. L. (1996). *Heterogeneous Catalysis for the Synthetic Chemist*. New York.
- Austad, T. and Milner, J. (2000). Surfactant Flooding in Enhanced Oil Recovery. Surfactants. In *Fundamentals and Applications in the Petroleum Industry* (pp. 203–250). UK: Cambridge University Press.
- Awang, M. and Seng, G. M. (2008). Sulfonation of phenols extracted from the pyrolysis oil of oil palm shells for enhanced oil recovery. *ChemSusChem*, *1*(3), 210–4. <http://doi.org/10.1002/cssc.200700083>
- Babajide, O. O., Petrik, L., Supervisors, C. and Ameer, F. (2011). Keywords Optimisation of Biodiesel Production via Different, (November).
- Babu, K., Maurya, N. K., Mandal, A. and Saxena, V. K. (2015). Synthesis and Characterization of Sodium Methyl Ester Sulfonate for Chemically-Enhanced Oil Recovery. *Brazilian Journal of Chemical Engineering*, *32*(03), 795–803.
- Babu, K., Pal, N., Bera, A., Saxena, V.K. and Mandal, A. (2015). Studies on interfacial tension and contact angle of synthesized surfactant and polymeric from castor oil for enhanced oil recovery. *Applied Surface Science*, *353*, 1126–1136. <http://doi.org/http://dx.doi.org/10.1016/j.apsusc.2015.06.196>
- Balakrishnan, K., Olutoye, M. A. and Hameed, B. H. (2013). Synthesis of methyl esters from waste cooking oil using construction waste material as solid base catalyst. *Bioresource Technology*, *128*, 788–91. <http://doi.org/10.1016/j.biortech.2012.10.023>
- Banerjee, A. and Chakraborty, R. (2009). Parametric sensitivity in transesterification of waste cooking oil for biodiesel production: A review. *Resources, Conservation and Recycling*, *53*, *9*, 490–497.
- Baran, J., Drozd, M., Gavrillko, T. A. and Styopkin, V. I. (2014). Structure, molecular dynamics, and thermotropic properties of stearic acid-ctab cationic surfactants with different molar ratios, *59*(3), 303–312.
- Barbosa, S. L., Dabdoub, M. J., Hurtado, G. R., Klein, S. I., Baroni, A. C. M. and Cunha, C. (2006). Solvent free esterification reactions using Lewis acids in solid phase catalysis. *Applied Catalysis A-General*, *313*(2), 146–150.
- Barnes, J. R., Smit, J. P. and Smit, J. R. (2003). Development of Surfactants for Chemical Flooding at Difficult Reservoir “Conditions”. “Conditions.” In *Shell Global Solutions*. Amsterdam, Netherlands; Retrieved from SPE 113313
- Barnwal, B. K and Sharma, M. P. (2005). Prospects of biodiesel production from vegetable oils in India. *Renewable and Sustainable Energy Reviews*, *9*, 363–78.
- Bastrzyk, A., Polowczyk, I., Szelag, E. and Sadowski, Z. (2012). Adsorption and co-adsorption of ppo-ppo-peo block copolymers and surfactants and their influence on

zeta potential of magnesite and dolomite. *Physicochemical Problems of Mineral Processing*, 48(1), 281.

- Behrens, E. J. (2013). Investigation of loss of surfactants during enhanced oil recovery applications - adsorption of surfactants onto clay materials, (June).
- Ben Shiau, B. J., Harwell, J. H., Lohateeraparp, P., Dinh, A.V., Roberts, B. L., Hsu, T. P. and Awuri, O. I. (2010). Designing Alcohol-Free Surfactant Chemical Flood for Oil Recovery'. *SPE Journal*.
- Bera, A., Kumar, T., Ojha, K. and Mandal, A. (2013). Adsorption of surfactants on sand surface in enhanced oil recovery: Isotherms, kinetics and thermodynamic studies. *Applied Surface Science*, 284(August 2015), 87–99.  
<http://doi.org/10.1016/j.apsusc.2013.07.029>
- Berchmans, H. J and Hirata, S. (2008). Biodiesel production from crude *Jatropha curcas* L. seed oil with a high content of free fatty acids. *Bioresource Technology*, 99, 1716–21.
- Berchmans, H. J., Morishita, K. and Takarada, T. (2010). Kinetic study of hydroxide-catalyzed methanolysis of *Jatropha curcas*-waster food oil mixture for biodiesel production. *Fuel Processing Technology*.
- Berger, P. D. and Lee, C. H. (2006). Improved ASP process using organic alkali. In *The SPE/DOE symposium on improved oil recovery*. Tulsa, Oklahoma. Retrieved from SPE 99581
- Bohmer, M. R. and Koopal, L. K. (1992). Adsorption of Ionic Surfactants on Variable-Charge Surfaces. In *1. Charge Effects and Structure of the Adsorbed Layer, Langmuir* (pp. 649–2659).
- Borges, M. E., Diaz, L., Alvarez-Galvan, M. C. and Brito, A. (2011). High performance heterogeneous catalyst for biodiesel production from vegetal and waste oil at low temperature. *Applied Catalysis B: Environmental*, 102, 310–5.
- Borugadda, V. B. and Goud, V. V. (2014). Epoxidation of Castor Oil Fatty Acid Methyl Esters (COFAME) as a Lubricant base Stock Using Heterogeneous Ion-exchange Resin (IR-120) as a Catalyst. *Energy Procedia*, 54(0361), 75–84.  
<http://doi.org/10.1016/j.egypro.2014.07.249>
- Bryan, J. and Kantzas, A. (2007). Enhanced heavy-oil recovery by alkali-surfactant flooding. In *SPE Annual Technical Conference and Exhibition*. Anaheim, California.
- Buhain, J. and Guo, M. (2007). Production of biodiesel from fresh vegetable oil and waste frying oil. *New Bio*.
- Cahn FRS, R. W. (2005). Concise Encyclopedia of Materials Characterization,. In *Elsevier Ltd Oxford* (2nd editio).
- Campanella, A. and Baltanas, M. A. (2006). Degradation of the oxirane ring of epoxidized vegetable oils in liquid–liquid heterogeneous reaction systems. *Chemical Engineering Journal. Eng. J.*, 118, 141–152.

- Campanella, A., Baltanas, M. A., Capel-Sanchez, M. C., Campos Martin, J. M. and Fierro, J. L. G. (2004). Soybean oil epoxidation with hydrogen peroxide using an amorphous Ti/SiO<sub>2</sub> catalyst. *Green Chem.*, *6*, 330–334.
- Campanella, A., Baltanas, M.A. and Fontanini, C. (2008). High yield epoxidation of fatty methyl esters with performic acid generated in-situ. *Chemical Engineering Journal*, *118*, 141–152.
- Campanelli, P., Banchemo, M. and Manna, L. (2010). Synthesis of biodiesel from edible, non- edible and waste cooking oils via supercritical methyl acetate transesterification. *Fuel Processing Technology*, *89*, 3675–82.
- Canakci, M. and Gerpen, J. V. (1999). Biodiesel production via acid-catalyst. No Title. *Trans. Autom. Sci. Eng.*, *42*, 1203–1210.
- Canakci, M. and Gerpen, J. V. (2003). A pilot plant to produce biodiesel from high free fatty acid feedstocks. *Trans. ASAE*, *46*, 945–954.
- Cappelletti, G., Bianchi, C. L. and Ardizzone, S. (2006). Xps study of the surfactant film adsorbed onto growing titania nanoparticles. *Applied Surface Science*, *253*(2), 519–524. <http://doi.org/http://dx.doi.org/10.1016/j.apsusc.2005.12.098>
- Carmona, M. (2014). The Role of Epoxidation On Camelina Sativa Biodiesel Properties, *16* (6), 1076–1084.
- Chan, K. S. and Shah, D. O. (n.d.). "The Molecular Mechanism for Achieving Low Interfacial Tension Minimum in a Petroleum Sulfonate/Oil/Brine System. In *Semi-Annual Report, Improved Oil Recovery Research Program*. University of Florida: Department of Chemical Engineering and Anesthesiology,.
- Chang, H. L., Zhang, Z. Q., Wang, Q. M., Xu, Z. S., Guo, Z. D., Sun H. Q., Cao, X. L. and Qiao, Q. (2006). Advances in Polymer Flooding and Alkaline/Surfactant/Polymer Processes as Developed and Applied in the People's Republic of China. *Journal of Petroleum Technology*, *58*, 84–89.
- Chavali, S., Lin, B., Miller, D. C. and Camarda, K. V. (2004). Environmentally benign transition metal catalyst design using optimization techniques. *Comp. Chem. Eng.*, *28*, 605.
- Cho, Y. B. and Seo, G. (2010). High activity of acid-treated quail eggshell catalyst in the transesterification of palm oil with methanol. *Bioresource Technology*, *101*, 8515–9.
- Clara, H., Larry, J. C., Lorenzo, A., Abel, B., Jie, Q., Phillip, C. D. and Malcolm, J. P. (2001). ASP system design for an offshore application in the La Salina field, Lake Maracaibo. In *SPE Latin American and Caribbean petroleum engineering conference*. Buenos Aires. Retrieved from SPE 69544
- Cullity, B. D. (1978). *Elements of X-ray Diffraction* (2nd editio). Addison Welsey, reading.
- Curbelo, F. D. S., Santanna, V. C., Neto, E. L. B., Dutra Jr., Dantas, T. N. C., Neto, A. A. D. and Garnica, A. I. C. (2007). Adsorption of nonionic surfactants in sandstones. *Colloids and Surfaces*, *293*, 1–4.

- Dandekar, A. Y. (2013). *Petroleum reservoir rock and fluid properties* (2nd editio). Boca Raton, FL: Taylor & Francis.
- Delshad, M., Han, C., Veedu, F. K. and Pope, G. A. (2013). A simplified model for simulations of alkaline–surfactant–polymer floods. *Journal of Petroleum Science and Engineering*, 108, 1.9.  
<http://doi.org/http://dx.doi.org/10.1016/j.petrol.2013.04.006>
- Demirbas, A. (2007). Biodiesel from sunflower oil in supercritical methanol with calcium oxide. *Energy Conversion Management*, 48, 937–941.
- Demirbas, A. (2008). Studies on cottonseed oil biodiesel prepared in non-catalytic SCF conditions. *Bioresoure Technology*, 99, 1125–30.
- Dennis, Y. C., Leung, X. W. and Leung, M. K. H. (2010). A review on biodiesel production using catalyzed transesterification. *Applied Energy*, 87, 1083–1095.
- Deshpande, P. S. (2013). Chapter 3 Epoxidation of oleic acid and vegetable oils : Synthesis , characterization and utilization as biolubricants and additives for plastics, (iv), 89–152.
- Devanesan, M. G., Viruthagiri, T. and Sugumar, N. (2007). Transesterification of Jatropha oil using immobilized *Pseudomonas fluorescens*. *African Journal of Biotechnology*, 6(21), 2497–2501.
- DeZabala, E. F. (1982). A Chemical Theory for Linear Alkaline Flooding". *SPE Journal*, 245–258.
- Di Serio, M., Tesser, R., Dimiccoli, M., Cammarota, F., Nasatasi, M., and Santacesaria, E. (2005). Synthesis of biodiesel via homogeneous Lewis acid catalysts. *J Mol Catal*, 239(January), 111–5.
- Di Serio, M., Tesser, R., Pengmei, L. and Santacesaria, E. (2008). Heterogeneous catalysts for biodiesel production. *Energy Fuels*, 22, 207–17.
- Dinda, S., Patwardhan, A. V., Goud, V. V. and Pradhan, N. C. (2008). Epoxidation of cottonseed oil by aqueous hydrogen peroxide catalyzed by liquid inorganic acids. *Bioresources Technology*, 99, 3737–3744.
- Donaldson, E. C. (2008). Wettability. Huston, Texas: Gulf Publishing Company.
- Dong, H. Z., Fang, S. F., Wang, D. M., Wang, J. Y., Liu, Z. and Hong, W. H. (2008). “Review of practical experience and Management by Polymer Flooding at Daqing.” In *SPE/DOE Symposium on Improved Oil Recovery*. Tulsa, Oklahoma.  
<http://doi.org/10.2118/114342-PA>
- Dorado, M. P., Ballesteros, E., Lopez, F. J. and Mittelbach, M. (2003). Optimization of Alkali-Catalyzed Transesterification of Brassica Carinata Oil for Biodiesel Production. *Energy and Fuels*, 18, (1), 77-83. *Energy and Fuels*, 18, (1), 77–83.

- Dossin, T. F., Reyniers, M. F., Berger, R. J. and Marin, G. B. (2006). Simulation of heterogeneously MgO-catalyzed transesterification for fine-chemical and biodiesel industrial production. *Appl Catal B: Environ*, 67, 136–48.
- Du, G., Tekin, A., Hammond, E. G. and Woo, L. K. 2004. (2004). Catalytic epoxidation of methyl linoleate. *Journal of American Oil Society*, 4, 477–480.
- Du, W., Xu, T. and Liu, D. (2003). Lipase catalyzed transesterification of soybean oil for biodiesel production during continuous batch operation. *Biotechnology Applied Biochemistry*, 38, 103–106.
- Dupuis, G., Rousseau, D., Tabary, R. and Grassl, B. (2010). “How to get the Best out of Hydrophobically Associative Polymers for IOR? New Experimental Insights.” In *2010 SPE Improved Oil Recovery Symposium* (pp. 1–12). Tulsa, Oklahoma: Society of Petroleum Engineers (SPE). Retrieved from SPE paper 129884
- Dwight Rust, S. W. (2008). A Market Opportunity Study Update, (December), 41.
- Eevera, T., Rajendran, K. and Saradha, S. (2009). Biodiesel production process optimization and characterization to assess the suitability of the product for varied environmental conditions. *Renewable Energy*, 34, 3, 762–765.
- Ehrlich, R and Wygal, R. J. (1977). “Interrelation of Crude Oil and Rock Properties with the Recovery of Oil by Caustic Waterflooding.” *SPE Journal*, (August), 263–270.
- Elraies, K. and Tan, I. M. and Saaid, I. (2009). Synthesis and Performance of a New Surfactant for, 3(1), 1–9.
- Elraies, K. A. and Tan, I. (2011). Design and Application of a New Acid-Alkali-Surfactant Flooding Formulation for Malaysian reservoirs No Title. In *SPE Asia Pacific Oil & Gas Conference and Exhibition*,. Bisbane. Retrieved from ,SPE 133005
- Elraies, K. A. and Tan, I. M. (2003). The Application of a New Polymeric Surfactant for Chemical EOR.
- Elraies, K. A., Tan, I. B. M. and Saaid, I. (2008). Synthesis and Performance of New Surfactant for Enhanced Oil Recovery. Malaysia: Geoscience and Petroleum and Chemical Engineering Department, Universiti Teknologi Petronas.
- Elraies, K. A., Tan, I., Fathaddin, M. and Abo-Jabal, A. (2011). Development of a New Polymeric Surfactant for Chemical Enhanced Oil Recovery. *Petroleum Science and Technology*, 29.
- Emegwalu, C. C. (2010). “Enhanced Oil Recovery for the Norne Field’s E-segment Using Surfactant Flooding.” NTNU.
- Emery, L. W., Mungan, N. and Nicholson, R. W. (1970). “Caustic Slug Injection in the Singleton Field.” *Journal of Petroleum Technology*, (December), 1569–1576.
- Enweremadu, C. C and Mbarawa, M. M. (2009). Technical aspects of production and analysis of biodiesel from used cooking oil -A review. *Renewable and Sustainable Energy Reviews*, (9 June), 2206–2219. <http://doi.org/10.1016/j.rser.2009.06.007>



- Espinoza Perez, J. D., Haagensohn, D. M., Pryor, S. W., Ulven, C. A. and Wiesenborn, D. P. (2009). Production and characterization of epoxidized canola oil. *American Society of Agricultural and Biological Engineers*, 52(4), 1289–1297. <http://doi.org/10.13031/2013.27772>
- Esteban, B., Riba, J. R., Baquero, G., Rius, A. and Puig, R. (2012). Temperature dependence of density and viscosity of vegetable oils. *Biomass and Bioenergy*, 42, 164–171. <http://doi.org/10.1016/j.biombioe.2012.03.007>
- Falls, A. H., Thigpen, D. R. and Nelson, R. C. (1992). “A Field Test of Co-surfactant-Enhanced Alkaline Flooding.” In *SPE/DOE 8th Symposium on Enhanced Oil Recovery*. Tulsa, Oklahoma, USA: OK. Retrieved from SPE 24117
- Fan, X. (2008). Optimization of Biodiesel Production from Crude Cottonseed Oil and Waste Vegetable Oil: Conventional and Ultrasonic Irradiation Methods. Graduate School of Clemson University.
- Farooqa, M., Ramlib, A. and Subbaraoa, D. (2013). Biodiesel production from waste cooking oil using bifunctional heterogeneous solid catalysts. *Journal of Cleaner Production*. Elsevier, (15 November), 131–140.
- Findlay, T. W., Swern, D. and Scanlan, J. T. (1945). Epoxidation of unsaturated fatty materials with peracetic acid in glacial acetic acid solution. *J Am Chem Soc*, 67, 412–4.
- Flaaten, A. K., Nguyen, Q. P., Pope, G. and Zhang, J. (2008). "A Systematic Laboratory Approach to Low-Cost, High-Performance Chemical Flooding. In *2008 SPE/DOE Improved Oil Recovery Symposium* (pp. 1–20). Tulsa, Oklahoma, USA: Society of Petroleum Engineers (SPE). Retrieved from SPE Paper 113469
- Fletcher, A. J. P. and Morrison, G. R. (2008). Developing a Chemical EOR Pilot Strategy for a Complex, Low Permeability Water Flood. In *2008 SPE/DOE Symposium on Improved Oil Recovery*. Tulsa, Oklahoma, USA: OK. Retrieved from SPE-112793
- Foster, N. C. and Hovda, K. (1997). . "Manufacture of Methyl Ester Sulfonates and other Derivatives, in Presentation Outlines of the Soaps. In *Detergents and Oleochemicals Conference/Exhibit*. AOCs Publication.
- Freedman, B., Pryde, E. and Mounts, T. (1984). Variables affecting the yields of fatty esters from transesterified vegetable oils. *Journal of the American Oil Chemists' Society*, 61(October), 1638–1643.
- French, W. H. (1971). In situ epoxidation process. Retrieved from US 3.360.531
- French, T. R. and Burchfield, T. E. (1990). “Design and Optimization of Alkaline Flooding Formulations.” In *SPE/DOE Seventh Symposium on Enhanced Oil Recovery*. Tulsa, Oklahoma, USA: OK. Retrieved from SPE 20238
- Fukuda, H. (2001). “Biodiesel fuel production by transesterification of oils.” *Journal of Bioscience and Bioengineering*, 92, 405–416.

- Gai, P. L. and B. E. D. (2003). *Electron Microscopy in Heterogeneous Catalysis*. Philadelphia: Institute of Physics Series in Microscopy in Materials Science.
- Galadima, A. and Garba, Z. N. (2009). Catalytic Synthesis of Ethyl Ester from Some Common Oils. *Science World Journal*, 4, 1597–6343. Retrieved from ISSN
- Gamage, P. K., O'Brien, M., & Karunanayake, L. (2009). Epoxidation of some vegetable oils and their hydrolysed products with peroxyformic acid - Optimised to industrial scale. *Journal of the National Science Foundation of Sri Lanka*, 37(4), 229–240. <http://doi.org/10.4038/jnsfsr.v37i4.1469>
- Gan, L. H., Goh, S. H. and Ooi, K. S. (1992). Kinetic studies of epoxidation and oxirane cleavage of palm olein methyl esters. *Journal of American Chemist's Society*, 69, 347–351.
- Gan-Zuo, L., Jian-Hai, M., Ying, L., and Shi-Ling, Y. (2000). "An experimental study of alkaline/surfactant/polymer flooding systems using natural mixed carboxylate." *Colloids Surf. A*, 173, 219–229.
- Georgogianni, K. G., Katsoulidis, A. K., Pomonis, P. J., Manos, G. and Kontominas, M. G. (2009). Transesterification of rapeseed oil for the production of biodiesel using homogeneous and heterogeneous catalysis. *Fuel Processing Technology*, 90, 1016–22.
- Geus, J. W. and van Veen, J. R. (1999). *An Integrated Approach to Homogeneous, Heterogeneous and Industrial Catalysis*. Elsevier, 467.
- Goodhew, P. J., Humphreys, J. and Beanland, R. (2001). *Microscopy and Analysis* (3rd Editio). London: Taylor & Francis.
- Goud, V. V., Patwardhan, A. V. and Pradha, N. C. (2007). Kinetics of in-situ epoxidation of natural triglycerides catalyzed by acidic ion exchange resin. *Ind. Eng. Chem. Res.*, 46, 3078–3085.
- Goud, V. V., Patwardhan, A. V. and Pradhan, N. C. (2006). Studies on the epoxidation of mahua oil (*Madhumica indica*) by hydrogen peroxide. *Bioresource Technology*, 97, 1365–1371.
- Greaser, G. R. and O. J. R. (2001). "New Thermal Recovery Technology and Technology Transfer for Successful Heavy Oil Development." In *2001 SPE International Thermal Operations and Heavy Oil Symposium*. Porlamar, Margarita Island, Venezuela. Retrieved from SPE 69731
- Green, D. W. and Willhite, G. P. (1998). *Enhanced Oil Recovery*. Society of Petroleum Engineers Richardson. Teas, USA.
- Gregorio, C. G. (2005a). *Fatty Acids and Derivatives from Coconut Oil* (6th ed.). Bailey's Industrial Oil and Fat Products.
- Gregorio, C. G. (2005b). *Fatty Acids and Derivatives from Coconut Oil* (6th Editio). Bailey's Industrial Oil and Fat Products.

- Guidotti, M., Psaro, R., Sgobba, M. and Ravasio, N. (2007). *Catalysis for Renewables: From Feedstock to Energy Production*. WILEY-VCH Verlag GmbH & Co.  
<http://doi.org/10.1002/9783527621118>
- Gunstone, F. D. (1997). Epoxidized oils. In *Lipid Technologies and Applications*. In B. Raton (Ed.), . CRC Press.
- Guo, W. K. (2000). “Commercial Pilot Test of Polymer Flooding in Daqing Oil Field.” In *2000 SPE/DOE Improved Oil Recovery Symposium*. Tulsa, Oklahoma, USA.  
 Retrieved from SPE 59275
- Gupta, R. and Mohanty, K. K. (2010). Temperature effects on surfactant-aided imbibition into fractured carbonates. *SPE Journal*, 15, 3, 588–597. Retrieved from SPE paper 110204
- Haber, J., Block, H. J. and Delmon, B. (1995). “Manual of Methods and Procedures for Catalyst Characterization.” *Pure and Applied Chemistry Journal*, 67(8-9), 1257–1306.
- Han, M., Xiang, W., Jiang, W. and Sun, F. (2006). “Application of EOR Technology by Means of Polymer Flooding in Bohai Oil Field.” In *International Oil & Gas Conference and Exhibition*. Beijing, China.
- Hang, X. and Yang, H. (1999). Model for a cascade continuous epoxidation process. *Journal of American Oil Chemistry Society*, 76, 89–92.
- Hanna, H. S. and Somasundaran, P. (n.d.). *Physico-Chemical Aspects of Adsorption at Solid/Liquid Interfaces: II- Mahogany sulfonate/Berea Sandstone, Kaolinite,* “*Improved Oil Recovery by Surfactant and Polymer Flooding*. (R. S. Shah, D. O., and Schechter, Ed.). New York: Academic Press, Inc.
- Hara, M. (2009). Environmentally benign production of biodiesel using heterogeneous catalysts T. *Chemical Engineering Communications*, 2(2), 129–35.
- Hattori, H. (2001). Solid base catalysts: generation of basic sites and application to organic synthesis. *Applied Catalysis A: General*, 222(1-2), 247–259.
- Hawash, S., El Diwani, G. and Abdel Kaber, E. (2011). Optimization of Biodiesel Production from Jatropha Oil by Heterogeneous Base Catalyst Transesterification. *International Journal of Engineering Science and Technology ( IJEST)*,  
<http://doi.org/0975-5462>
- Hayyan, A., Alam M. Z., Mirghani, M. E. S., Kabbashi, N. A., Hakimi, N. I. and Siran, Y. M. (2010). Sludge palm oil as a renewable raw material for biodiesel production by two-step processes. *Bioresource Technology*, 101, 7804–11.
- Hayyan, A., Alam, M., Mirghani, M., Kabbashi, N., Hakimi, N., Siran, Y. and Tahiruddin, S. (2010). Production of biodiesel from Sludge Palm Oil by Esterification Process. *Journal of Energy and Power Engineering*, 4, 13–14.

- Helwani, Z., Othman, M. R., Aziz, N., Fernando, W. J.N. and Kim, J. (2009). Technologies for production of biodiesel focusing on green catalytic techniques: A review. *Fuel Processing Technology*, 90, 1502–1514.
- Hermans, L. A. M. and Geus, J. W. (1979). *Preparation of Catalysts II*. Amsterdam, Netherlands: Elsevier Ltd.
- Highina, B. I., Bugajel, I. M. and Umar, B. (2011). Biodiesel production from *Jatropha caucous* oil in a batch reactor using zinc oxide as catalyst. *Journal of Petroleum Technology and Alternative Fuels*, 146–149.
- Hill, K. (2001). Fats and Oils as Oleochemical Raw Materials. *Journal of Oleo Science*, 50(5), 433–444. <http://doi.org/10.5650/jos.50.433>
- Hindryawati, N., Maniam, G. P., Karim, M. R. and Chong, K. F. (2014). Transesterification of used cooking oil over alkali metal (Li, Na, K) supported rice husk silica as potential solid base catalyst. *Engineering Science and Technology, an International Journal*, 17(2), 95–103. <http://doi.org/10.1016/j.jestch.2014.04.002>
- Hirasaki, G. J. and Zhang, D. L. (2003). “Surface Chemistry of Oil Recovery from Fractured, Oil-Wet, Carbonate Formations.” In *SPE International Symposium on Oilfield Chemistry*. Houston, Texas.
- Holmberg, K., Jönsson, B., Kronberg, B. and L. B. (2003). *Surfactants and Polymers in Aqueous Solution* (2nd ed.). Chichester, New York: Wiley.
- Hongping, H., Ray, F. L. and Jianxi, Z. (2004). Infrared study of HDTMA<sup>+</sup> intercalated montmorillonite. *Spectrochimica Acta Part A: Molecular and Biomolecular Spectroscopy*, 60(12), 2853–2859. <http://doi.org/10.1016/j.saa.2003.09.028>
- Hosna Talebian, S., Mohd Tan, I., Sagir, M. and Muhammad, M. (2015). Static and dynamic foam/oil interactions: Potential of CO<sub>2</sub>-philic surfactants as mobility control agents. *Journal of Petroleum Science and Engineering*, 135, 118–126. <http://doi.org/http://dx.doi.org/10.1016/j.petrol.2015.08.011>
- Hou, S. (2001). Study of the Effect of ASP Solution Viscosity on Displacement Efficiency. In *2001 SPE annual technical conference and exhibition*. New Orleans, LA. Retrieved from SPE 71492
- Hovda, K. (1996). “Sulfonation of Fatty Acid Esters.” USA.
- Hsu, A., Jones, K. C., Foglia, T. A. and Marmer, W. N. (2004). Continuous production of ethyl esters of grease using an immobilized lipase. *Journal of American Oil Chemical Society*, 81(8), 749–752.
- Imelik, B. and Vadrine, J. C. (1994). *Catalyst Characterization: Physical Techniques for solid materials*. New York: Plenum Press.
- Inagaki, T. (2001). Development of a-Sulfo fatty acid esters. In *Proceedings World Conference on Oleochemicals*. Kuala Lumpur, Malaysia.
- Ishiguro, T., Ogushi, T., Ishiwada, Y. and Asahara, T. (1965). No Title, 14, 284.

- Ivanova, N. I., Volchkova, I. L. and Shchukin, E. D. (1995). No Title. *Colloids Surfaces-A*, 101, 239.
- Ivonete, P. G., Maria, A., Luvizotto, J. M. and Lucas, E. F. (2007). Polymer flooding: A sustainable enhanced oil recovery in the current scenario. Buenos Aires, Argentina.
- Jackson, A. C. (2006). Experimental Study of the Benefits of Sodium Carbonate on Surfactants for Enhanced Oil Recovery. Texas, USA: University of Texas at Austin.
- Jacobson, K., Gopinath, R., Meher, L. C. and Dalai, A. K. (2008). Solid acid catalyzed biodiesel production from waste cooking oil. *Applied Catalysis B: Environmental*, 85, 86–91.
- Janaun J. and Ellis, N. (2010). Perspectives on biodiesel as a sustainable fuel. *Renewable and Sustainable Energy Reviews*, 14, 1312–1320.
- Jiang, T., Hirasaki, G.J. and Miller, C. A. (2010). Characterization of kaolinite  $\zeta$  potential for interpretation of wettability alteration in diluted bitumen emulsion separation. *Energy & Fuels*, 24(4), 2350–2360. <http://doi.org/10.1021/ef900999h>
- Kamari, A., Sattari, M., Mohammadi, A.H. and Ramjugernath, D. (2015). Reliable method for the determination of surfactant retention in porous media during chemical flooding oil recovery. *Fuel*, 158, 122–128. <http://doi.org/http://dx.doi.org/10.1016/j.fuel.2015.05.013>
- Karimov, A. (2011). Impact of Wettability Alteration on Recovery Factor.
- Karlheinz, H. (2000). “Fats and oils as oleochemical raw materials.” *Pure Applied Chemistry*, 72, 1255–1264.
- Kaufmam. (1990). *International News on Fats Oils and Related Materials*, 1, 1034.
- Kemp, W. H. (2006). *Biodiesel Basics and Beyond: A Comprehensive Guide to Production and Use for the Home and Farm*. Ontario, Canada: Aztext Press.
- Kim, H. J., Kang, B. S., Kim, M. J., Park, Y. M., Kim, D. K., Lee, J. S. and Lee, K. Y. (2004). Transesterification of vegetable oil to biodiesel using heterogeneous base catalyst. *Catalysis Today*, 93-95, 315–320.
- Klass, M. and Warwel, S. (1995). Complete and partial epoxidation of plant oils by lipase-catalysed perhydrolysis. *Industrial Crops and Products*.
- Ko, S. O., Schlautman, M. A. and Carraway, E. R. (1998). Partitioning of hydrophobic organic compounds to sorbed surfactants. 1. Experimental studies. *Environmental Science Technology*, 32, 2769–2775.
- Kondamudi, N., Mohapatra, S. K. and Misra, M. (2011). Quintinite as a bifunctional heterogeneous catalyst for biodiesel synthesis. *Applied Catalysis A: General*, 393(1-2), 36–43. <http://doi.org/10.1016/j.apcata.2010.11.025>

- Kongyai C., C. B. and H. M. (2013). Epoxidation of waste used-oil biodiesel: Effect of reaction factors and its impact on the oxidative stability. *Korean Journal Chemical Engineering*, 30, 327–336.
- Kotwal, M. S., Niphadkar, P. S., Deshpadkar, S. S., Bokade, V. V. and Joshi, P. N. (2009). Transesterification of sunflower oil catalyzed by fly ash-based solid catalysts. *Fuel*, 88, 1773–1778.
- Krumrine, P. H., Falcone, J. S. and Campbell, T. C. (1982). “Surfactant Flooding 1: The Effect of Alkaline Additives on IFT, Surfactant Adsorption, and Recovery Efficiency.” *SPE Journal*, (August), 503–513.
- Kulkarni, M. G. and Dalai, A. K. (2006). Waste cooking oils - an economical source for biodiesel: A Review. *Ind. Eng. Chem. Res.*, 45, 2901–2913.
- Kumari, V., Shah, S. and Gupta, M. N. (2007). Preparation of biodiesel by lipase catalyzed transesterification of high free fatty acid containing oil from *Madhuca indica*. *Energy and Fuels*, 21, 368–372.
- Lake, L. W. (2011). *Enhanced Oil Recovery*. Englewood Cliffs, New Jersey: Prentice-Hall.
- Langmuir. (1916). The Constitution and Fundamental Properties of Solids & Liquids. *Journal of American Chemist's Society*, 38(11), 2221–2295.
- Lashkarbolooki, M., Ayatollahi, S. and Riazi, M. (. (2014). The impacts of aqueous ions on interfacial tension and wettability of an asphaltenic–acidic crude oil reservoir during smart water injection. *Journal of Chemical & Engineering Data*, 59(11), 3624–3634. <http://doi.org/10.1021/je500730e>
- Lathi, P. and Mattiasson, B. (2007). “Green approach for the preparation of biodegradable lubricant base stock from epoxidized vegetable oil”. *Applied Catalysis B: Environmental*, 69, 207–212.
- Lee, H. V., Juan, J. C., Binti Abdullah, N. F., Nizah Mf, R. and Taufiq-Yap, Y. H. (2014). Heterogeneous base catalysts for edible palm and non-edible *Jatropha*-based biodiesel production. *Chemistry Central Journal*, 8(1), 30. <http://doi.org/10.1186/1752-153X-8-30>
- Lee, S., Posarac, D. and Ellis, N. (2012). An experimental investigation of biodiesel synthesis from waste canola oil using supercritical methanol. *Fuel*, 91, 229–37.
- Leung, D. Y. C., Wu, X. and Leung, M. K. H. (2010). A review on biodiesel production using catalyzed transesterification. *Applied Energy*, 87(4), 1083–95.
- Levitt, D. B. (2006). “Experimental Evaluation of High Performance EOR Surfactants for a Dolomite Oil Reservoir.” Austin, Texas: The University of Texas at Austin.
- Li, H. (2004). IR Studies of the Interaction of Surfactants and Polyelectrolytes Adsorbed on TiO<sub>2</sub> Particles. Tianjin, China.

- Li, G., Mu, J., Li, Y. and Yuan, S. (2000). *An experimental study on alkaline/surfactant/polymer flooding systems using nature mixed carboxylate, Colloids and Surfaces A: Physicochemical and Engineering Aspects.*
- Liljeblad, J. (2006). "Quaternary Ammonium Surfactants Adsorbed at the Solid-Liquid Interface A VSFS-Study." Stockholm.
- Lingfeng, C., Guomin, X., Bo, X. and Guangyuan, T. (2007). Transesterification of cotton seed oil to biodiesel using heterogeneous solid basic catalysts. *Energy Fuels*, 21, 3740–3743.
- Liu, S. (2008). Alkaline Surfactant Polymer Enhanced Oil Recovery Process. Houston, Texas: Rice University.
- Liu, S, Li, R. F., Miller, C. A. and Hirasaki, G. J. (n.d.). "Alkaline/Surfactant/Polymer Processes: Wide Range of Conditions for Good Recovery." No Title. *SPE Journal*, 15(2), 282–293. Retrieved from SPE-113936-PA
- Liu, S., Zhang, D. L., Yan, W., Puerto, M., Hirasaki, G. J. and Miller, C. A. (2008). "Favourable Attributes of Alkali-Surfactant-Polymer Flooding." *SPE Journal*, 13(1), 5–16. <http://doi.org/10.2118/99744-PA>
- Liu, X., He, H., Wang, Y. and Zhu, S. (2007). Transesterification of Soybean oil to biodiesel as a solid base catalyst. *Catalysis Communication*, 8, 1107–1111.
- Lu, J., Goudarzi, A., Chen, P., Kim, D.H., Delshad, M., Mohanty, K.K., Sepehrnoori, K., Weerasooriya, U.P. and Pope, G. A. (2014). Enhanced oil recovery from high-temperature, high-salinity naturally fractured carbonate reservoirs by surfactant flood. *Journal of Petroleum Science and Engineering*, 124, 122–131. <http://doi.org/http://dx.doi.org/10.1016/j.petrol.2014.10.016>
- Lyons, W. and Plisga, B. S. (2005). *Standard Handbook of Petroleum & Natural Gas Engineering* (2nd ed.). Burlington, MA: Elsevier Inc.
- M. Saifuddin, P. E. Goh, W. S. and Ho, K. M. M. (2014). Biodiesel Production From Waste Cooking Palm Oil and Environmental Impact Analysis. *Bulgarian Journal of Agricultural Science*, 20(1), 186–192.
- Ma, K. (2013). Transport of Surfactant and Foam in Porous Media for Enhanced Oil Recovery Processes.
- Ma, F. and Hanna, M. A. (1999). Biodiesel production: a review. *Bioresource Technology*, 70(1), 1–15.
- Ma, K., Cui, L., Dong, Y., Wang, T., Da, C., Hirasaki, G. J. and Biswal, S. L. (2013). Adsorption of cationic and anionic surfactants on natural and synthetic carbonate materials. *Journal of Colloid and Interface Science*, 408(1), 164–172. <http://doi.org/10.1016/j.jcis.2013.07.006>
- Maheshwari, Y. K. (2011). Comparative Simulation Study of Chemical EOR Methodologies (Alkaline, Surfactant and/or Polymer) Applied to Norne Field E-Segment. Trondheim: NTNU.

- Mannhardt, K. (1988). "Modeling adsorption of Foam-Forming surfactant. *Revue del'Institut Francais Du Petrol*, 43(5), 659–671.
- Manrique E., Thomas C., Ravikiran R., Izadi M., Lantz M., R. J. and A. V. (2010). "EOR: Current Status and Opportunities." In *2010 SPE Improved Oil Recovery Symposium* (pp. 1–21). Tulsa, Oklahoma, U. S.A: Society of Petroleum Engineers (SPE). Retrieved from SPE Paper 130113
- Marchetti, J. M., Miguel, V. U. and Errazu, A. F. (2007). Heterogeneous esterification of oil with high amount of free fatty acids. *Fuel*, 86, 906–910.
- Martínez, A., Prieto, G. and Rollán, J. (2009). "Nanofibrous  $\gamma$ -Al<sub>2</sub>O<sub>3</sub> as support for Co-based Fischer-Tropsch catalysts: Pondering the relevance of diffusional and dispersion effect on catalytic performance." *Journal of Catalysis*, 263, 292–305.
- Math, M. C., Kumar, S. P. and Chetty, S. V. (2010). Technologies for biodiesel production from used cooking oil – a review. *Energy for Sustainable Development*, 14, 339–45.
- Mattingly, B., Manning, P., Voon, J., Himstedt, H. and Clausen, E., Popp, M. (2004). Comparative esterification of agricultural oils for biodiesel blending: Final Report Award Number MBTC-2052. Mack Blackwell Transportation Centre.
- Mayer, E. H., Berg, R. L., Carrnichale, J. D. and Weinbrandt, R. M. (1983). Alkaline injection for enhanced oil recovery - a status report. Tulsa, USA. Retrieved from SPE 8848
- Mazzocchia, C., Modica, G., Kaddouri, A. and Nannicini, R. (2004). Fatty acid methyl esters synthesis from triglycerides over heterogeneous catalysts in the presence of microwaves. *CR Chim*.
- Meher, L. C., Vidya Sagar, D. and Naik, S. N. (2006). Technical aspects of biodiesel production by transesterification" a review. *Renewable and Sustainable Energy Reviews*, 10, 248–268.
- Mehta, S. K., Chaudhary, S., Bhasin, K. K., Kumar, R. and Aratono, M. (2007). Conductometric and spectroscopic studies of sodium dodecyl sulfate in aqueous media in the presence of organic chalcogen. *Colloids and Surfaces A: Physicochemical and Engineering Aspects*, 304(1-3), 88–95. <http://doi.org/10.1016/j.colsurfa.2007.04.031>
- Milner, J. A. T. (1996). *Chemical Flooding of Oil Reservoirs 7. Oil Exclusion by Spontaneous Imbibition of Brine with and without Surfactant in Mixed-Wet, Low Permeability Chalk Material*.
- Mohadesi, M., Hojabri, Z. and Moradi, G. (2014). Biodiesel production using alkali earth metal oxides catalysts synthesized by sol-gel method. *Biofuel Research Journal* /, 2012–2015.
- Mohan, K. (2009). Alkaline Surfactant Flooding for Tight Carbonate Reservoirs. In *The Annual Technical Conference and Exhibition*. New Orleans. Retrieved from SPE 129516



- Morikawa, K., Shirasaki, T. and Okada, M. (1967). *Advances in Catalysis and related subjects, vol. 20*. New York: New York: Academic Press.
- Morrow, N. R. (1990). Wettability and Its Effect on Oil Recovery. New Mexico Institute Of Mining and Technology: Society of Petroleum Engineers (SPE). Retrieved from SPE 21621
- Muherei, M. A. (2009). Equilibrium Adsorption Isotherms of Anionic, Nonionic Surfactants and Their Mixtures to Shale and Sandstone. *Modern Applied Science*, 3, 2.
- Mul, G. and Hirschon, A. S. (2001). Effect of preparation procedures on the activity of supported palladium/lanthanum methanol decomposition catalysts. *Catalysis Today*, 65(1), 69–75.
- Mushtaq, A., Ajab, K. M., Muhammad, Z. and Shazia, S. (2011). Biodiesel from Non Edible Oil Seeds: a Renewable Source of Bioenergy. *Economic Effects of Biofuel Production, 2005*. <http://doi.org/17887>
- Mushtaq, M., Tan, I. B., Devi, C. and Majidaie, S. (2011). Epoxidation of Fatty Acid Methyl Esters derived from Jatropha Oil. Department of Chemical Engineering. Tronoh, Perak, Malaysia.: Department of Geosciences and Petroleum Engineering, Universiti Teknologi Petronas.
- Nakama, Y., Harusawa, F. and Murotani, I. (1990). Cloud Point Phenomena in Mixtures of Anionic and Cationic Suffactants in Aqueous Solution, 717–721.
- Nasr-El-Din, H. A., Hawkins, B. F. and Green, K. A. (1992). Recovery of Residual Oil Using the Alkaline/Surfactant/Polymer Process: Effect of Alkali Concentration. *Journal of Petroleum Science and Engineering*, 6, 381–388.
- Nelson, R. C., Lawson, J. B., Thigpen, D. R. and Stegemeier, G. L. (1984). “Co-Surfactant Enhanced Alkaline Flooding. *SPE Journal*. Retrieved from SPE 12672
- Neth, C. (1964). *No Title*. (6th ed.). Henkel & Cie. Appl.
- Ngamcharussrivichai, C., Nunthasanti, P., Tanachai, S. and Bunyakiat, K. (2010). Biodiesel production through transesterification over natural calciums. *Fuel Processing Technology*, 91, 1409–1415.
- Nielsen, P. M., Brask, J. and Fjerbaek, L. (2008). Enzymatic biodiesel production: technical and economical considerations. *European Journal of Lipid Science Technology*, 110, 692–700.
- Okieimen, F. E., Bakare, O. I. and Okieimen, C. O. (2002). Studies on the epoxidation of rubber seed oil. *Industrial Crops and Products*, 15(2), 139–144. [http://doi.org/10.1016/S0926-6690\(01\)00104-2](http://doi.org/10.1016/S0926-6690(01)00104-2)
- Olajire, A. A. (2014). Review of ASP EOR (alkaline surfactant polymer enhanced oil recovery) technology in the petroleum industry: Prospects and challenges. *Energy*, 77, 963–982. <http://doi.org/http://dx.doi.org/10.1016/j.energy.2014.09.00>

- Olsen, D. K., Hicks, M. D., Hurd, B. G., Sinnokrot, A. A. and Sweigart, C. N. (1990). "Design of a Novel Flooding System for an Oil-Wet Central Texas Carbonate Reservoir." In *SPE Seventh Symposium on Enhanced Oil Recovery*. Tulsa, Oklahoma, U. S.A: OK. Retrieved from SPE20224
- Pages, X. and Alfos, C. (2001). Synthesis of new derivatives from vegetable sunflower oil methyl esters via epoxidation and oxirane opening. *OCL-OL CORP*, 8(2), 122–125.
- Paria, S., Manohar, C. and Khilar, K. C. (2004). Effect of cationic surfactant on the adsorption characteristics of anionic surfactant on cellulose surface. *Colloids and Surfaces A: Physicochemical and Engineering Aspects*, 232(2-3), 139–142. <http://doi.org/10.1016/j.colsurfa.2003.10.016>
- Paria, S. and Khilar, K. C. (2004). Review on Experimental Studies of Surfactant Adsorption at the Hydrophilic Solid-Water Interface. In *Advances in Colloid and Interface Science* (pp. 75–95).
- Pashley, R. M. and Karaman, M. E. (2004). *Applied Colloid and Surface Chemistry*. England: John Wiley & Sons.
- Pasupulety, N., Gunda, K., Liu, Y., Rempel, G. L. and Ng, F. T. T. (2013). Production of biodiesel from soybean oil on CaO/Al<sub>2</sub>O<sub>3</sub> solid base catalysts. *Applied Catalysis A: General*, 452, 189–202. <http://doi.org/10.1016/j.apcata.2012.10.006>
- Patil, P., Deng, S., Rhodes, J. I. and Lammers, P. J. (2010). Conversion of waste cooking oil to biodiesel using ferric sulfate and supercritical methanol processes, 89, 360–4.
- Pei, X.M., Yu, J.J., Hu, X. and Cui, Z. G. (2014). Performance of palmitoyl diglycol amide and its anionic and nonionic derivatives in reducing crude oil/water interfacial tension in absence of alkali. *Colloids and Surfaces A: Physicochemical and Engineering Aspects*, 444, 269–275. <http://doi.org/http://dx.doi.org/10.1016/j.colsurfa.2013.12.068>
- Perego, C. and Villa, P. (1997). Catalyst preparation methods. *Catalysis Today*, 292–294.
- Peterson, G. R and Scarrah, W. P. (1984). Rapeseed oil transesterification by heterogeneous catalysis. *Journal of the American Oil Chemists' Society*, 61, 1593–7.
- Pethkar, A.V. and Paknikar, K. M. (1998). Recovery of gold from solution using *Cladosporioides* biomass beads. *Journal of Biotechnology*, 63, 211–220.
- Piazza, G. J., Nunez, A. and Foglia, T. A. (1998). "Hydrolysis of Mono-and Diepoxyoctadecanoates by Alumina." *Journal of American Oil Chemistry Society*, 110, 6492–6497.
- Piispanen, P. S. (2002). *Synthesis and Characterization of Surfactants Based on Natural Products*.
- Pingping, S., Jialu, W., Shiyi, Y., Taixian, Z. and Xu, J. (2009). Study of Enhanced-Oil-Recovery Mechanism of Alkali/Surfactant/Polymer Flooding in Porous Media from Experiments. *SPE Journal*, 14, 237–244.

- Pitts, M. J. Dowling, P., Wyatt, K., Surkalo, H. and Adams, C. (2006). Alkaline-Surfactant-Polymer Flood of the Tanner Field. In *SPE/DOE Symposium on Improved Oil Recovery*. Tulsa, USA: OK. Retrieved from SPE-100004
- Ponce F, R.V., Carvalho, M. S. and Alvarado, V. (2014). Oil recovery modeling of macro-emulsion flooding at low capillary number. *Journal of Petroleum Science and Engineering*, 119, 112–122.  
<http://doi.org/http://dx.doi.org/10.1016/j.petrol.2014.04.020>
- Pope, G. A., Sahni, V., Dean, R. M., Britton, C., Kim, D. H. and Weerasooriya, U. (2010). The Role of Co-Solvents and Co-Surfactants in Making Chemical Floods Robust' SPE. *SPE Journal*.
- Pratap, M. and Gauma, M. S. (2004). Field Implementation of Alkaline-Surfactant-Polymer (ASP) Flooding: A maiden effort in India. In *The Asia Pacific Oil and Gas Conference and Exhibition*. Perth. Retrieved from SPE 88455
- Puerto, M. Hirasaki, G. J. and Miller, C. A. (2010). “Surfactant Systems for EOR in High-Temperature, High-Salinity Environment.” In J. R. Barnes (Ed.), *SPE Improved Oil Recovery Symposium* (pp. 24–28). Tulsa Oklahoma, USA: Shell Global Solutions International B.V. Retrieved from SPE 129675
- Pye, D. (1964). Improved Secondary Recovery by Control of Water Mobility. *Journal of Petroleum Technology*, (August).
- Qiang, L., Mingzhe, D., Shanzhou, M. and Yun, T. (2006). “Surfactant enhanced alkaline flooding for Western Canadian heavy oil recovery.” *Colloids and Surfaces A: Physicochemical and Engineering Aspects*, 293, 63–71.
- Qiao, Q., Gu, H., Li, D. and Dong, L. (2000). The Pilot Test of ASP (Alkaline/Surfactant/Polymer Flooding) Combination Flooding In Karamay Oil Field. In *SPE Oil & Gas International Conference*. Beijing, China. Retrieved from SPE-64726
- Qiao, W., Cui, Y., Zhu, Y. and Cai, H. (2012). Dynamic interfacial tension behaviors between guerbet betaine surfactants solution and daqing crude oil. *Fuel*, 102, 746–750. <http://doi.org/http://dx.doi.org/10.1016/j.fuel.2012.05.046>
- Quesada-Medina, J. and Olivares-Carrillo, P. (2011). Evidence of thermal decomposition of fatty acid methyl esters during the synthesis of biodiesel with supercritical methanol. *The Journal of Supercritical Fluids*, 56, 56–63.
- Qutubuddin, S., Miller, C.A., and Benton, W.J. (1985). Effects of polymers, electrolytes, and pH on microemulsion phase behavior, in Macro- and Microemulsions. *American Chemical Society Symposium Series*, 272, 223–251.
- Ramakrishnan, T. S. and Wasan, D. T. (1983). “A Model for Interfacial Activity of Acidic Crude Oil/Caustic Systems for Alkaline Flooding.” *SPE Journal*, (August), 602–612.
- Rangarajan, B., Havey, A., Grulke, E. A. and Culnan, P. D. (1995). Kinetic parameters of a two phase model for in-situ epoxidation of soybean oil. *Journal of American Oil Chemistry Society*, 1161–1169.

- Rao, D. N., Ayirala, S. C., Abe, A. A. and Xu, W. (2006). Impact of low-cost dilute surfactants on wettability and relative permeability. In *SPE/DOE Symposium on Improved Oil Recovery*. Tulsa, Oklahoma, USA. Retrieved from SPE paper 99609
- Rashid, U. and Anwar, F. (2008). Production of biodiesel through optimized alkaline-catalyzed transesterification of rapeseed oil. *Fuel*, *87*, 265–273.
- Rawajfih, Z. and Nsour, N. (2006). Characteristics of Phenol and Chlorinated Phenols Sorption onto Surfactant-Modified Bentonite. *Journal of Colloid Interface Sci*, *298*, 39–49.
- Reichenbach-Klinke, R., Langlotz, B., Wenzke, B., Spindler, C. and Brodt, G. (2011). “Hydrophobic Associative Copolymer with Favourable Properties for the Application in Polymer Flooding.” In *SPE International Symposium on Oilfield Chemistry*. (pp. 1–11). The Woodlands, Texas, U.S.A: Society of Petroleum Engineers. Retrieved from SPE Paper 141107
- Rodenbush, C. M, Hsieh, F. H. and Viswanath, D. S. (1999). Density and viscosity of vegetable oils. *Journal of American Oil Chemical Society*, *76*, 1415–9.
- Romero-Zerón, L. B. and Kittisrisawai, S. (2015). Evaluation of a surfactant carrier for the effective propagation and target release of surfactants within porous media during enhanced oil recovery. Part I: Dynamic adsorption study. *Fuel*, *148*, 238–245. <http://doi.org/http://dx.doi.org/10.1016/j.fuel.2015.01.034>
- Rosen, M. J. and Kunjappu, J. T. (2012). “*Surfactants and Interfacial Phenomena*” (4th ed.). Hoboken, New Jersey.
- Rosen, M. J., Wang, H., Shen, P. and Zhu, Y. (2005). Ultra-low interfacial tension for enhanced oil recovery at very low surfactant concentrations. *Langmuir Journal*, *21*, 3749–3756.
- Royon, D., Daz, M., Ellenrieder, G. and Locatelli, S. (2007). Enzymatic production of biodiesel from cotton seed oil using t-butanol as a solvent. *Bioresource Technology*, *98*, 648–653.
- Ryles, R. G. (1988). “Chemical stability Limits of water-Soluble Polymers Used in Oil recovery Processes.” *Journal of SPE Reservoir Engineering*, *3*(1), 23–34.
- Sabudak, T. Y. M. (2010). Biodiesel production from waste frying oils and its quality control. *Waste Management*, *30*, 799–803.
- Sadikhzadeh, E. (2006). Evaluation of polymer flooding for improved recovery in the Statfjord Formation of the Gullfaks Field.
- Sahoo, P. K. and Das, L. M. (2009). Process optimization for biodiesel production from Jatropha, Karanja and Polanga oils. *Fuel*, *88*, 1588–94.
- Saka, S. and Isayama, Y. (2009). . A new process for catalyst-free production of biodiesel using supercritical methyl acetate. *Fuel*, *88*, 1307–13.

- Saka, S., Isayama, Y., Ilham, Z. and Jiayu, X. (2010). New process for catalyst-free biodiesel production using subcritical acetic acid and supercritical methanol. *Fuel*, 89, 1442–6.
- Salari, Z., Ahmadi, M. A., Kharrat, R. and Abbaszadeh, S. A. (2011). Experimental Studies of Cationic Surfactant Adsorption onto Carbonate Rocks, 5(12), 808–813.
- Salinas, D., Guerrero, S. and Araya, P. (2010). Transesterification of canola oil on potassium-supported TiO<sub>2</sub> catalysts. *Catalysis Communications*, 11, 773–7.
- Salles, A. L., Bregeault, J. M. and Thouvenot, R. (2000). Comparison of oxoperoxophosphatotungstate phase transfer catalysis with methyltrioxorhenium two-phase catalysis for epoxidation by hydrogen peroxide. *Comptes Rendus de l'Académie Des Sciences*, 183–187.
- Sanchez-Martin, M. J., Dorado, M. C., del Hoyo, C., M.S. Rodriguez-Cruz, M. S. and Hazard, J. (2008). *Ma. Mater*, 150, 115.
- Sassen, C. L. (1991). “The Influence of Pressure on the Phase Behaviour of Water + Oil + Surfactant Systems.” The Netherlands: Delft University Press.
- Sassen, C. L., Bredee, J. H., de Loos, T. W. and de S. A. J. (1989). Influence of pressure and electrolyte on the phase behaviour of water + oil + nonionic surfactant systems. *Journal of Physics and Chemistry*, 93, 6511–6516.
- Sassen, C. L., Casielles, A. G., de Loos, Th. W. and de Swaan Aron, J. (1992). The influence of pressure and temperature on the phase behaviour of the system H<sub>2</sub>O + C<sub>12</sub> + C<sub>7</sub>E<sub>5</sub> and relevant binary subsystems. *Fluid Phase Equilibria*, 72, 173–187.
- Sastry, N. V., S'equaris, J. M. and Schwuger, M. J. (1995). Adsorption of polyacrylic acid and sodium dodecylbenzenesulfonate on kaolinite. *Journal of Colloid Interface Sci*, 171, 224–233.
- Satterfield, C. N. (1980). *Heterogeneous Catalysis in Practice*. Mc- Graw-Hill.
- Sawangkeaw, R., Tejvirat, P., Ngamcharassrivichai, C. and Somkiat Ngamprasertsith, S. (2012). Supercritical Transesterification of Palm Oil and Hydrated Ethanol in a Fixed Bed Reactor with a CaO/Al<sub>2</sub>O<sub>3</sub> Catalyst. *Energy and Fuels*, 5, 1062–1080.
- Scala, J. and Wool, R. P. (2002). Effect of FA composition on epoxidation kinetics of TAG. *Journal of the American Oil Chemists' Society*, 79(4), 373–378. <http://doi.org/10.1007/s11746-002-0491-9>
- Scala, J. and Wool, R. P. (2002). Effect of FA composition on epoxidation kinetics of TAG. *Journal of American Oil Chemistry Society*, 79, 373–378.
- Schramm, L. L. (2000). *Surfactants: Fundamentals and Application in the Petroleum Industry*, 129.
- Schramm, L. L. (2012). “*Surfactants: Fundamentals and applications in the petroleum industry*.” Cambridge, UK.

- Schuchardta, U., Serchelia, R. and Vargas, R. M. (1998). Transesterification of vegetable oils: a review. *Journal of Brazilian Chemical Society*, 9(1), 199–210.
- Seethepalli, A., Adibhatla, B. and Mohanty, K. K. (2004). “Wettability Alteration during Surfactant Flooding of Carbonate Reservoirs.” In *SPE/DOE 14th Symposium on Improved Oil Recovery*. Tulsa Oklahoma, USA: OK. Retrieved from SPE 89423
- Sepulveda, J. S., Teixeira and Schuchardt, U. (2007). Alumina-catalyzed epoxidation of unsaturated fatty esters with hydrogen peroxide. *Applied Catalysis A: General*, 310, 213–217.
- Seright, R. S. and Henrici, B. J. (2009). “Xanthan Stability at Elevated Temperature.” *Journal of SPE Reservoir Engineering*, 5(1), 52–60.
- Seright, R. S., Fan, T., Wavrik, K., Wan, H., Gaillard, N. and Favero, C. (2011). “Rheology of a New Sulfonic Associative Polymer in Porous Media.” *SPE Reservoir Evaluation & Engineering*, 14(6)(December), 726–134.
- Shah, S., Sharma, S. and Gupta, M. N. (2004). Biodiesel preparation by lipase-catalyzed transesterification of Jatropha oil. *Energy & Fuels*, 18, 154–159.
- ShamsiJazeyi, H., Verduzco, R. and Hirasaki, G. J. (2014). Reducing adsorption of anionic surfactant for enhanced oil recovery: Part I. Competitive adsorption mechanism. *Colloids and Surfaces A: Physicochemical and Engineering Aspects*, 453, 162–167. <http://doi.org/http://dx.doi.org/10.1016/j.colsurfa.2013.10.042>
- Sharma, Y. C., Singh, B. and Korstad, J. (2011). Latest developments on application of heterogeneous basic catalysts for an efficient and eco-friendly synthesis of biodiesel: A review. *Fuel*, 90, 1309–1324.
- Sharma, Y. C., Singh, B. and Korstad, J. (2010). Latest developments on application of heterogeneous basic catalysts for an efficient and eco-friendly synthesis of biodiesel: A review. *Fuel*, 90, 1309–1324.
- Sharma, Y. C., Singh, B. and Upadhyay, S. N. (2008). Advancements in development and characterization of biodiesel: A review. *Fuel*, 87, 2355–2373.
- Sheng, J. (2013). Chapter 8 - alkaline-surfactant flooding. In *Enhanced oil recovery field case studies* (pp. 179–188). Boston: Gulf Professional Publishing.
- Sheng, J. J. (2011). Chapter 12 - alkaline-surfactant flooding. In *Modern chemical enhanced oil recovery* (J. J. Shen, pp. 473–500). China: Boston: Gulf Professional Publishing.
- Silverstein, R. M., Webster F. X., & Kiemle, D. J. (2005). No Title. *John Wiley & Sons, Inc.*
- Sinadinovic-Fiser, S., Jankovic, M. and Petrovic, Z. S. (2001). Kinetics of In-Situ epoxidation of soybean oil in bulk catalyzed by ion exchange resin. *Journal of American Oil Society*, 78, 725–731.

- Singhal, A. (2011). Preliminary Review of IETP Projects Using Polymers. Calgary, Alberta, Canada: Premier Reservoir Engineering Services LTD.
- Sivakumar, P., Anbarasu, K. and Renganathan, S. (2011). Bio-diesel production by alkaline catalyzed transesterification of dairy waste scum. *Fuel*, *90*, 147–151.
- Skauge, A. and Fotland, P. (1990). Effect of pressure and temperature on the phase behavior of microemulsions. *SPE Reservoir Engineering*, *5*, 601–608.
- Smith, P. C., Ngothai, Y., Nguyen, Q. D. and Neill, B. K. (2009). Alkoxylation of biodiesel and its impact on low-temperature properties. *Fuel*, *88*(4), 605–612. <http://doi.org/10.1016/j.fuel.2008.10.026>
- Solomon, T. W. G. (2002). *Solomons Organic Chemistry* (6th ed.). New York: John Wiley & Sons.
- Somasundaran, P. and Huang, U. L. (2000). Adsorption/aggregation of surfactants and their mixtures at solid/liquid interfaces. *Advances in Colloid Interface Science*, *88*, 179–208.
- Somasundaran, P., Columbia, U.H. and Shafick Hanna, U. C. (2000). “Adsorption/Desorption of Sulfonates by Reservoir Rock Minerals in Solutions of Varying Sulfonate Concentrations.”
- Sosis, P. and Dringoli, L. (1970). “Sulfation of synthetic linear primary alcohols with chlorosulfonic acid.” *Journal of the American Oil Chemists’ Society*, *47*, 229–232.
- Spildo, K., Sun, L., Djurhuus, K. and Skauge, A. (2014). A strategy for low cost, effective surfactant injection. *Journal of Petroleum Science and Engineering*, *117*, 8–14. <http://doi.org/http://dx.doi.org/10.1016/j.petrol.2014.03.006>
- Spinler, E.A., Baldwin, B.A. and Graue, A. (2002). Experimental artefacts caused by wettability variation in chalk. *Journal of Petroleum Science Engineering*, *33*((1-3)), 49 – 59.
- Standnes, D.C. and Austad, T. (2000). Wettability alteration in chalk. 2. Mechanism Surfactants, wettability alteration from oil-wet to water-wet using surfactants. *Journal of Petroleum Science and Engineering*, *28*(3), 123–143.
- Standnes, D.C., Nogaret, L.A.D., Chen, H.-L. and Austad, T. (2002). An evaluation of spontaneous imbibition of water into oil-wet carbonate reservoir cores using a nonionic and a cationic surfactant. *Energy & Fuels*, *16*(6), 1557–1564.
- Stein, W. and Baumann, H. (1975).  $\alpha$ -Sulfonated fatty acids and esters: Manufacturing process, properties, and applications. *Journal of the American Oil Chemists Society*, *52*(9), 323–329. <http://doi.org/10.1007/BF02639188>
- Suarez, P. A. Z., Pereira, M., Doll, K. M., Sharma, B. K. and Erhan, S. Z. (2009). Epoxidation of Methyl Oleate Using Heterogeneous Catalyst. *Industrial & Engineering*, *48*, 3268–3270.

- Sun, S., Ke, X., Cui, L., Yang, G., Bi, Y., Song, F. and Xu, X. (2011). Enzymatic epoxidation of *Sapindus mukorossi* seed oil by perstearic acid optimized using response surface methodology. *Industrial Crops and Products*, 33(3), 676–682. <http://doi.org/10.1016/j.indcrop.2011.01.002>
- Swern, D. (1947). Electronic interpretation of the reaction of olefins with organic peracids. *Journal of American Chemist's Society*, 69, 1692–8.
- Sydansk, R. D. (2006). *Polymers, Gels, Foams and Resins*. USA: Society of Petroleum Engineers (SPE).
- Tabatabal, A., Gonzalez, M. V., Harwell, J. H. and Scamehorn, J. F. (1993). Reducing Surfactant Adsorption in Carbonate Reservoirs. *SPE Reservoir Engineering*, 8(2). <http://doi.org/10.2118/24105-PA>
- Tan, K. T., Lee, K. T. and Mohamed, A. R. (2011). Prospects of non-catalytic supercritical methyl acetate process in biodiesel production. *Fuel Processing Technology*, 92, 1905–9.
- Teichner, S. J., Nicolaon, G. A., Vicarini, M. A. and Gardes, G. E. (1976). Adv Coll. Inter. Sci. *Advances in Colloid Interface Science*, 5, 245.
- Teng, G., Gao, L., Xiao, G. and Liu, H. (2009). Transesterification of soybean oil to biodiesel over heterogeneous solid base catalyst. *Energy Fuels*, 23, 4630–4634.
- Thomas, W. J. (1998). *Barry Crittenden "Adsorption Technology and Design"*. Elsevier Science & Technology Books.
- Tichelkamp, T., Teigen, E., Nourani, M. and Øye, G. (2015). Systematic study of the effect of electrolyte composition on interfacial tensions between surfactant solutions and crude oils. *Chemical Engineering Science*, 132, 244–249. <http://doi.org/http://dx.doi.org/10.1016/j.ces.2015.04.032>
- Toda, M., Takagaki, A., Okamura, M., Kondo, J. N., Hayashi, S., Domen, K. and Hara, M. (2005). Biodiesel made with sugar catalyst. *Nature*, 438, 178.
- Tornvall, U., Orellana-Coca, C., Hatti-kaul, R. and Adlercreutz, D. (2007). stability of immobilized *Candida antarctica* lipase B during chemo-enzymatic epoxidation of fatty acids. *Enzyme Microbial Technology*, 40, 447–451.
- Touhami, Y., Rana, D., Hornof, V. and Neale, G. H. (2001). Effects of Added Surfactant on the Dynamic Interfacial Tension Behaviour of Acidic Oil/Alkaline Systems. *Journal of Colloid and Interface Science*, 239, 226–229.
- Upadhyaya, A., Acosta, E. J., Scamehorn, J. F. and Sabatini, D. a. (2007). Adsorption of anionic-cationic surfactant mixtures on metal oxide surfaces. *Journal of Surfactants and Detergents*, 10(4), 269–277. <http://doi.org/10.1007/s11743-007-1045-3>
- Van Gorp, K. (1996). Preparation of heterogeneous catalysts from organometallic precursors. Utrecht University.



- Van Isahak, W. N. R., Ismail, M., Mohd, J. and Yarmo, M. A. (2010). Transesterification of palm Oil using Nano-Calcium oxide as a Solid Base catalyst. *World Applied Sciences Journal (Special Issue of Nanotechnology)*, 17–22.
- Varma, M. N. and Madras, G. (2007). Synthesis of biodiesel from castor oil and linseed oil in supercritical fluids. *Industrial & Engineering Chemistry Research*, 46, 1–6.
- Verma, A. and P. M. K. (2010). Synthesis, characterization and physical properties studies of an anionic surfactant. *Indian Journal of Chemical Technology*, 233–237.
- Verziu, M., Coman, S. M., Richards, R. and Parvulescu, V. I. (2011). Transesterification of vegetable oils over CaO catalysts. *Catalysis Today*, 167, 64–70.
- Vicente, G., Martinez, M. and Aracil, J. (2004). Integrated biodiesel production: a comparison of different homogeneous catalysts systems. *Bioresources Technology*, 92(3), 297–305.
- Viriya-empikul, N., Krasae, P., Puttasawat, B., Yoosuk, B., Chollacoop, N. and Faungnawakij, K. (2010). Waste shells of mollusk and egg as biodiesel production catalysts. *Bioresource Technology*, 101, 3765–7.
- W., L. L. (2010). “Enhanced Oil Recovery.” Florence, Italy: Society of Petroleum Engineers (SPE).
- Wagner, O. R. and Leach, R. O. (1959). “Improving Oil displacement Efficiency by wettability Adjustment.” *Petroleum Transactions*, 216, 65–72.
- Wanchao, S., Chengzhi, Y. and Dakuang, H. (1995). Alkali-Surfactant-Polymer Combination Flooding for Improving Recovery of the Oil with High Acid Value. In *International Meeting on Petroleum Engineering*. Beijing, PR China.
- Wang, D. and Wang, G. (2010). “Novel Surfactants that Attain Ultra-Low Interfacial Tension between Oil and High Salinity Formation Water without adding Alkali, Salts, Co-surfactants, Alcohol and Solvents.” In *SPE EOR Conference at Oil & Gas West Asia*. Muscat, Oman.
- Wang, D., Cheng, J., Yang, Z., Li, Q., Wu, W. and Yu, H. (2001). “Successful Field Test of the First Ultra-Low Interfacial Tension Foam Flood.” In *SPE Asia Pacific Improved Oil Recovery Conference*. Kuala Lumpur, Malaysia. <http://doi.org/10.2118/72147-MS>
- Wang, D., Han, P. and Shao, Z. (2006). Sweep Improvement Options for Daqing Oil Field. SPE/DOE symposium on improved oil recovery. *SPE Journal*.
- Wang, L. and Mohanty, K. K. (2013). Improving Oil Recovery in Gas-Flooded, Oil-Wet Carbonate Reservoirs by Wettability Altering Surfactant. In *SPE International Symposium on Oilfield Chemistry*. Texas, USA.
- Wangqi, H. D. and Dave, F. (2004). “Surfactant Blends for Aqueous Solutions Useful for Improving Oil Recovery.” U. S. Patent 6 828 281 B1.
- Waterman, K. C., Turro, N. J., Chandar, P. and Somasundaran, P. (1986). No Title. *Journal of Physical Chemistry*, 90, 6828.

- Weil, J. K., Stirton, J. Ault, W. and Bistline, R. (1953). Salts of alpha-sulfonated fatty acid esters. *Journal of American Chemist's Society*, 4859–4860.
- Wen, Z., Yu, X., Tu, S.T., Yan, J. and Dahlquist, E. (2010). Biodiesel production from waste cooking oil catalyzed by TiO<sub>2</sub>–MgO mixed oxides. *Bioresource Technology*, 101, 9570–9576.
- Wesson, L. L. and Harwell, J. H. (2010). “Surfactant Adsorption in Porous Media”, *Surfactants: Fundamentals and Applications in the Petroleum Industry*. University Press Cambridge.
- Wesson, L. L. and Harwell, J. H. (2010). “Surfactant adsorption in porous media”, *surfactants: Fundamentals and applications in the petroleum industry*. University Press Cambridge.
- Willi, W. (1994). “Process for the Production of Surfactant Mixtures Based on Ether Sulfonates and Their Use.”
- Williams, D. B. and Carter, C. B. (1996). *Transmission Electron Microscopy I Basics*. New York: Plenum Press.
- Wu, W. H., Foglia, T. A., Marmer W. N. and Phillips, J. G. (1999). Optimizing production of ethyl esters of grease using 95% ethanol by response surface methodology. *Journal of American Oil Chemical Society*, 76(4), 517–521.
- Wu, Y., Shuler P., Blanco M., Tang Y. and Goddard, W. A. (2005). “A Study of Branched Alcohol Propoxylate Sulfate Surfactants for Improved Oil Recovery.” In *2005 SPE Annual Technical Conference and Exhibition* (pp. 1–10). Dallas, Texas, U.S.A: Society of Petroleum Engineers (SPE) Inc.
- Wuest, W., Eskuchen, R. and Richter, B. (1994). Process for the Production of Surfactant Mixtures Based on Ether Sulfonates and Their Use.
- Xie, W. and Huang, X. (2006). Synthesis of biodiesel from soybean oil using heterogeneous KF/ZnO catalyst. *Catalysis Today*, 107, 53–59.
- Xie, W. and Li, H. (2006). Alumina-supported potassium iodide as a heterogeneous catalyst for biodiesel production from soybean oil. *Journal of Molecular Catalysis A: Chemical*, 255, 1–9.
- Xie, W., Peng, H. and Chen, L. (2006). Calcined Mg–Al hydrotalcites as solid base catalysts for methanolysis of soybean oil. *Journal of Molecular Catalysis A: Chemical*, 246, 24–32.
- Xie, X. and Morrow, N. R. (2001). “Oil Recovery by Spontaneous Imbibition from Weakly Water-Wet Rocks.” *Petrophysics*, 42(4), 313.
- Xie, X., Weiss, W.W., Tong, Z. and Morrow, N. R. (2004). Improved oil recovery from carbonate reservoirs by chemical stimulation. In *2004 SPE/DOE Fourteenth Symposium on Improved Oil Recovery*. Tulsa. Retrieved from SPE

- Xin, J., Imahara, H. and Saka, S. (2008). Oxidation stability of biodiesel fuel as prepared by supercritical methanol. *Fuel*, 87, 1807–13.
- Xu, Q., Vasudevan, T.V. and Somasundaran, P. (1991). Adsorption of anionic—nonionic and cationic—nonionic surfactant mixtures on kaolinite. *Journal of Colloid and Interface Science*, 141(2), 528–534. [http://doi.org/http://dx.doi.org/10.1016/0021-9797\(91\)90083-K](http://doi.org/http://dx.doi.org/10.1016/0021-9797(91)90083-K)
- Yaakob, Z., Mohammad, M., Alherbawi, M., Alam, Z. and Sopian, K. (2013). Overview of the production of biodiesel from Waste cooking oil. *Renewable and Sustainable Energy Reviews*, 18, 186–191.
- Yalman, E. (2012). Biodiesel Production from Safflower Using Heterogeneous CAO Based Catalysts. A Thesis Submitted to in Energy Engineering, (July).
- Yang, S. S. (2000). “Mechanisms of wettability for crude oil/brine/mica system.” Rice: Rice University.
- Yang, X., Liao, G., Han, P., Yang, Z. and Yao, Y. (2003). “An Extended field Test Study on Alkaline-surfactant-polymer flooding in Beiyiduanxi of Daqing Oilfield.” In *SPE Asia Pacific Oil and Gas Conference and Exhibition*. Jakarta, Indonesia. Retrieved from SPE 80532
- Yermakov, Y. I., Kuznetsov, B. N. and Zakharov, V. A. (1981). *Catalysis by Supported Complexes*. Amsterdam: Elsevier.
- Yuan, F.-Q., Cheng, Y.-Q., Wang, H.-Y., Xu, Z.-C., Zhang, L., Zhang, L. and Zhao, S. (2015). Effect of organic alkali on interfacial tensions of surfactant solutions against crude oils. *Colloids and Surfaces A: Physicochemical and Engineering Aspects*, 470, 171–178. <http://doi.org/http://dx.doi.org/10.1016/j.colsurfa.2015.01.059>
- Zabeti, M., Wan Daud, W. M. A. and Aroua, M. K. (2009). Optimization of the activity of CaO/Al<sub>2</sub>O<sub>3</sub> catalyst for biodiesel production using response surface methodology. *Applied Catalysis A-General*, 366(1), 154–159.
- Zabeti, M., Wan Daud, W., Mohd, A. and Aroua, M. K. (2009). Activity of solid catalysts for biodiesel production: a review. *Fuel Process Technology*, 90(6), 770–777.
- Zaitoun, A. and Potie, B. (1983). "Limiting Conditions for the Use of Hydrolysed Polyacrylamides in Brines Containing Divalent Ions: In *Proceeding of SPE Oilfield and Geothermal Chemistry Symposium*. Denver, Colorado, USA.
- Zargartalebi, M., Kharrat, R. and Barati, N. (2015). Enhancement of surfactant flooding performance by the use of silica nanoparticles. *Fuel*, 143, 21–27. <http://doi.org/http://dx.doi.org/10.1016/j.fuel.2014.11.040>
- Zhang, Q.-Q., Cai, B.-X., Xu, W.-J., Gang, H.-Z., Liu, J.-F., Yang, S.-Z. and Mu, B.-Z. (2015). The Rebirth of Waste Cooking Oil to Novel Bio-based Surfactants. *Scientific Reports*, 5, 9971. <http://doi.org/10.1038/srep09971>

- Zhang, R. and Somasundaran, P. (2006). Advances in adsorption of surfactants and their mixtures at solid/solution interfaces. *Advances in Colloid and Interface Science*, 123-126(SPEC. ISS.), 213–229. <http://doi.org/10.1016/j.cis.2006.07.004>
- Zhang, D. L., Liu, S., Yan, W., Puerto, M., Hirasaki, J. and Miller, C. A. 2006. (2006). “Favorable Attributes of Alkali-Surfactant-Polymer Flooding.” In *SPE/DOE Symposium on Improved Oil Recovery*. Tulsa, Oklahoma, U. S.A.
- Zhang, R. and Somasundaran, P. (2006). Advances in Adsorption of Surfactant and their Mixtures at Solid/Solution interfaces. *Advances in Colloid Interface Science*, 123-126, 213–229.
- Zhang, R. and Somasundaran, P. (2006). Advances in adsorption of surfactants and their mixtures at solid/solution interfaces. *Advances in Colloid and Interface Science*, 123-126(SP, 213–229. <http://doi.org/10.1016/j.cis.2006.07.004>
- Zhang, Y. P., Sayegh, S. G. and Huang, S. (2005). “The role of effective interfacial tension in alkaline/surfactant/ polymer flooding.” In *Proceedings of Canadian International Petroleum Conference*. Society of Petroleum Engineers (SPE).
- Zhang, Y., Dube, M. A., McLean, D. D. and Kates, M. (2003). Biodiesel production from waste cooking oil: 1. Process design and technological assessment. *Bioresource Technology*, 89(1), 1–16.
- Zhao, Y. and Shadman, F. (1993). Production of oxygen from lunar ilmenite. *Resources of Near-Earth Space*. Retrieved from <http://uapress.arizona.edu/onlinebks/ResourcesNearEarthSpace/resources07.pdf>
- Zhao, F., Ma, Y., Hou, J., Tang, J. and Xie, D. (2015). Feasibility and mechanism of compound flooding of high-temperature reservoirs using organic alkali. *Journal of Petroleum Science and Engineering*, 135, 88–100. <http://doi.org/http://dx.doi.org/10.1016/j.petrol.2015.08.014>
- Zheng, S., Kates, M., Dube, M. A. and McLean, D. D. (2006). Acid-catalyzed production of biodiesel from waste frying oil. *Biomass and Bioenergy*, 30(3), 267–272.
- Zhou, W. M. D. & Liu, Q. (2005). Experimental Investigation of Surfactant Adsorption on Sand and Oil-Water Interface in Heavy Oil/Water/Sand Systems. *Petroleum Society Journals*.
- Zhou, Z. H. and Gunter, W. D. (1992). The nature of the surface charge of kaolinite. *Clays Minerology*, 40, 365–368.
- Zhu, Y., Zhang, Y. and Hou, Q. (2013). Effect of Main Factors on Oil Recovery of Surfactant- Polymer Flooding. In *International Petroleum Technology Conference*. China.
- Zong, M. H., Duan, Z. Q., Lou, W. Y., Smith, T. J. and Wu, H. (2007). Preparation of a sugar catalyst and its use for highly efficient production of biodiesel. *Green Chemistry*, 9, 434–437.

Zullaikah, S., Lai, C. C., Vali, S. R. and Ju, Y. H. (2005). A two-step acid-catalyzed process for the production of biodiesel from rice bran oil. *Bioresource Technology*, 96(17), 1889–96.

## APPENDICES

### Appendix A- Sample Calculations on FAME Production

#### A.1 Free fatty acids determination

Using waste palm oil (WPO)

$$\text{FFA} \left( \frac{\text{mg}}{\text{g}} \right) = (V_2 - V_1) \times \frac{1.4}{\rho_{\text{oil}}}$$

Where  $V_1$  = Volume of standard solution without WPO and  $V_2$  = Volume of standard solution with addition of WPO

**Table 29:** Titration readings for WPO

Samples	$V_1$	$V_2$
1	0.1	15.10
2	0.3	15.30
3	0.2	15.00
4	0.2	15.20
<b>Average</b>	0.2	15.15

The density of waste palm oil at 25 °C is obtained using the mathematical expression using below (Rodenbush *et al.*, 1999; Esteban *et al.*, 2012):

$$\rho = a + b \times T$$

where  $\rho$  is the density expressed in  $\text{g/cm}^3$ ,  $T$  is the temperature expressed in °C,  $a$  is the intercept and  $b$  is a negative slope.

For waste palm oil the parameters of the density-temperature fit are:  $a = 0.9250$  and  $b = -6.5612 (\times 10^{-4})$ , respectively (Esteban *et al.*, 2012).

Then its density at 25 °C:  $\rho = 0.9250 + (-6.5612 \times 10^{-4}) \times 65) = 0.9086 \text{ g/cm}^3$

$$\text{FFA} \left( \frac{\text{mg}}{\text{g}} \right) = (50.15 - 0.2) \times \frac{1.4}{0.9086}$$

$$\text{FFA} = 76.96 \text{ mg/g}$$

For waste sunflower oil (WSO)

**Table 30:** Titration readings for WSO

Samples		V <sub>1</sub>	V <sub>2</sub>
1		0.05	0.3
2		0.1	0.4
3		0.0.05	0.3
4		0.1	0.3
Average		0.075	0.325

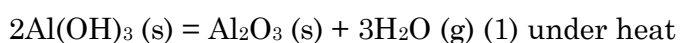
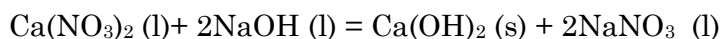
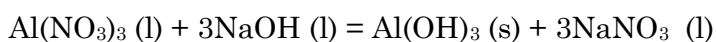
For sunflower oil the parameters of the density-temperature fit are:  $a = 0.9310$  and  $b = -6.4145 (\times 10^{-4})$

At 25 °C:  $\rho = 0.9310 + (-6.4145 \times 10^{-4}) \times 25) = 0.91496 \text{ g/cm}^3$

❖ FFA = 0.3825 mg/g

## A.2. FAME Production Calculations

Preparation of 80% CaO/Al<sub>2</sub>O<sub>3</sub> catalyst by co-precipitation method



M<sub>w</sub> of Al<sub>2</sub>O<sub>3</sub> = 101.96 g/mol

M<sub>w</sub> of CaO = 56.0774 g/mol

M<sub>w</sub> of Ca(NO<sub>3</sub>)<sub>2</sub> = 164.088 g/mol

M<sub>w</sub> of Al(NO<sub>3</sub>)<sub>3</sub> = 212.996 g/mol

M<sub>w</sub> of Al(NO<sub>3</sub>)<sub>3</sub>.9H<sub>2</sub>O = 374.996 g/mol

M<sub>w</sub> of Ca(NO<sub>3</sub>)<sub>2</sub>.4H<sub>2</sub>O = 236.172 g/mol

**100 g of combined catalyst = 80 g CaO/20 g Al<sub>2</sub>O<sub>3</sub>**

moles of Al<sub>2</sub>O<sub>3</sub> =  $m_{\text{Al}_2\text{O}_3} / M_{\text{wAl}_2\text{O}_3} = 20/101.96 = 0.2$  moles of Al<sub>2</sub>O<sub>3</sub>

Since 1 mol of Al(NO<sub>3</sub>)<sub>3</sub> = 1/2 mole of Al<sub>2</sub>O<sub>3</sub> = 0.5 moles

Then moles of aluminium nitrate =  $0.2/0.5 = 0.4$  moles of Al(NO<sub>3</sub>)<sub>3</sub>

Mass of Al(NO<sub>3</sub>)<sub>3</sub>.9H<sub>2</sub>O =  $0.4 \times 375 = 150$  g of Al(NO<sub>3</sub>)<sub>3</sub>.9H<sub>2</sub>O

Moles of CaO =  $80/56.0774 = 1.4266$  moles

1 mol of  $\text{Ca}(\text{NO}_3)_2 = 1$  mol of  $\text{Ca}(\text{OH})_2 = 1$  mol CaO

Then moles of  $\text{Ca}(\text{NO}_3)_2 = \sim 1.4266$  moles

Mass of  $\text{Ca}(\text{NO}_3)_2 \cdot 4\text{H}_2\text{O} = n_{\text{Ca}(\text{NO}_3)_2} \times \text{Mw}_{\text{Ca}(\text{NO}_3)_2 \cdot 4\text{H}_2\text{O}} = 1.4266 \times 236.172 = 336.923$  g of Calcium nitrate =  $\sim 340$  g of Calcium nitrate

### ***Preparation of the precipitating agent (NaOH) solution***

$155/2 = \{78 \text{ g Aluminium nitrate}\}$

$340/2 = \{170 \text{ g of Calcium nitrate}\}$

New moles of  $\text{Al}(\text{NO}_3)_3 \cdot 9\text{H}_2\text{O} = 78/375 = 0.21$  moles

1 mol of  $\text{Al}(\text{NO}_3)_3 \cdot 9\text{H}_2\text{O} = 3$  moles of NaOH

moles of NaOH =  $0.21 \times 3 = 0.63$  moles

New moles of  $\text{Ca}(\text{NO}_3)_2 = 170/236.2 = 0.72$  moles

1 mol of  $\text{Ca}(\text{NO}_3)_2 = 2$  mol of NaOH

moles of NaOH =  $0.72 \times 2 = 1.44$  moles

Total moles of NaOH = 2.07 moles

1L = 2 moles of NaOH

0.03 moles = x

❖  $0.03/2 = 0.015$  L which equals 150 mL of 2M solution

❖ 508 mL of 4M solution of NaOH

❖ 160 g in 1L of NaOH

### **A.3. FAME Production Calculations**

#### **i. Values Used**

$V_{\text{oil}} = 50 \text{ mL} = 50 \text{ cm}^3$

$\rho = 0.9250 + (-6.5612 \times 10^{-4}) \times 65 = 0.8824 \text{ g/cm}^3$

$\text{Mw}_{\text{oil}} = 846.1 \text{ g/mol}$  (Arjun *et al.*, 2008)

#### **ii. Mass and Moles of WPO**

$$\rho = \frac{m}{V}$$



$$m_{WPO} = 0.8824 \frac{\text{g}}{\text{cm}^3} \times 50 \text{cm}^3$$

$$m_{WPO} = 44.12 \text{ g}$$

$$n = \frac{m}{Mr}$$

$$n_{WPO} = \frac{44.12}{846.1} = 0.0522 \text{ moles of WPO}$$

### iii. Mass and Moles of Methanol

$$n_{MeOH} = 9 \times 0.0522$$

$$n_{MeOH} = 0.4698 \text{ moles of MeOH}$$

$$n = \frac{m}{Mr}$$

$$m_{MeOH} = n_{MeOH} \times Mw_{MeOH}$$

$$m_{MeOH} = 0.4698 \text{ mol} \times 32.04 \frac{\text{g}}{\text{mol}}$$

$$m_{MeOH} = 15.52 \text{ g of MeOH}$$

$$V_{MeOH} = \frac{15.52 \text{ g}}{0.79180 \text{ g/mL}}$$

$$V_{MeOH} = 19.60 \text{ mL}$$

### iv. Catalyst Weight Determination

*Catalyst loading = 4 wt. %*

$$0.04 = \frac{m_{cat}}{m_{WPO} + m_{MeOH} + m_{cat}}$$

$$m_{cat} = 0.04 \times (44.12 + 15.52 + m_{cat})$$

$$m_{cat} = 2.485 \text{ g of catalyst}$$

The same calculations were performed when waste sunflower oil (WSO) was used. Where its density and molecular weight were 0.9216 g/cm<sup>3</sup> and 856 g/mol. correspondingly (Guerrero *et al.*, 2011).

Afterwards the FAME produced by transesterifying the different waste vegetable oils was analysed using the GC-MS. The results are presented in Tables 35 to 40.

### V. FAME Yield Calculation

Here the calculations were performed using the FAME produced at 60%CaO/Al<sub>2</sub>O<sub>3</sub>

$$\text{Ratio} = \frac{\text{Total peak area of the fatty acid methyl esters}}{\text{Peak of the internal standard}}$$

where the internal standard weight is 0.05 g, the peak of the internal standard is 0.1769% and the total FAME area when 60%CaO/Al<sub>2</sub>O<sub>3</sub> catalyst was used is 96.1314%.

$$\diamond \text{ Ratio} = \frac{96.1314\%}{0.1769\%} = 543.4223$$

In calculating the fatty acid methyl esters mass produced, the concentration of the internal standard was multiplied by the ratio of the peak of the fatty acid methyl ester and the peak of the internal standard. Weight percent of FAME was calculated using Equation 10

$$\text{FAME Yield (\%)} = \frac{\text{Weight of FAME produced (g)}}{\text{Weight of oil used (g)}} \times 100$$

where the weight of FAME produced equals  $0.05 \text{ g} \times 543.4223 = 27.17111 \text{ g}$

$$\diamond \text{ FAME Yield (\%)} = \frac{27.171 \text{ g}}{50 \text{ g}} \times 100 \% = 54.342 \% \sim 54 \%$$

**Table 31:** Effect of catalyst ratio on the FAME yield of WSO using 60% CaO/Al<sub>2</sub>O<sub>3</sub> at reaction temperature of 65 °C, methanol/oil molar ratio of 9:1 and reaction time of 4 hours and agitation speed of 800 rpm

FAME	Area %
Heptane, 2,2,4,6,6-pentamethyl	0.027
Decane, 4-methyl	0.0365
Decane, 2,3,7-trimethyl	0.0525
Hexadecane, 7,9-dimethyl	0.0296
Tetradecane	0.0473
Phenol, 2,4-bis(1,1-dimethylethyl)	0.2069
Docosane	0.0478
9-Hexadecenoic acid, methyl ester, (Z) or Palmitoleic acid, methyl ester	0.1937
Triacontane	0.0405
Hexadecanoic acid, methyl ester or Palmitic acid, methyl ester	11.0083
Linoleic acid	0.068
Heptadecanoic acid, methyl ester or Margaric acid methyl ester	0.1769
8,11-Octadecadienoic acid, methyl ester	55.6214
14-Octadecenoic acid, methyl ester	15.3867
Octadecanoic acid, methyl ester or Stearic acid methyl ester	10.1408
9,12-Octadecadienoic acid (Z,Z)-, methyl ester or Linoleic acid, methyl ester	0.3581
9-Octadecenoic acid (Z) or Oleic acid	0.6618

9,12-Octadecadienoic acid (Z,Z)-, ethyl ester or Linoleic acid ethyl ester	0.2188
9,12-Octadecadienoic acid, methyl ester, (E,E) or Linolelaidic acid, methyl ester	0.2094
(2.alpha.,5a.alpha.,9a.beta.)-(+.-)-Hexahydro-3H,6H-2,5a-methano-1,2-benzazepine	0.1929
2-Methyl-7H-1,3,4-thiadiazolo[3,2-A]pyrimidin-7-one	0.1805
cis-3-Butyl-4-vinyl-cyclopentene	0.1793
7-methyl-1-oxo-2,3-dihydrothieno[2,3-c]pyridine	0.901
4,6-Dimethoxy-2-phenylindole	0.4576
Eicosanoic acid, methyl ester or Arachidic acid methyl ester	0.7834
P-dimethoxy-N-phosphorylated dimethylsulphoximide	0.3144
10H-PYRAZINO[2,3-B][1,4]BENZOTHIAZINE	0.0586
2-Propenamide	0.077
Docosanoic acid, methyl ester or Behenic acid, methyl ester	1.7814
Tetracosanoic acid, methyl ester or Lignoceric acid methyl ester	0.4294
<b>Total FAME Area (%)</b>	<b>96.1314</b>
<b>Ratio of the peak of the fatty acid methyl ester and the peak of the internal standard</b>	<b>543.4223</b>
<b>Internal standard = 50 µl (microliters) = 0.05 grams</b>	<b>0.05</b>
<b>Weight of FAME in grams (g)</b>	<b>27.17111</b>

**Table 32:** Effect of catalyst ratio on the FAME yield of WSO using 70% CaO/Al<sub>2</sub>O<sub>3</sub> at reaction temperature of 65 °C, methanol/oil molar ratio of 9:1 and reaction time of 4 hours and agitation speed of 800 rpm

<b>FAME 7</b>	<b>Area %</b>
Heptane, 2,2,4,6,6-pentamethyl or 2,2,4,6,6-Pentamethylheptane	0.0271
Decane, 4-methyl or 4-Methyldecane	0.0324
Nonadecane or n-Nonadecane	0.0546
Nonadecane or n-Nonadecane	0.0265
Silane, dimethoxydimethyl	0.0357
n-Pentadecane	0.042
Phenol, 2,4-bis(1,1-dimethylethyl)	0.0727
n-Docosane	0.0428
9-Hexadecenoic acid, methyl ester, (Z) or Palmitoleic acid, methyl ester	0.1054
Undecane, 2,9-dimethyl-	0.0104
Hexadecanoic acid, methyl ester or Palmitic acid, methyl ester	19.4651
9-Octadecenoic acid (Z)-, methyl ester or Oleic acid, methyl ester	0.071
Heptadecanoic acid, methyl ester or Margaric acid methyl ester	0.1334
8,11-Octadecadienoic acid, methyl ester	55.9241
METHYLELAIDATE	0.1448
Octadecanoic acid, methyl ester or Stearic acid, methyl ester	16.8806
Linoleic acid	0.0187

9-Octadecenoic acid (Z) or Oleic acid	0.02819
9,12-Octadecadienoic acid (Z,Z)-, methyl ester or Linoleic acid, methyl ester	0.351
Bicyclo[3.2.0]heptane, 2-methylene-	0.0018
2,4-Hexadienedioic acid, 3-methyl-4-propyl-, dimethyl ester, (Z,E)	0.0189
9,12,15-Octadecatrienoic acid, methyl ester	0.3476
11-Eicosenoic acid, methyl ester	0.5972
2-Chloro-5,6,7,8-tetrahydroquinoline	0.0192
(5-Ethyl-cyclopent-1-enyl)-methanol	0.0027
Eicosanoic acid, methyl ester or Arachidic acid methyl ester	2.9904
(E)-3-Methoxy-4-nitro-2-butenic acid	0.0203
4-Amino-2-(1-hydroxy-1-ethylpropyl)quinoline	0.0125
Benzaldehyde, 3-chloro-, oxime	0.0493
Docosanoic acid, methyl ester or Behenic acid, methyl ester	2.2287
Tetracosanoic acid, methyl ester or Lignoceric acid methyl ester	0.6795
<b>Total FAME Area (%)</b>	<b>99.6406</b>
<b>Ratio of the peak of the fatty acid methyl ester and the peak of the internal standard</b>	<b>746.931</b>
<b>Internal standard = 50 µl (microliters) = 0.05 grams (g)</b>	<b>0.05</b>
<b>Weight of FAME in grams (g)</b>	<b>37.34655</b>

**Table 33:** Effect of catalyst ratio on the FAME yield of WSO using 80% CaO/Al<sub>2</sub>O<sub>3</sub> at reaction temperature of 65 °C, methanol/oil molar ratio of 9:1 and reaction time of 4 hours and agitation speed of 800 rpm

<b>FAME</b>	<b>Area %</b>
Heptane, 2,2,4,6,6-pentamethyl	0.0257
Octane, 2,4,6-trimethyl	0.0259
2-PENTADECYL-4,4,7,7-TETRADEUTERO-1,3-DIOXAPANE	0.0299
Nonadecane	0.0364
n-Triacontane	0.0406
Tetradecanoic acid, methyl ester or Myristic acid, methyl ester	0.0876
9-Hexadecenoic acid, methyl ester, (Z) or Palmitoleic acid, methyl ester	0.1823
n-Heneicosane	0.0359
Hexadecanoic acid, methyl ester or Palmitic acid, methyl ester	10.4385
AMBRETTOLIDE	0.0697
Heptadecanoic acid, methyl ester or Margaric acid methyl ester	0.0997
9,12-Octadecadienoic acid, methyl ester, (E,E) or Linolelaidic acid, methyl ester	54.1723
9-Octadecenoic acid (Z)-, methyl ester or Oleic acid, methyl ester	13.6226
Octadecanoic acid, methyl ester or Stearic acid, methyl ester	11.0568

Linoleic acid	0.2691
9,12-Octadecadienoic acid (Z,Z)-, ethyl ester or Linoleic acid ethyl ester	0.4472
9-Octadecenoic acid (Z)-, ethyl ester or Oleic acid, ethyl ester	0.2523
Octadecanoic acid or Stearic acid	0.4699
9,11-Octadecadienoic acid, methyl ester, (E,E)	0.5737
cis-Bicyclo[5.2.0]non-8-ene	0.188
Camphene or Bicyclo[2.2.1]heptane, 2,2-dimethyl-3-methylene	0.0888
4-Oxo-.beta.-isodamascol	0.283
Ethyl linoleate or LINOLEIC ACID, ETHYL ESTER	0.1003
6-Butyl-1,4-cycloheptadiene	0.1009
METHYL ESTER OF RICINOLEIC ACID or methyl ricinoleate	0.933
2,4-Hexadienedioic acid, 3-methyl-4-propyl-, dimethyl ester, (Z,E)	0.168
1-nitrophenanthro[4,5-bcd]thiophene	0.0536
Eicosanoic acid, methyl ester or Arachidic acid methyl ester	1.8428
3-Methylthio-5-(4-(4-methoxyphenyl)-1,3-butadienyl)isoxazole	0.0168
Phenothiazine	0.1205
10H-PYRAZINO[2,3-B][1,4]BENZOTHIAZINE	0.1402
Benzaldehyde, 4-chloro-, oxime Benzaldehyde, p-chloro-, oxime	0.07
Methyl 2-octylcyclopropene-1-octanoate	0.0078
N-tert-Butyl-3-(methylthio)furan-2-carboxamide	0.0166
Docosanoic acid, methyl ester or Behenic acid, methyl ester	2.8986
Tetracosanoic acid, methyl ester or Lignoceric acid methyl ester	0.6458
<b>Total FAME Area (%)</b>	<b>97.1535</b>
<b>Ratio of the peak of the fatty acid methyl ester and the peak of the internal standard</b>	<b>974.4584</b>
<b>Internal standard = 50 µl (microliters) = 0.05 grams (g)</b>	<b>0.05</b>
<b>Weight of FAME in grams (g)</b>	<b>48.72292</b>

**Table 34:** Effect of catalyst ratio on the FAME yield of WPO using 60% CaO/Al<sub>2</sub>O<sub>3</sub> at reaction temperature of 65 °C, methanol/oil molar ratio of 9:1 and reaction time of 4 hours and agitation speed of 800 rpm

<b>FAME</b>	<b>Area %</b>
Dodecanoic acid, methyl ester	0.4563
Methyl tetradecanoate	1.2211
9-Hexadecenoic acid, methyl ester, (Z)-	0.2415
Hexadecanoic acid, methyl ester	35.0077
Heptadecanoic acid, methyl ester	0.112
10,13-Octadecadienoic acid, methyl ester	12.1928
9-Octadecenoic acid, methyl ester, (E)-	44.9739

Octadecanoic acid, methyl ester	4.5698
11-Eicosenoic acid, methyl ester	0.2875
Eicosanoic acid, methyl ester	0.8602
<b>Total FAME Area (%)</b>	<b>99.8108</b>
<b>Ratio of the peak of the fatty acid methyl ester and the peak of the internal standard</b>	<b>891.1679</b>
<b>Internal standard = 50 µl (microliters) = 0.05 grams (g)</b>	<b>0.05</b>
<b>Weight of FAME in grams (g)</b>	<b>44.55839</b>

**Table 35:** Effect of catalyst ratio on the FAME yield of WPO using 70% CaO/Al<sub>2</sub>O<sub>3</sub> at reaction temperature of 65 °C, methanol/oil molar ratio of 9:1 and reaction time of 4 hours and agitation speed of 800 rpm

<b>FAME</b>	<b>Area %</b>
Heptane, 2,2,4,6,6-pentamethyl	0.021
Decane, 4-methyl	0.0303
Undecane, 5,7-dimethyl	0.0498
Undecane, 5-methyl	0.0264
Decane, 3-methyl	0.0147
Octanoic acid, methyl ester or n-Caprylic acid methyl ester	0.0755
2-PENTADECYL-4,4,7,7-TETRADEUTERO-1,3-DIOXAPANE	0.05
Decane, 3-ethyl-3-methyl	0.0362
n-Nonadecane	0.0378
n-Heneicosane	0.0275
Phenol, 2,4-bis(1,1-dimethylethyl)	0.01625
Dodecanoic acid, methyl ester or Lauric acid, methyl ester	0.6943
n-Eicosane	0.0247
Tetradecanoic acid, methyl ester -(CAS) or Myristic acid, methyl ester	1.9602
Pentadecanoic acid, methyl ester (CAS) or Methyl n-pentadecanoate	0.0445
9-Hexadecenoic acid, methyl ester, (Z)- or Palmitoleic acid, methyl ester	0.3658
5,5-Dibutylnonane	0.0508
Hexadecanoic acid, methyl ester or Palmitic acid, methyl ester	35.6668
Heptadecane, 9-octyl- (CAS)or 9-N-OCTYLHEPTADECANE	0.01029
9-Octadecenoic acid (Z)-, methyl ester -(CAS) or Oleic acid, methyl ester	0.0688
Heptadecanoic acid, methyl ester (CAS) or Margaric acid methyl ester	0.1605
9-Octadecenoic acid (Z)-, methyl ester -(CAS) or Oleic acid, methyl ester	49.4711
Octadecanoic acid, methyl ester -(CAS) or Stearic acid, methyl ester	7.5655
9,12-Octadecadienoic acid (Z,Z)-, methyl ester -(CAS) or Linoleic acid, methyl ester	0.4049
9,11-Octadecadienoic acid, methyl ester, (E,E)	0.165

1-Methylcycloheptanol or 1-Methylcycloheptanol-1 \$\$	0.1092
1,1-Dimethyl-1-silacyclo-3-pentene	0.712
11-Eicosenoic acid, methyl ester	0.2984
Z-.beta.-dihydroterpineol	0.01682
Eicosanoic acid, methyl ester or Arachidic acid methyl ester	0.8688
9-Octadecenoic acid, 12-hydroxy-13-methoxy-, methyl ester	0.0942
Naphthalene, 2-isothiocyanato or Isothiocyanic acid, 2-naphthyl ester	0.346
10H-PYRAZINO[2,3-B][1,4]BENZOTHIAZINE	0.01324
10H-PYRAZINO[2,3-B][1,4]BENZOTHIAZINE	0.01209
Docosanoic acid, methyl ester or Behenic acid, methyl ester	0.433
Tetracosanoic acid, methyl ester or Lignoceric acid methyl ester	0.3484
<b>Total FAME Area (%)</b>	<b>98.5252</b>
<b>Ratio of the peak of the fatty acid methyl ester and the peak of the internal standard</b>	<b>613.8642</b>
<b>Internal standard = 50 µl (microliters) = 0.05 grams (g)</b>	<b>0.05</b>
<b>Weight of FAME in grams (g)</b>	<b>30.69321</b>

**Table 36:** Effect of catalyst ratio on the FAME yield of WPO using 80% CaO/Al<sub>2</sub>O<sub>3</sub> at reaction temperature of 65 °C, methanol/oil molar ratio of 9:1 and reaction time of 4 hours and agitation speed of 800 rpm

<b>FAME</b>	<b>Area %</b>
Dodecanoic acid, methyl ester	0.662
Methyl tetradecanoate	1.4917
9-Hexadecenoic acid, methyl ester, (Z)-	0.2606
Hexadecanoic acid, methyl ester	34.9854
Heptadecanoic acid, methyl ester	0.1816
9,12-Octadecadienoic acid (Z,Z)-, methyl ester	11.5043
6-Octadecenoic acid, methyl ester, (Z)-	44.2424
Octadecanoic acid, methyl ester	5.9296
[1,1'-Biphenyl]-3-amine	0.008
11-Eicosenoic acid, methyl ester	0.1588
Eicosanoic acid, methyl ester	0.6269
Docosanoic acid, methyl ester	0.1764
<b>Total FAME Area (%)</b>	<b>100.0381</b>
<b>Ratio of the peak of the fatty acid methyl ester and the peak of the internal standard</b>	<b>550.8706</b>
<b>Internal standard = 50 µl (microliters) = 0.05 grams (g)</b>	<b>0.05</b>
<b>Weight of FAME in grams (g)</b>	<b>27.54353</b>

- **Reusability Tests**

**Table 37:** Effect of catalyst ratio on the FAME yield of WPO using 60% CaO/Al<sub>2</sub>O<sub>3</sub> at reaction temperature of 65 °C, methanol/oil molar ratio of 9:1 and reaction time of 4 hours and agitation speed of 800 rpm

<b>FAME</b>	<b>Area %</b>
Dodecanoic acid, methyl ester	0.4563
Methyl tetradecanoate	1.2211
9-Hexadecenoic acid, methyl ester, (Z)	0.2415
Hexadecanoic acid, methyl ester	30.0077
Heptadecanoic acid, methyl ester	0.112
10,13-Octadecadienoic acid, methyl ester	10.0817
Linoleic acid	14.0845
9-Octadecenoic acid, methyl ester, (E)	38.8633
Octadecanoic acid, methyl ester	3.5698
11-Eicosenoic acid, methyl ester	0.2875
Eicosanoic acid, methyl ester	0.9602
<b>Total FAME Area (%)</b>	<b>85.6891</b>
<b>Ratio of the peak of the fatty acid methyl ester and the peak of the internal standard</b>	<b>765.08125</b>
<b>Internal standard = 50 µl (microliters) = 0.05 grams (g)</b>	<b>0.05</b>
<b>Weight of FAME in grams (g)</b>	<b>38.2540625</b>
<b>Yield of FAME (%)</b>	<b>76.508125</b>

**Table 38:** Effect of catalyst ratio on the FAME yield of WSO using 80% CaO/Al<sub>2</sub>O<sub>3</sub> at reaction temperature of 65 °C, methanol/oil molar ratio of 9:1 and reaction time of 4 hours and agitation speed of 800 rpm

<b>FAME</b>	<b>Area %</b>
Heptane, 2,2,4,6,6-pentamethyl	0.0257
Octane, 2,4,6-trimethyl	0.0259
2-PENTADECYL-4,4,7,7-TETRADEUTERO-1,3-DIOXAPANE	0.0299
Nonadecane	0.0364
n-Triacontane	0.0406
Tetradecanoic acid, methyl ester or Myristic acid, methyl ester	0.0876
9-Hexadecenoic acid, methyl ester, (Z) or Palmitoleic acid, methyl ester	0.1823
n-Heneicosane	0.0359
Hexadecanoic acid, methyl ester or Palmitic acid, methyl ester	7.4385
AMBRETTOLIDE	0.0697
Heptadecanoic acid, methyl ester or Margaric acid methyl ester	0.0997



9,12-Octadecadienoic acid, methyl ester, (E,E) or Linolelaidic acid, methyl ester	49.1723
9-Octadecenoic acid (Z)-, methyl ester or Oleic acid, methyl ester	10.6226
Octadecanoic acid, methyl ester or Stearic acid, methyl ester	8.0568
Linoleic acid	0.2691
9,12-Octadecadienoic acid (Z,Z)-, ethyl ester or Linoleic acid ethyl ester	0.4472
9-Octadecenoic acid (Z)-, ethyl ester) or Oleic acid, ethyl ester	0.2523
Octadecanoic acid or Stearic acid	0.4699
9,11-Octadecadienoic acid, methyl ester, (E,E)	0.2737
cis-Bicyclo[5.2.0]non-8-ene	0.188
Camphene or Bicyclo[2.2.1]heptane, 2,2-dimethyl-3-methylene	0.8887
4-Oxo-.beta.-isodamascol	0.183
Ethyl linoleate or LINOLEIC ACID, ETHYL ESTER	0.1003
6-Butyl-1,4-cycloheptadiene	4.2009
METHYL ESTER OF RICINOLEIC ACID or methyl ricinoleate	0.933
2,4-Hexadienedioic acid, 3-methyl-4-propyl-, dimethyl ester, (Z,E)	1.068
1-nitrophenanthro[4,5-bcd]thiophene	0.0536
Eicosanoic acid, methyl ester (CAS) or Arachidic acid methyl ester	0.8428
3-Methylthio-5-(4-(4-methoxyphenyl)-1,3-butadienyl)isoxazole	0.0168
Phenothiazine	4.1205
10H-PYRAZINO[2,3-B][1,4]BENZOTHIAZINE	1.1402
Benzaldehyde, 4-chloro-, oxime Benzaldehyde, p-chloro-, oxime	2.0675
Methyl 2-octylcyclopropene-1-octanoate	5.0078
N-tert-Butyl-3-(methylthio)furan-2-carboxamide	0.0966
Docosanoic acid, methyl ester) or Behenic acid, methyl ester	1.0986
Tetracosanoic acid, methyl ester or Lignoceric acid methyl ester	0.4458
<b>Total FAME Area (%)</b>	<b>79.8535</b>
<b>Ratio of the peak of the fatty acid methyl ester and the peak of the internal standard</b>	<b>800.9378</b>
<b>Internal standard = 50 µl (microliters) = 0.05 grams (g)</b>	<b>0.05</b>
<b>Weight of FAME in grams (g)</b>	<b>40.04689</b>
<b>Yield of FAME (g)</b>	<b>80.09378</b>

## Appendix B – Spectrum and Chromatograms of Epoxidized Fatty Acid Methyl esters

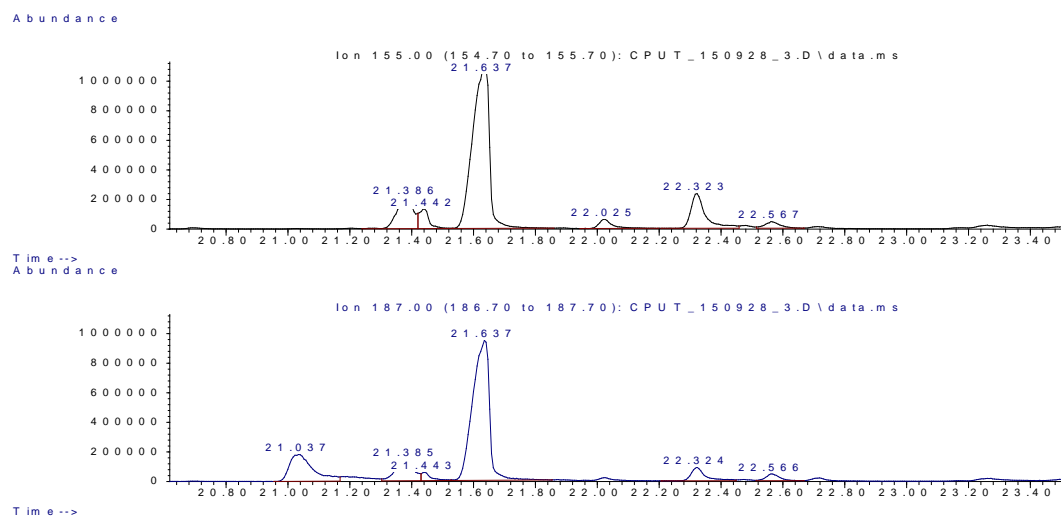


Figure 49: Mass spectrum of solvent-free EFAME at 25 °C

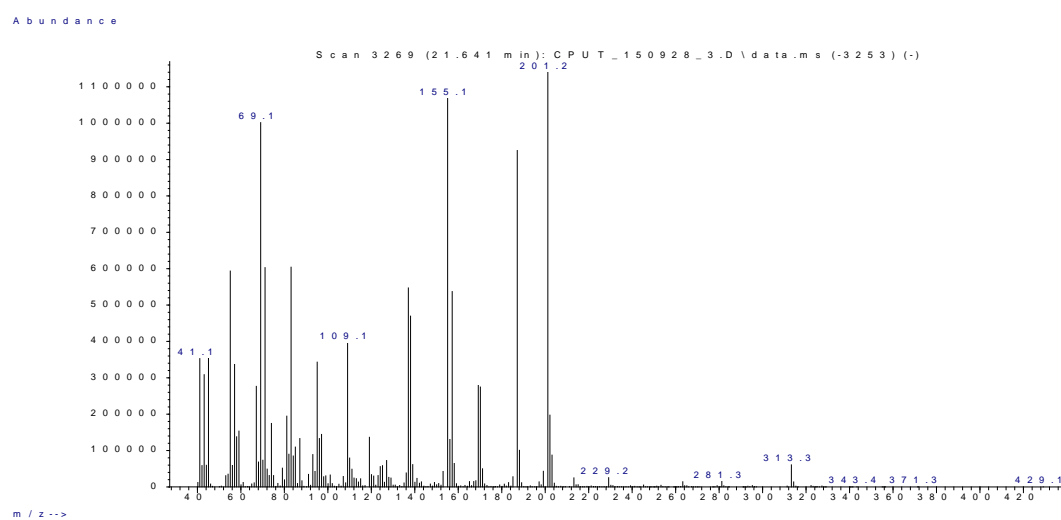
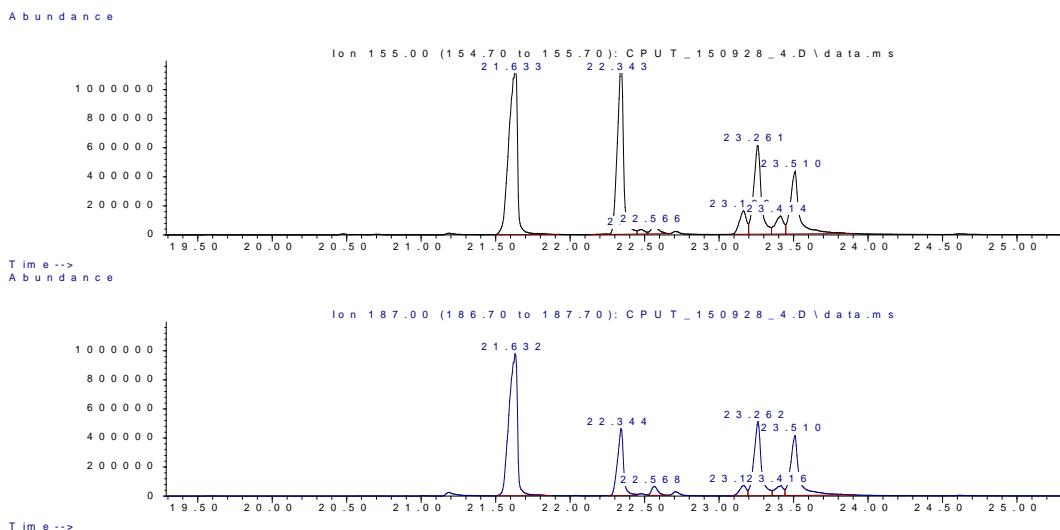
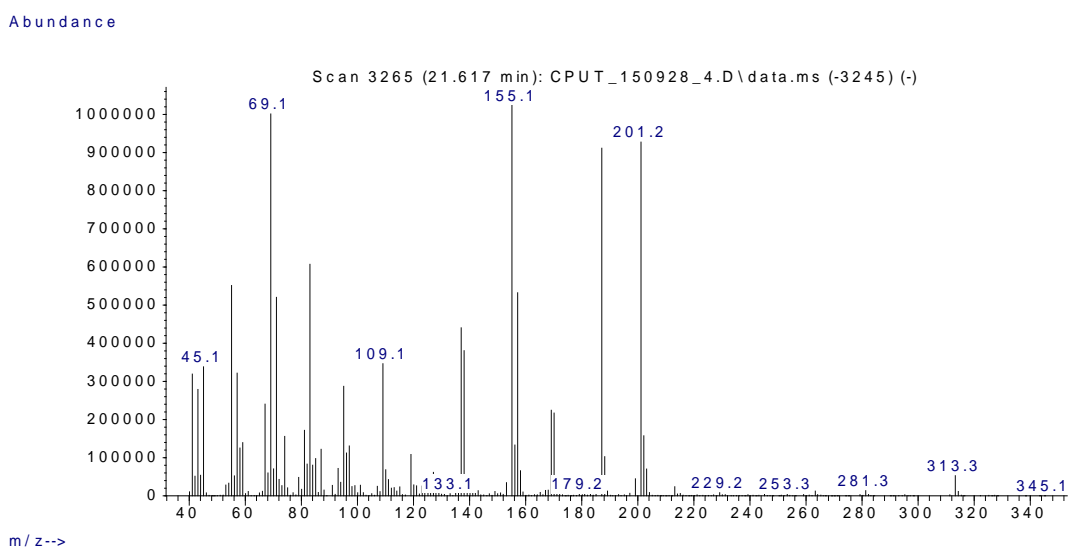


Figure 50: GC-MS Chromatogram of solvent-free EFAME at 25 °C



**Figure 51:** Mass spectrum of EFAME with toluene at 25 °C



**Figure 52:** GC-MS Chromatogram of EFAME with toluene at 25 °C

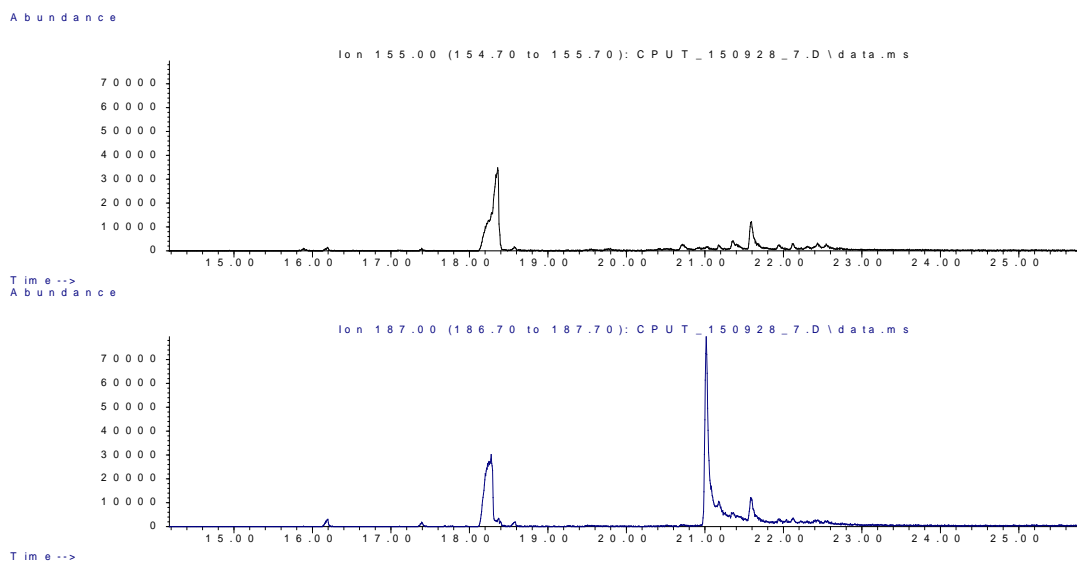


**Figure 53:** Mass spectrum of EFAME with propan-2-ol at 30 °C

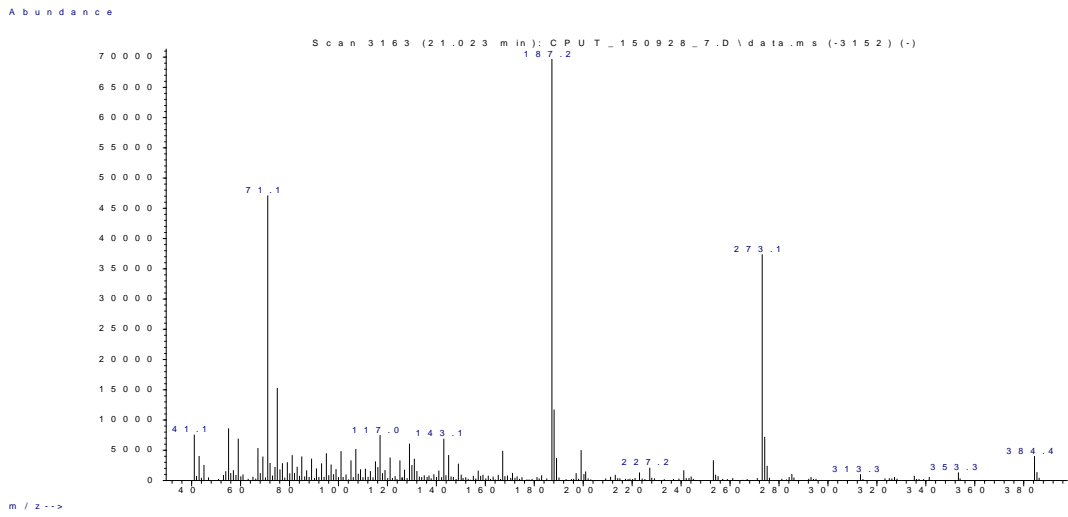


**Figure 54:** GC-MS Chromatogram of EFAME with propan-2-ol at 30 °C

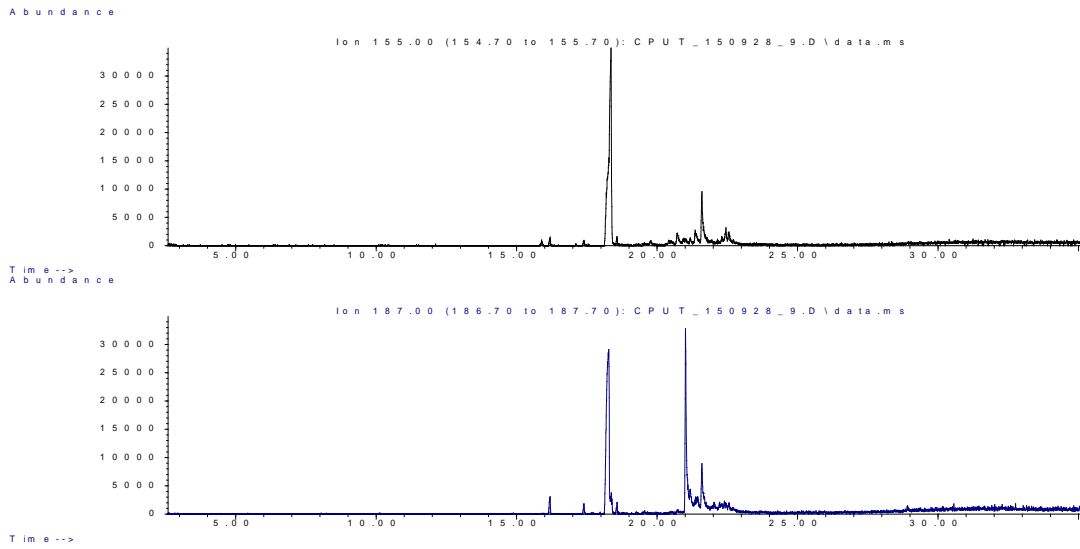


**Figure 55:** Mass spectrum of EFAME with n-hexane at 30 °C

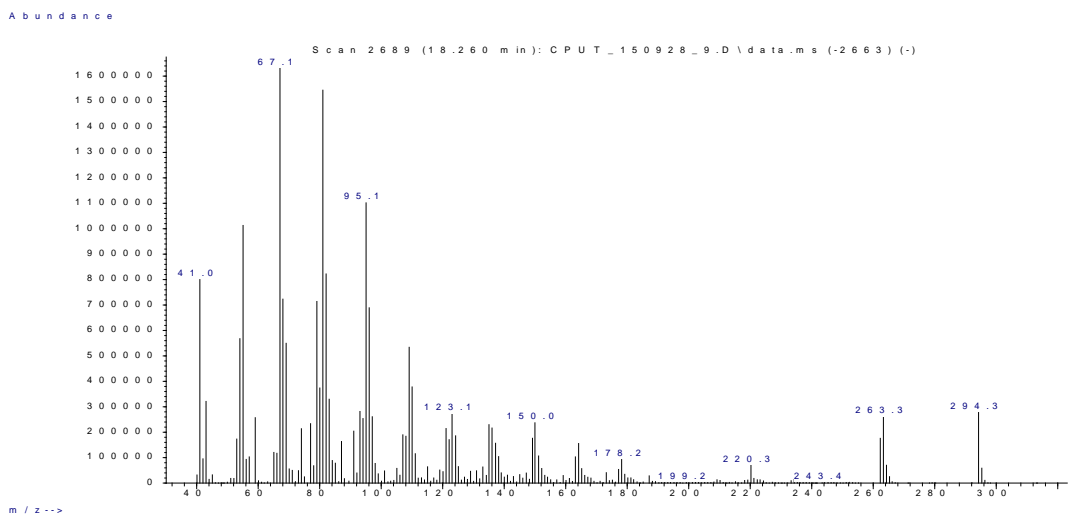


**Figure 56:** GC-MS chromatogram of EFAME with n-hexane at 30 °C

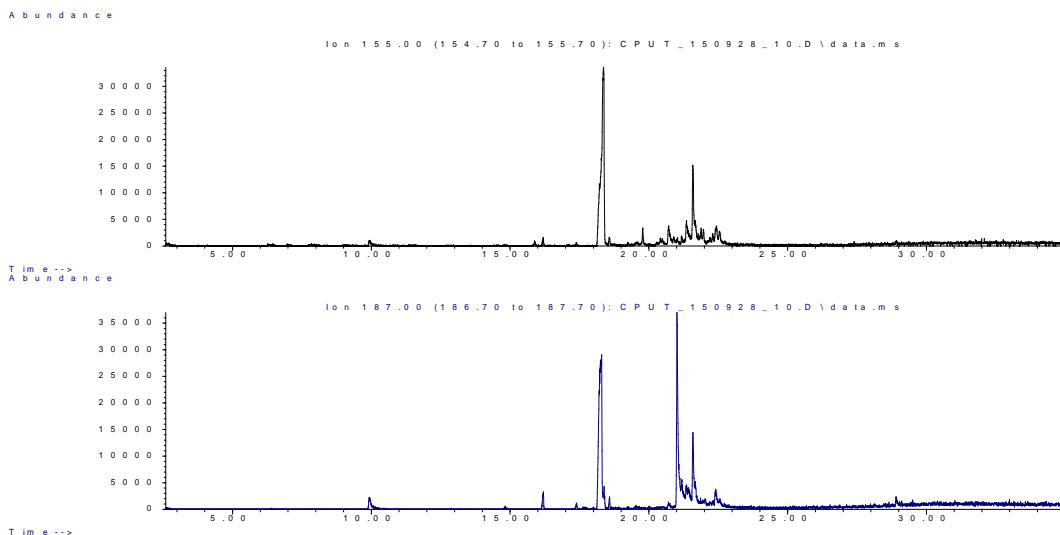


**Figure 57:** Mass spectrum of EFAME with n-hexane at 50 °C

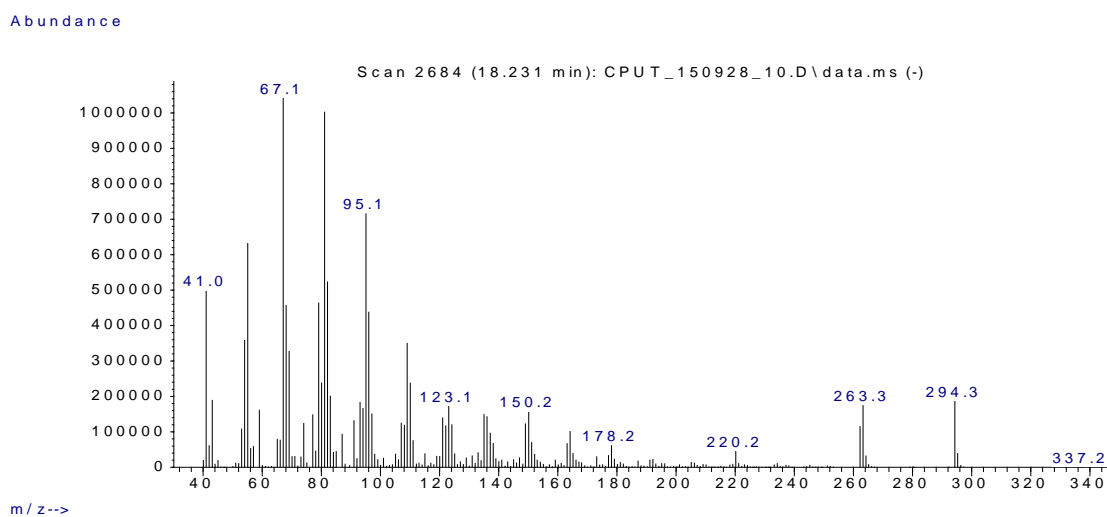


**Figure 58:** GC-MS chromatogram of EFAME with n-hexane at 50 °C

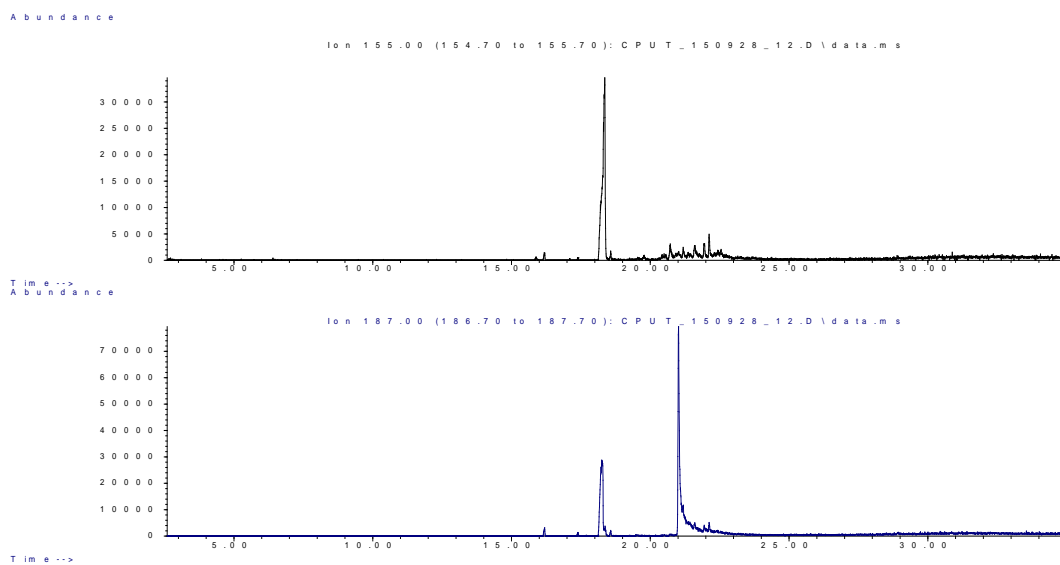


**Figure 59:** Mass spectrum of EFAME with propan-2-ol at 50 °C

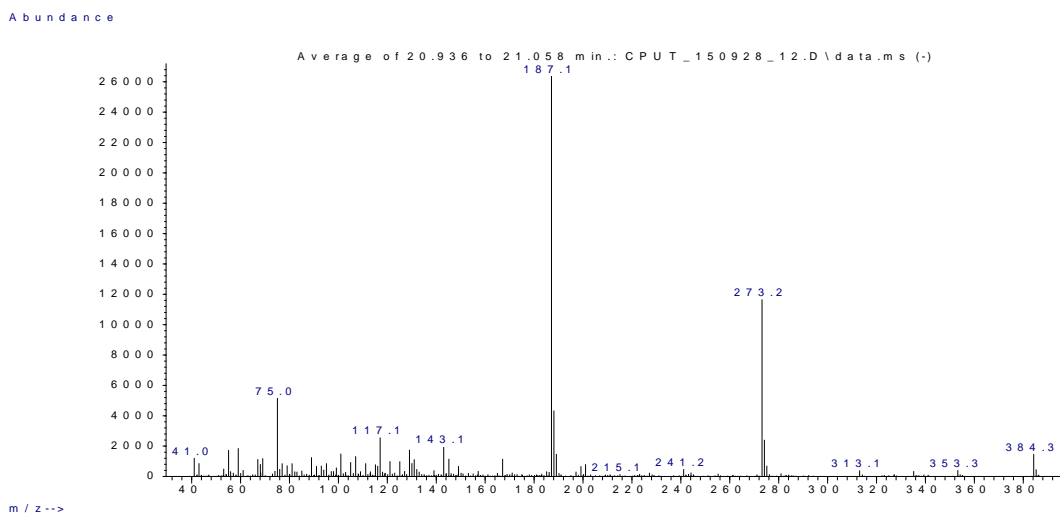


**Figure 60:** GC-MS chromatogram of EFAME with propan-2-ol at 50 °C

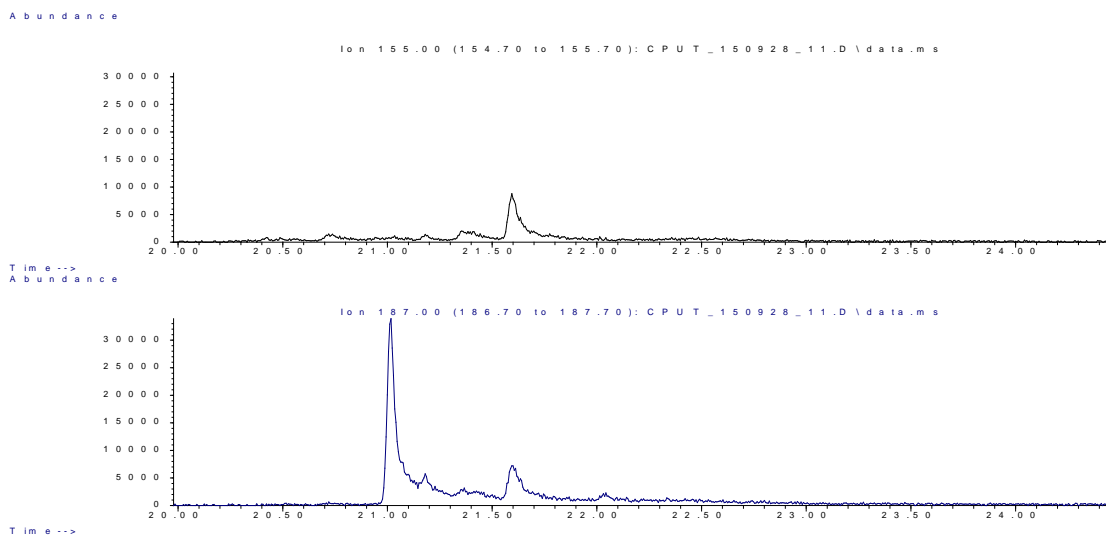


**Figure 61:** Mass spectrum of EFAME with toluene at 50 °C

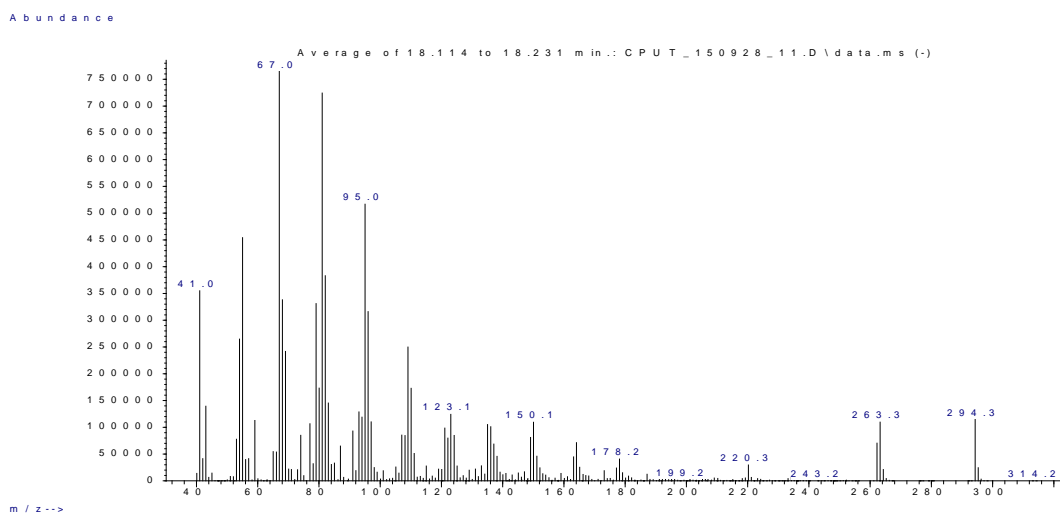


**Figure 62:** GC-MS chromatogram of EFAME with toluene at 50 °C

## Appendix C- Sample Calculations for Adsorption Density Determination

### C.1. Adsorption of CTAB on kaolin clay powder

Measure the conductivity of initial surfactant stock solution (30 g of surfactant in 2 vol% NaCl brine solution) before dilution with water using the conductivity meter

CTAB stock solution conductivity = 12.36 g/L = 12360 ppm where 1g/L = 1000 ppm

The volume of the solutions was calculated using the following expression:  $C_1V_1 = C_2V_2$

Then at 50 ppm surfactant solution the volume of solution will be:

$$12360 \text{ ppm} \times 1 \text{ ml} = 50 \text{ ppm} \times V_2$$

$$V_2 = 247.2 \text{ ml}$$

**Table 39:** Total volumes of CTAB solutions prepared and initial CTAB concentrations measured in part per million before adsorption on kaolin powder

Test	Initial Surfactant Concentration, $C_i$ (ppm)	Volume of surfactant solution (mL)	Measured surfactant concentration (ppm)
1	50	247.2	51
2	75	164.8	73
3	100	123.6	103
4	125	98.88	124
5	150	70.63	152
6	175	61.8	174
7	200	54.93	205
8	225	49.44	223
9	250	41.2	251
10	275	38.03	277
11	300	35.31	302
12	325	32.96	328
13	350	30.9	352
14	400	29.08	401
15	450	27.47	453
16	500	24.72	503
17	550	22.47	554
18	600	20.6	605

Afterwards, it was mixed with the reservoir material (kaolin clay) in a solid: liquid ratio of 1:20 and left to equilibrate for 14 days. The residual equilibrium concentration was read and recorded.

**Table 40:** CTAB equilibrium surfactant concentration after filtration

Residual Surfactant Concentration, $C_e$ (ppm)
23.500
45.856
64.124

85.270
94.460
106.691
126.334
135.567
152.080
167.793
187.603
209.342
226.194
277.046
327.542
376.631
428.845
478.456

The amount of surfactant absorbed (adsorption density) was calculated as the unit mass of surfactant adsorbed per 1 gram of rock (mg/g) using the expression below:

$$\Gamma = \left( \frac{(C_i - C_e) \times M_s}{(M_c)} \right) \times 10^{-3}$$

Where,  $C_i = 51$  ppm,  $C_e = 23.5$  ppm,  $M_s = 30$  g and  $M_c = 2$  g.

$$\Gamma = \left( \frac{(51 - 23.5) \times 30}{(2)} \right) \times 10^{-3} = 0.4125 \frac{\text{mg}}{\text{g}} \text{ kaolin clay}$$

**Table 41:** Static adsorption density of CTAB at different concentrations on kaolin clay at in 2 vol% NaCl solution at ambient temperature

CTAB Adsorption Density, $\Gamma$ (mg/g)	$C_i - C_e$
0.4125	26.5
0.4072	29.144
0.5831	35.8757
0.5810	39.73
0.8631	55.5404
1.0096	68.3087
1.1800	73.666
1.3115	89.4329
1.4838	97.92
1.6381	107.207
1.7160	112.397
1.7799	115.658
1.8871	123.806
1.8593	122.954



1.8819	122.458
1.8955	123.369
1.8773	121.155
1.8982	121.544

*The same method was applied when determining the adsorption of SDS and SEMES on Kaolin clay in 2 vol % NaCl solution at ambient temperature.*

**Table 42:** Total volumes of SDS solutions prepared and initial SDS concentrations measured in part per million before adsorption on kaolin clay powder

Test	Initial Surfactant Concentration, $C_i$ (ppm)	Total volume of Surfactant solution (ml)	Measured Surfactant Concentration, $C_i$ (ppm)
1	50	300	52
2	75	200	71
3	100	150	101.12
4	125	120	127.10
5	150	120	152.53
6	175	100	173.60
7	200	85.71	206.30
8	225	75	224
9	250	66.66	252
10	275	60	275.80
11	300	54.55	304.10
12	325	50	327.3
13	350	46.15	352.70
14	400	42.86	402
15	425	37.5	425.20
16	450	35.29	451.30
17	475	33.33	476.50
18	500	31.58	501.51
19	550	30	553.11
20	600	27.27	610

**Table 43:** Residual concentrations and static adsorption density of SDS at different concentrations on kaolin clay in 2 vol % NaCl solution at ambient temperature

Residual Surfactant Concentration, $C_e$ (ppm)	SDS Adsorption Density, $\Gamma$ (mg/g)	$C_i-C_e$
23.6	0.43	28.4
46.5	0.37	24.5
68	0.50	33.12
86.7	0.61	40.4
106.7	0.69	45.83
122.1	0.77	51.5
144.5	0.93	61.8

157.1	1.00	66.9
174	1.17	78
195.8	1.20	80
224.5	1.19	79.6
246.6	1.21	80.7
270.9	1.23	81.8
319.3	1.24	82.7
341	1.26	84.2
368.1	1.25	83.2
395.5	1.22	81
419.2	1.23	82.31
471.9	1.22	81.21
530.3	1.20	79.7

*CTAB, SDS and SEMES* static adsorption on alumina in 2 vol. % NaCl solution at ambient temperature.

**Table 44:** Total volumes of CTAB solutions prepared and initial CTAB concentrations measured in part per million before adsorption on alumina

Tests	Initial Surfactant Concentration, $C_i$ (ppm)	Total Volume of Surfactant Solution (mL)	Measured Surfactant Concentration, $C_i$ (ppm)
1	50	225.80	53.1
2	75	150.53	76
3	100	112.90	103
4	125	90.32	126.2
5	150	75.27	153.1
6	175	64.51	173.8
7	200	56.45	202
8	225	50.18	227
9	250	45.16	251
10	275	41.05	278
11	300	37.63	304
12	325	34.74	326.3
13	350	32.26	352
14	400	28.23	404.12
15	425	26.56	425.6
16	450	25.09	451
17	475	23.77	478
18	500	22.58	501
19	550	20.53	553
20	600	18.82	604

**Table 45:** Residual concentration and static adsorption density of CTAB at different concentrations on alumina in 2 vol. % NaCl solution at ambient temperature

Residual Surfactant Concentration, $C_e$ (ppm)	CTAB Adsorption Density, $\Gamma$ (mg/g)	$C_i-C_e$
27.6	0.3825	22.4
45.5	0.4575	29.5
69	0.5100	31
88.7	0.5625	36.3
105.7	0.7110	44.3
122.1	0.7755	52.9
140.5	0.9225	59.5
163.1	0.9585	61.9
186	0.9750	64
215.8	0.9330	59.2
239.5	0.9675	60.5
260.6	0.9855	64.4
288.9	0.9465	61.1
339.3	0.9723	60.7
363	0.9390	62
385.1	0.9885	64.9
412.4	0.9840	62.6
436.6	0.9660	63.4
487.9	0.9765	62.1
538.35	0.9848	61.65

**Table 46:** Total volumes of SDS solutions prepared and initial SDS concentrations measured in part per million before adsorption on alumina

Test	Initial Surfactant Concentration, $C_i$ (ppm)	Volume of surfactant solution (mL)	Measured Surfactant Concentration, $C_i$ (ppm)
1	50	247.2	53
2	75	164.8	73
3	100	123.6	103
4	125	98.88	124
5	150	70.63	152
6	175	61.8	174
7	200	54.93	205
8	225	49.44	223
9	250	41.2	251
10	275	38.03	277
11	300	35.31	302
12	325	32.96	328
13	350	30.9	352
14	400	29.08	401
15	450	27.47	453

16	500	24.72	503
17	550	22.47	554
18	600	20.6	605

**Table 47:** Residual concentrations and static adsorption density of SDS at different concentrations on alumina in 2 vol. % NaCl solution at ambient temperature

Residual Surfactant Concentration, $C_e$ (ppm)	SDS Adsorption Density, $\Gamma$ (mg/g)	$C_i - C_e$ (ppm)
23.5	0.4425	29.5
45.856	0.4072	27.144
63.12431	0.5981	39.8757
85.27	0.5810	38.73
92.45958	0.8931	59.5404
101.6913	1.0846	72.3087
117.334	1.3150	87.666
132.5671	1.3565	90.4329
145.08	1.5888	105.92
153.7932	1.8481	123.207
171.6031	1.9560	130.397
183.342	2.1699	144.658
212.1943	2.0971	139.806
265.0462	2.0393	135.954
316.542	2.0469	136.458
365.631	2.0605	137.369
415.8454	2.0723	138.155
460.456	2.1682	144.544

*CTAB, SDS and SEMES* static adsorption on silica in 2 vol. % NaCl solution at ambient temperature.

**Table 48:** Total volumes of CTAB solutions prepared and initial CTAB concentrations measured in part per million before adsorption on silica

Tests	Initial Surfactant Concentration, $C_i$ (ppm)	Volume of Surfactant Solution (mL)	Measured Surfactant Concentration, $C_i$ (ppm)
1	50	247.2	52.3
2	75	164.8	73.5
3	100	123.6	102.1
4	125	98.88	124
5	150	70.63	152
6	175	61.8	174.5
7	200	54.93	205
8	225	49.44	224
9	250	41.2	251.12

10	275	38.03	276.2
11	300	35.31	301.3
12	325	32.96	326
13	350	30.9	352.2
14	400	29.08	404
15	450	27.47	451
16	500	24.72	502
17	550	22.47	553.21
18	600	20.6	603.1

**Table 49:** Residual CTAB concentrations and static adsorption density of CTAB at different concentrations on silica in 2 vol. % NaCl solution at ambient temperature

Residual Surfactant Concentration, $C_e$ (ppm)	CTAB Adsorption Density, $\Gamma$ (mg/g)	$C_i - C_e$ (ppm)
12.5	0.5970	37.5
39.856	0.5047	35.144
54.12431	0.7196	45.8757
75.27	0.7310	49.73
84.45958	1.0131	65.5404
100.6913	1.1071	74.3087
118.334	1.3000	81.666
124.5671	1.4915	100.433
134.08	1.7556	115.92
145.7832	1.9563	129.217
152.6031	2.2305	147.397
179.342	2.1999	145.658
202.1943	2.2501	147.806
254.0462	2.2493	145.954
303.542	2.2119	146.458
354.631	2.2105	145.369
408.8454	2.1655	141.155
454.456	2.2297	145.544

**Table 50:** Total volumes of SDS solutions prepared and initial SDS concentrations measured in part per million before adsorption on silica

Tests	Initial Surfactant Concentration, $C_i$ (ppm)	Total Volume of Surfactant Solution (mL)	Measured Surfactant Concentration, $C_i$ (ppm)
1	50	229.4	52.1
2	75	152.93	74.3
3	100	114.70	101.1
4	125	91.76	126.2
5	150	76.47	151
6	175	65.54	172.11

7	200	57.35	203
8	225	50.98	226
9	250	45.88	254.5
10	275	41.71	274
11	300	38.23	301.2
12	325	35.29	328
13	350	32.77	350
14	400	28.68	405
15	425	26.99	427.1
16	450	25.49	452
17	475	24.15	476
18	500	22.94	502.31
19	550	20.85	554
20	600	19.12	601

**Table 51:** Residual SDS concentrations and static adsorption density of SDS at different concentrations on silica in 2 vol. % NaCl solution at ambient temperature

<b>Residual Surfactant Concentration, <math>C_e</math>(ppm)</b>	<b>SDS Adsorption Density, <math>\Gamma</math> (mg/g)</b>	<b><math>C_i-C_e</math> (ppm)</b>
43.6	0.1275	6.4
66.5	0.1275	8.5
94.2	0.0870	5.8
114.7	0.1545	10.3
138.7	0.1695	11.3
164.1	0.1635	10.9
188.5	0.1725	11.5
216.1	0.1335	8.9
241.4	0.1290	8.6
268.8	0.0930	6.2
289.5	0.1575	10.5
312.6	0.1860	12.4
341.9	0.1215	8.1
388.3	0.1755	11.7
415.4	0.1440	9.6
439.1	0.1635	10.9
468.5	0.0975	6.5
487.9	0.1815	12.1
538.9	0.1665	11.1
592.35	0.1148	7.65

*CTAB, SDS and SEMES static adsorption on ilmenite in 2 vol. % NaCl solution at ambient temperature.*

**Table 52:** Total volumes of CTAB solutions prepared and initial CTAB concentrations measured in part per million before adsorption on ilmenite

Tests	Initial Surfactant Concentration, $C_i$ (ppm)	Total Volume of Surfactant Solution (mL)	Measured Surfactant Concentration, $C_i$ (ppm)
1	50	213.80	51
2	75	142.53	73
3	100	106.90	103
4	125	85.52	124
6	175	61.09	174
7	200	53.45	205
8	275	38.87	277
9	300	35.63	302
10	375	28.51	377.1
11	400	26.73	401
12	475	22.51	472
13	500	21.38	503
14	550	19.44	554
15	600	17.82	605

**Table 53:** Residual CTAB concentrations and static adsorption density of CTAB at different concentrations on ilmenite in 2 vol. % NaCl solution at ambient temperature

Residual Surfactant Concentration, $C_e$ (ppm)	CTAB Adsorption Density, $\Gamma$ (mg/g)	Co-Cs
26.5	0.3675	23.5
39.856	0.4972	35.144
64.12431	0.5831	35.8757
85.27	0.5810	39.73
120.6913	0.7996	54.3087
138.334	1.0000	61.666
168.7832	1.6233	106.217
192.6031	1.6410	107.397
264.1943	1.6936	110.806
288.0462	1.6943	111.954
359.542	1.6869	115.458
393.631	1.6405	106.369
441.8454	1.6823	108.155
494.456	1.6582	105.544

**Table 54:** Total volumes of SDS solutions prepared and initial SDS concentrations measured in part per million before adsorption on ilmenite

Tests	Initial Surfactant Concentration, $C_i$ (ppm)	Total Volume of Surfactant Solution (mL)	Measured Surfactant Concentration, $C_i$ (ppm)
1	50	239.40	52.1
2	75	159.60	74.3
3	100	119.70	101.1
4	125	95.76	126.2
5	175	68.40	172.11
6	200	59.85	203
7	275	43.53	274
8	300	39.90	301.2
9	350	34.2	350
10	400	29.92	405
11	475	25.20	476
12	500	23.94	502.31
13	550	21.76	554
14	600	19.95	603.1

**Table 55:** Residual SDS concentrations and static adsorption density of SDS at different concentrations on ilmenite in 2 wt. % NaCl solution at ambient temperature

Residual Surfactant Concentration, $C_e$ (ppm)	SDS Adsorption Density, $\Gamma$ (mg/g)	$C_i-C_e$ (ppm)
33.9	0.27	18.2
56.7	0.26	17.6
84.2	0.25	16.9
100.7	0.38	25.5
144.1	0.42	28.01
171.5	0.47	31.5
218.8	0.83	55.2
235.5	0.99	65.7
290.9	0.89	59.1
350.3	0.82	54.7
421.5	0.82	54.5
441.9	0.91	60.41
494.9	0.89	59.1
539.35	0.96	63.75

**Table 56:** The effect of different alkali concentrations on the adsorption isotherms of SDS

Concentration of NaOH (wt. %)	$C_i$ (ppm)	$C_e$ (ppm)	$\Gamma$ (mg/g)
0	252	174	1.17
0.2	252	186	0.99
0.3	252	196.5	0.8325



0.4	252	194.1	0.8685
0.5	252	202.6	0.741
0.6	252	204.2	0.717
0.7	252	211.2	0.612
0.8	252	214.5	0.5625
1	252	223.3	0.4305

**Table 57:** The effect of different alkali concentrations on the adsorption isotherms of CTAB

Concentration of NaOH (wt. %)	$C_i$ (ppm)	$C_e$ (ppm)	$\Gamma$ (mg/g)
0	352	226.1943	1.887086
0.2	352	220.4	1.974
0.3	352	208.2	2.157
0.4	352	199.1	2.2935
0.5	352	186.7	2.4795
0.6	352	189	2.445
0.7	352	186.3	2.4855
0.8	352	185.9	2.4915
1	352	183.8	2.523

**Table 58:** The effect of different alkali concentrations on the adsorption isotherms of SEMES

Concentration of NaOH (wt. %)	$C_i$ (ppm)	$C_e$ (ppm)	$\Gamma$ (mg/g)
0	202	149.4	0.789
0.2	202	152.2	0.747
0.3	202	165.5	0.5475
0.4	202	174.1	0.4185
0.5	202	181.86	0.3021
0.6	202	185.8	0.243
0.7	202	189.9	0.1815
0.8	202	193	0.135
1	202	196.3	0.0855

**Table 59:** The effect of different salt concentrations on the adsorption isotherms of SDS

Concentration of NaCl (wt. %)	$C_i$ (ppm)	$C_e$ (ppm)	$\Gamma$ (mg/g)
0	252	202	0.75
1	252	183	1.035
2	252	174	1.17
3	252	101.2	2.262
4	252	87.4	2.469
5	252	71.8	2.703

**Table 60:** The effect of different salt concentrations on the adsorption isotherms of CTAB

Concentration of NaCl (wt. %)	$C_i$ (ppm)	$C_e$ (ppm)	$\Gamma$ (mg/g)
0	352	179.2	2.592
1	352	201.3	2.2605
2	352	226.1943	1.887086
3	352	273.2	1.182
4	352	301.4	0.759
5	352	323.9	0.4215

**Table 61:** Adsorption data for the adsorption isotherm of SDS+CTAB system with fixed salinity

Tests	$C_i$ (ppm)	Volume (ml)	$C_i$ measured (ppm)	$C_e$ (ppm)	Adsorption Density, $\Gamma$ (mg/g)
12	325	32.96	325.3	183.342	2.13
13	350	30.9	351.2	205.19	2.19
14	400	29.08	402	250.0462	2.28
15	450	27.47	452.1	300.52	2.27
16	500	24.72	501	349.31	2.28
17	550	22.47	553.21	401.8454	2.27
18	600	20.6	603.4	451.6	2.28

**Table 62:** Adsorption data for the adsorption isotherm of SEMES+CTAB system with fixed salinity

Tests	$C_i$ (ppm)	Volume (ml)	$C_i$ measured (ppm)	$C_e$ (ppm)	Adsorption Density, $\Gamma$ (mg/g)
12	325	32.96	326	195.42	1.9587
13	350	30.9	352.01	209.9	2.13165
14	400	29.08	401	255.062	2.18907
15	450	27.47	451.2	305.52	2.1852
16	500	24.72	502.1	356.31	2.18685
17	550	22.47	552.12	406.84	2.1792
18	600	20.6	602.3	455.9	2.196